Haemostatic Products as a Potential Therapy for Vesicant-contaminated Wounds

By

Charlotte Amy Hall

A thesis submitted to

The University of Birmingham for the degree of

DOCTOR OF PHILOSOPHY

School of Biosciences

The University of Birmingham

May 2012

UNIVERSITY OF
BIRMINGHAM

University of Birmingham Research Archive

e-theses repository

This unpublished thesis/dissertation is copyright of the author and/or third parties. The intellectual property rights of the author or third parties in respect of this work are as defined by The Copyright Designs and Patents Act 1988 or as modified by any successor legislation.

Any use made of information contained in this thesis/dissertation must be in accordance with that legislation and must be properly acknowledged. Further distribution or reproduction in any format is prohibited without the permission of the copyright holder.

ABSTRACT

There is potential for haemorrhaging injuries to become contaminated with toxic chemicals e.g. sulphur mustard (SM) in certain scenarios. There are currently no specific medical countermeasures for such injuries. It is proposed that haemostats could simultaneously stop bleeding and decontaminate wounds. Products must be able to clot SM-contaminated blood and reduce SM percutaneous absorption to be considered suitable. Blood clot viscosity was assessed *ex vivo* using thrombelastography (TEG). Sulphur mustard did not significantly affect coagulation following application *in vitro* or *in vivo*. Overall, SM did not affect the pro-coagulatory function of haemostats. Although, three of the seven haemostats tested were ineffective at increasing the rate of coagulation. Additionally, clot strength in WoundStat™ treated blood was adversely affected by SM *in vitro.*

Porcine skin provides a suitable model for human skin and allows direct comparison between *in vitro* and *in vivo* percutaneous absorption studies. Static diffusion cells are an established system for the measurement of percutaneous absorption *in vitro* and allow the screening of candidate products for decontaminant efficacy. Both liquid and polysaccharide-based haemostats significantly increased the rate and amount of SM penetrating through undamaged skin and were excluded from further study. Removal of the barrier layer of the skin (stratum corneum and epidermis) significantly increased the percutaneous absorption of SM (rate and amount) which was mitigated by the timely application of WoundStat™. This haemostat was comparable in performance to standard military topical decontaminants.

Sulphur mustard percutaneous absorption data showed good agreement between *in vivo* and *in vitro* data with a significant reduction in the reported latent period between SM exposure and presentation of dermal toxicity in a damaged skin porcine model. Moreover, the altered toxicodynamics imply that the latent period associated with SM pathology is due, in part, to rate of absorption and not solely caused by biochemical pathways. Microarray analysis has identified that SM exposure via damaged skin causes previously unidentified changes in gene expression which may warrant further investigation as potential therapeutic targets. Furthermore, WoundStat™ was shown to reduce SM percutaneous absorption and subsequent pathology *in vivo* and warrants further investigation as haemostatic decontaminant.

ACKNOWLEDGEMENTS

Firstly, I would like to thank my supervisors Professors Kevin Chipman and Rob Chilcott for their guidance throughout the project and helping to keep me positive when things did not quite go to plan! This Thesis would not have been possible without their support and advice.

I would like to acknowledge the Defence Threat Reduction Agency for providing funding for this project and my Ph.D. training as a whole. I would also like to thank staff at the US Army Medical Research Institute of Chemical Defence, who assisted me whilst working there, in particular Ed Clarkson and John Graham for devising the overall project with Rob and for critical review of abstracts and publications. I would also like to thank staff at the Defence Science and Technology laboratories for assisting me during my time there. Special thanks go to Chris Dalton and the staff at the EAH particularly Stefan, Matt and Charles. Special thanks also go to Dr S Javed (HPA), Tim Williams and Lorraine Wallace for all their help and expertise with the microarray studies and Dr Emma Rayner and Professor Graham Hall for their assistance with reviewing and scoring my histopathology slides.

My Thesis would not have been possible without the help of everyone in the CBRN and Chemical Toxicology research group at HPA – Porton: Rob Chilcott, Bob Maynard, Hazem Matar, Rhys Jones and Helen Lydon. I am extremely grateful to Haz and Rhys for all their assistance with the *in vivo* experiments and for their "amazing" sense of humour which has helped keep me sane over the last four years.

A special acknowledgement must go to my partner in crime, H who has been a fantastic lab buddy, messy housemate and all-round awesome friend. I would like to thank her for the cups of tea, Twirls, cakes, and support in and out of the lab.

I could not have survived the last four years without my daily banter-filled tea breaks at Porton and the people who shared these with me to make my Ph.D. enormously more enjoyable (in no particular order): Ruth, Debs, Barry, Ant, Jennie, Sajid, Simon, Hannah, Leanne, Gemma, Stacey, Claire and Suzanna. Thank you for the amazing cakes, competitive baking contests, constant mocking of my accent, and making "that's what she said" part of my daily vocabulary.

I would like to thank my fantastic parents, who have given me endless emotional (and financial!) support over my academic career and have always encouraged me to be the best I could. Thank you to my amazing little sister Bex for always being "dead proud of me".

Finally, I am extremely grateful to my wonderful fiancé Mike for providing emotional support, helping with scientific illustrations, making me endless cups of tea during my Thesis write-up, and for giving me a hug and a very large gin and tonic after a bad day in the lab.

TABLE OF CONTENTS

LIST OF FIGURES

CHAPTER 1

CHAPTER 2

CHAPTER 3

CHAPTER 4

CHAPTER 5

LIST OF TABLES

CHAPTER 2

CHAPTER 3

CHAPTER 4

CHAPTER 5

CHAPTER 6

CHAPTER 7

LIST OF ABBREVIATIONS

3Rs	Ethical framework for the National Centre for the Replacement, Refinement and Reduction of Animals in Research (NC3Rs)
AC	Alternating current
ACS+®	Advanced clotting sponge plus®
ANGPTL	Angiopoietin-like
ANOVA	Analysis of variance
AREG	Amphiregulin
ATP	Adenosine triphosphate
BSA	Bovine serum albumin
CAIII	Carbonic anhydrase III
CaM	Calmodulin
CAT	Catalase
cDNA	Complement deoxyribonucleic acid
CEES	Chloroethyl ethyl sulphide
cRNA	Complement ribonucleic acid
CI	Coagulation index
Cy3	Cyanine 3
CYPs	Cytochrome P450 family of monooxygenases
CIELAB	Commission International d'Eclairage L*a*b*
CW	Chemical warfare
Da	Daltons
DISC	Death inducing signal complex
DNA	Deoxyribonucleic acid
DPM	Disintegrations per minute
EAH	Experimental animal house
ECG	Electrocardiogram
EDTA	Ethylenediaminetetraacetic acid
EGF	Epidermal growth factor
FADD	Fas-associated death domain
FDR	False discovery rate
FE	Fuller's earth
FLVCR	Feline leukaemia virus subgroup C cellular receptor
GC-FP	Flame photometric gas chromatography
GC – MS	Gas chromatography – mass spectrometry
$GPII_b/III_a$	Glycoprotein II_b/III_a

GST	Glutathione-S-transferase
GSH	Reduced glutathione
GPx	Glutathione peroxidase
H_2O_2	Hydrogen peroxide
IL	Interleukin
iNOS	Inducible nitric oxide synthase
IP_3R	Inositol 1,4,5-triphosphate receptors
IRF-1	Interferon regulatory factor-1
IRT	Infrared thermography
K_d	Diffusion parameter
K_m	Partition coefficient
LD_{50}	Median lethal dose
LDI	Laser Doppler imaging
Log P	Partition coefficient
LSC	Liquid scintillation counting
MAPK	Mitogen activated protein kinases
MMP	Metalloprotease
MOMP	Mitochondrial outer membrane pore
mRNA	Messenger ribonucleic acid
NAD^+	Nicotinamide adenine dinucleotide
NADH	Reduced nicotinamide adenine dinucleotide
NADPH	Reduced nicotinamide adenine dinucleotide phosphate
NCOA	Nuclear receptor coactivator
NO	Nitric oxide
NF-κB	Nuclear factor - κB
$O_2^{\bullet-}$	Superoxide radical
OECD	Organisation for Economic Co-operation and Development
$ONOO^-$	Peroxynitrite radical
PAI-1	Plasminogen activator inhibitor
PARP	Poly (adenosine diphosphate) polymerase
PI3Kγ	Phosphoinositide-3-kinase γ
PMN	Polymorphonuclear neutrophil
qRT-PCR	Quantitative real time polymerase chain reaction
QC	QuikClot Advanced clotting sponge plus®
RIN	RNA integrity number
RNA	Ribonucleic acid

RNS	Reactive nitrogen species
ROI	Region of interest
ROS	Reactive oxygen species
RSDL®	Reactive Skin Decontamination Lotion®
SC	Stratum corneum
SD	Standard deviation
SEMS	Shear elastic modulus strength
SM	Sulphur mustard
SNC	Self-normalisation and calibration
SOD	Superoxide dismutase
SRS	Skin reflectance spectroscopy
TDG	Thiodiglycol
TEWL	Transepidermal water loss
TEG	Thrombelastography
TF	Tissue factor
TNFα	Tumour necrosis factor alpha
t-PA	Tissue-type plasminogen activator
TXNIP	Thioredoxin interacting protein
UPK2	Uroplakin II
UV	Ultraviolet
uPA	Urokinase
VIP	Vacuum infiltration tissue processor
vWF	von Willebrand factor

Chapter 1

Introduction

INTRODUCTION

Sulphur mustard (SM) has been recognised as a significant chemical hazard to military personnel since its first reported use against allied troops in Ypres, Belgium during the First World War (Marshall. 1919). However, it may also pose a threat to civilian populations (Wattana and Bey. 2009). Over the last 25 years, the reported exposure of civilians to SM during the Iran-Iraq conflict (late 1980s), the sarin attacks on the Tokyo underground (1995) and the more recent 9/11 and 7/7 terrorist attacks in New York and London have heightened the perceived threat to civilian populations from "dirty bomb" scenarios, in which penetrating injuries or abraded skin could become contaminated with highly toxic chemicals such as SM.

Current regimes for decontamination of said injuries involve the use of dilute (0.5%) hypochlorite solutions and aggressive irrigation and lavage of the wound. However, use of hypochlorite solutions in wounds is contraindicated, particularly for use in abdominal cavity wounds which can result in peritoneal fibrosis and adhesions (Levine and Saltzman. 1996). Standard military topical skin decontaminants (fuller's earth, Reactive Skin Decontamination Lotion®; RSDL® and M291) are also contraindicated for use in wounds. The fine granular nature of fuller's earth and M291 hinders complete removal from wounds and residual particulate matter could potentially illicit an immune response, ultimately resulting in fibrosis and granulomatous reactions in the surrounding tissue (Gibbs and Pooley. 1994, Sakula. 1961). Reactive Skin Decontamination Lotion® has been shown to adversely affect wound healing processes resulting in decreased collagen content and reduced wound strength in an animal model (Walters*, et al*. 2007). Therefore, there is a considerable need for the development of a decontaminant which is safe for use on abraded skin and in open wounds. In addition to

the capacity to decontaminate wounds, a product which could simultaneously stop bleeding would be advantageous.

The aim of this Thesis was to investigate if commercially available haemostats could be suitable to fulfil this dual decontamination/haemostasis requirement. Haemostats promote the coagulation of blood by either adsorbing plasma to locally concentrate clotting factors, activating extrinsic and intrinsic coagulation pathways or a combination of both.

SKIN AND PERCUTANEOUS ABSORPTION

Skin

The skin is a key interface between the internal biological milieu and the environment, preventing loss of water and nutrients, ingress of microorganisms and limiting absorption of UV radiation and hazardous compounds (Poet and McDougal. 2002). Human skin consists of three layers: the stratified, avascular epidermis, the dermis consisting of blood vessels, nerve endings and connective tissue and the hypodermis which is primarily comprised of subcutaneous fat providing a thermal barrier, mechanical cushion and energy store (Barry. 1991).

Epidermis

The epidermis is the outermost layer of the skin and is connected to the dermis by the basement membrane (Figure 1.1). The epidermis is predominately comprised of keratinocytes (90 – 95%) which can be further subdivided into distinct stratified layers (Haake*, et al*. 2001). Other cell types present within the epidermis include melanocytes,

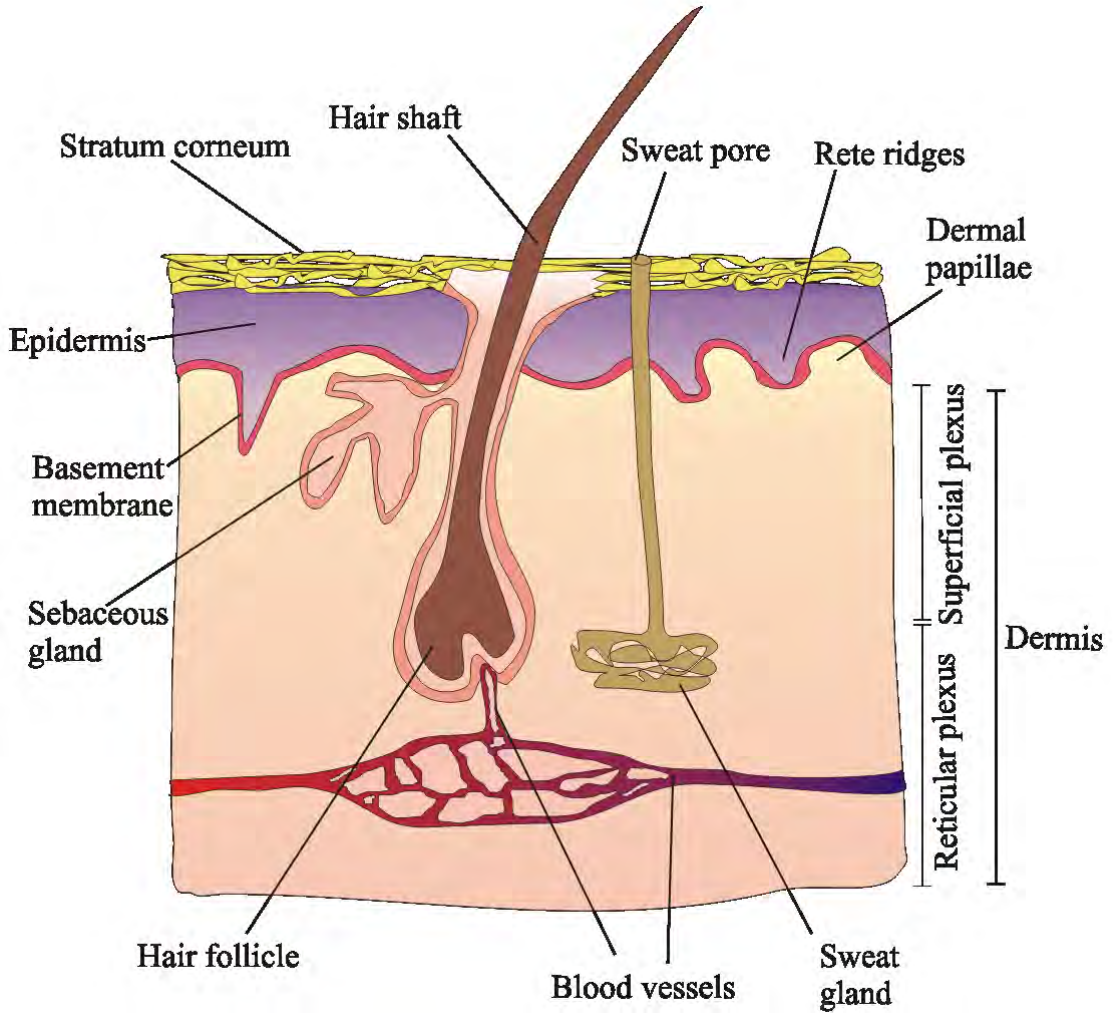

Figure 1.1: Diagrammatic cross-section of a typical section of human skin

The dermis is connected to the epidermis via the basement membrane or basale lamina. A sub-layer of the epidermis (stratum corneum) provides the main barrier function of the skin. The epidermis is avascular whilst the dermis is well perfused and contains lymphatic vessels and nerve ending (not shown). Appendages to the skin (hair follicle, sebaceous and sweat glands) are also shown and these may provide additional routes of penetration through the stratum corneum into the viable layers of the skin.

Langerhans cells and Merkel cells which are involved in pigment formation, immunological function and sensory perception, respectively (Forslind and Lindberg. 2003). There is an increasing calcium concentration from the lower layers of the epidermis (the stratum basale and stratum spinosum) to the upper layers (the stratum granulosum and the stratum corneum; SC) which correspond to increasing levels of differentiation in the epidermis (Kanitakis. 2002, Akiyama. 2011). In addition to these layers, hairless skin which has a thick epidermis (e.g. skin on the soles of the feet) has a stratum lucidum layer below the SC (McGrath*, et al*. 2010).

The stratum basale is a single layer of viable keratinocytes, approximately 10% of which are stem cells, that occupies the basement membrane. The stratum basale is attached to the basement membrane via hemidesmosomes (McGrath*, et al*. 2010). Adjoining keratinocytes are attached via desmosomes which are maintained upon differentiation to form a continuous layer (Forslind and Lindberg. 2003). The cells undergo apical migration from the basement membrane to form the remaining layers of the epidermis (McGrath*, et al*. 2010).

The stratum spinosum comprises several cell layers, adjoined by desmosomes and tight junctions which give the layer its characteristic spiny appearance when viewed microscopically (McGrath*, et al*. 2010). These cells also contain a greater number of keratin filaments compared to the cells in the stratum basale (Hwa*, et al*. 2011).

The stratum granulosum is characterised by the presence of keratohyalin granules, increased number of lamellar bodies and the flattening of the epidermal cells compared to the lower layers of the epidermis (Jennemann*, et al*. 2007). The stratum granulosum has an abundance of lamellar bodies, which are a major component in the synthesis of epidermal lamellar lipids such as ceramides, fatty acids and cholesterol

which contribute to the hydrophobicity of the upper epidermal layers. The keratohyalin granules contain profilaggrin, loricrin, cysteine-rich proteins and keratins 1 and 10 (Dale*, et al*. 1983, Baroni*, et al*. 2012). These proteins are important in maintaining skin barrier properties (Akiyama. 2011).

The outermost layer of the epidermis is the stratum corneum (SC) which is considered to be the primary barrier of the skin (Figure 1.1) (Blank. 1965). The three components which contribute to the barrier properties of the SC include: cornified cell envelope (corneocytes), intercellular lipid bilayer and keratin-filaggrin degradation products (McGrath and Uitto. 2008). Keratinocytes undergo terminal differentiation and cornification to form non-viable corneocytes. In the proposed "brick and mortar" model of the SC, the corneocytes (bricks) are surrounded by intercellular lipids (ceramides, fatty acids and cholesterol) and proteins secreted from the lamellar bodies (mortar) (Michaels*, et al*. 1975). However, other models have suggested the SC may not be so structured with cisternae of fluid interspersed throughout the SC (Warner*, et al*. 2003). Filaggrin is a 37 kDa protein proteolytically cleaved product of profilaggrin which is involved in corneocyte formation (Gan*, et al*. 1990). Filaggrin binds to keratin fibres causing them to bundle into insoluble macrofibrils (Markova*, et al*. 1993). Aggregation of keratin and subsequent collapse of the cytoskeleton results in the formation of corneocytes. The SC is maintained at a constant thickness through the process of desquamation whereby corneocytes are "sloughed off" as cells from the lower layers move up. In the upper layers of the SC, filaggrin is proteolysed into a mixture of hygroscopic amino acids known as skin natural moisturising factor (NMF) which helps modulate SC hydration (Markova*, et al*. 1993).

Dermis

The dermis is connected to the epidermis via the basement membrane (Figure 1.1) and is comprised of two layers; the upper (papillary) layer and lower (reticular) layer. The papillary dermis projects into the epidermis, increasing the interface between the two integument layers. These projections are termed dermal papillae whilst the corresponding epidermal projections are described as rete ridges (Figure 1.1). The major cell types of the dermis, fibroblasts, mast cells and macrophages, are surrounded by extracellular matrix comprised of collagen, elastin and proteoglycans (McGrath*, et al*. 2010). The dermis is highly vascularised; networks of blood vessels, lymphatic vessels as well as nerve fibres, provide nutrients to the avascular epidermis. There is not a distinct boundary between the papillary and reticular layers but the reticular layer contains a more mature elastin fibre network within the collagen matrix (Haake*, et al*. 2001).

Appendages

Additional structures present within the dermis including hair follicles, sweat glands and sebaceous glands are termed appendages or adnexa. The presence and density of these structures varies widely between species and anatomical regions (Monteiro-Riviere. 2005). The appendageal structures pass from the dermis through the epidermis and SC to form openings or "pores" on the surface of the skin (Figure 1.1). There is particular interest in these structures as an alternative route of absorption into the skin (Figure 1.2), especially for chemicals whose molecular weight is too high to penetrate the SC under normal conditions (Monteiro-Riviere. 2005).

Biotransformations in Skin

The skin has been shown to perform both Phase I and Phase II detoxification reactions and is capable of xenobiotic metabolism (Rettie*, et al.* 1986, Roper*, et al.* 1997, Steinsträsser and Merkle. 1995, Yourick and Bronaugh. 2000). These activities may influence both toxicity and percutaneous absorption in the skin. Metabolism of xenobiotics is a multistep process whereby a chemical has functional groups added (Phase I) before conjugation (Phase II) and elimination. There are a number of Phase I and Phase II enzymes present within the skin including; cytochrome P450 superfamily, esterases, dehydrogenases and transferases. Immuno-localisation studies have identified the basal cells and viable keratinocytes of the epidermis, sebaceous glands and hair follicle cells as the primary sites of enzyme activity (Steinsträsser and Merkle. 1995, Cheung*, et al.* 1999).

Phase I enzymes

Cytochrome P450

The cytochrome P450 (CYP) superfamily is considered a key group of Phase I enzymes, particularly regarding their ability to activate chemicals to toxic intermediates. Cytochromes P450 are haem-containing, mixed function oxidases which catalyse the insertion of a single oxygen atom (from molecular oxygen) into the xenobiotic. Generally, the amount of CYP is much lower in the skin compared to the liver (Pham*, et al.* 1990, Zhu*, et al.* 2002), although the expression of some isoforms e.g. CYP2S1 is considerably higher in the skin (Smith*, et al.* 2003).

It is generally accepted that CYP activity does not affect percutaneous absorption due to the location of these enzymes (lower epidermis). However, increased toxicity of xenobiotics (due to activation by CYP) has been well documented (Rogan, *et al.* 1993, Bronaugh, *et al.* 1994). Sulphur mustard has previously been shown to inhibit CYP activity *in vitro* (Brimfield, *et al.* 2009, Brimfield, *et al.* 2012) and upregulate CYP expression in lung epithelium following an aerosol challenge (Pons, *et al.* 2001). Currently, the effect of SM on CYP activity within the skin *in vivo* is unknown.

Esterases

Esterases are ubiquitously expressed in mammalian tissues including the skin (Satoh and Hosokawa 1998). The most significant group present in the skin (in terms of xenobiotic metabolism) are the carboxylesterases, which catalyse the hydrolysis of carboxylic acid esters to a carboxylic acid and an alcohol group (Steinsträsser and Merkle. 1995). Carboxylesterase activity is localised to the basal keratinocytes, sebaceous glands and hair follicles (Jewell, *et al.* 2007a, Jewell, *et al.* 2007b, Meyer and Neurand. 1976) although non-specific esterase activity has also been identified in the stratum corneum (Beisson, *et al.* 2001).

Esterases are known to be robust enough to withstand freezing and esterase activity has been identified in previously frozen skin (Hewitt, *et al.* 2000). It is widely accepted that hydrolysis resulting from esterase activity will reduce the systemic absorption of the parent compound (Williams, *et al.* 1990). Whilst this may reduce systemic toxicity attributed to the parent compound, the resulting carboxylic acid and alcohol groups could be further metabolised to more reactive metabolites. Esterase activity may also promote percutaneous absorption once the compound has entered the

SC by increasing the water solubility (and hence increasing the ability to diffuse through the more aqueous layers of the epidermis) (Liederer and Borchardt. 2006).

Alcohol and Aldehyde Dehydrogenases

Alcohol dehydrogenase (ADH) oxidises alcohol groups to aldehyde groups via the removal of two hydrogen atoms, using NAD+ as a co-substrate. Aldehyde dehydrogenase (ALDH) also uses NAD+ as a co-substrate to oxidise aldehyde groups to carboxylic acid groups. Both enzymes appear to have a potential role in the mechanism of skin sensitisation (Cheung, *et al.* 2003). Aldehydes formed by ADH may subsequently react with (and covalently bind) proteins within the epidermis resulting in haptenisation (Lockley, *et al.* 2004, Lockley, *et al.* 2002).

Phase II enzymes

Transferases

There are a number of transferase enzymes located within the dermal tissues that are able to conjugate both the parent compound and the functionalised compounds generated from Phase I metabolism. These reactions generally result in the pharmacological inactivation or detoxification of chemicals and help facilitation elimination from the body (McCarver and Hines. 2002). The higher relative activity of Phase II enzymes (compared to Phase I) within the skin highlights the important detoxification capacity of the cutaneous tissues (Götz, *et al.* 2012). Phase II enzymes are thought to be important in terms of detoxifying reactive oxygen species (ROS) originating from ultra violet (UV) exposure (Götz, *et al.* 2012). Generally, they are not

thought to modulate percutaneous absorption due to their localisation in the stratum basale and dermal appendages.

Transferases identified within the skin include glucuronyl transferases, N-acetyltranferases, sulphotransferases and glutathione transferases. Glutathione transferases catalyse the conjugation of reduced glutathione (a cysteine-containing tripeptide) with electrophilic chemicals including SM (Gross, *et al.* 1993). Glutathione (GSH) plays a central role in the detoxification of ROS within the skin and depletion of GSH may contribute to SM-induced cell death (Kumar, *et al.* 2001, Rappeneau, *et al.* 2000).

Percutaneous absorption and penetration

The penetration of xenobiotics through the skin is largely considered to be a passive diffusion process (Hadgraft. 2001). There is active intraepidermal transport of large organic cations via an organic anion transporting polypeptide (Schiffer, *et al*. 2003) but this is unlikely to impact upon percutaneous absorption.

The function of skin as a barrier to absorption

The primary barrier to dermal absorption is the SC (Blank. 1965). Whilst the SC is not impermeable to chemicals it does function to limit the penetration and absorption of the vast majority of compounds (Schaefer, *et al*. 2011). Corneocytes and intercellular lamellar lipids are two of the main components of the SC and it is thought that the intercellular lamellar lipids provide a route through which chemicals can be absorbed in the skin (Wertz. 2004).

Routes of dermal absorption

There are several routes by which molecules can pass through the SC and into the viable epidermis/dermis (and hence potentially reach the systemic circulation); these are termed intercellular, transcellular and appendageal routes (Figure 1.2). In the intercellular route, chemicals pass between the corneocytes in the SC via the lipid matrix. This is widely considered to be the principal route of percutaneous absorption (Kitson and Thewalt. 2000). The transcellular route of absorption occurs when a substance passes through both the corneocytes and the lipid matrix within the SC. However, the physiological significance of this route is questionable due to the unfavourable thermodynamics of chemicals passing through multiple layers of corneocytes and intercellular lipids (Flynn. 1990). The appendageal route of absorption involves chemicals by-passing the SC to enter the lower epidermal or dermal layers. This can be achieved by passage of chemicals through appendage structures including hair follicles and sweat glands (Maibach *et al*. 1971). However, the density of the appendages varies greatly between different anatomical locations and species (Scheuplein. 1967).

It is thought this route of percutaneous absorption may be most important immediately after application of a penetrant or if the penetrant is large or very polar (Scheuplein. 1967). It is likely to have higher significance as a route of absorption in animals with high follicle densities (Illel*, et al*. 1991). The significance of the appendageal route can be measured using the skin sandwich model (Essa*, et al*. 2002) to determine the follicular versus bulk transport (penetration through SC) ratio.

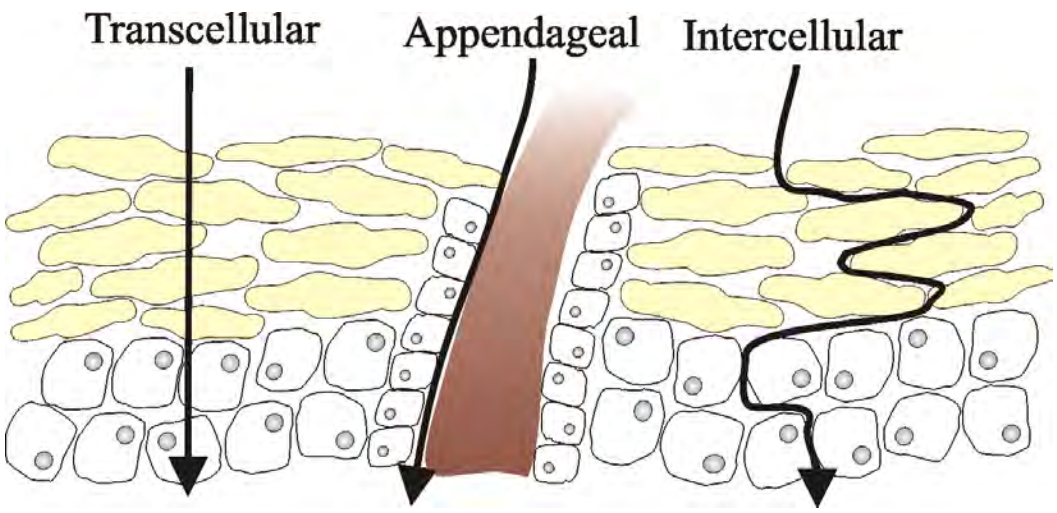

Figure 1.2: Routes of percutaneous penetration through the stratum corneum.

Kinetics of dermal absorption

Skin absorption occurs when a chemical, such as SM, undergoes passive diffusion through the SC into the viable layers of the skin. Diffusion can be defined as the process by which matter moves from one part of a system to another as a result of random molecular motion and can be characterised by Fick's laws (Brisson. 1974). The four main factors influence the rate of skin absorption (J; Equation 1.1) based on Fick's laws of diffusion include: partitioning (partition coefficient; K_m), diffusivity (diffusivity coefficient; D), distance (h) and concentration (C). Fick's first law of diffusion applies to "steady state" or "infinite dose" conditions where the amount of chemical available for diffusion does not significantly decrease. Fick's second law of diffusion applies to "finite dose" conditions where the amount of chemical available for diffusion is significantly reduced over time (due to rapid percutaneous absorption or evaporation).

$$J = \frac{D \cdot C \cdot K_m}{h} \qquad \textit{Equation 1.1}$$

Equation 1.1: Calculation of the overall rate (or flux) of diffusion (J) across the skin (g cm^{-2} h^{-1}). Where D is diffusivity coefficient, C is concentration, h is the thickness of the SC, and K_m is the partition coefficient.

Diffusivity (or diffusivity coefficient) (D) is a temperature-dependent parameter related to the mobility of a penetrating molecule within the SC and is expressed as cm^2 h^{-1}. This parameter is affected by a number of factors including: potential for interactions between the molecule and SC (hydrogen bonding or electrostatic interactions) and the size of molecule (steric hindrance). The extent to which a chemical moves into the SC from the skin surface is expressed as the partition coefficient (K_m) and is primarily determined by the relative solubility of the chemical in water or octanol (log P value).

The distance parameter (h; cm) refers to the mean diffusional path length through the SC as this is the main rate-limiting membrane which a chemical must transverse. Finally, the concentration (C; g cm^{-1}) of a chemical is assumed to be equal to its liquid density at a given temperature.

Fick's first law makes the assumption that diffusion is driven by concentration gradients. However, thermodynamic activity (based on Fick's second law) is the driving force for diffusion of chemicals across the skin (Barry*, et al*. 1985) and diffusion is not solely reliant on concentration gradients due to physiological processes such as sweating. Sweating results in the formation of an aqueous layer over the skin surface. If a hydrophobic chemical were applied to the skin the presence of an aqueous layer like sweat would decrease the concentration of the chemical. However, the presence of a hydrophobe in an aqueous solution results in disruption of the hydrogen bonding network between water molecules in the solution (less thermodynamically favourable) and increase fugacity. Fugacity can be defined as the tendency of a molecule to move from one environment to another dependent on its physiochemical properties (Pugh and Chilcott. 2008). In the case of lipophilic chemicals this results in increased diffusion from the aqueous phase (less favourable) to the more lipid-rich SC (more favourable).

The maximum rate of absorption of a chemical can be determined experimentally from the gradient of the slope from the linear phase (steady-state flux) of cumulative amount absorbed (g cm^{-1}) over time (h; Figure 1.3). True steady-state can only be measured under infinite dose conditions. However, a pseudo steady-state can be measured under finite dose conditions from the linear portion of the graph (Figure 1.3). The lag time, which is defined as the time intercept of the linear portion of the cumulative absorption time curve, can be calculated using Equation 1.2.

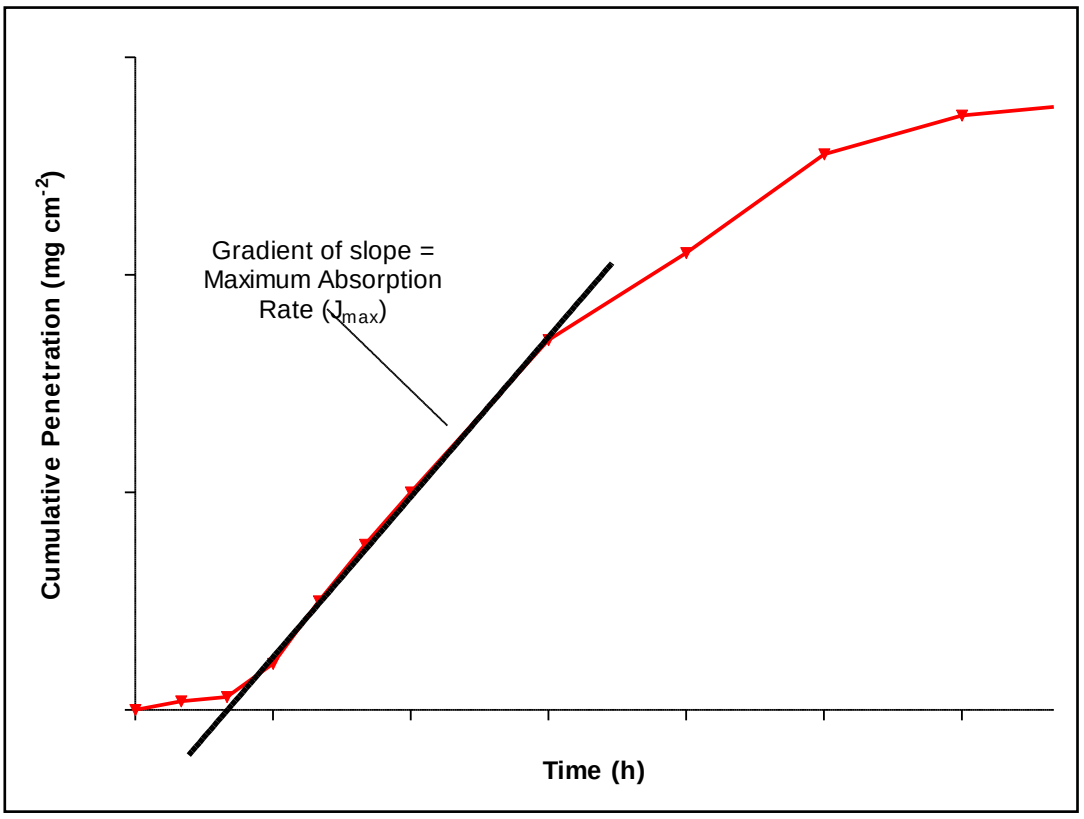

Figure 1.3: Example of cumulative penetration profile for a chemical under finite dose conditions.

Maximum absorption rate is determined from the gradient of the slope from the linear phase of the graph.

Equation 1.2

Equation 1.2: Calculation of lag time where, T_L is the lag time, L is the effective thickness of the skin, C is the concentration of the chemical applied to the skin surface (assumed to be constant in steady-state), D is the diffusion coefficient of the skin and k_d is the diffusion parameter (defined as $k_d = D/L^2$) (Twizell and Kubota. 1994).

Physicochemical factors affecting dermal absorption

The main physicochemical factors that can influence percutaneous absorption include: the lipophilicity of the penetrant, the size of the penetrant (molecular weight), if the penetrant is applied to the skin in a vehicle and the volume of the dose applied.

Molecular weight of a penetrant

Smaller molecules (low molecular weight) will pass through the skin much more rapidly than those with a higher molecular weight. The importance of different routes of absorption may also depend on the molecular weight of a molecule; for instance, the appendageal route is more important for the absorption of larger molecules than for smaller molecules (Scheuplein. 1967). However, as a general guide it is considered that chemicals with a molecular weight greater than 500 Da do not penetrate the skin under 'normal' circumstances (Bos and Meinardi. 2000).

Hydrophobicity of a penetrant

Hydrophobicity, expressed as Log P (the logarithm to base ten of the partition coefficient between octanol and water), is a major factor in determining the dermal penetration of a chemical. The higher the Log P value, the more lipophilic the chemical is. Compounds with a Log P above 3 are considered highly lipophilic. The relative hydrophilicity and lipophilicity affects dermal absorption because, as previously described, in terms of entropy and free energy within a system it is more thermodynamically favourable for lipophilic chemicals to partition into the SC. Conversely it is likely to be less favourable for these chemicals to partition into the more aqueous viable epidermis and dermis and pass into systemic circulation (Bronaugh. 2004). Thus potentially forming a reservoir within the skin.

Solvent vehicle for application of a penetrant

Applying a chemical to the skin surface in a solvent vehicle can affect the percutaneous absorption of the chemical. The absorption of a chemical into the skin may be impeded if it is more soluble in the vehicle it is applied in than the SC (Jacobi*, et al*. 2006). Contrary to this, if a chemical is more soluble in the SC than its application vehicle, then the chemical is more likely to penetrate into the SC. The rate of percutaneous absorption for a chemical is highest when it is at saturated concentration in its application vehicle (because thermodynamic activity is maximal). Hence, the same concentration of a lipophilic chemical will be absorbed more rapidly if it is dissolved in an aqueous vehicle compared with a more lipophilic vehicle. Furthermore, some solvent vehicles are able to act as penetration enhancers (Ma*, et al*. 2010, Williams and Barry.

2004, Duracher*, et al*. 2009), either by perturbing the arrangement of SC lipids, or by entering the SC and creating a reservoir for dissolution of the chemical penetrant. Therefore, it is important to take into consideration these effects if a chemical is applied in a solvent vehicle. Additionally, this is an important consideration for decontaminants which aim to prevent the absorption of chemicals into the skin and therefore the chemical (to be decontaminated) should have a higher solubility in the decontaminant than the SC.

Dose of a penetrant

Whether the dose of a chemical is applied to the skin as a finite or infinite dose can have a significant influence on dermal absorption. Infinite doses require the application of a sufficient volume of penetrant to the skin that will not significantly deplete (due to absorption or evaporation) over time. This allows the maximum rate of absorption and permeability coefficient of the penetrant to be measured under steady-state conditions. However, these conditions are not generally reflective of a typical exposure scenario. Application of a finite dose of penetrant to the skin surface (which is depleted over time by evaporation or absorption) is more relevant to exposure scenarios. However, absorption may not reach steady-state as the dose applied becomes depleted over time due to absorption and evaporation dependent on the physicochemical properties of the penetrant (Franz. 1978).

Biological factors affecting dermal absorption

Biological factors relate to the variability seen in the structure or chemical structure of the skin. Differences in the influence of biological factors can be seen intra or inter-individually, as well as between different species. The main biological factors that influence dermal absorption include the anatomical location of the skin, gender, age, skin damage/disease and also species.

Anatomical location of the skin

The anatomical location is an important consideration when investigating dermal absorption due to differing skin permeability depending on location of the site on the body (Maibach*, et al*. 1971). Where the SC is thickest, such as the palms of the hands and soles of the feet the skin is less permeable to chemicals than areas of the body where the SC much thinner, such as the scrotum or eyelids (Scheuplein and Blank. 1971). Differences between anatomical locations are not limited to skin thickness there is also variation in the corneocyte arrangement and the lipid composition of the SC between sites on the same individual and intra-individually (Lampe*, et al*. 1983). However, no correlation between specific SC lipids and barrier function has been observed (Norlen*, et al*. 1999).

Conversely, intra-individual variations in filaggrin, which is a major structural protein in the SC, have been shown to impact barrier function in a mouse model (Kawasaki *et al.* 2012). Filaggrin contributes to the mechanical strength and integrity of the SC (Dale*, et al*. 1985) and is also further processed to hygroscopic amino acids which are important in SC hydration (Rawlings and Harding. 2004). Therefore,

decreased levels of this protein may result in SC barrier disruption and increase percutaneous absorption of some chemicals.

Gender and Age

Gender-specific differences in the structure, permeability and protein composition of the SC have been observed (Jacobi*, et al*. 2005). However, it is unclear whether these anatomical differences correlate with significant differences in percutaneous penetration between the sexes. Age-related changes in the skin structure between older (>65 years) and younger (<40 years) volunteers that may potentially increase skin permeability have been reported (Roskos*, et al*. 1989). These included decreased SC hydration status, reduced skin surface lipids and flattening of the dermal-epidermal junction (loss of rete ridges and corresponding dermal papillae) (Roskos*, et al*. 1989). Conversely, age-related decreases in cutaneous perfusion may act to decrease rates of penetration (Monteiro-Riviere. 2004).

Skin damage

The effect of skin damage on the penetration of chemicals has been previously investigated using a variety of methods. These have included; chemical disruption to skin barrier e.g. sodium lauryl sulphate (Borrás-Blasco*, et al*. 1997, Jakasa*, et al*. 2006) and physical damage to skin e.g. removal of SC via tape stripping or abrasion (Bashir*, et al*. 2001, Akomeah*, et al*. 2008). As the SC is the main barrier to dermal absorption it is reasonable to assume that its removal would increase the rate and amount of a chemical absorbed through the skin. However, *in vitro* damaged skin studies which

have completely removed the epidermis have shown that enhanced absorption favours hydrophilic molecules more than hydrophobic ones (Gattu and Maibach. 2011). Presumably this is due to the aqueous nature of the epidermis/dermis being less thermodynamically favourable for diffusion of hydrophobic molecules compared to hydrophilic ones.

Species differences

Key factors which appear to influence the suitability of different animal skin to model human skin include the thickness of the SC and hair follicle density. Ideally the skin used for percutaneous absorption studies would be human. This would reduce the problem of trying to account for species differences when extrapolating to *in vivo* predictions (Bronaugh and Franz. 1986). However, it is unethical to use human volunteers for percutaneous absorption studies using toxic or potentially toxic penetrants and obtaining sufficient quantities of suitable human skin for *in vitro* studies is difficult. Therefore, animal models are needed but the SC thickness differs greatly between commonly studied mammalian species (Bartek, *et al*. 1972, Monteiro-Riviere, *et al*. 1990). Rodent species have a thinner epidermis compared to human skin resulting in overestimate absorption of chemicals (Dalton, *et al*. 2006). Pig skin has a similar thickness to human skin (Monteiro-Riviere, *et al*. 1990) and is widely accepted as the most suitable animal model for human skin absorption (Barbero and Frasch. 2009, Simon and Maibach. 2000). Hair follicle density also varies greatly between species. The dorsal skin of the rat and mouse has 289 and 658 follicles per cm^2, respectively. In contrast, human dorsal skin has 11 follicles per cm^2 (Bronaugh, *et al*. 1982). As previously described the higher follicle density means the appendageal route of

absorption is likely to represent a more significant route of penetration in rodent skin compared to human skin (Illel*, et al*. 1991).

Measurement of percutaneous absorption - *in vitro* techniques

Highly toxic chemicals such as SM cannot be administered to human volunteers *in vivo*. Thus, *in vitro* assessment of dermal absorption provides an ethical alternative to *in vivo* studies. Measurement of dermal absorption using skin mounted in diffusion cells is a well established method (Chilcott*, et al*. 2005, Hattersley*, et al*. 2008, Miller and Kasting. 2010, Franz. 1975). Generally, absorption data obtained from *in vitro* studies correlate with *in vivo* absorption data (Williams. 2006). Penetration of chemicals *in vivo* may be influenced by blood flow, or inflammation in response to the chemical applied at the skin surface (Williams. 2006). These events cannot be replicated using excised skin in the diffusion cell system. Therefore, penetration of a chemical *in vitro* may not accurately predict *in vivo* penetration (Williams. 2006). This may be particularly relevant to SM which has been shown to reduce dermal perfusion (Brown*, et al*. 1998, Reid*, et al*. 2007) and increase expression of pro-inflammatory cytokines (Price*, et al*. 2009, Ricketts*, et al*. 2001, Sabourin*, et al*. 2000). Therefore, SM may induce blood flow or inflammatory response changes which may influence the dermal or systemic absorption of SM.

Diffusion Cells

Two main types of diffusion cell are used to measure *in vitro* percutaneous absorption; static and the flow-through. The principle behind both systems is the same: chemicals

are applied to the skin surface and the amount of chemical penetrating through the skin into the receptor fluid below can be measured. In the flow-through diffusion cell (Bronaugh and Stewart. 1985) receptor fluid is constantly removed from the receptor fluid chamber and replenished with fresh receptor. The flow-through system was not used in this Thesis and so will not be discussed further.

As the name suggests, in static diffusion cell systems the receptor fluid is static and allows the penetrant to accumulate (Franz. 1975). The diffusion cells used in this Thesis were of the water-jacketed variety allowing control over receptor fluid and skin surface temperature via a heated-water circulator (Figure 1.4). Skin is mounted between a donor and receptor chamber and clamped in placed. Serial samples of the receptor fluid can be taken via the sampling port and the cumulative penetration of a chemical over time can be measured (Figure 1.3). The amount of chemical remaining on the skin surface, within the skin layers or within the receptor fluid at the end of the study can also can be measured.

Receptor fluid

Common used receptors included physiological saline (0.9%) with and without bovine serum albumin (BSA) and culture medium containing nutrients (Rubio*, et al*. 2011, Kasting*, et al*. 1997). The partitioning of a chemical into the receptor fluid is limited by the chemical's solubility and affinity for the receptor fluid phase. Underestimation of skin permeability may result if the thermodynamic activity of the penetrant in the receptor fluid exceeds 10% of that in the donor chamber due to loss of infinite sink conditions (Cooper and Berner. 1985). Therefore, it is important that the volume and composition of the receptor fluid are appropriate for the test compound to ensure

efficient removal of the penetrant from the skin/receptor fluid interface and maintenance of effective "sink" conditions (Guy, *et al*. 1985). The absorption of more lipophilic chemicals can be facilitated by the addition of BSA (Bronaugh. 2004). Given the low solubility of SM (less that 0.1% at 22°C) 50% aqueous ethanol is used as a receptor fluid as it facilitates the partitioning of SM into the receptor phase (Hattersley, *et al*. 2008, Ramsey, *et al*. 1994, Scott and Ramsey. 1987). Moreover, SM is rapidly hydrolysed in 50% aqueous ethanol (T½ ~ 30 seconds) maintaining the concentration gradient and infinite sink conditions (Chilcott 2000). This reduces the problem of underestimating the amount or rate of absorption, which is particular concern for toxic chemicals such as SM.

Skin Preparation

In vitro dermal absorption studies have be conducted using various skin preparations including full thickness skin (Vallet, *et al*. 2007, Chilcott, *et al*. 2000, Van de Sandt, *et al*. 2004), split thickness skin (dermatomed) (Dalton, *et al*. 2006, Van de Sandt, *et al*. 2004, Schmook, *et al*. 2001) or epidermal membranes (Hattersley, *et al*. 2008, Chilcott, *et al*. 2000). However, use of full-thickness skin may affect the penetration of lipophilic chemicals due to the lack of functioning circulation *in vitro* (Wilkinson, *et al*. 2006, Hawkins and Reifenrath. 1986). Epidermal membranes are separated from the underlying dermis and would not be suitable for generating a superficial wound *in vitro* model. Therefore, split-thickness (or dermatomed) skin is widely regarded as a suitable *in vitro* model for measuring percutaneous absorption and has shows better agreement with *in vivo* data than full-thickness skin (Hawkins and Reifenrath. 1986).

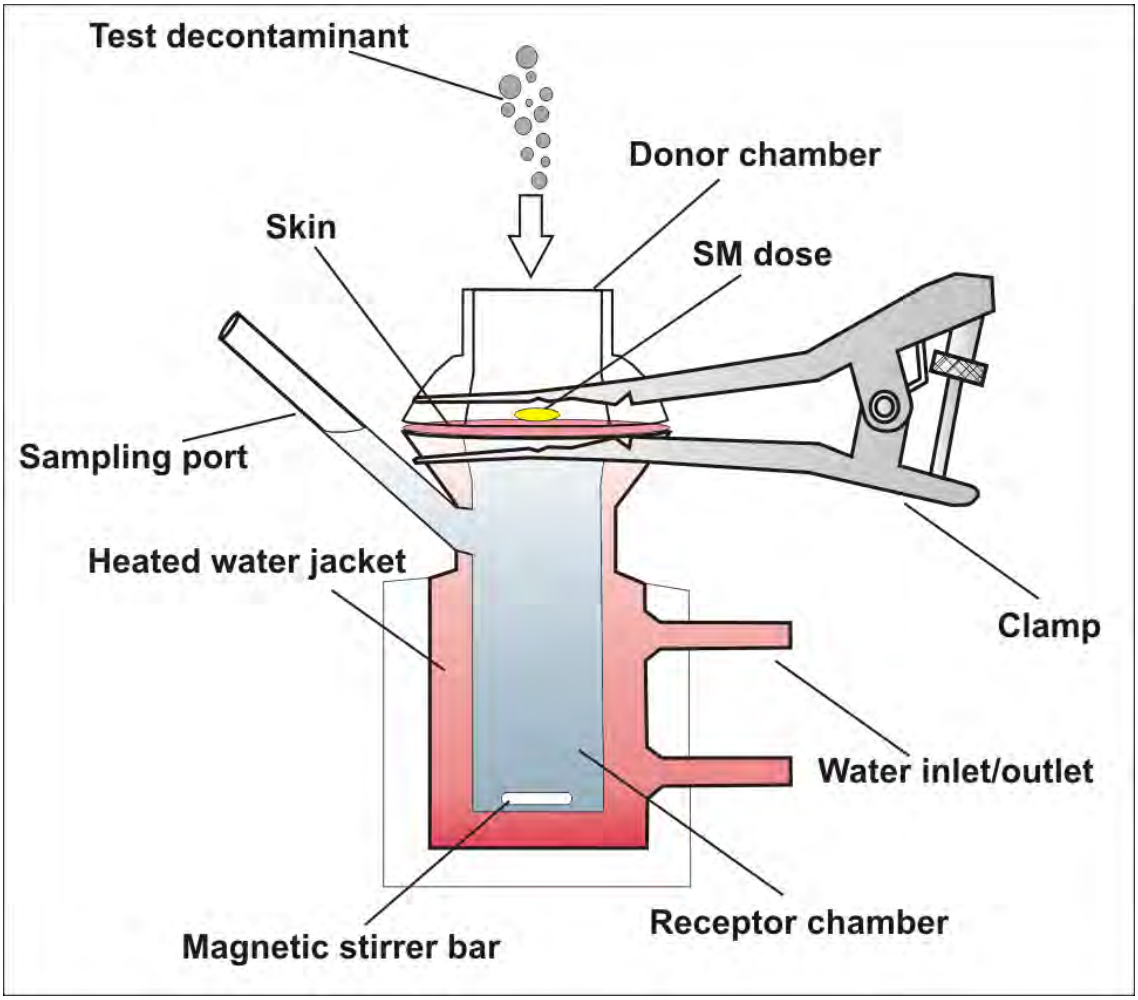

Figure 1.4: A Schematic diagram of static diffusion cell.

Skin is mounted between an upper (donor) and lower (receptor/acceptor) chamber and clamped in place. The lower chamber is filled with an appropriate fluid which is maintained at a constant temperature via an external source of heated water. A stirring mechanism is used to ensure mixing of the receptor chamber fluid.

Split-thickness skin is obtained by removing a layer of skin using a dermatome, allowing the SC and the epidermis to be removed from the majority of the dermis.

Measurement of dermal barrier integrity

Measuring the physical integrity (SC integrity) prior to a dermal penetration study is a requirement of the Organisation for Economic Co-operation and Development (OECD) guidelines (OECD. 2004) and is used to check that skin barrier function has not become unintentionally compromised (which could affect the penetration of the chemical through the skin). There are several methods used to measure barrier integrity including: transepidermal water loss (TEWL) (Elkeeb*, et al*. 2010), penetration of tritiated water (^{3}H) (Lawrence. 1997) and electrical resistance across the skin (Davies*, et al*. 2004, Chilcott, *et al.* 1996). However, there is disagreement over the effectiveness of TEWL as a measure of barrier function *in vitro* (Chilcott*, et al*. 2002). Briefly, the electrical resistance of the skin, when physiological saline is applied to the donor and receptor chamber, is measured using an alternating current (AC) impedance meter. If the skin were damaged then the passage of an electrical current through the skin would be easier (lower resistance). Skin is generally considered undamaged if the resistance is greater than 1.5 $k\Omega\ cm^{-2}$ (Davies*, et al*. 2004).

Measurement of percutaneous absorption - *in vivo* techniques

Determining percutaneous absorption *in vivo* could involve the use of relevant laboratory species or human volunteers. However, use of human volunteers is unethical for measuring the absorption of toxic chemicals such as SM. For the reasons mentioned

earlier, the use of rodents (in measuring SM absorption) may not accurately predict human dermal absorption due to higher hair follicle density and thinner SC and epidermis. However, the pig is a well established model for measuring percutaneous absorption and SM lesion development (Reid*, et al*. 2007, Brown and Rice. 1997, Chilcott*, et al*. 2007, Graham*, et al*. 2001). The *in vivo* system has a number of advantages over the *in vitro* system including: the presence of relevant physiological processes (inflammation and xenobiotic metabolism) and the presence of cutaneous blood flow (Monteiro-Riviere*, et al*. 1990).

The dermal absorption of chemicals *in vivo* can be measured in similar ways to *in vitro* including the use of radiolabelled (typically ^{14}C) chemicals (Chilcott*, et al*. 2005, Van de Sandt*, et al*. 2000) or quantification and speciation of parent or metabolite compounds using liquid or gas chromatography combined mass spectrometry (Black*, et al*. 1992, Fairhall*, et al*. 2008, Lawrence*, et al*. 2008).

Another method of determining percutaneous absorption *in vivo* is to quantify the biological response to the chemicals (Wester and Maibach. 2001). One major advantage of this technique is that it is non invasive but inter-individual variation may limit the accuracy of this method (Levin and Maibach. 2005). The use of biophysical measurements is limited to chemicals which elicit a visible or measurable effect upon the skin. Sulphur mustard is known to elicit a number of skin effects which can be quantified using a range of techniques including transepidermal water loss (skin barrier function), laser Doppler imaging (dermal blood flow), skin reflectance spectroscopy (skin colour) and infrared thermography (skin surface temperature) (Chilcott. 2000, Braue*, et al*. 2007, Graham*, et al*. 2002).

Transepidermal water loss is the outward diffusion of water through the dermal layers (Oestmann, *et al*. 1993). Transepidermal water loss measurements can provide an indication of the structural integrity of the skin barrier (Kalia, *et al*. 1996) by measuring the water vapour-pressure gradient of the air adjacent to the skin surface (Nilsson. 1977). A correlation between increased TEWL and increased *in vivo* percutaneous absorption has been observed for both lipophilic and hydrophilic compounds for human (Oestmann, *et al*. 1993, Lotte, *et al*. 1987) and murine (Kanikkannan, *et al*. 2002) skin. Increases in TEWL following SM vapour exposure have been observed in intact porcine skin *in vivo* (Chilcott. 2000). As the lipids of the SC are thought to provide the primary barrier to loss of water (Golden, *et al*. 1987), it is reasonable to postulate that removal or damage to the SC may increase TEWL.

Laser Doppler imaging (LDI) is based on the principle that the movement of the reflecting body (i.e. erythrocytes within the superficial cutaneous vasculature) will cause a frequency shift (Doppler shift) in the reflected light detected (Forrester, *et al*. 2002, Droog, *et al*. 2001). By scanning the laser beam over the tissue, an image of cutaneous blood flow can be produced. Laser Doppler imaging is an established non-invasive technique for the assessment of burn severity, wound healing and inflammation (Graham, *et al*. 2002, Droog, *et al*. 2001) and has shown good correlation with histopathological findings (Brown, *et al*. 1998, Braue, *et al*. 2007).

Infrared thermography (IRT) allows the visualisation of changes in anatomical heat distribution in response to various stimuli (Ring. 1990). Factors which can affect skin surface temperature (other than environmental factors) include: inflammation and changes in dermal blood flow (Lahiri, *et al*. 2012, Cole, *et al*. 1990, Bharara, *et al*. 2006, Ruminski, *et al*. 2007). Sulphur mustard has previously been shown to affect

dermal perfusion (Brown, *et al*. 1998) and IRT has been used to assess the efficacy of debridement for as a treatment for SM-induced skin lesions (Dalton, *et al.* 2006).

Skin reflectance spectrophotometry (SRS) allows a quantitative assessment of skin colour changes including; erythema (Lahti, *et al*. 1993) and blanching (Waring, *et al*. 1993, Pershing, *et al*. 1992). The reflectance spectrophotometer measurements were recorded in the Commission International d'Eclairage L*a*b* (CIELAB) colour space values (Weatherall and Coombs. 1992) where changes in; lightness (L*), chroma (a*; redness) and hue (b*; blueness) can be attributed to eschar formation, erythema/blanching and cyanosis, respectively. Skin reflectance spectrophotometry has been previously described for the quantification of skin colour changes following SM exposure (Chilcott. 2000).

COAGULATION AND HAEMOSTASIS

Coagulation is a tightly controlled biochemical system, which must balance the rapid production of a fibrin clot against the maintenance of blood flow through the vasculature. Chronic effects of SM on coagulation include thrombocytopenia and anaemia (Balali-Mood, *et al*. 2005, Mahmoudi, *et al*. 2005, Krumbhaar and Krumbhaar. 1919). Very little is known about the acute effects of SM on coagulation but, given its ability to alkylate biological macromolecules, there is potential for SM to alkylate components of the coagulation system.

The cell-based model of coagulation proposes three overlapping coagulation phases; initiation, amplification and propagation (Hoffman. 2003). The activation of the initial clotting factors occurs on tissue factor (TF) bearing cells (Figure 1.5).

This multi-domain cell surface receptor acts as both a binding site and cofactor for factor VII and is constitutively expressed on a wide range of extravascular cells (Hoffman. 2003). It is only when injury is sustained to the vascular wall that the TF expressing cells are exposed to circulating blood and are able to bind factor VII_a, which circulates in small amounts in normal plasma. During the initiation phase, the bound factor VII_a is able to activate factor VII, which binds to TF to form the factor VII_a-TF complex. This complex is then able to activate factor IX and X in the presence of Ca^{2+} which activate prothrombin (II) to thrombin (Monroe*, et al*. 2002).

During the amplification phase, blood components (including platelets and von Willebrand factor; vWF) come into contact with TF-bearing cells (Figure 1.5). The small amounts of activated thrombin activate platelets and clotting factors including V (released from activated platelets), VIII (cleavage product of vWF) and XI. The activated platelets adhere to the injury site and aggregate to form an initial plug. Pro-inflammatory cytokines such as IL-1β, IL-6 and TNF-α have been shown to demonstrate pro-coagulatory activity and increase the rate of clotting and platelet numbers (Collombet*, et al*. 2005, Watts*, et al*. 1996). Sulphur mustard has been shown to increase expression of these cytokines *in vivo* (Arroyo*, et al*. 2004a, Yaraee*, et al*. 2009) and so, SM exposure could potentially increase the rate of coagulation.

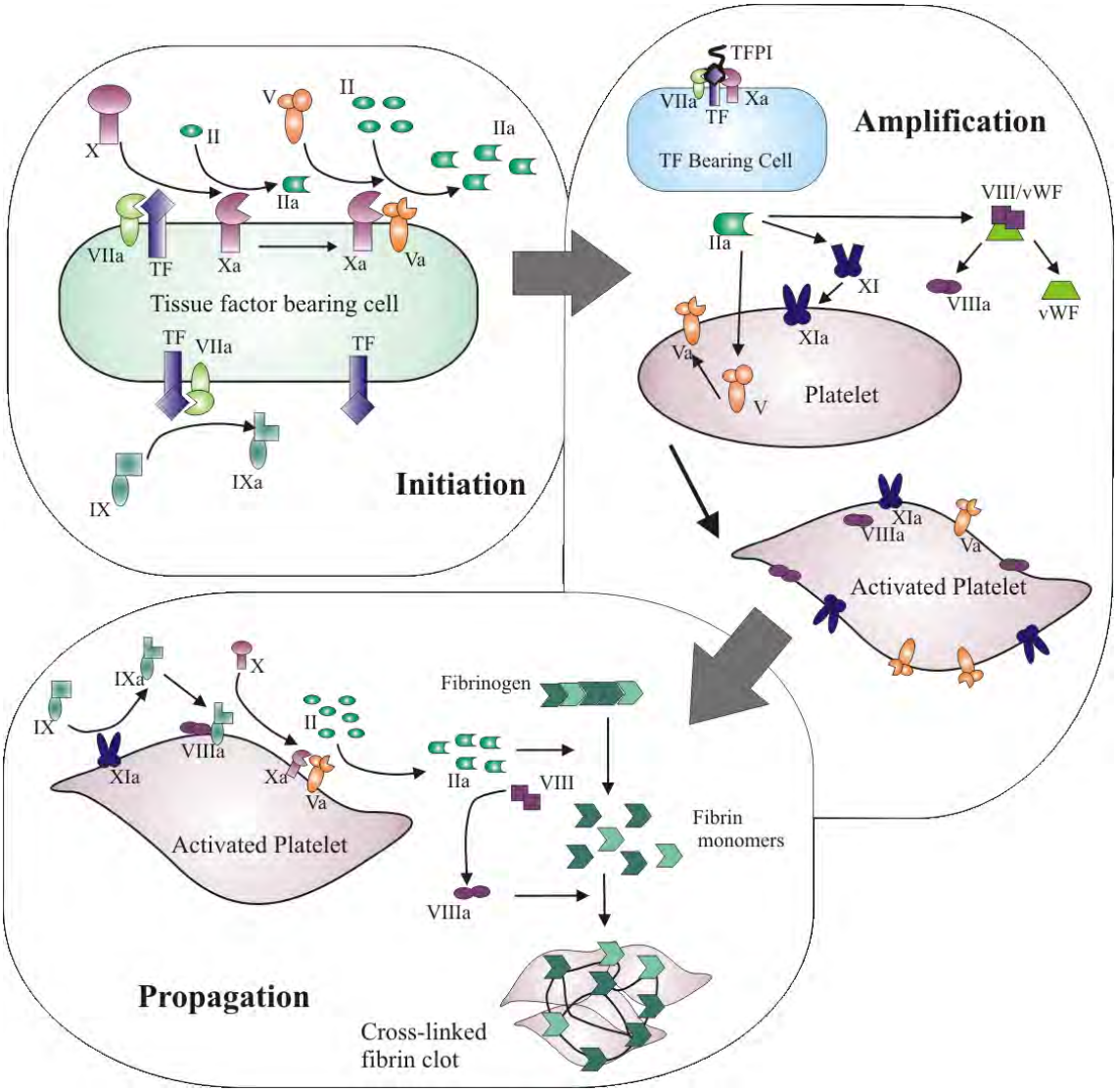

Figure 1.5: The cell-based model of coagulation showing the three overlapping phases; initiation, amplification and propagation.

Activation of clotting factors on tissue factor (TF) bearing cells produces nominal levels of activated thrombin (II). During the amplification phase, blood components (including platelets and von Willebrand factor; vWF) come into contact with TF-bearing cells. Thrombin activates platelets and clotting factors which results in large amount of thrombin being activated (propagation phase). Thrombin cleaves fibrinogen to produce fibrin monomers. These form a fibril network incorporating the platelet plug and are covalently linked by factor XIIIa to produce a stable fibrin clot. The small a denotes activated form (adapted from Hoffman, 2003).

During the propagation phase, factor X_a is able to complex with factor V_a, Ca^{2+} and platelet factor 3 to form the prothrombinase complex (Figure 1.5). This complex converts prothrombin to its active form, thrombin, which stimulates a number of positive and negative feedback loops in addition to catalysing the cleavage of fibrinogen to fibrin peptides A and B and fibrinogen monomers (Tuthill*, et al*. 2001). The fibrin monomers arrange into fibrils and eventually form a network of fibres. Thrombin uses Ca^{2+} as a co-factor to activate factor XIII which transaminates the non-covalent bonds between the monomer fibres (Nielsen*, et al*. 2004). This covalently cross-links the fibrin monomer fibrils to form a stable fibrin clot that is resistant to proteolytic degradation by plasmin (Sierra. 1993). Sulphur mustard alkylates a number of amino acid residues including; histidine, glutamic acid, aspartic acid and valine (Black*, et al*. 1997, Noort*, et al*. 1996). Histidine and aspartic acid are critical amino acids in the active site of thrombin (Ye*, et al*. 1991) and thus alkylation could result in conformational or functional changes to thrombin leading to a reduction in clotting.

Thrombin regulates its own production by activating physiological pathways to localise its formation at the injury site and prevent the clot from extending to uninjured endothelial surfaces (Mahdy and Webster. 2004, Roberts*, et al*. 2004). Regulatory pathways and the fibrinolytic pathway are crucial for overall haemostasis within the body and to prevent thrombosis. The thrombin regulatory pathways inhibit thrombin activity (antithrombin III) as well as clotting factors upstream of thrombin to prevent further production of thrombin (protein C pathway, antithrombin III and tissue factor pathway inhibitor).

The function of the fibrinolytic pathway is the dissolution of cross-linked fibrin clots (Castellino. 1981). Conversion of the zymogen (plasminogen) to activated plasmin

is achieved by specific plasminogen activators (Castellino. 1984). Once activated, plasmin degrades clots via cleaving fibrin, disrupting platelet function, collagenases activation and inactivation of factors V_a and $VIII_a$. Plasminogen activators include tissue type plasminogen activator (t-PA) and urinary type plasminogen activator or urokinase (uPA) (Francis and Marder. 1987). Both t-PA and uPA are inhibited by type 1 plasminogen activator inhibitor (PAI-1) and plasmin is also directly inhibited by α2-antiplasmin (Kunamneni*, et al*. 2008). Sulphur mustard has been shown to increase uPA activity *in vitro* by 20 – fold within 24 h of exposure (Detheux*, et al*. 1997) which could result in increased fibrinolysis. Thus overall, there are three potential mechanisms through which SM may exert an anti-coagulatory effect.

In vitro measurement of coagulation – Thrombelastography

Thrombelastography (TEG) measures the viscoelastic properties of whole blood during clotting and was first described by Hartert (Hartert. 1948). Unlike classical coagulation tests (prothrombin time, partial thromboplastin time and activated prothrombin time), TEG measures the clotting ability of a whole blood sample (Mallett and Cox. 1992). Thrombelastography measures the physical properties of clot formation using an oscillating cup and pin. A plastic cup or cuvette containing the blood sample is maintained at 37˚C and is rotated in each direction through 4˚45’ at a frequency of 0.1 Hz (Figure 1.6A) (Khurana*, et al*. 1997). The plastic pin is coaxially suspended into the cup and becomes coupled to the motion of the cup once the fibrin clot forms. The pin is attached to a torsion wire which acts as torque transducer. The resistance of the clot to deformation is plotted as a function of time and provides a quantitative assessment of the rigidity of the clot (Figure 1.6B) (Khurana*, et al*. 1997).

Six clotting parameters are measured using TEG: R Time, K Time, α angle maximum amplitude, shear elastic modulus strength (SEMS) and coagulation index (CI) (Figure 1.6B). These parameters provide details of the clotting dynamics and clot strength and relate to the phases of coagulation in the cell-based model (Figure 1.5) (Hoffman. 2003). R Time is the latent interval from the start of the recording to the formation of a three-dimensional fibrin gel network with a defined rigidity of 2 mm.

The R time is a measure of the enzymatic function (clotting factors) and corresponds to the initiation phase (Johansson*, et al*. 2009). K Time is the interval from the R time to a fixed amplitude point (20 mm). This reflects the amplification phase of coagulation pathway (Kawasaki*, et al*. 2004). The α-angle is the angle of the slope of the TEG trace from R time to K time. The alpha angle is indicative of the thrombin "burst" stage of the amplification phase (Johansson*, et al*. 2008). K time combined with α angle reflects the overall clotting kinetics. The maximum amplitude is the greatest amplitude achieved on the TEG trace and is representative of total clot strength (Johansson*, et al*. 2009). Shear elastic modulus strength (SEMS) is a function of the maximum amplitude and is a measure of the clot elasticity to shearing forces (Khurana*, et al*. 1997). Two components contribute to the overall strength of the clot, the fibrin clot matrix and platelet aggregation. The coagulation index (CI) is derived from a linear equation and assigning a coagulation score based on R Time, K Time, α-angle and maximum amplitude.

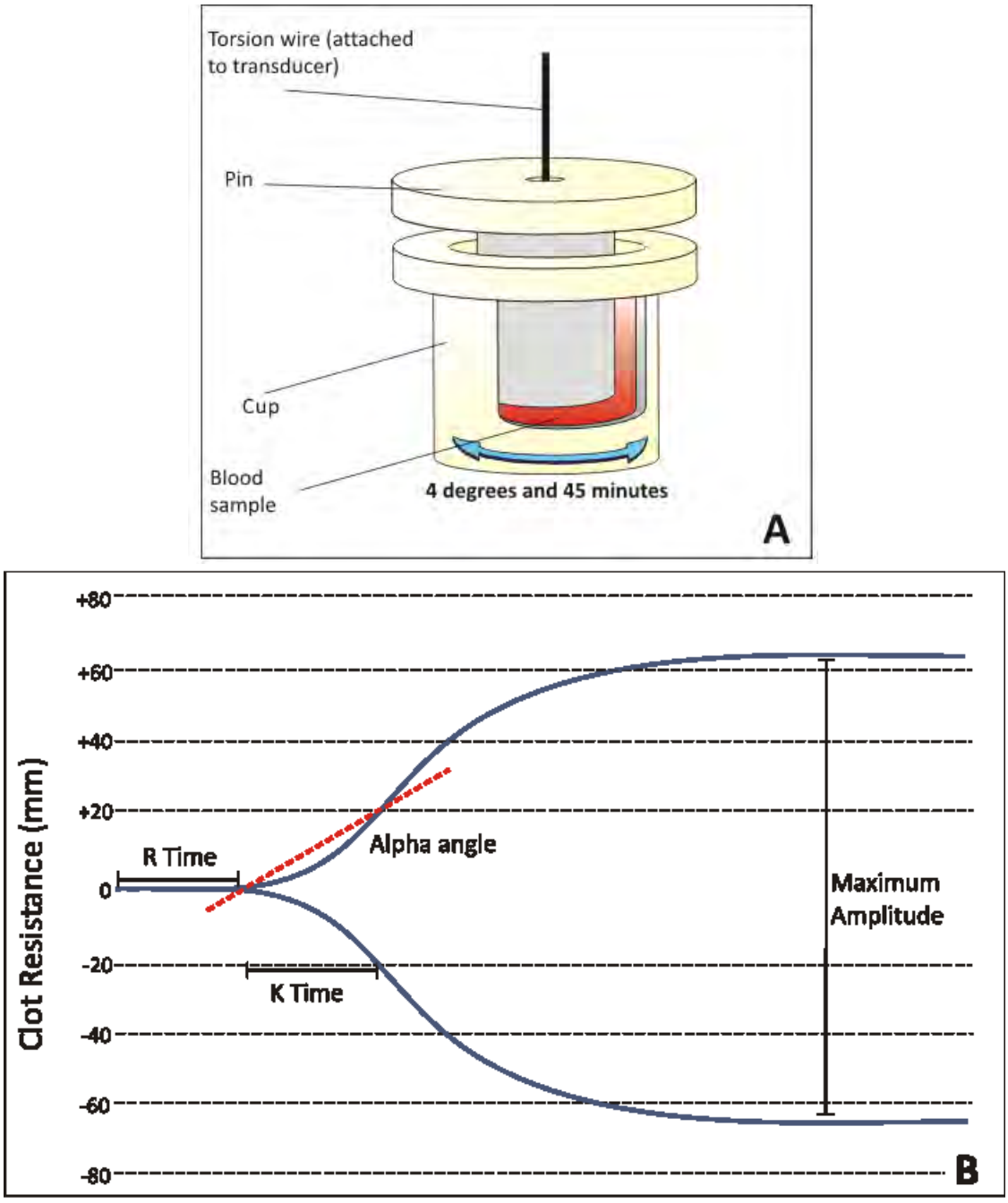

Figure 1.6: Schematic diagram of Haemoscope Thrombelastograph® pin and cup setup (A) and example TEG trace with the four key parameters labelled (R Time, K time, α-angle and maximum amplitude) (B).

Haemostatic products

The haemostatic products tested in this Thesis are intended for application to wounds in order to arrest haemorrhage and have demonstrated efficacy *in vivo* (Kheirabadi*, et al*. 2009, Ahuja*, et al*. 2006, Alam*, et al*. 2004, Alam*, et al*. 2003). A variety of formulations were tested including dressings, granular and liquid products.

Three products (WoundStat™, QuikClot Advanced Clotting Sponge plus®; QuikClot ACS+® and ProQR®) are categorised as inorganic particles or granules. Overall, these products are thought to arrest bleeding via adsorption of water from plasma into the lattice structure of the product, resulting in localisation and subsequent activation of clotting factors (Kheirabadi*, et al*. 2009).

Additionally, QuikClot ACS+® (a non mineral zeolite bead) is also thought to facilitate the coagulation phenomenon known as the "glass effect", whereby its negative surface charge promotes coagulation via the activation of factor XII (and subsequent activation of factor IX; Figure 1.5) in the same manner as the negative surface charge of glass (Cochrane*, et al*. 1973). WoundStat™ is an aluminium silicate member of the smectite clay family (Carraway*, et al*. 2008). The haemostatic activity of WoundStat™ is largely attributed to the tetrahedral sheet-like organisation of the clay which can absorb large amounts of water resulting in localised concentration of clotting factors (Bowman*, et al*. 2011). Additionally, aluminium silicate clays have zones of negative and positive charges which are able to activate the coagulation process via factors XII and XI (Figure 1.5). Similarly to QuikClot ACS+® it has been proposed that negative surface charges on the promote coagulation via the activation of factor XII. ProQR® is a granular non-zeolite mineral haemostat comprised of a mixture of a hydrophilic polymer and potassium iron oxyacid salt (Ho and Hruza. 2007). In addition to plasma

adsorption the potassium salt in combination with hydrophilic polymer, provides a scaffold for red blood cells and platelets to bind, resulting in the formation of an artificial eschar (Ho and Hruza. 2007).

Two chitosan-based products (HemCon® and Celox™) achieve haemorrhage control by forming a seal at the site of vessel injury via mucoadhesive properties (Brown, *et al*. 2007, Pusateri, *et al*. 2003a, Pusateri, *et al*. 2003b). Electrostatic interactions with blood cells (resulting in erythrocyte and platelet aggregation) have also been suggested as contributory mechanisms (Brown, *et al*. 2007, Kozen, *et al*. 2008, Kozen, *et al*. 2007).

Finally, two liquid haemostats (FastAct® and VitaGel™) were also chosen for testing. The intention of this Thesis was to combine these liquid products with a novel decontaminant (described in Chapter 2) to produce a reactive decontaminant/haemostat mixture. Both products contain activated clotting factors such as thrombin and factors VII, IX and X, which can trigger the amplification and propagation phases of coagulation (Figure 1.5) (Alam, *et al*. 2004, Prior, *et al*. 2000).

SULPHUR MUSTARD

Sulphur mustard (bis (2-chloroethyl) sulphide) is a vesicant or blistering agent, which is able to alkylate a range of biological macromolecules (Figure 1.7) (Papirmeister, *et al*. 1985). The relatively high percutaneous LD_{50} (100 mg kg^{-1}; rabbit) for SM means that it is generally considered a non-lethal weapon but instead causes considerable incapacitation (Graham, *et al*. 2005). Sulphur mustard is poorly soluble in water (0.07% at 10°C), and has a relatively low volatility and high freezing point (14°C) and so is

able to persist in the environment for long periods especially in damp, cooler climates (Balali-Mood and Hefazi. 2005).

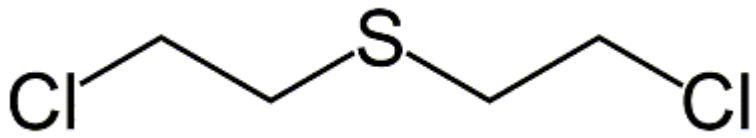

Figure 1.7: Chemical structure of sulphur mustard.

Characteristics of sulphur mustard-induced injuries

The three main target organs for SM are the skin, eyes and lungs. High exposures to SM can also results in systemic toxicity, characterised by fever, gastrointestinal tract effects (diarrhoea), and bone marrow suppression (leukocytopenia and thrombocytopenia) (Kehe and Szinicz. 2005, Dacre and Goldman. 1996). The focus of this Thesis was on the cutaneous route of exposure and subsequent pathology and so further details on respiratory or ocular toxicity have not been included.

Due to its lipophilic nature (Log P 1.37), SM can easily penetrate through epithelial tissue and thus skin plays a very important role as a route of entry for SM (Renshaw. 1946). The typical skin pathology induced by SM can be divided into three overlapping phases; initial erythema followed by blistering and finally ulceration (Kehe and Szinicz. 2005). There is a well documented latent period between the time of exposure and the onset of clinical symptoms, with an inverse correlation between the exposure dose and the latency period (Papirmeister *et al.* 1991). Following a latency period of 4 – 8 h erythema is observed at threshold doses (10 – 20 μg cm^{-2}) whilst blistering is seen at higher doses (40 – 100 μg cm^{-2}) (Papirmeister *et al.* 1991).

Toxicokinetics

There is good correlation between SM penetration rates using human skin *in vitro* and human volunteers, with rates of 71 – 294 μg cm^{-2} hr^{-1} and 60 – 240 μg cm^{-2} hr^{-1} for *in vitro* and human volunteer studies, respectively (Chilcott*, et al*. 2000, Kehe and Szinicz. 2005, Nagy*, et al*. 1946). The amount of SM needed to produce blisters has been found to be 20 μg cm^{-2} of liquid SM (Papirmeister*, et al*. 1984). However, only 4 μg cm^{-2} of saturated SM vapour is needed to produce the same result (Nagy*, et al*. 1946). This discrepancy is due to the fact that of the applied liquid dose, 80% will evaporate with 20% of the dose penetrating (Renshaw 1946). Therefore, occluded conditions will increase the skin penetration and severity of SM–induced skin lesion (Chilcott*, et al*. 2000). There is some disagreement in the literature over what percentage of SM remains in the skin, how much is absorbed systemically and whether or not there is a reservoir within the skin of unreacted SM (Hattersley*, et al*. 2008, Renshaw. 1946, Chilcott*, et al*. 2001). The reported amount retained within the skin varies from 10 – 20% up to 60% of the applied dose, with variability in the amount absorbed systemically also seen (ranging from 40% to 80 – 90% of the applied dose) (Hattersley*, et al*. 2008, Renshaw. 1946). Once SM has entered the systemic circulation, it is quickly cleared and mostly excreted in the urine, with 60% of the absorbed dose found to be excreted within 24 hours. Metabolites of SM found in the urine result from either hydrolysis or direct oxidation at the sulphur atom or from reactions with glutathione (Black*, et al*. 1992, Black and Read. 1995). Two separate studies using rats have found that conjugation with glutathione is more important than hydrolysis in terms of SM breakdown products (Davison*, et al*. 1961, Roberts and Warwick. 1963). Whole body autoradiography studies with mice using ^{35}S–SM found that there was increased

radioactivity localised to the kidney, liver, intestines and nasal regions following both intravenous and percutaneous administration (Clemedson, *et al*. 1963).

Gross skin pathology

Sulphur mustard skin lesion pathology is characterised by the appearance of erythema followed by the formation of small vesicles which coalesce to form gross blisters or large bullae (Papirmeister, *et al*. 1984). The blisters, which initially appear as small vesicles, display positive Nikolsky signs and occur within the area of erythema approximately 18 h post – exposure (Papirmeister, *et al*. 1984). Blistering is a result of separation of the epidermal–dermal layer with the upper portion of the lamina lucida (Kehe, *et al*. 2009, Sayer, *et al*. 2010). Sulphur mustard–induced micro–blisters coalesce to form large blisters, which are thin-walled and filled with a clear yellow-amber coloured fluid which does not contain active SM (Kehe, *et al*. 2009). Macroblistering, resulting from the coalescence of micro-blisters, is almost exclusive to humans (Maynard. 2007). At 48 hours post-exposure, blistering becomes more marked and large blisters usually break leading to erosions, full thickness skin loss and ulceration (Sidell, *et al*. 1997). Necrosis may occur at these sites followed by formation of an eschar at 72 hours post exposure (Maynard. 2007). The eschar usually begins to slough by 4 – 6 days leaving a scar which may be characterised by hypo- or hyper-pigmentation (Balali-Mood and Hefazi. 2005). The severity of SM-induced injury is also dependent on anatomical location with skin at warm, moist body areas, including: the axilla and scrotum, being more susceptible to SM injuries (Sidell, *et al*. 1997).

Microscopic effects

Following SM exposure there is both marked keratinocyte cell death as well as terminal differentiation of keratinocytes within the basal layer of the skin, with the build up of necrotic and apoptotic cells and signs of a substantial inflammatory response (Sayer*, et al*. 2010, Smith. 1999, Simbulan-Rosenthal*, et al*. 2006). Histopathology has revealed that SM-exposed skin shows vasodilation and neutrophil infiltration, indicative of vasoactive and chemo attractant mediator production within the exposed area (Brown and Rice. 1997). Vasodilation would present clinically as erythema (Smith*, et al*. 1997). Basal cells of the epidermis appear to be the most sensitive to SM toxicity, possibly as these cells are actively dividing and so are more susceptible to the alkylating properties of SM (Papirmeister *et al.* 1991). SM is able to alkylate a variety of cellular components, including DNA and proteins (Papirmeister*, et al*. 1985). The primary site of DNA alkylation is the N7 position of deoxyguanosine residues (Wheeler. 1962). The main targets for SM alkylation of proteins include carboxyl, sulphydryl and α-amino groups as well as the imidazole ring of histidine (Balali-Mood and Hefazi. 2005).

Proposed mechanisms of sulphur mustard toxicity

Although SM was first used over 90 years ago and despite many decades of research, there is currently no conclusive mechanism of action for SM. However, most recently proposed mechanisms focus on the ability of SM to alkylate cellular components, including DNA and proteins and induced cellular oxidative stress. There is also no defined mechanism to explain why SM causes epidermal-dermal separation or preferentially targets the basal cells of the epidermis. Similarities between SM-induced

blisters and clinical blistering diseases such as epidermolysis bullosa have been observed (Monteiro-Riviere and Inman. 2000, Monteiro-Riviere, *et al*. 1999). Protease involvement in vesication has been proposed following the observation that a transmembrane protein (BP180) was present on both the roof and the floor of a SM blister (Greenberg, *et al*. 2006). The most upregulated matrix metalloprotease (MMP) in the skin following SM exposure *in vivo* has been identified as MMP-9 (Ruff and Dillman III. 2007, Shakarjian, *et al*. 2006, Vallet, *et al*. 2012, Dachir, *et al*. 2010). However, SM-induced vesication is unlikely to be due to MMP involvement alone.

Sulphur mustard selectively targets the basal cells of the epidermis and induces cell death in a dose dependent manner (Sun, *et al*. 1999, Dabrowska, *et al*. 1996, Kehe, *et al*. 2000). At higher concentrations (≥500 μM endothelial cells, 1000 μM HeLa cells), cell death is by necrosis, whilst at lower concentrations (≤200 μM endothelial cells, 100 μM HeLa cells) cell death is due to apoptosis (Sun, *et al*. 1999, Dabrowska, *et al*. 1996). This concentration-dependent variability in mechanism is particularly important for dermal exposure to liquid SM due to the effects of surface spreading (Szinicz, *et al*. 2007). Work by Chilcott *et al*. (2000) observed rapid spreading of radiolabelled-SM on skin surface following application of a 20 μL droplet, even though the droplet bead was still visible. Therefore, there will be a higher concentration of SM at the contact point, subsequently decreasing as it spreads (Chilcott, *et al*. 2000). This may present a considerable challenge when trying to identify targets for therapeutics as there is likely to be different modes of cell death occurring.

The aim of this section is to give an outline on how SM specifically induces apoptosis and does not aim to give an in-depth account of apoptosis. Both apoptosis and necrosis are defined and well orchestrated processes (Rosenthal, *et al*. 1998, Rosenthal,

et al. 2001, Festjens*, et al*. 2006). However, intracellular levels of adenosine triphosphate (ATP) influence the mode of cell death because the process of apoptotic cell death requires sufficient amounts of ATP to allow full completion whilst necrosis does not (Eguchi*, et al*. 1997). Due to the delay between SM exposure and appearance of visible cutaneous injury it has been suggested that apoptosis predominates as the mode of cell death (Kehe*, et al*. 2009).

Key processes involved in apoptosis which have been shown to be influenced by SM are summarised in Figure 1.8. Sulphur mustard has been shown to initiate both the intrinsic and extrinsic apoptotic pathways culminating in activation of effector caspase-3 and apoptotic cell death (Rosenthal*, et al*. 1998, Ray*, et al*. 2005, Steinritz*, et al*. 2007, Kehe*, et al*. 2008). The activated Fas receptors cluster to form Fas-associated death domain (FADD) upon activation. An initiator procaspase (such as caspase-8) is recruited to form a death inducing signalling complex (DISC).

Expression of the pro-apoptotic ligands Fas and tumour necrosis factor alpha (TNF-α) and the Fas receptor, which can form a death inducing signalling complex with caspase-8, have been shown to be up-regulated in keratinocytes by SM (Arroyo*, et al*. 2004a, Rosenthal*, et al*. 2003). However, whilst cell expressing negative Fas-associated death domain (activated Fas receptors which have clustered together) show reduced apoptosis in response to SM exposure it is not obliterated, suggesting the involvement of additional pathways (Arroyo*, et al*. 2004a). Sulphur mustard has also been shown to shift the balance between pro and anti-apoptotic members of the Bcl-2 family in favour of apoptosis. This pro-apoptosis shift can result in the opening of the mitochondrial outer membrane pore (MOMP). Sulphur mustard has been found to induce MOMP,

cytochrome c release and caspase-9 activation in bronchial cells (Sourdeval, *et al*. 2006).

Sulphur mustard has been shown to promote the dephosphorylation of Bad (a Bcl-2 family member), promoting apoptotic death via the calmodulin pathway (Shakarjian, *et al*. 2010). Basal cells exposed to SM exhibit morphological characteristics of apoptosis including: membrane blebbing, perinuclear budding and pyknosis (Petrali, *et al*. 1991, Petrali, *et al*. 1994).

DNA Damage

Sulphur mustard is able to react and alkylate many cellular components including DNA, forming mono and bifunctional adducts (Wheeler. 1962). Each 2-chloroethyl side chain of the SM molecule is able to undergo first order (SN1) intramolecular cyclisation with the release of the chloride ion. The ethylene sulfonium cation intermediate forms the highly reactive carbonium ion which reacts with nucleophiles such as DNA, RNA and proteins (Figure 1.9) (Papirmeister, *et al*. 1985). Adenine and guanine residues are more favourable for adduct formation, with N7 position of guanine nucleotides being the most common accounting for an approximately 61% of total alkylations (Kehe and Szinicz. 2005). Inter or intrastrand cross links resulting from bifunctional adducts account for nearly 17% of all SM alkylations (Brookes and Lawley. 1961, Brookes and Lawley. 1960, Lawley and Brookes. 1968). However, the DNA lesion postulated to be most critical for cell damage is O6-(2-ethylthioethyl) guanine, despite the low frequency of occurrence (~0.1% of all DNA lesions), due to a lack of repair mechanism in humans (Ludlum, *et al*. 1984, Ludlum, *et al*. 1986).

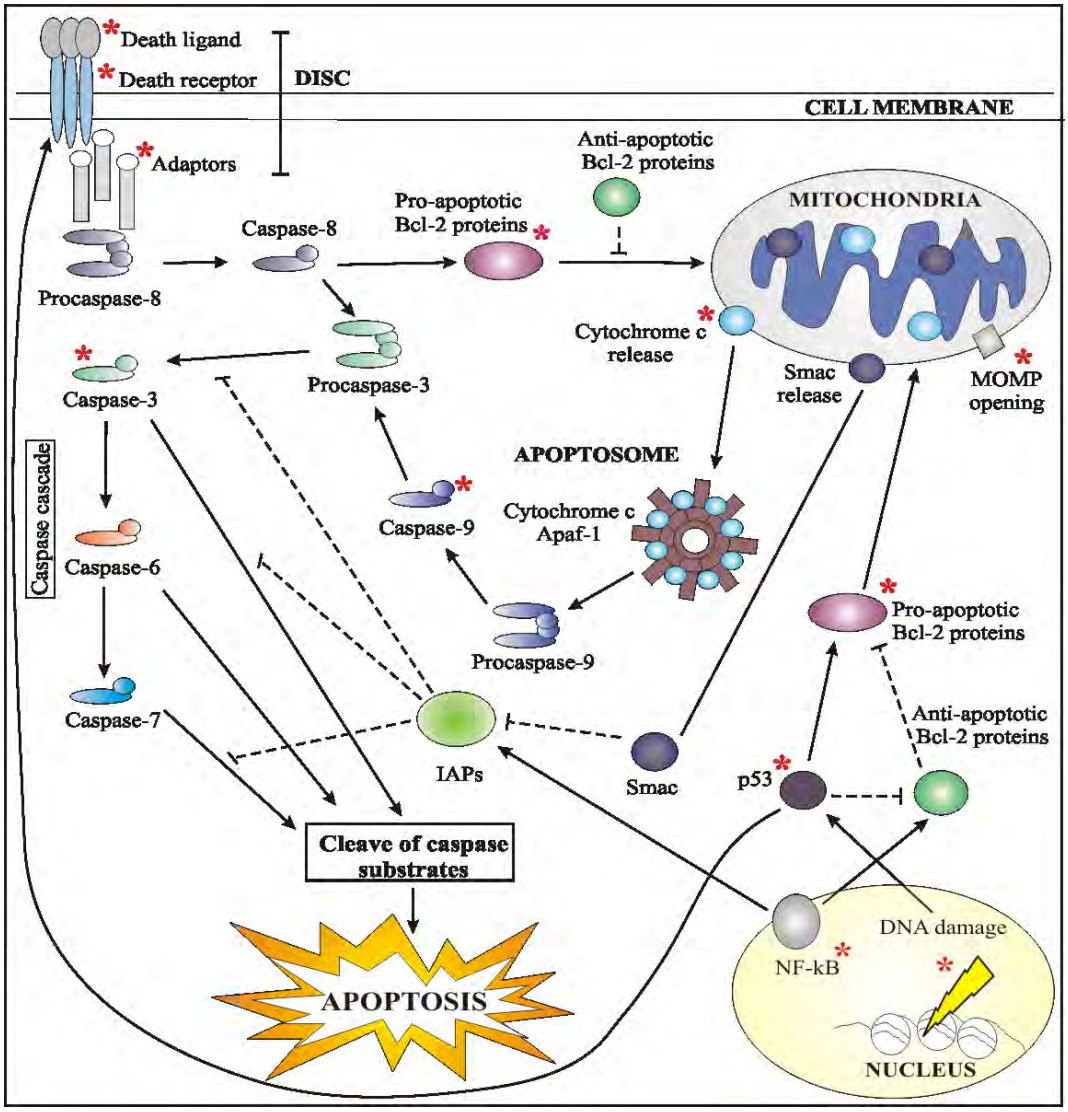

Figure 1.8: Schematic of major apoptotic pathways affected by SM.

Sulphur mustard triggers apoptosis directly by destabilising p53 and indirectly via DNA damage, activating pro-apoptotic members of the Bcl-2 family, resulting in increased expression of death receptors and ligands. Death receptors activate adaptor proteins e.g. procaspase-8 to form a death inducing signalling complex (DISC). The caspase cascade is activated via caspase-3. Mitochondrial outer membrane pore (MOMP) opening in response to SM results in Smac protein and cytochrome c release. Cytochrome c activates caspase-9 via the apoptosome which subsequently activates the caspase cascade via caspase-3. Smac proteins inhibit inhibitors of apoptotic proteins (IAPs) activity. Nuclear factor κB (NF-κB) promotes IAP and anti-apoptotic Bcl-2 protein activity. Red asterisks indicate proteins are known to be effected by SM exposure.

Double DNA strand breaks results in two outcomes that contribute to cell death. Firstly, strand breaks arrest the cell cycle at either G1 or G2 stage checkpoints in a SM dose-dependent manner (Rosenthal, *et al*. 1998, Ismail, *et al*. 2005). Secondly, DNA strand breaks can activate protein kinases (ataxia-teleangiectasa mutated protein and ataxia-teleangiectasa and Rad3-related kinase) which are able to phosphorylate pro-apoptotic downstream targets including; p53, Chk 1 and Chk2 (Jowsey, *et al*. 2012, Jowsey, *et al*. 2009, Banin, *et al*. 1998, Enders. 2008). Deoxyribose nucleic acid repair may prompt terminal differentiation or programmed cell death via apoptosis (Kehe, *et al*. 2009, Rosenthal, *et al*. 1998).

The DNA repair process triggered in response to SM-induced damage may also contribute to cell death. Several groups have proposed a role for poly (adenosine diphosphate) polymerase (PARP) in contributing to SM-induced cell death and subsequent blister formation (Papirmeister *et al.* 1991, Kehe, *et al*. 2008, Debiak, *et al*. 2009, Bhat, *et al*. 2001). The isoform of particular interest is PARP-1 which is activated by DNA strand breaks such as those seen with SM exposure (Bhat, *et al*. 2001). Studies by Rosenthal *et al.* (1998) observed significant increases in activity within one hour of SM exposure in human keratinocytes. Overactivation of PARP, due to increased genomic stress, can result necrotic cell death due to depletion of intracellular nicotinamide adenine dinucleotide (NAD^+) and ATP in a SM concentration-dependent manner (Kan, *et al*. 2003). However, the cytotoxic action of SM cannot be solely attributed to PARP as the inhibition of PARP only provides limited cytoprotection in the first few hours following SM exposure (Martens and Smith. 2008). There also appears to be cell-specific response to SM as PARP over-activation determines the mode of cell death in fibroblasts but not keratinocytes (Rosenthal, *et al*. 2001).

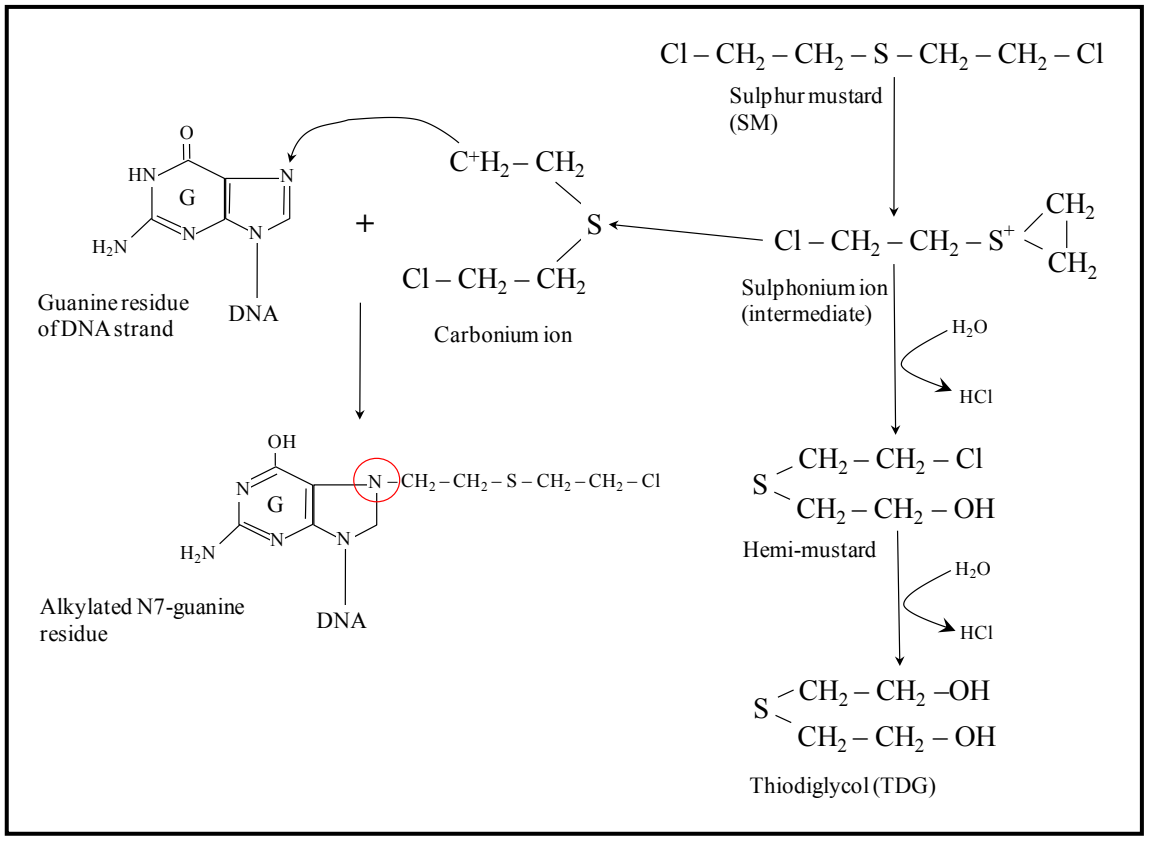

Figure 1.9: Sulphur mustard breakdown products and DNA adduct formation.

During SM hydrolysis from SM to thiodiglycol (TDG), a sulphonium ion intermediate is formed. This can generate a highly reactive carbonium ion which reacts with and alkylates DNA (or RNA) residues e.g. N7-guanine.

Ca^{2+} signalling and calmodulin

A number of studies have reported a SM-induced irreversible rise in intracellular levels of Ca^{2+} although the exact mechanism for this remains unclear (Hua*, et al*. 1993, Mol and Smith. 1996, Hamilton*, et al*. 1998, Sawyer and Hamilton. 2000). There is a reported cell type-dependent response in the lag time between SM exposure and intracellular Ca^{2+} response for fibroblasts (5 – 10 min) and primary keratinocytes (3 – 24 h) (Mol and Smith. 1996, Sawyer and Hamilton. 2000). Responses for secondary cultures of confluent human keratinocytes (≤ 2 min) are similar to fibroblast responses (Hamilton*, et al*. 1998). The physiological relevance of such observations is unclear as the reported rises in intracellular Ca^{2+} were only moderate (less than two fold) (Kehe*, et al*. 2009, Ruff and Dillman III. 2007) but would be sufficient to induce terminal differentiation, which is a form of Ca^{2+} dependent cell death in keratinocytes (Lippens*, et al*. 2005). Low Ca^{2+} concentrations allow for proliferation in the basal layers but as the Ca^{2+} concentration progressively increases in the upper epidermal layers, cornification is triggered by converting cells into corneocytes (Simbulan-Rosenthal*, et al*. 2006, Whitfield*, et al*. 1995). The markers of terminal differentiation include the suppression of fibronectin, induction of keratin 1 and 10 and cross linking of involucrin (Rosenthal*, et al*. 1998).

Sulphur mustard has also been shown to alter gene expression of the calcium binding proteins, calmodulin (CaM) and calcineurin (Simbulan-Rosenthal*, et al*. 2006). The Ca^{2+}-CaM-calcineurin pathway may have a role in SM-induced apoptosis, possibly via dephosphorylation of the pro-apoptotic Bcl-2 family member, Bad (Kehe*, et al*. 2009, Simbulan-Rosenthal*, et al*. 2006). Once activated Bad is able to interact with Bcl-2 and Bcl-xl and induce MOMP opening and subsequently induce apoptosis (Figure

1.8) (Simbulan-Rosenthal, *et al*. 2006). Sulphur mustard activated Ca^{2+}-CaM complexes can also directly regulate apoptosis. The CaM-Ca^{2+} complex is able to directly bind Fas receptor as well as activate caspases and endonucleases resulting in DNA cleavage and apoptotic DNA ladders (Kehe, *et al*. 2009, Simbulan-Rosenthal, *et al*. 2006, Ankarcrona, *et al*. 1996). Increased Ca^{2+} and calmodulin levels can also have downstream effects on other pathways including nitric oxide production and oxidative stress (Bloch, *et al*. 2007, Gao, *et al*. 2007).

Nitric oxide, reactive oxygen species and oxidative stress

Cell death resulting from SM exposure has also been linked to nitric oxide production and oxidative stress (Paromov, *et al*. 2008). Under normal physiological conditions, reactive oxygen species (ROS) are constantly produced within the cell and the free radicals are removed by the antioxidant defence system. Three key enzymes are involved in this pathway; superoxide dismutase (SOD), glutathione peroxidases (GPx) and catalase (CAT) (Sies. 1997, Sies. 1993). Superoxide dismutase converts free radical superoxide to hydrogen peroxide which is subsequently catalysed to water by GPx and CAT (Figure 1.10). Oxidative stress results as a consequence of the normal cellular defence system becoming overwhelmed (e.g. through glutathione depletion) and may contribute to SM induced cell death (Kumar, *et al*. 2001, Rappeneau, *et al*. 2000, Giuliani, *et al*. 1997, Gross, *et al*. 1993).

Expression of inducible nitric oxide synthase (iNOS) has been shown to increase following SM exposure (Gao, *et al*. 2008). Nitric oxide (NO) is a physiological messenger involved in blood vessel homeostasis (Champion, *et al*. 2003), immune and inflammatory response (Kanwar, *et al*. 2009) and wound healing (Luo and Chen. 2005).

Nitric oxide is also able to react with superoxide (O_2^-) to form peroxynitrite ($ONOO^-$) (Figure 1.10) which can subsequently form other reactive nitrogen species (RNS) (Squadrito and Pryor. 1998). Peroxynitrite and RNS are able to induce cytotoxicity in a similar fashion to ROS through oxidation and covalent modification of membrane lipids, proteins and DNA (Sawyer, *et al*. 1996, Korkmaz, *et al*. 2006). Both peroxynitrite and superoxide both trigger DNA single strand breaks which will subsequently increase PARP activation and so highlights how SM exposure can result in cumulative cytotoxic effects.

Inflammation

Sulphur mustard exposure results in increased expression of pro-inflammatory cytokines including; IL 1α/β, 6 and 8 and TNFα (Ruff and Dillman III. 2007, Arroyo, *et al*. 2001b, Smith, *et al*. 1998, Arroyo, *et al*. 2001a). Nuclear factor–κB (NF-κB) pathway and mitogen-activated protein kinases (MAPKs) have been shown to be involved in the regulation of genes for inflammatory cytokines following SM injury (Minsavage and Dillman III. 2007, Rebholz, *et al*. 2008).

Sulphur mustard activates NF-κB pathway resulting in translocation of NF-κB to the nucleus, where it can mediate cellular stress, apoptosis and inflammatory responses (Figure 1.8) (Minsavage and Dillman III. 2007, Karin and Ben-Neriah. 2000, Hayden and Ghosh. 2008, Karin and Greten. 2005). Sulphur mustard has also been shown to activate the p38 MAPK pathway which is involved in cell apoptosis and terminal differentiation through the phosphorylation of p38 in a dose dependent manner (Rebholz, *et al*. 2008). Inhibition of p38 has been found to reduce SM-induced inflammatory cytokine production (Dillman III, *et al*. 2004).

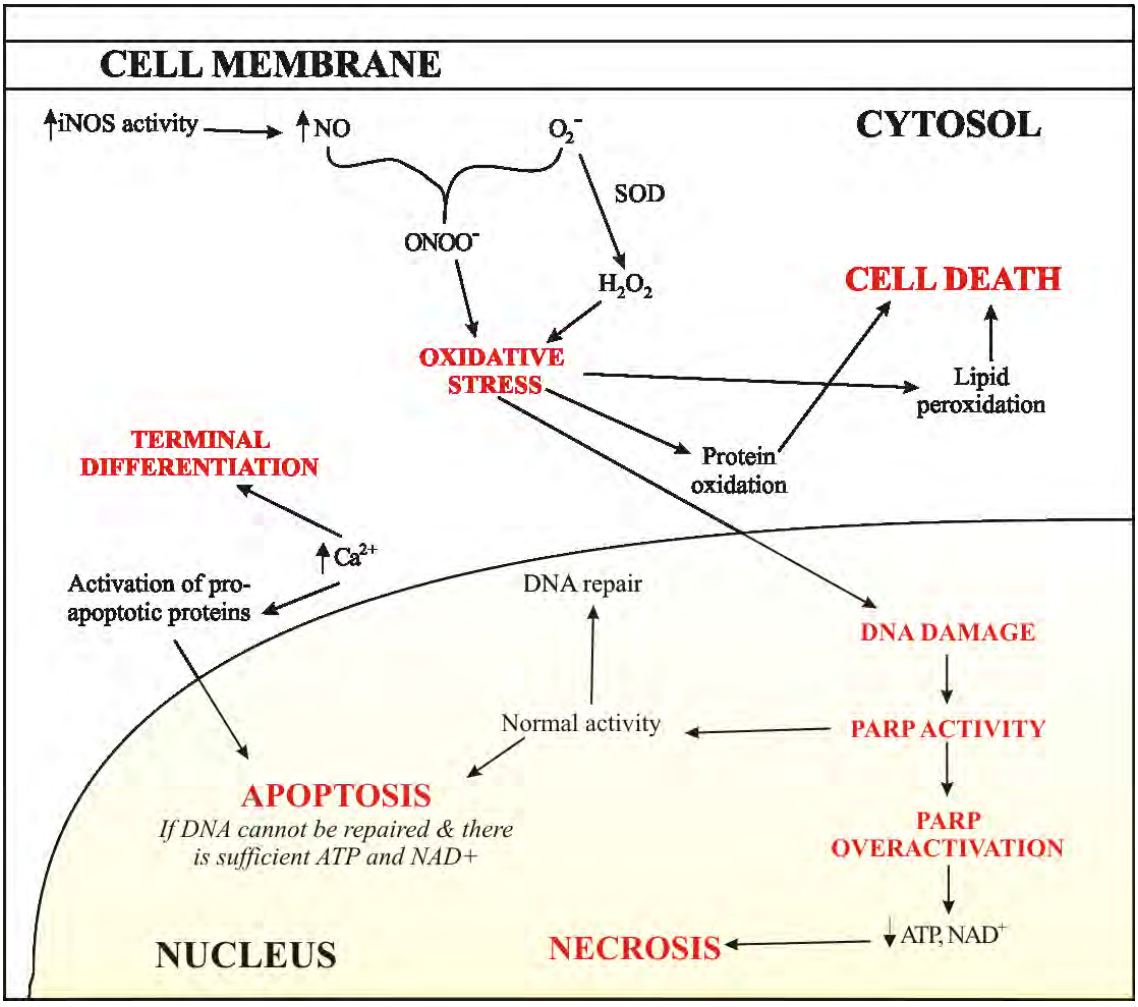

Figure 1.10: Summary of mechanisms for SM-induced cytotoxicity.

SM can induce oxidative stress resulting in DNA damage or cause DNA damage directly. Poly (ADP-ribose) polymerase (PARP) becomes activated. If the DNA damage cannot be repaired apoptosis results. If the damage is sufficiently severe, PARP becomes overactivated leading to ATP and NAD^+ depletion and necrotic cell death. SM has also been found to increase intracellular Ca^{2+}, which can activate pro-apoptotic members of the Bcl-2 family. SM has also been found to activate pro-apoptotic proteins and stabilise p53, resulting in cell death. SM also triggers increased production of nitric oxide (NO; possibly via iNOS) and superoxide (O_2^-) culminating in increased production of peroxynitrite. Excessive peroxynitrite, hydrogen peroxide and superoxide can overwhelm the normal antioxidant processes resulting in oxidative stress and subsequent lipid peroxidation, protein oxidation and DNA damage.

HYPOTHESIS AND AIMS

The majority of haemostats increase the rate of coagulation by passively adsorbing plasma which subsequently results in increased local concentration of clotting factors resulting in activation of the coagulation process (Figure 1.5). Passive adsorption is also the mechanism of action for in-service military decontaminants including fuller's earth (Taysse*, et al*. 2007, Taysse*, et al*. 2011). Therefore, haemostatic products appear to have the potential function as both decontaminants and clotting agents. This may help resolve the issue of how to simultaneously treat and decontaminate haemorrhaging wounds which are contaminated with toxic chemicals such as SM.

To evaluate the suitability of haemostats to function as decontaminants the following hypotheses were investigated:

- The efficacy of haemostats to increase the rate of coagulation *in vitro* is not affected by the presence of SM in the blood.
- The rate and extent of SM absorption is significantly increased *in vitro* and *in vivo* when applied via superficially damaged skin.
- Haemostats are effective in significantly reducing the rate and extent of SM absorption *in vitro* and *in vivo*.

Chapter 2

General Methods

GENERAL METHODS

Chemicals

Sulphur mustard (SM; bis (2-chloroethyl) sulphide) used for thrombelastography studies was purchased from the Defence Science and Technology Laboratory (Dstl) and was reported to be >98 % pure by NMR. Sulphur mustard for all other studies and its radiolabelled (^{14}C) analogue were custom synthesised by TNO Defense. The purity of the agents was determined to be 99.2% and >97% for SM (NMR analysis) and ^{14}C-SM (GC-MS and HPLC analysis), respectively. The ^{14}C-SM solution was diluted with unlabelled SM to give a working solution (nominal activities 0.635 mCi g^{-1}; static diffusion studies, 11 mCi g^{-1}; *in vivo* studies) which was stored for up to three months at 4°C. The storage and use of chemical warfare (CW) agents was in full compliance with the Chemical Weapons Convention (1993).

Supplier details are summarised in Table 2.1. All reagents were purchased from Sigma-Aldrich unless otherwise stated. All general consumables were purchased from Fisher Scientific UK Ltd.

Animals

Specific pathogen-free, out-bred domestic pigs (*Sus scrofa domestica;* Large White strain, female) were purchased from a reputable supplier (weight range 15 – 25 kg) and were individually housed in approved pens under a 12 h/12 h light/dark cycle.

Reagents, consumables or equipment	Supplier Name	Supplier Address
Microarray supplies	Agilent Technologies UK Ltd.	Wokingham, UK
RNA storage & isolation	Ambion, Applied Biosystems	Warrington, UK
AC resistance meter	AVO multimeter	Dover, UK
In vivo consumables	BD	Franklin Lakes, USA
Precellys®	Bertin Technologies	Montigny-le-Bretonneux, France
AquaFlux evaporimeter	Biox Systems	London, UK
Surgical consumables	Burtons Medical Equipment Ltd.	Marden, UK
Camera	Canon	Uxbridge, UK
SM (non-radiolabelled)	Defence Science and Technology Laboratory (Dstl)	Porton Down, UK
Custom pig sling	Ellegaard	Dalmose, Denmark
Dermatome	Eurosurgical Ltd.	Guildford, UK
Histology supplies	Fisher Scientific UK Ltd.	Loughborough, UK
Infrared camera	FLIR Systems	West Malling, UK
Pipettes	Gilson Scientific Ltd.	Luton, UK
Statistical analysis software	GraphPad Software	San Diego, USA
Surgical equipment	Harvard Apparatus Ltd.	Edenbridge, UK
Homogeniser	IKA®-Werke GmbH & Co.	Staufen, Germany
Reflectance spectrometer	Konica Minolta	Warrington, UK
Thrombelastography supplies	MediCell Ltd.	London, UK
Laser Doppler line scanner	Moor Instruments	Axminster, UK
Liquid scintillation counter supplies and tissue solubliser	PerkinElmer	Beaconsfield, UK
Static diffusion cells	PermeGear	Chicago, USA
RNA isolation kit	QIAGEN	Crawley, UK
Hyponoval® sedative	Roche Products Ltd.	Welwyn Garden City, UK
Histology supplier	Sakura Finetek UK Ltd	Thatcham, UK
Chemicals	Sigma-Aldrich	Gillingham, UK
Scintillation vials	Simport Scientific	Beloeil, Canada
Anti-coagulant blood tubes	Teklab Ltd	Sacriston, UK
Nanodrop spectrometer	Thermo-Fisher Scientific	Waltham, USA
^{14}C-SM	TNO Defense	Rijswijk, The Netherlands
Monitoring equipment	Welch Allyn (UK) Ltd.	Aston Abbotts, UK
Alfaxan® anaesthetic and Dolethal®	Vétoquinol UK Ltd.	Buckingham, UK

Table 2-1: Supplier's details for materials and equipment used in Thesis.

Daily husbandry was carried out by staff in the experimental animal house (EAH) at Dstl. Animals had access to water and food *ad libitum*. All animals were frequently inspected by a qualified veterinary surgeon. Animal weights were recorded on a regular basis to provide an objective measure of each animal's general health status. All *in vivo* experiments (Chapters 5 and 6) were conducted under terminal anaesthesia. Animal studies were performed under a specific project licence granted by the UK Home Office (reference PPL 30/2662). All staff involved with animal work were fully trained and held appropriate (Home Office) personal licences. The use of animals was conducted in accordance with the Animals (Scientific Procedures) Act (1986).

Haemostatic Products and Decontaminants

Haemostatic products (Table 2.2) were stored in accordance with manufacturers' instructions and fresh packets were used on the day of each experiment. Three skin decontaminants used by the military (fuller's earth, Reactive Skin Decontaminant Liquid®; RSDL® and M291) were used to provide a benchmark of decontamination efficacy (Table 2.3). A novel decontaminant comprised of tetraglyme, oxime and poly (ethyleneimine) (TOP) was also tested. The TOP formulation was prepared fresh on the day of each experiment to produce a working solution comprising tetraglyme (30% w/v), 2-pyridine aldoxime mesylate (2-PAM; 50mM) and poly(ethyleneimine) solution (50% w/v) in phosphate buffered saline (pH 8.0 ± 0.1).

Haemostatic Product	Manufacturer	Description
Celox®	Medtrade Products Ltd., Crewe, UK	Granules made from chitosan
FastAct®	Wortham Laboratories Inc, Chattanooga, USA	Bovine-derived activated clotting factors
HemCon®	HemCon Medical Technologies, Inc., Tigard, USA	Chitosan-based dressing
ProQR®	Biolife, Sarasota, USA	Hydrophilic polymer and potassium-ferrite oxyacid salt
QuikClot Advanced Clotting Sponge plus®	Z-Medica, Wallingford, USA	Synthetic zeolite beads
WoundStat™	TraumaCure, Inc., Bethesda, USA	Granules made from smectite clay
Vitagel™	Orthovita, Inc., Malvern, USA	Collagen and thrombin in calcium chloride solution

Table 2-2: Summary of haemostatic products

Decontaminant	Manufacturer	Description
M291 containing Ambergard XE-555 resin	Kindly supplied by Dr Edward Clarkson (United States Army Medical Research Institute of Chemical Defense, Aberdeen Proving Ground, MD, USA)	Activated charcoal absorbent, polystyrene polymeric and ion exchange resin
RSDL®		Reactive liquid decontaminant
Fuller's earth	Sigma-Aldrich, Gillingham, UK	Montmorillonite powder
Tetraglyme, oxime and poly(ethyleneimine) (TOP)	Kindly provided by Dr Richard Gordon for evaluation (WRAIR, Silverspring, MD, USA)	Reactive liquid decontaminant

Table 2-3: Summary of decontaminants

Thrombelastography

Experimental Apparatus

Parameters relating to blood-clotting were measured using an eight-channel thrombelastograph system (TEG 5000®; MediCell Ltd.). All TEG-related consumables were purchased from MediCell Ltd. Daily calibrations of the electromagnetic detector and torsion wire were performed as per manufacturer's instructions, as were weekly quality control standards (Biological QC Level I and Level II).

Experimental Procedures

Daily samples of blood (8 ml) were acquired from each of the animals (n=6) following sedation with midazolam (Hyponoval®; 6 ml intramuscular administration, Roche Products Ltd.) and light anaesthesia (3 – 5% isofluorane in 8 L min^{-1} O_2). Blood samples were drawn from the cephalic vein or cranial vena cava into dried polystyrene tubes containing 3.2 % sodium citrate (Teklab Ltd.) and were equilibrated on a tube roller (ambient temperature; 30 min) prior to use. The actual anatomical location via which venous samples were obtained was altered on a regular basis to ensure minimum discomfort to the animals.

Each TEG channel was set to 37°C and allowed to equilibrate (10 min) prior to use to minimise effect of temperature-driven coagulation. Treatment groups are shown in Table 2.4. Haemostatic products (9 mg of granular or dressings or 9 µl of liquids) were placed into 5 ml polyethylene vials and mixed with citrated whole blood (2 ml). In the case of SM treatment groups, 1 µl SM was added to blood (with or without haemostat) to give a 4 mM SM concentration.

Treatment Group	Haemostat?	Sulphur Mustard?
Control	No	No
Haemostat	Yes	No
SM	No	Yes
Haemostat + SM	Yes	Yes

Table 2-4: Treatment groups for thrombelastography study

	Machine 1		Machine 2		Machine 3		Machine 4	
Channel	1	2	3	4	5	6	7	8
Sample ID	Haemostat plus SM or SM only treatment groups (duplicates)				Haemostat only or control (untreated) treatment groups (duplicates)			

Table 2-5: Channel setup for the four thrombelastography (TEG) machines.

Channels 5 – 8 were solely used with uncontaminated (not SM treated) blood, with all SM contaminated blood analysis performed using channels 1 – 4.

The vials were capped and gently mixed for 30 s. Following mixing, aliquots (340 µl) were transferred to TEG cups pre-treated with calcium chloride (20 µl; 0.2 M). Calcium chloride was present to overcome anticoagulant effect of sodium citrate and reactivate endogenous haemostatic pathways. An untreated blood sample served as a control. Samples were tested in duplicate and TEG traces were recorded until acquisition of maximum clot amplitude.

Due to Health and Safety requirements, two loan machines could not be used with SM-contaminated blood. Therefore, all SM treatment groups (Table 2.4) were analysed using Health Protection Agency owned TEG machines (termed "Channels 1 – 4", Table 2.5). The loan machines (termed "machine 3 and 4", Channels 5 – 8) were only used with blood which had not been treated with SM. To quantify whether there was bias between the machines, all channels were calibrated simultaneously (using QC standards I & II) before use.

Data Analysis

The coagulation parameters investigated by TEG were R time (min), K time (min), alpha angle (degrees) and maximum amplitude (mm). From these data, two further parameters were calculated: shear elastic modulus strength (SEMS or G; dynes cm^{-2}; Equation 2.1) and Coagulation Index (CI; (Equation 2.2).

$$\frac{\qquad}{-} \qquad \textbf{\textit{Equation 2.1}}$$

Equation 2.1: Calculation of SEMS (G; dynes cm^{-2}) where MA is maximum amplitude

- - - ***Equation 2.2***

Equation 2.2: Calculation of coagulation index (CI) where R is R time, K is K time, MA is maximum amplitude and α is alpha angle.

In Vitro Dermal Absorption Studies

Experimental Apparatus

In vitro dermal absorption was measured using Franz-type glass diffusion cells purchased from PermeGear (Figure 1.4). Split-thickness skin was clamped between the upper (donor) and lower (receptor) chambers with an area of 1.76 cm^2 available for diffusion. Each receptor chamber was filled with an appropriate receptor fluid. Magnetic stirrer-bars (polytetrafluoroethylene; 12 x 4.5 mm, cylindrical, Fisher Scientific UK Ltd.) which provided adequate and rapid mixing of the receptor fluid but did not produce a vortex (Ng, *et al*. 2010) were placed in the receptor chamber. Assembled diffusion cells were placed into holding blocks above a magnetic stirrer (V9-CB Stirrer, PermeGear). Warm (36°C) water was continuously circulated around each cell's water jacket using a recirculating water heater to give a skin surface temperature of ~32°C (confirmed by infrared thermography; FLIR P620, FLIR Systems).

A liquid scintillation counter (Model 2810 Tri-Carb, PerkinElmer) was used for the quantification of radioactivity in all samples. The instrument was calibrated before use using the self-normalization and calibration (SNC) standards for ^{14}C, ^{3}H and background.

Experimental Procedures

Skin Preparation and Storage

Undamaged skin studies (study 1 – 3) were performed using abdominal skin. Dorsal skin was used for the damaged skin investigation (study 4) due to problems associated with the dermatoming of abdominal skin. Undamaged dorsal skin was also used as a control in study 4, as a validation step to allow comparison between the undamaged skin and damaged skin experiments.

Intact Skin Preparation

Abdominal skin was obtained post mortem from female pigs (weight range 20 – 25 kg). The skin was stored flat between aluminium foil sheets at -25°C and thawed at 5°C for 18 h prior to the commencement of each study. The excised skin was carefully close-clipped and sectioned to a nominal depth of 500 μm using an electric dermatome (Humeca D42, Eurosurgical Ltd.). The actual skin section thickness was ~ 570 μm when measured using a micrometer. The skin was visually inspected to identify areas of damage. Sections were cut to size (approximately 2.5 cm^2) using a scalpel.

Damaged Skin Preparation

Pig dorsum skin was obtained and stored using the same method as above. Uniform damage to the skin surface was achieved using an electric dermatome (Humeca D42, Eurosurgical Ltd.) through the removal of a nominal 100 μm layer from the skin surface (corresponding to the removal of the SC and the majority of the epidermis). Further skin sections were taken at a nominal thickness of 500 μm.

Assessment of skin integrity and receptor fluid composition

The structural integrity of the membrane was assessed by measuring electrical resistance across the membrane (Chilcott, *et al*. 1996) skin sections were clamped between the receptor and donor chamber with the SC side upward. The donor and receptor chamber were filled with 0.9% saline solution (~ 13 ml and 500 µl for receptor chamber and donor chamber, respectively) and allowed to equilibrate for 1 h. Membrane resistance was measured using an AC resistance meter (M3004 AVO multimeter) and membranes with a resistance below 1.5 kΩ were rejected. The saline solution was removed and receptor chamber medium (50% aqueous ethanol) was added so that the meniscus in the sampling arm was level with the surface of the skin. The surface of the skin was swabbed to remove any residual saline solution. The cells were connected to the circulating water jacket and equilibrated for a further 24 h.

Skin absorption and related measurements

Following equilibration, baseline samples (250 µl) of receptor fluid were taken. A 10 µl droplet of ^{14}C-SM was subsequently applied to the skin surface and left *in situ* for the study duration (24 h). Thirty seconds post exposure, haemostatic products or standard decontaminants (Table 2.2 and 2.3) were applied to the contaminated skin surface (200 mg or 200 µl for dry and liquid products, respectively). Contaminated skin with no decontamination served as controls. All products were left *in situ* for the duration of the study (24 h). Samples of receptor fluid (250 µl) were taken (via the sampling port) at regular intervals (3 h) for 24 h post-exposure. Hourly samples were taken for the control samples for the initial 6 h. Samples were placed into liquid scintillation counting

fluid (5 ml; LSC, Ultima Gold, PerkinElmer) within opaque, plastic scintillation vials (6.5 ml; Simport Scientific). After sampling, fresh 50% aqueous ethanol (250 µl) was added to each receptor chamber to maintain a constant volume.

Dose distribution

Twenty-four hours post-exposure, the diffusion cells were removed from the heated manifold and dismantled. The receptor fluid media and decontaminant were recovered separately into 20 ml glass Wheaton vials. Twenty millilitres of LSC fluid was added to each vial containing recovered decontaminant. The skin surface was swabbed using dry cotton wool and placed into 10 ml isopropanol. The skin was removed from the diffusion cell and placed into a pre-weighed 20 ml glass Wheaton vial. The skin weight was recorded and 10 ml Soluene-350™ (quaternary ammonium hydroxide in toluene, PerkinElmer) was added to solubilise the skin. Vials were stored at ambient temperature for up to 5 days (with occasional vigorous shaking) to facilitate dissolution into the respective solvent. Aliquots (250 µl) of all dose recovery samples were placed into 5 ml LSC fluid.

Reference standards (containing known quantities of ^{14}C-SM) were prepared for the skin, test products and receptor fluid to obtain the specific activity (disintegrations per minute per gram; DPM g^{-1}) and to ascertain the quenching effects of the skin or products. From the specific activity, the amount of radioactivity within each sample could be converted to amount of ^{14}C-SM.

Test product (haemostat or decontaminant) standards were prepared in triplicate by the addition of ^{14}C-SM (2 µl) to vials containing product (200 mg or 200 µl for dry and liquid products, respectively). Separate skin standards were prepared for each

experiment. Three representative sections of unexposed dermatomed skin were placed into individual glass vials and ^{14}C-SM (5 µl) was applied. Soluene-350™ (10 ml) was added to solubilise the skin. All vials were stored for 5 days (ambient temperature) with occasional vigorous shaking to assist dissolution. Triplicate aliquots (250 µl) from each standard were added to 5 ml LSC fluid.

Receptor fluid standards were made by the addition of ^{14}C-SM (10 µl) to 50% aqueous ethanol (10 ml). Sub-samples (100, 75, 50 and 25 µl) were taken in triplicate and added separately to 5 ml LSC fluid.

Liquid Scintillation Counting

All samples were allowed to equilibrate in the counter for 1 h prior to measurement. Radioactivity (disintegrations per minutes; DPM) was quantified using a 2 minute count time calibrated to Ultima-Gold liquid scintillation fluid using a pre-installed ^{14}C quench curve.

Evaluation of ^{14}C-SM desorption from haemostats

Desorption or vapour loss of ^{14}C-SM from the products was measured at ambient temperature using a modified static diffusion cell experiment. Diffusion cells were assembled as previously described with the dermatomed skin replaced with aluminium foil (2.5 cm^2), which served as an impermeable membrane. The difference in recovery of ^{14}C-SM between occluded and unoccluded cells was measured. A droplet of neat ^{14}C-SM (2 µl) was applied to the foil surface and the haemostats or decontaminants (200 mg bolus) were added to the donor chamber. Following the addition of ^{14}C-SM

cells were occluded (where applicable) using foil applied to the top of the donor chamber using silicon-based vacuum grease to form a seal. The haemostats or decontaminants remained *in situ* for 3 h. Diffusion cells which were treated with ^{14}C-SM but not haemostat or decontaminant served as the control group. Three hours post exposure, the diffusion cells were dismantled and the foil (occluding and membrane) and haemostat were recovered separately in 20 ml glass vials. Dry cotton swabs were used to swab the inside surface of the donor chamber and were retained for analysis.

Quantification of ^{14}C-SM

The activity of ^{14}C-radiolabel (DPM) measured in samples of receptor chamber fluid, surface swabs, skin and decontaminant was converted to amount of ^{14}C-SM by calculating the specific activity (DPM g^{-1}). The specific activities for the standards used were calculated using Equation 2.3.

- ——————— ***Equation 2.3***
-

The DPM measured for each unknown sample were converted into amount of ^{14}C-SM using Equation 2.4.

- ——————— ***Equation 2.4.***
-

The ^{14}C-SM vapour loss from the haemostatic products was approximated using Equation 2.5.

- ——————————— ***Equation 2.5.***

The maximum rate of penetration (J_{max}) was calculated from the gradient of the slope of the straight line for between the 3, 6 and 9 h time points (Equation 2.6).

Equation 2.6.

Equation 2.6: Where; m = slope, x = x-intercept at time point, c = y-intercept at time point

<u>*In Vivo* Dermal Absorption Studies</u>

Experimental Apparatus

Physiological parameters (pulse oximetry; % oxygen saturation, capnography; exhaled CO_2, core body temperature, electrocardiogram; ECG, respiratory rate and blood pressure) were monitored throughout the study using a Propaq® Encore 204-EL (Welch Allyn (UK) Ltd.). Surgical and anaesthesia equipment was provided by Dstl and was subject to annual servicing and calibration. Animals were placed in ventral recumbence in a custom sling (Ellegaard) and sling frame (kindly provided by EAH staff at Dstl) whilst in the fume-hood. Due to the air-flow within the fume-hood, animals were placed on a thermal blanket (Harvard Apparatus Ltd.) to maintain core body temperature (37.5 ± 1°C).

A range of biophysical measurements were taken during the study including; LDI (LDLS, Moor Instruments), SRS (CM-2600d, Konica Minolta), IRT (FLIR SC620; FLIR Systems), TEWL (AquaFlux AF200; Biox Systems) and standard digital

photographs (EOS 40d; Canon). Where appropriate, all equipment was calibrated before use in accordance with manufacturer's guidelines.

Experimental Procedures

Surgical Procedures

Following an overnight fast, each animal was sedated with midazolam (up to 6 ml; 2 mg ml^{-1} Hypnoval®, Roche Products Ltd.) prior to induction of anaesthesia using 3.5 – 5% isoflurane delivered via a facemask. After an equilibration period of 5 to 15 minutes, an endotracheal tube was introduced via which anaesthesia (1.5 – 2.5% isofluorane) was maintained for subsequent surgery. The carotid artery and the internal jugular vein were surgically cannulated using 8 French gauge sterile catheters (2.7 outer diameter; Burtons Medical Equipment Ltd.). This provided access for arterial blood sampling and subsequent intra-venous administration of anaesthetic (Alfaxan; alfaxalone, Vétoquinol UK Ltd.). Alfaxan (10 mg ml^{-1}) was administered at a rate of 1.0 – 1.2 mg kg^{-1} h^{-1} for the remainder of the study. The level of consciousness was monitored throughout the study with adjustments made to the rate of alfaxan infusion when required (range used 12 – 26 ml hr^{-1}).

Experimental measurements

The left side of the dorsum was close clipped and up to 4 dosing rings attached to indicate areas for pre-damage biophysical measurements. Treatment groups were randomly assigned to multiple dorsal sites to reduce any effect of anatomical bias (Figure 2.1). For sites requiring damaged skin, a small (~ 3 cm^2) area was dermatomed

(Humeca Model D42, Eurosurgical Ltd.) to a nominal depth of 100 μm. This resulted in transient, punctuate bleeding and so the area was subsequently swabbed with cotton gauze soaked in saline to remove extraneous material such as dried blood. The study design was such that only one site per animal was exposed to ^{14}C-SM.

Once the appropriate sites had been dermatomed, baseline (pre SM-exposure) biophysical measurements and blood samples were taken. Following removal of SM from the skin surface (1 h post-exposure), biophysical measurements (LDI, SRS, IRT, TEWL and standard digital photographs) were taken at 60 min intervals until 6 hours post-exposure. All equipment was calibrated according manufacturer's instructions and equipment settings are given in Table 2.6.

Physiological parameters and blood sampling

Physiological parameters (pulse rate, ECG, arterial blood pressure, breathing rate, core temperature, CO_2 and SpO_2) were monitored and recorded for the study duration. Arterial blood samples (4 ml) were acquired during pre-damage and baseline measurements and at hourly intervals thereafter. Each sample was placed into 3.2% sodium citrate treated vials (Teklab Ltd.) for radiometric (2 ml) and thrombelastography (2 ml) analysis.

Sulphur Mustard Challenge

Following baseline measurements a multi-vesicating (10 μl) dose of ^{14}C-SM was applied as a discrete droplet to skin within the dosing area. The agent was left *in situ* for 60 minutes before removal with cotton swabs and surgical gauze.

Equipment	Calibration Procedures	Measurement settings	Export file type
LDI	Laser turned on prior to measurements (1 h) to stabilise	Repeat line scanner images taken in triplicate (200 ms per line). Raw images were converted to the maximum resolution and the region of interest (ROI; area within dosing ring) was selected and exported (LDLS V1.1a software; Moor Instruments).	ASCII file Imported in Microsoft Excel®
SRS	Zero and white calibrations procedures performed daily	The observer angle was set to 2° and D65 was selected as the primary illuminant. Measurements were taken in triplicate (specular component included and excluded). Absorbance values (360 nm – 740 nm) and CIELAB parameters, L*a*b* were exported from SpectraMagic NX (Konica Minolta).	CSV file Imported in Microsoft Excel®
IRT	Internal auto calibration	Thermographs of the treatment sites were obtained in triplicate. The ROI (area within dosing ring) was selected and exported (ThermaCAM™ Researcher software; FLIR Systems Ltd.).	CSV file Imported in Microsoft Excel®
TEWL	Calibrated daily and allowed to equilibrate (1 h) prior to measurements.	Flux values recorded in triplicate and exported.	TXT file Imported in Microsoft Excel®
Standard photography	N/A	Photos were taken with Canon EOS 40D; 17 – 85 mm lens using the following settings; F-Stop; f/5.6, ISO; 400 and exposure time; 1/60.	JPG file

Table 2-6: Measurement and calibration settings for biophysical equipment used.

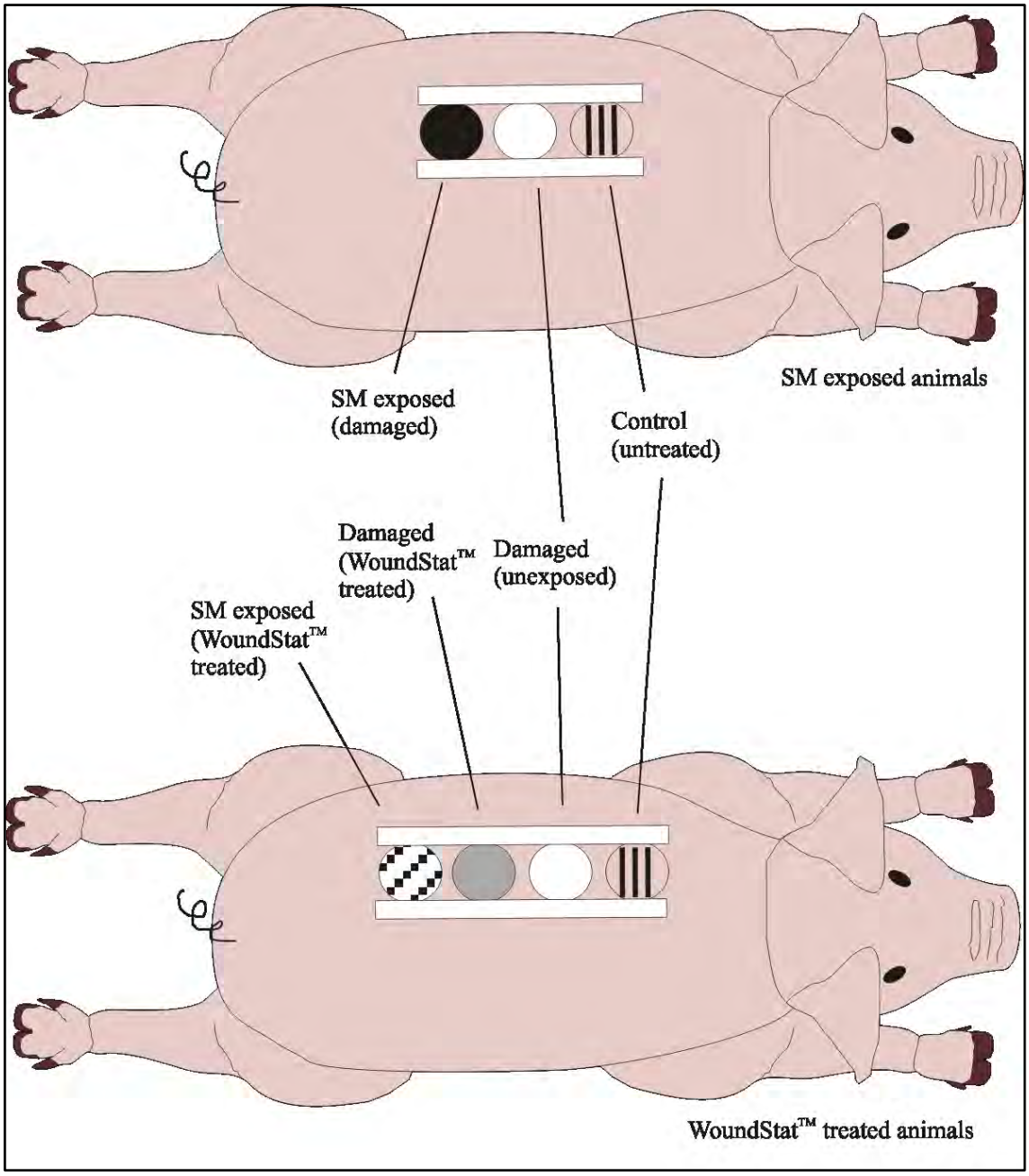

Figure 2.1: Schematic of dosing site setup for in vivo experiments.

Metal dosing rings were taped to the dorsum. Each animal in the SM group (Chapter 5) had 3 treatment sites; control (untreated; striped), damaged unexposed (white) and SM exposed damaged (black). Each animal in the WoundStat™ treated group (Chapter 6) had 4 treatment sites; control (untreated; striped), damaged unexposed (white), damaged WoundStat™ treated (grey) and SM exposed WoundStat™ treated (white & black diamonds).

Removal of the SM from the treatment site was a Health and Safety requirement to limit transfer of ^{14}C-SM to the measuring equipment. All sites received this treatment and swabs were retained for radiometric analysis.

Application of WoundStat™

WoundStat™ (2 g) was applied (30 s post-exposure) to the appropriate exposure site. The product was applied so that it covered the area within the dosing ring. WoundStat™ was also applied to an unexposed, damaged site to assess whether the treatment would cause any adverse reactions *in vivo.* The product was removed 60 min post-exposure and retained for radiometric analysis. To aid recovery of the product, 1 ml of sterile water was applied to the haemostat immediately before removal so that it formed a clay-like mass.

Termination of study and post mortem

Animals were euthanized (6 h post-exposure) by intravenous administration of a lethal dose of Dolethal (pentobarbital; 200 mg ml^{-1}, Vétoquinol UK Ltd.). Animals were exsanguinated and the skin at each treatment site was excised and weighed. Representative samples were taken for histological, genomic and radiometric analysis.

Post mortem examinations were carried out on animals and the main organs (brain, heart, lung, liver, kidney, pancreas and spleen) were removed, weighed and representative samples taken for radiometric analysis. Representative sections of small intestine were also taken for radiometric analysis.

Dose distribution of ^{14}C-sulphur mustard

Skin, swab and WoundStat™

Skin exposure sites were placed into vials containing up to 40 ml tissue solubiliser (Soluene-350™). Cotton swabs and surgical gauze were placed into isopropanol (20 ml). Vials were stored at ambient temperature for at least 14 days (with occasional vigorous shaking) to allow dissolution and extraction into the respective solvent.

Standard solutions were prepared by adding 5 µl ^{14}C-SM to vials containing (i) 20 ml isopropanol, (ii) cotton swab or (iii) skin. Vials containing cotton swabs and skin were treated as per experimental samples with the addition of isopropanol (20 ml) or Soluene-350™ (up to 40 ml), respectively. Vials were stored at ambient temperature for the same period of time as experimental samples. Aliquots (250 µl) of all standard and experimental samples (gauze swabs, sponges and dissolved skin) were removed and placed into 5 ml LSC fluid and analysed by liquid scintillation counting as previously described.

Blood and Organs

A modification of an existing method was used to prepare blood samples for liquid scintillation counting (Moore. 1981). Triplicate aliquots of blood (0.4 ml) were mixed with 1 ml Soluene-350™ and isopropanol solution (1:2 ratio) and incubated (60°C; 2 h). After cooling, samples were treated with hydrogen peroxide (0.5 ml; 30 % v/v) and incubated (ambient temperature; 30 min). Samples were subsequently heated (60°C; 30 min) and cooled prior to the addition of liquid scintillation fluid (20 ml).

Organ samples (100 mg) were prepared in triplicate by the addition of Soluene-350™ (2 ml) followed by incubation (60°C; 4 h). Samples were allowed to cool prior to the subsequent addition of 20 ml liquid scintillation fluid. Blood and organ samples for reference standards were obtained from non-exposed animals. Samples were treated with ^{14}C-SM (5 µl) and prepared in triplicate following the methods above.

The density of the blood and organs were measured to account for difference in volume when calculating the amount of ^{14}C in the solubilised sample (Table 2.7). Samples of each organ (5 g) were homogenised using a stator-rotor homogeniser (T 10 ULTRA-TURRAX®, IKA®-Werke GmbH & Co.). Aliquots (1 ml) were sampled and weighed in triplicate using a positive displacement pipette (Microman®, Gilson Scientific Ltd).

All samples were analysed by LSC with an analysis time of 5 minutes per sample. The amounts of radioactivity in each sample were converted to amount of ^{14}C-radiolabelled SM by comparison to the corresponding reference standards (measured simultaneously).

Radiolabel (^{14}C) elimination kinetics for the blood were calculated from linear regression analysis of a semi-logarithmic plot of blood concentration against time at steady state where the decrease in concentration of ^{14}C-SM with time was constant (Shen. 2008). The kinetic parameters were calculated from equations 2.7 – 2.10 based on the standard equation of a straight line ($y = mx + c$) where y = blood concentration, m = gradient of slope and c = y-axis intercept.

Sample	Density (g ml^{-1})
Brain	0.87
Heart	0.89
Lungs	0.77
Liver	0.98
Spleen	0.96
Pancreas	0.84
Kidney	0.91
Small intestine	0.89
Blood	1.05

Table 2-7: Measured organ density for use in radiometric calculations.

———— ***Equation 2.7.***

Equation 2.7: Calculation of half life of elimination ($T½$) where, C_o is initial blood concentration (equal to the y-axis intercept, 'c').

- ***Equation 2.8.***

Equation 2.8: Calculation of the elimination constant (K_{el}) where, m is the gradient of the slope.

— ***Equation 2.9.***

Equation 2.9: Calculation of the apparent volume of distribution (V_d) where, D_a is the original applied dose.

Equation 2.10.

Equation 2.10: Calculation of dose (D) where, C_{max} is the maximum (experimentally measured) whole blood concentration of ^{14}C (derived from ^{14}C–SM).

Histology

Sample collection and preparation

A section of excised skin from each site was pinned flat to a cork board (21 gauge needles; BD) and skin samples were submerged in 10% neutral buffered formalin (NBF; 20 times sample weight). Samples remained in the fixative for at least one week (up to 6 months).

Sample processing

Samples were removed from the fixative and rinsed with distilled water. Skin samples were trimmed (width 5 mm) and placed in tissue processing cassettes (Tissue-Tek® Uni-cassettes®, Sakura Finetek UK Ltd.). Skin samples were processed using an automated vacuum infiltration tissue processor (VIP; Tissue Tek®, Sakura Finetek UK Ltd.).The VIP processing schedule comprised dehydration of samples through a series of ethanol gradients (80, 90 and 3 x 100%; 1 h each) followed by three changes of 100% chloroform (changes 1 and 2; 1 h, change 3; 2 h) and 15 min in 50% xylene/chloroform. The samples were then placed in xylene (100%) for 10 min prior to the paraffin wax infiltration (2 changes; 2 h, 1 change; 1 h). Once the infiltration step was complete, the samples were embedded using paraffin wax (transverse side down) in metal embedding moulds and chilled on a cooling block (-5°C).

Sectioning and Staining procedures

The paraffin-embedded skin was mounted in a microtome and sections cut to a nominal thickness of 5 μm. Consecutive sections were floated on a 30% ethanol bath and transferred to a warm water (~40°C) bath to help the sections flatten. Sections were lifted onto glass microscope slides (Superfrost Plus; Fisher Scientific UK Ltd.) and placed into a drying oven (37°C) overnight. Sections from each sample were subsequently stained with Haematoxylin and Eosin.

Sections were deparaffinised in 3 changes of xylene (1 min each) and rehydrated through an ethanol series (100%, 100%, 95%, 95% and 50%; 1 min each). Slides were placed in distilled water (1 min) and stained with Haematoxylin (Mayer's

Haematoxylin; 5 min). Slides were rinsed and differentiated in running tap water (1 min), 1% acid alcohol (1 min), running tap water (1 min) and alkaline alcohol (1% sodium hydroxide; 1 min). Sections were counter-stained in alcoholic Eosin Y (0.25%; 1 min) and rinsed in distilled water (1 min). Sections were dehydrated through an ethanol series (95%, 100% and 100%; 2 min each) and immersed in 3 changes of xylene (1 min each). Slides were cover-slipped using Tissue-Tek® Film Coverslipper™ (Sakura Finetek UK Ltd.) and allowed to dry prior to examination.

Histopathological analysis

Stained skin sections were examined by a qualified histopathologist. Each section was subjectively scored for the occurrence and severity of several indicators including; keratinocyte necrosis, escharification, sub-epidermal separation or vesication, blood vessel dilation and inflammatory cell infiltrate.

Genomic analysis

Tissue preparation and RNA extraction

Skin samples from each treatment site (approximately 0.5 cm^3) were placed into 1.5 ml microcentrifuge tubes containing RNAlater® (Ambion, Applied Biosystems; at least 5 times v/w). Samples were incubated at 4°C overnight to allow full absorption into the tissue and stored at -20°C until required (up to 1 year).

Total ribonucleic acid (RNA) was extracted using RNeasy Fibrous Tissue Mini kit (QIAGEN) with minor modifications to the protocol. Briefly, 30 mg skin samples were transferred to RLT lysis buffer (300 µl; QIAGEN) containing 1% β-

mercaptoethanol and homogenised using a Precellys® 24 tissue homogeniser (Bertin Technologies). Samples were processed at 6300 rpm for 23 s for 4 cycles. Between cycles samples were incubated on ice (1 min). The resulting homogenate was mixed in a fresh 2 ml microcentrifuge tube with 590 µl nuclease-free water, 10 µl Proteinase K and incubated at 55°C for 10 min. Following incubation, tubes were centrifuged at 10,000 x g at ambient temperature for 3 min. The supernatant (approximately 900 µl) was transferred to a fresh 2 ml tube containing 1 ml acid-phenol:chloroform:isoamyl alcohol (pH 4.5; 25:24:1, Ambion). Tubes were vortexed (1 min) and incubated on ice for 15 min prior to centrifugation (10,000 x g; 20 min, 4°C). The aqueous phase was transferred to a fresh 2 ml microcentrifuge tube containing 0.5 volume of ethanol (99.9%; molecular biology grade) and incubated at -20°C for 16 h. Samples were transferred to an RNeasy mini spin column (QIAGEN) and processed as per the manufacturer's instructions with the optional on-column DNase I digest performed.

Ribonucleic acid was quantified by spectrophotometry (Nanodrop ND1000 UV-Vis spectrophotometer; Thermo-Fisher Scientific) and stored at -80°C (Equation 2.11). An A_{260}/A_{280} ratio greater than 1.8 was deemed a suitable indication of RNA purity (Appendix 1; Table 1). Samples with a RNA concentration below 60 ng μl^{-1} or an A_{260}/A_{280} ratio below 1.8 underwent further processing (sodium acetate-ethanol precipitation step) to concentrate the RNA and remove organic solvent or salt contamination. Briefly, the RNA sample was mixed and incubated (-80°C; 1 h or -20°C; 16 h) with sodium acetate (1/10 volume; 3 M, pH 5.2, Ambion) and ethanol (2 volumes; ice-cold, molecular biology grade). The sample was centrifuged (16,000 x g; 30 min, 4°C) and the supernatant discarded. The RNA pellet was resuspended in ethanol (70%; ice-cold) and centrifuged (16,000 x g; 15 min, 4°C). The supernatant was

removed and the pellet was allowed to air-dry before resuspension in nuclease-free water (20 µl).

The integrity of the RNA was confirmed using RNA 600 Nano chips and BioAnalyzer 2100 (Agilent Technologies UK Ltd.). Samples with genomic DNA contamination (indicated by large product bands on the gel) were treated with TURBO DNA-free™ (Ambion) according to manufacturer's instructions. A RNA integrity number (RIN) of above 6.0 and clear peaks at 18S and 28S were considered indicators of good quality RNA that could be used for microarray analysis (Appendix 1; Table 1). If the RNA quality was unsatisfactory the entire process was repeated using stored skin tissue.

Labelling procedure

All equipment, slides and reagents using for labelling RNA samples and processing microarray slides were purchased from Agilent Technologies (Agilent Technologies UK Ltd.) unless otherwise stated. The RNA was reverse-transcribed, labelled and converted from complement DNA (cDNA) to complement RNA (cRNA) using the Agilent One Colour Low Input Quick Amp Labelling kit (Figure 2.2). The labelling was carried out according to manufacturer's instructions with One-Colour RNA Spike mix included as a control. Once labelled, the amplified RNA was purified using RNeasy mini-spin columns (QIAGEN) to remove uncoupled cyanine-3 (Cy3) dye. Briefly, cRNA sample was diluted with nuclease-free water (84 µl) and mixed with RLT lysis buffer (350 µl) and ethanol (250 µl; molecular biology grade). The sample was transferred to a spin column and centrifuged (10,000 x g; 30 s, 4°C). The sample was washed twice with RPE wash buffer (500 µl) and centrifuged (10,000 x g; 30 s, 4°C) after each wash step.

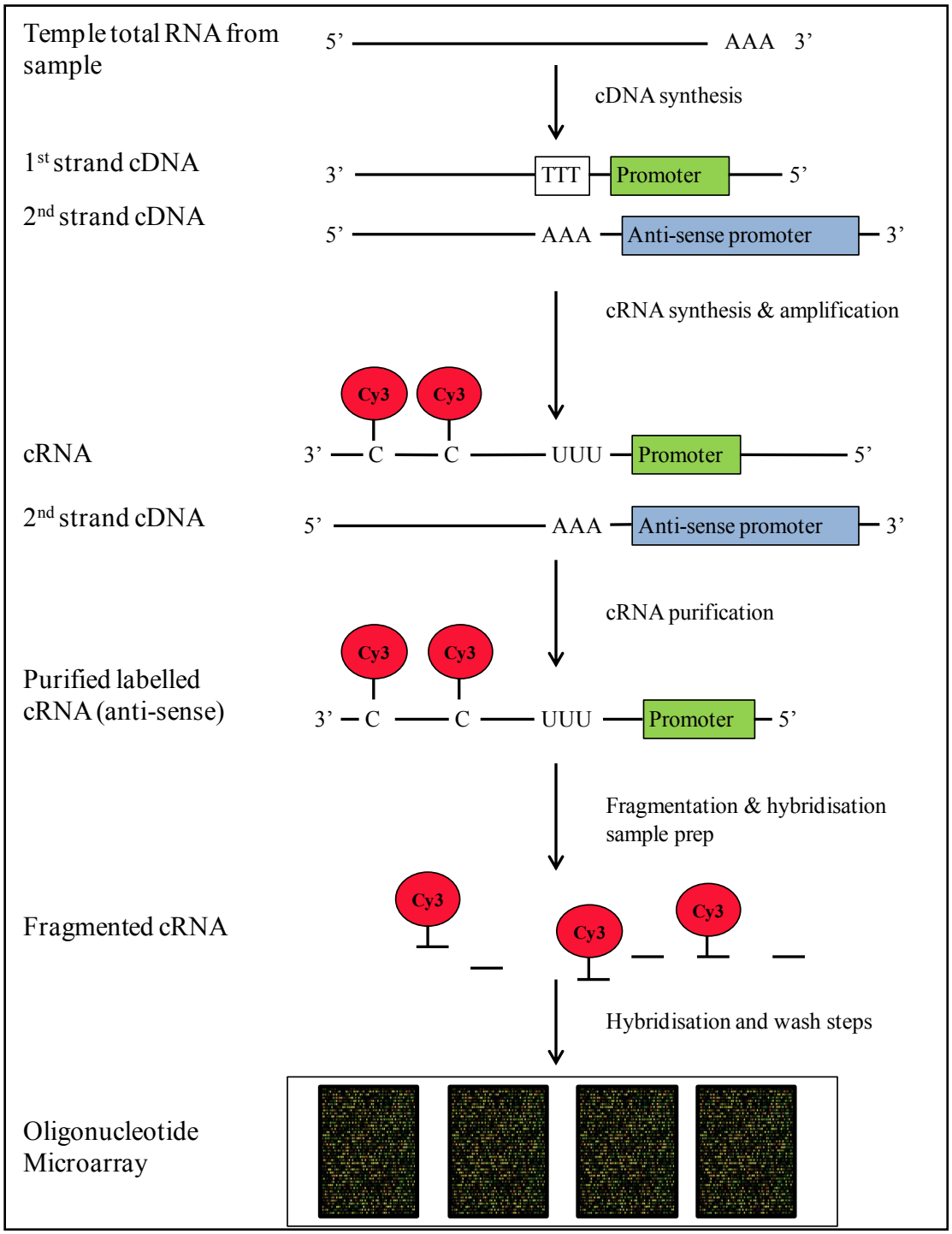

Figure 2.2: Schematic of amplified cRNA synthesis and hybridisation to oligonucleotide microarrays.

Total RNA was reverse-transcribed to cDNA. cRNA was synthesised and amplified from this template, incorporating Cy3 fluorescent dye. cRNA was purified, fragmented and hybridised to an oligonucleotide microarray. Following hybridisation slides were washed and scanned.

Flow-through was discarded after each step. The column was transferred to a fresh 1.5 ml tube and centrifuged (10,000 x g; 1 min, 4°C) to remove any remaining RPE wash buffer. The cRNA sample was transferred to a fresh 1.5 ml tube and incubated with nuclease-free water (30 µl). The column was centrifuged (10,000 x g; 30 s, 4°C) to elute the sample and incubated on ice.

Labelling efficiency was determined by spectrophotometry (Nanodrop ND1000 UV-Vis spectrophotometer; Thermo-Fisher Scientific). A yield of ≥1.65 µg cRNA and a specific activity (Cy3 dye incorporation) of >6 pmol μg^{-1} cRNA was deemed acceptable.

Hybridisation procedure

Hybridisation samples were prepared by mixing labelled cRNA (1.65 µg) with 10X blocking agent (11 µl), 25X fragmentation buffer (2.2 µl) and adjusted to the final volume (55 µl) with nuclease-free water. Samples were incubated (60°C; 30 min) to fragment the RNA and then immediately cooled on ice (1 min). Fragmented samples were mixed with an equal volume of 2X GEx Hybridisation buffer (HI-RPM) and centrifuged (10,000 x g; 1 min, ambient temperature). Samples were stored on ice prior to loading onto a gasket slide. The 4x44K gasket slide was placed into the SureHyb chamber base and samples (100 µl) were pipetted into randomly assigned gasket wells.

The microarray slide (porcine gene expression oligonucleotide microarray; 4X44K) was placed on top of the gasket slide (oligonucleotide-side facing down) followed by the chamber top. The assembled chamber was clamped together and rotated to ensure air bubbles were mobile and the solution fully covered the array slide. Slides were incubated (65°C; 17 h) in a rotating hybridisation oven to allow the labelled

cRNA to anneal to the oligonucleotide probes. Following incubation, the chamber was disassembled and the gasket-microarray slide "sandwich" was placed in gene expression wash buffer 1. Once separated from the gasket slide, array slides were washed in gene expression wash buffer 1 (1 min; ambient temperature) and gene expression wash buffer 2 (1 min, ~31°C). Slides were scanned immediately to minimise the impact of environmental oxidants using Agilent High-Resolution Microarray Scanner (G2565BA). Slides were scanned (5 μm resolution; double pass) and the data from the images (.tif) were extracted using Agilent Feature Extraction Software (Version 10.7.3.1) using the grid and protocol supplied with the array slide to produce text files (.txt) of the signal intensity.

Bioinformatics analysis

The concentration of RNA for each sample was quantified from the absorbance at 260 nm (Equation 2.11).

Equation 2.11

*Equation 2.11: Quantification of RNA using a manipulation of the Beer-Lambert law, w*here; c is RNA concentration (ng μl^{-1}) A_{260} is absorbance at 260 nm, b is path-length (1 cm) and ε is RNA extinction coefficient (40 ng cm^{-1} μl^{-1}).

The signal intensity data from the scanned slides were analysed using GeneSpring GX 11 (Agilent Technologies Ltd.). Agilent standard normalisations for one-colour arrays were applied to all data sets and spots of poor quality (low intensity, poor morphology or saturated intensity), controls and gene probes which were absent in more than 50%

of samples were excluded from further analysis. Expression data for each treatment group were normalised to controls (intact, unexposed skin) for each animal. The difference in the relative gene expression for different treatment groups (Table 2.8) were tested for statistical significance.

Statistical analysis

GraphPad Prism version 5.00 for Windows (GraphPad Software) was used for normality testing and statistical analysis of the data. The normal distribution of the data was assessed using a D'Agostino and Pearson omnibus normality test and Gaussian non-linear regression curve fit. Normally distributed data were expressed as mean ± standard deviation. Data which did not fit Gaussian distribution were expressed as mean ± 95% confidence intervals. Significance was pre-defined at an alpha-level of 0.05.

One-way analysis of variance (ANOVA) with a Bonferroni's multiple comparisons post test was used for inter-group comparisons of data which met normal distribution criteria. A Student's t-test was used to analyse differences between two normally distributed groups. Kruskal-Wallis one-way ANOVA with Dunns post test was used to analyse multiple inter-group comparisons for data that did not fit Gaussian distribution. Comparisons between two groups for data which did not meet normal distribution criteria were analysed using a two-tailed Mann-Whitney U test. Gene expression data were analysed pair wise using a t-test followed by Benjamini Hochberg multiple test correction with a false discovery rate (FDR) of 0.05.

Treatment Group Comparisons		Statistical Test
SM-exposed, damaged skin	Unexposed damaged skin	Paired t-test
Unexposed, damaged skin + WoundStat™ treatment	SM-exposed, damaged skin + WoundStat™ treatment	Paired t-test
SM-exposed, damaged skin	SM-exposed, damaged skin + WoundStat™ treatment	Unpaired t-test

Table 2-8: Treatment group comparisons for gene expression data.

Treatment sites on each animal were compared (paired t-test) or data were pooled for animals (n=6) and compared (unpaired t-test). All expression data were normalised to control (untreated) skin.

Chapter 3

The Effect of Sulphur Mustard on Coagulation and the Efficacy of Haemostats in Untreated and SM-Treated Blood

INTRODUCTION

Sulphur mustard exposure is known to have adverse chronic effects on coagulation e.g. thrombocytopenia and anaemia (Balali-Mood, *et al*. 2005, Mahmoudi, *et al*. 2005, Krumbhaar and Krumbhaar. 1919). However, there is little published on the acute effects of SM on blood coagulation and it is unclear what effect SM contamination would have on a haemorrhaging injury. Sulphur mustard has been shown to increase the expression of uPA in fibroblast cell culture (Detheux, *et al*. 1997). Plasminogen is cleaved to form plasmin by uPA (Vasquez, *et al*. 1998). Plasmin is responsible for cleavage of the cross-linked fibrin clot to produce fibrin monomers, resulting in clot lysis (Pryzdial, *et al*. 1999). Thus it is possible that SM could enhance clot lysis through activation of uPA. Alternatively, it is known that SM alkylates a number of amino acid residues including; histidine, glutamic acid, aspartic acid and valine (Black, *et al*. 1997, Noort, *et al*. 1996). Thrombin is a key enzyme in the initiation and amplification phases of coagulation (Chapter 1 Figure 1.5) and its active site contains histidine, serine and aspartic acid residues. Therefore, it is also possible that SM could alkylate crucial amino acid residues resulting in conformational or functional changes to thrombin leading to reduced coagulation.

Thrombelastography (TEG) is an established clinical method of assessing coagulation of whole blood (Bowbrick, *et al*. 2000, Karoutsos, *et al*. 1999, Kaufmann, *et al*. 1997, Williams, *et al*. 1999). The technique has also been used to measure the clotting efficacy of haemostatic products *in vitro* using uncontaminated porcine blood (Kheirabadi, *et al*. 2009, Kheirabadi, *et al*. 2010). Therefore, TEG appears to be a suitable model for investigating the effects of SM on blood coagulation in untreated and haemostat-treated blood.

Aims

To utilise thrombelastography to investigate;

- the effect of SM on blood coagulation *in vitro* and *in vivo*,
- whether haemostatic products were efficacious and,
- whether the presence of SM had an adverse effect on the clotting efficacy of haemostatic products.

MATERIALS AND METHODS

Full details of the methods used in this study are described in Chapter 2. Briefly, the *in vitro* clotting efficacy of haemostatic products (Table 2.2) was evaluated in untreated and SM-treated blood using thrombelastography (Figure 3.1). Clotting efficacy was assessed by a number of thrombelastography parameters (time to initial fibrin formation; R time, clotting kinetics; K time and α-angle, total clot strength; maximum amplitude, total clot elasticity; shear elastic modulus strength and overall coagulation index). The coagulation parameters of arterial blood samples from the circulation of animals which had been exposed to SM with and without subsequently decontaminated with WoundStat™ *in vivo* were also measured. Full details of the methods used to perform the *in vivo* SM challenge and subsequent WoundStat™ treatment (where applicable) are detailed in Chapter 2. However, the results are shown here rather than in Chapters 5 or 6 to allow comparison between the *in vitro* and *in vivo* results.

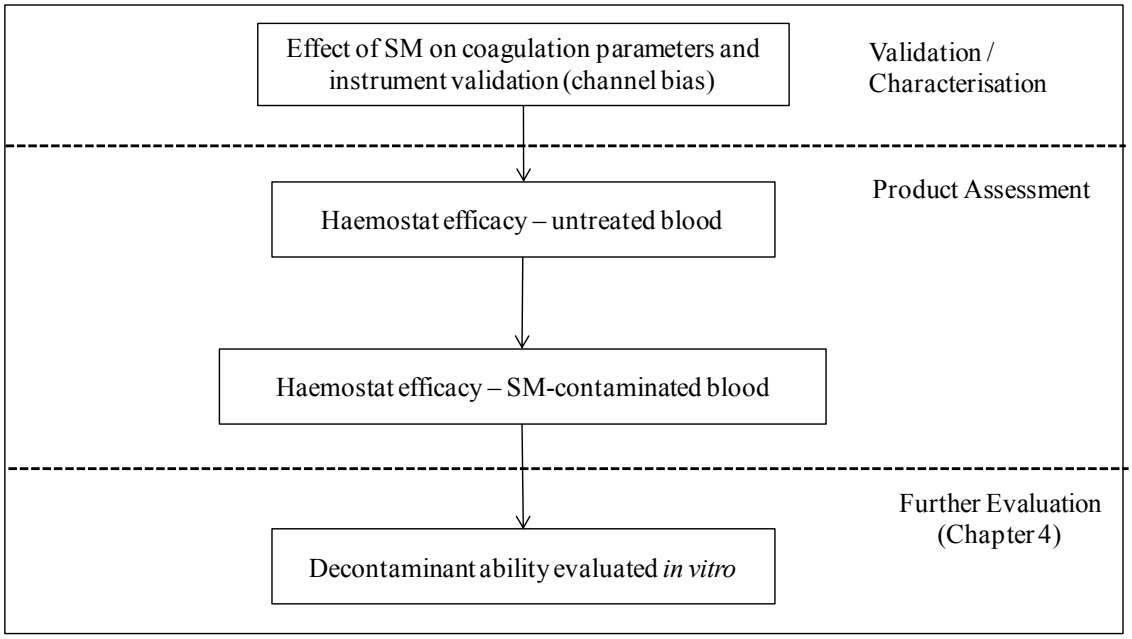

Figure 3.1: Testing strategy for haemostatic products in untreated and SM-contaminated blood.

RESULTS

Instrument validation – channel bias

Due to the potential risk of contaminating the TEG machine with SM, only two machines (Channels 5 – 8) were used with SM contaminated blood (SM and SM plus haemostat treated). The two other machines were only used for uncontaminated blood (control and haemostat treated). There was no statistically significant difference between individual channels (Figure 3.2).

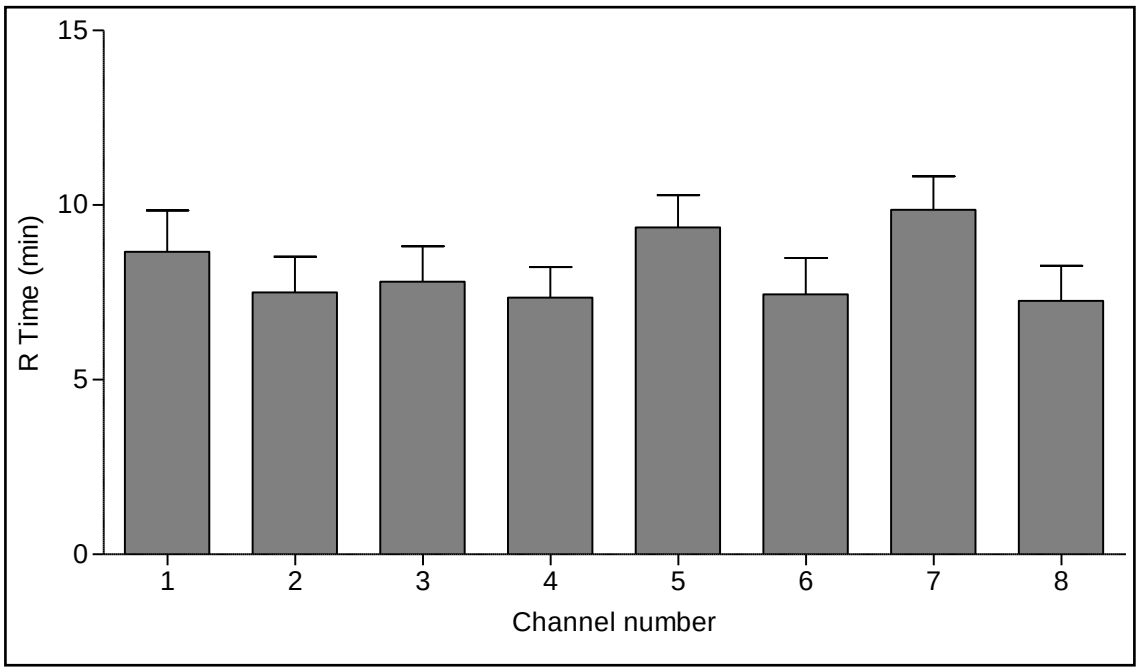

Figure 3.2: Time to initial fibrin formation (R time) for the 8 channels used.

Data acquired from SM-treated blood (channels 1 – 4) and control (untreated blood) (channels 5 – 8), expressed as mean ± S.D. (n= 45).

Effect of sulphur mustard on *in vitro* coagulation parameters

Time to initial fibrin formation (R Time) was not significantly affected by SM contamination (Figure 3.3). There was a significant, negative correlation between α angle and K Time ($p < 0.001$) for both the control and SM treatment groups (Figure 3.4). However, no significant difference was found between the two groups.

Sulphur mustard did not significantly affect the total clot strength or elasticity (maximum amplitude and SEMS, respectively) nor did it affect the overall coagulation index (Table 3.1).

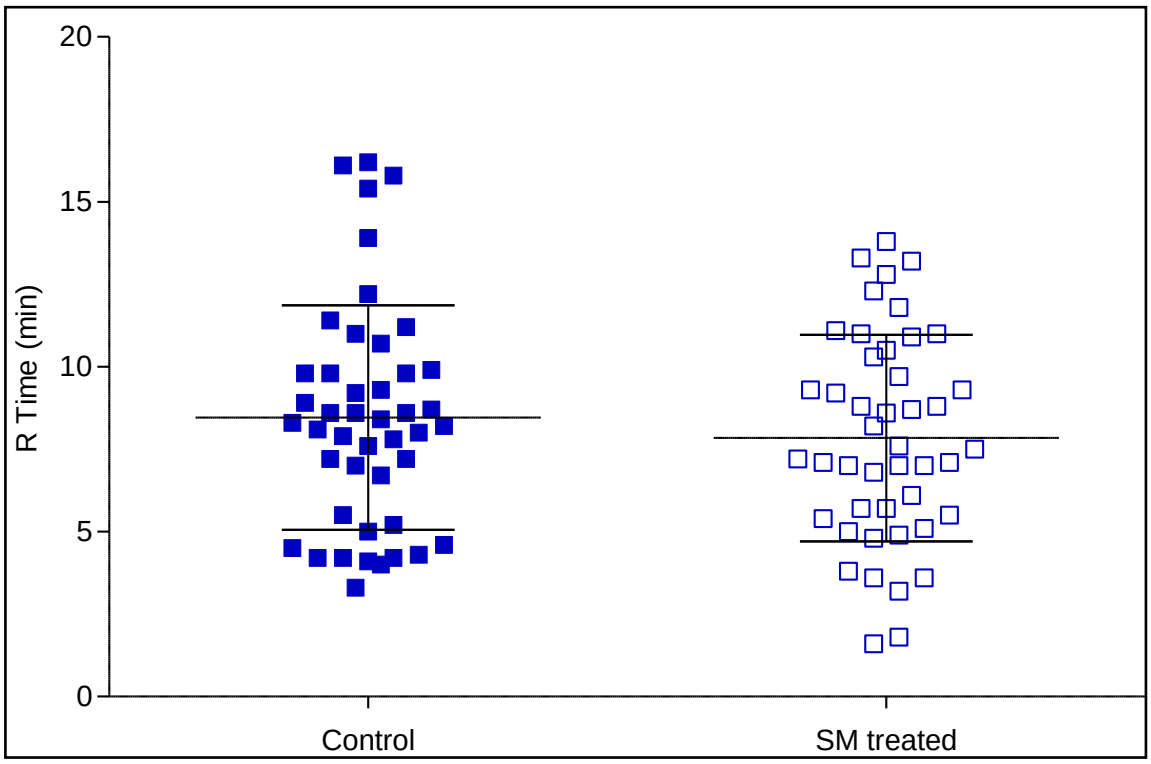

Figure 3.3: Initial fibrin formation (R Time; min) of whole blood following the addition of SM (4 mM).

Individual values are shown as well as mean (central line; n=45) and standard deviation (outermost lines).

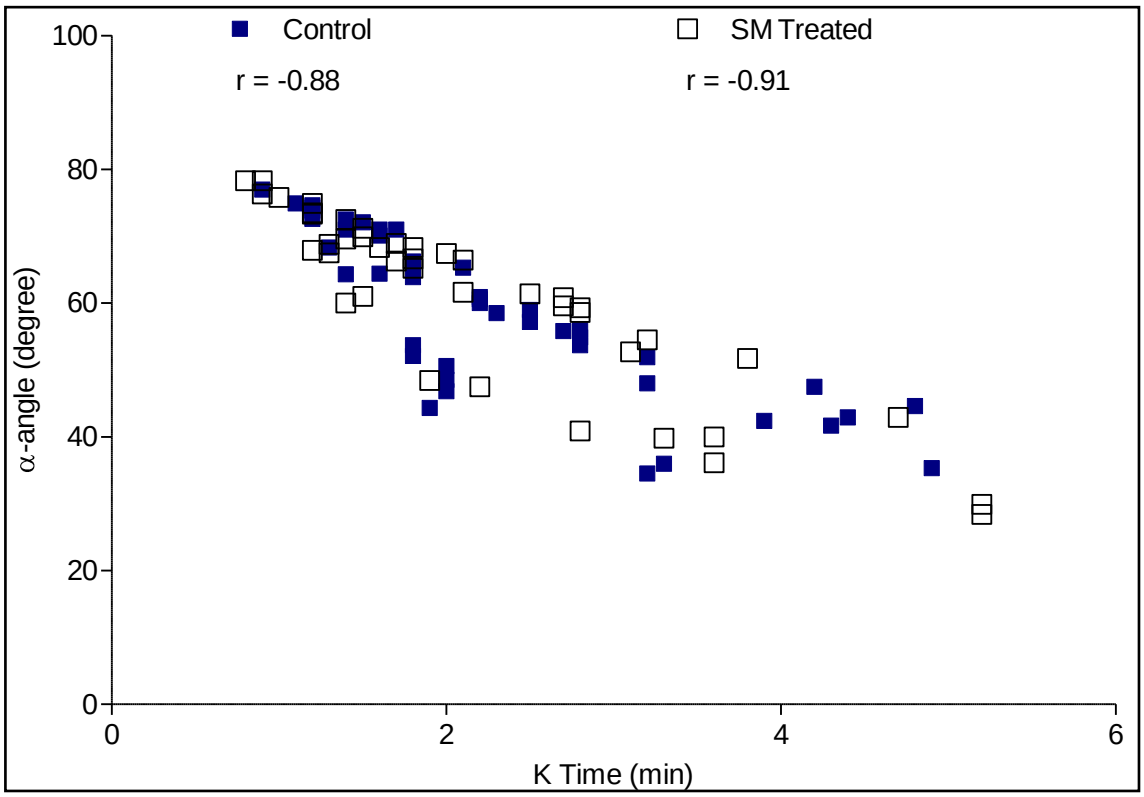

Figure 3.4: Clotting kinetics (K Time; min, α angle; degrees) of whole blood following the addition of SM (4 mM).

The correlation between clotting parameters K time and α angle was determined to be significant by Spearman correlation coefficient (p value <0.001 for both control and SM treated blood, n=45).

Treatment Group	Control (n=45)	SM treated (n=45)
Maximum Amplitude (mm)	72.8 (71.5 – 74.2)	66.2 (61.2 – 71.3)
SEMS (dynes cm^{-2})	3569 (3502 – 3637)	3244 (2997 – 3491)
Overall Coagulation Index (CI)	3.6 (3.4 – 3.9)	2.6 (1.9 – 3.3)

Table 3-1: Total clot strength and elasticity of whole blood following application of SM.

Data are shown for maximum amplitude, shear elastic modulus strength (SEMS) and coagulation index. Data expressed as mean (± 95% confidence intervals; n= 45).

The *in vitro* efficacy of test haemostats tested using thrombelastography

Four haemostatic products (WoundStat™, VitaGel™, FastAct® and ProQR®) significantly decreased R Time compared to control blood ($p < 0.001$; Figure 3.5). However, three products were not effective *in vitro* with no statistically significant difference in R Time compared to control values (QuikClot ACS+®, Celox™ and HemCon®; Figure 3.5).

The same four haemostats (WoundStat™, VitaGel™, FastAct® and ProQR®) also significantly improved clotting kinetics (reduced K time and increased α-angle) compared to control blood (Table 3.2).

VitaGel™ significantly increased the total clot strength (maximum amplitude), clot elasticity (shear elastic modulus strength) and overall coagulation index compared to control (untreated) samples ($p < 0.05$; Table 3.2 and Figures 3.6 and 3.7).

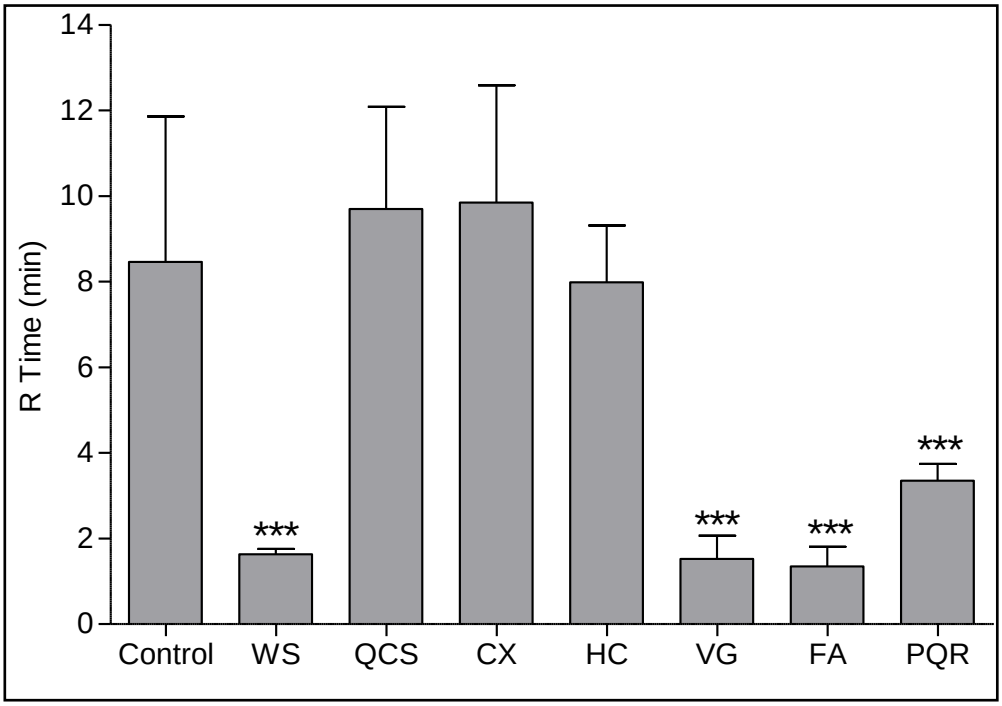

Figure 3.5: Initial fibrin formation (R Time; min) of whole blood following addition of haemostatic products.

*Haemostats tested included: WoundStat™; WS, VitaGel™; VG, Celox™; CX, FastAct®; FA, ProQR®; PQR, HemCon®; HC and QuikClot ACS+®; QCS. Untreated blood served as a control. Individual values are mean ± standard deviation of n=6. Statistically significant differences are shown, where *** represents a p value of <0.001.*

Treatment Group	**K Time (min)**	**Alpha angle (degree)**	**Maximum Amplitude (mm)**
Control (n=45)	2.3 (1.9 – 2.6)	58.5 (54.8 – 62.1)	72.8 (71.5 – 74.2)
WS (n=6)	***0.8 (0.8 – 0.8)	***80.7 (80.3 – 81.1)	74.7 (72.9 – 76.5)
VG (n=6)	**1.0 (0.75 – 1.2)	**77.0 (75.6 – 78.4)	*79.2 (75.6 – 82.8)
CX (n=6)	2.4 (1.9 – 2.9)	56.1 (46.7 – 65.6)	72.4 (65.4 – 79.4)
FA (n=6)	**1.1 (0.8 – 1.5)	**75.7 (70.7 – 80.8)	75.6 (69.8 – 81.4)
PQR (n=6)	***1.0 (0.9 – 1.4)	**72.7 (69.1 – 76.3)	73.0 (68.9 – 77.4)
HC (n=6)	1.7 (1.4 – 2.0)	64.0 (58.8 – 69.2)	75.0 (71.5 – 78.4)
QCS (n=6)	2.6 (1.8 – 3.4)	57.6 (50.6 – 64.7)	71.6 (6739 – 75.3)

Table 3-2: Clotting kinetics (K Time and α-angle) and clot strength (maximum amplitude) of whole blood following addition of haemostatic products.

*Haemostats tested included: WoundStat™, VitaGel™, Celox™, FastAct®, ProQR®, HemCon®, and QuikClot ACS+®. Untreated blood served as a control. Statistically significant differences are shown, where * and ** represent a p-value of <0.05 and <0.01, respectively. Data expressed as mean (± 95% confidence intervals; n= 6 to 45).*

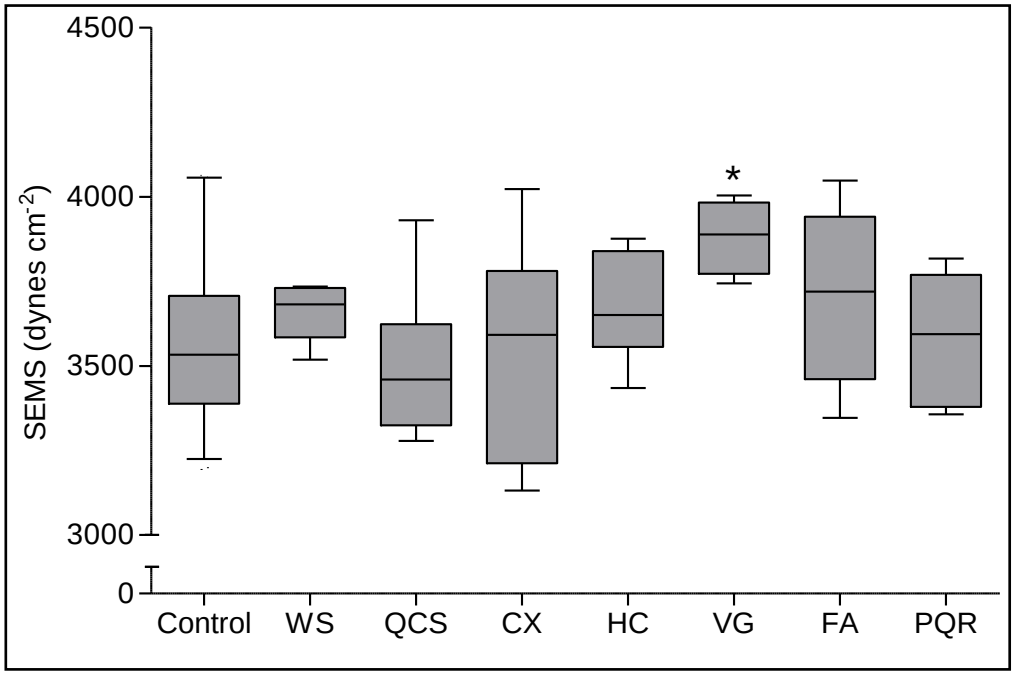

Figure 3.6: Total clot elasticity (shear elastic modulus strength; SEMS, dynes cm^{-2}) of whole blood following addition of haemostatic products.

*Haemostats tested included: WoundStat™, VitaGel™, Celox™, FastAct®, ProQR®, HemCon®, and QuikClot ACS+®. Untreated blood served as a control. Data are expressed as mean, 95% confidence intervals and inter-quartile range represented by the mid-line, outer lines and box, respectively (n= 6 to 45). Statistically significant differences are shown, where * represents a p-value of <0.05.*

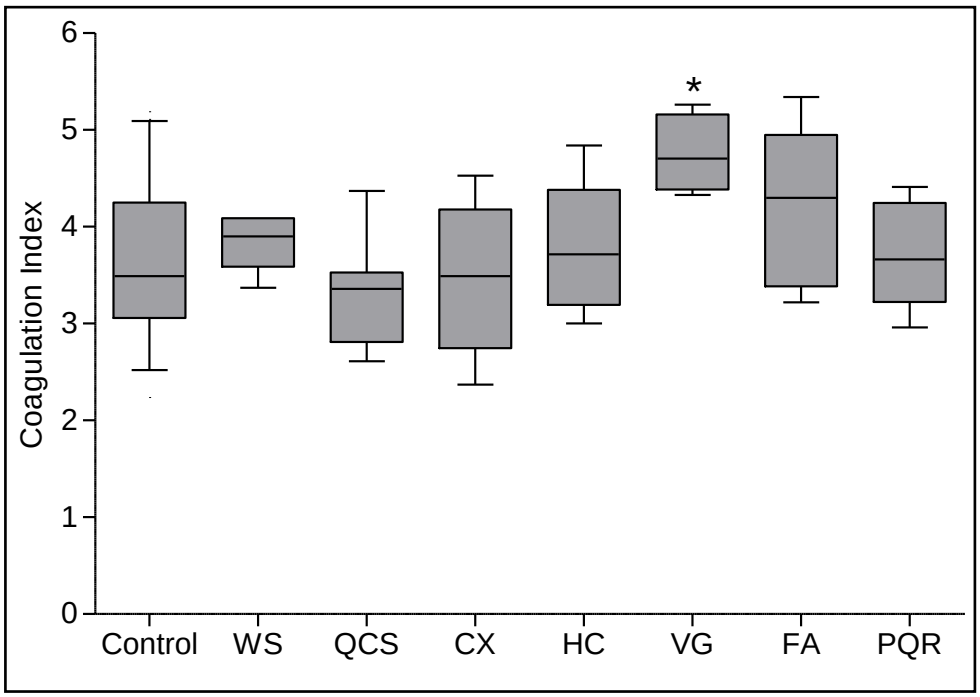

Figure 3.7: Overall assessment of coagulation (Coagulation Index; CI) of whole blood following addition of haemostatic products.

*Haemostats tested included: WoundStat™, VitaGel™, Celox™, FastAct®, ProQR®, HemCon®, and QuikClot ACS+®. Untreated blood served as a control. Coagulation Index provides an overall score for clotting based on R Time, K Time, alpha angle and maximum amplitude. Data are expressed as mean, 95% confidence intervals and inter-quartile range represented by the mid-line, outer lines and box, respectively (n= 6 to 45). Statistically significant differences are shown, where * represents a p value of <0.05.*

The effect of sulphur mustard on coagulation haemostat-treated blood coagulation *in vitro*

The four haemostats (WoundStat™, VitaGel™, FastAct® and ProQR®) that were effective at reducing R Time in uncontaminated blood were not affected by SM contamination (Figure 3.8). The other haemostats tested (QuikClot ACS+®, HemCon® and Celox™) were ineffective in reducing the time to initial clot formation (Figure 3.8).

WoundStat™, VitaGel™, FastAct® and ProQR® significantly increased overall clotting kinetics (decreased K time and increased α-angle) in SM-contaminated blood compared to control (untreated) blood (Table 3.3). Moreover, no significant difference in clotting kinetics (K time and α-angle) was observed between naive and SM-contaminated blood for the haemostats.

Interestingly, the ability of WoundStat™ to increase total clot strength and elasticity was compromised in SM-contaminated blood, with significant decreases in maximum amplitude and shear elastic modulus strength (2- and 4.1-fold decreases, respectively) compared to control (untreated) blood ($p < 0.01$) and WoundStat™ treated uncontaminated blood ($p < 0.01$; Table 3.3 and Figure 3.9). Sulphur mustard also significantly decreased the coagulation index for this group compared to both control (untreated) blood and WoundStat™-treated uncontaminated blood ($p < 0.01$; Figure 3.10). The relative efficacy of the haemostatic products to coagulate blood (with or without addition of SM) is summarised in Table 3.4.

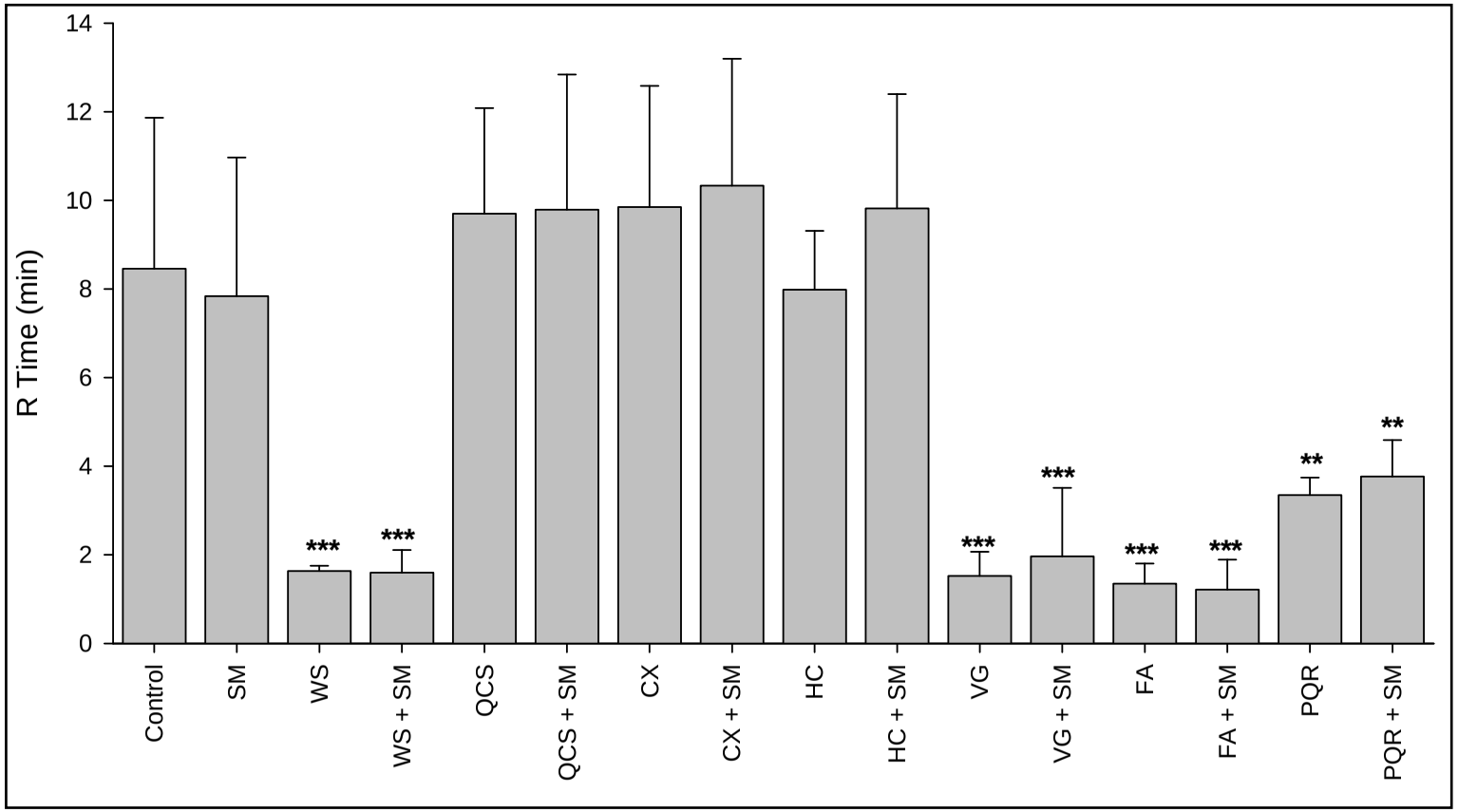

Figure 3.8: Initial fibrin formation (R Time; min) of whole blood following addition of SM and haemostatic products

*Haemostats were tested in combination with SM. Haemostats tested included : WoundStat™; WS, VitaGel™; VG, Celox™; CX, FastAct®; FA, ProQR®; PQR, HemCon®; HC and QuikClot ACS+®; QCS. Untreated blood served as a control. Individual values are mean ± standard deviation (n=6 to 45). Statistically significant differences between haemostat and control values are shown, where ** and *** represent a p value of <0.01 and <0.001, respectively.*

Treatment Group	K Time (min)	Alpha angle (degree)	Maximum Amplitude (mm)
Control (n=45)	2.3 (1.9 – 2.6)	58.5 (54.8 – 62.1)	72.8 (71.5 – 74.2)
SM (n=45)	2.2 (1.9 – 2.6)	60.7 (56.6 – 64.9)	70.6 (67.8 – 73.3)
WS (n=6)	***0.8 (0.8 – 0.8)	***80.7 (80.3 – 81.1)	74.7 (72.9 – 76.5)
WS + SM (n=6)	*1.1 (0.7 – 1.6)	**76.3 (71.7 – 80.8)	**36.5 (22.1 – 50.8)
VG (n=6)	**1.0 (0.75 – 1.2)	**77.0 (75.6 – 78.4)	*79.2 (75.6 – 82.8)
VG + SM (n=6)	***0.9 (0.7 – 1.0)	***79.4 (77.3 – 81.4)	**78.9 (75.7 – 82.1)
CX (n=6)	2.4 (1.9 – 2.9)	56.1 (46.7 – 65.6)	72.4 (65.4 – 79.4)
CX + SM (n=6)	2.8 (1.5 – 4.2)	48.2 (28.4 – 68.0)	66.5 (48.0 – 85.0)
FA (n=6)	**1.1 (0.8 – 1.5)	**75.7 (70.7 – 80.8)	75.6 (69.8 – 81.4)
FA + SM (n=6)	**1.0 (0.7 – 1.3)	***77.7 (73.2 – 82.2)	**78.3 (75.4 – 81.2)
PQR (n=6)	***1.0 (0.9 – 1.4)	**72.7 (69.1 – 76.3)	73.0 (68.9 – 77.4)
PQR + SM (n=6)	**1.1 (0.8 – 1.3)	**75.8 (72.5 – 79.1)	**76.6 (75.3 – 77.9)
HC (n=6)	1.7 (1.4 – 2.0)	64.0 (58.8 – 69.2)	75.0 (71.5 – 78.4)
HC + SM (n=6)	2.8 (1.5 – 4.1)	51.3 (39.5 – 63.2)	75.0 (72.5 – 77.4)
QCS (n=6)	2.6 (1.8 – 3.4)	57.6 (50.6 – 64.7)	71.6 (6739 – 75.3)
QCS + SM (n=6)	2.9 (1.8 – 4.0)	52.0 (40.8 – 63.1)	71.6 (50.8 – 72.7)

Table 3-3: Clotting kinetics (K Time and α-angle) and clot strength (maximum amplitude) of whole blood following addition of SM and haemostatic products.

*Haemostats were tested in combination with SM. Haemostats tested included: WoundStat™, VitaGel™, Celox™, FastAct®, ProQR®, HemCon®, and QuikClot ACS+®. Untreated blood and SM-exposed served as negative and positive controls, respectively. Statistically significant differences between haemostat + SM and control are shown, where *, ** and *** represent a p value of <0.05, <0.01 and <0.001, respectively. Black line represents significant difference between haemostat (naive blood) and haemostat (SM-contaminated blood) treatment groups. Data are expressed as mean (± 95% confidence intervals; n= 6 to 45).*

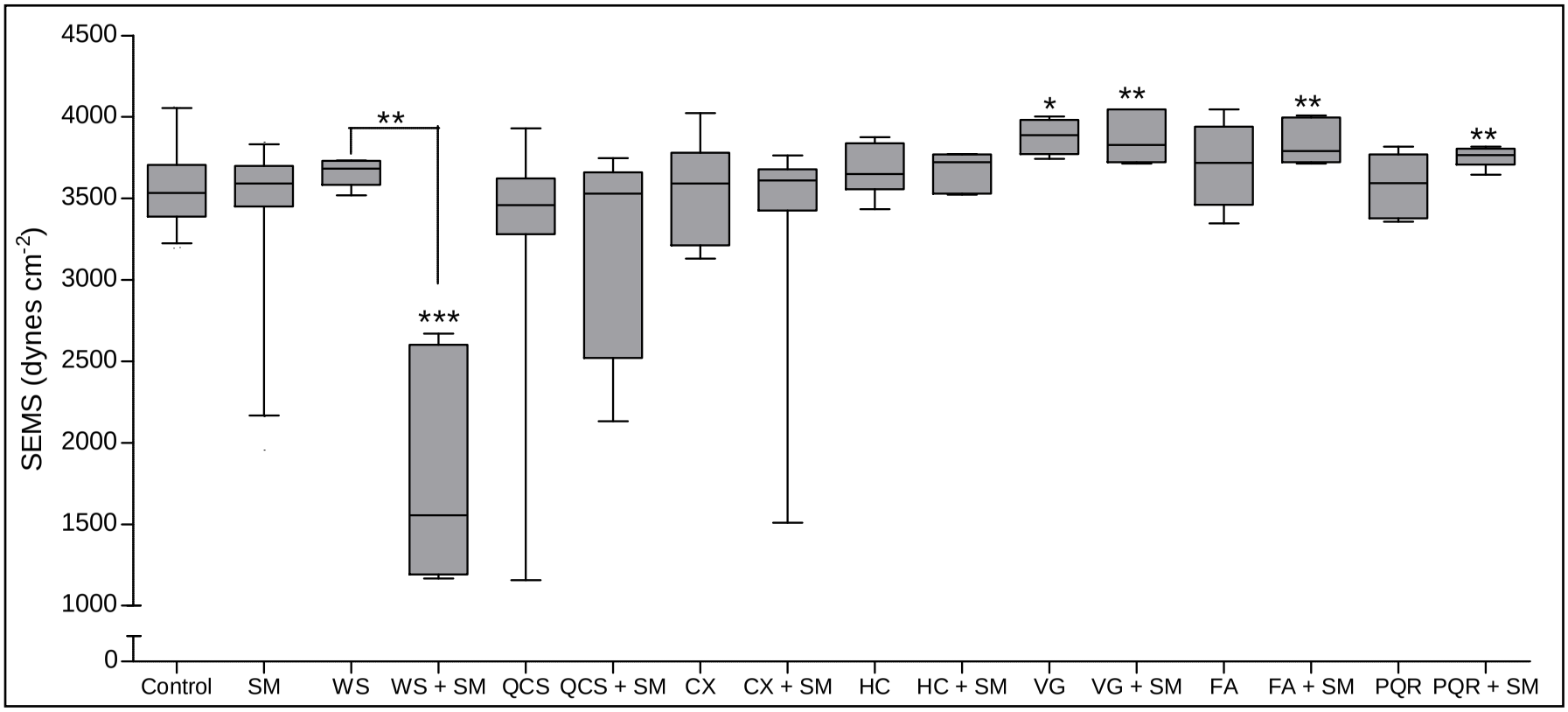

Figure 3.9: Total clot elasticity (shear elastic modulus strength; SEMS, dynes cm-2) of whole blood following addition of SM and haemostatic products.

*Haemostats were tested in combination with SM. Haemostats tested included: WoundStat™, VitaGel™, Celox™, FastAct®, ProQR®, HemCon®, and QuikClot ACS+®. Untreated blood and SM-exposed served as negative and positive controls, respectively. Black line represents significant difference between haemostat (naive blood) and haemostat (SM-contaminated blood) treatment groups. Significant differences between haemostat (SM-contaminated blood) and SM treatment groups are shown, where * and ** represent a p value of <0.05 and <0.01, respectively. Data are expressed as mean, 95% confidence intervals and inter-quartile range represented by the mid-line, outer lines and box, respectively (n= 6 to 45).*

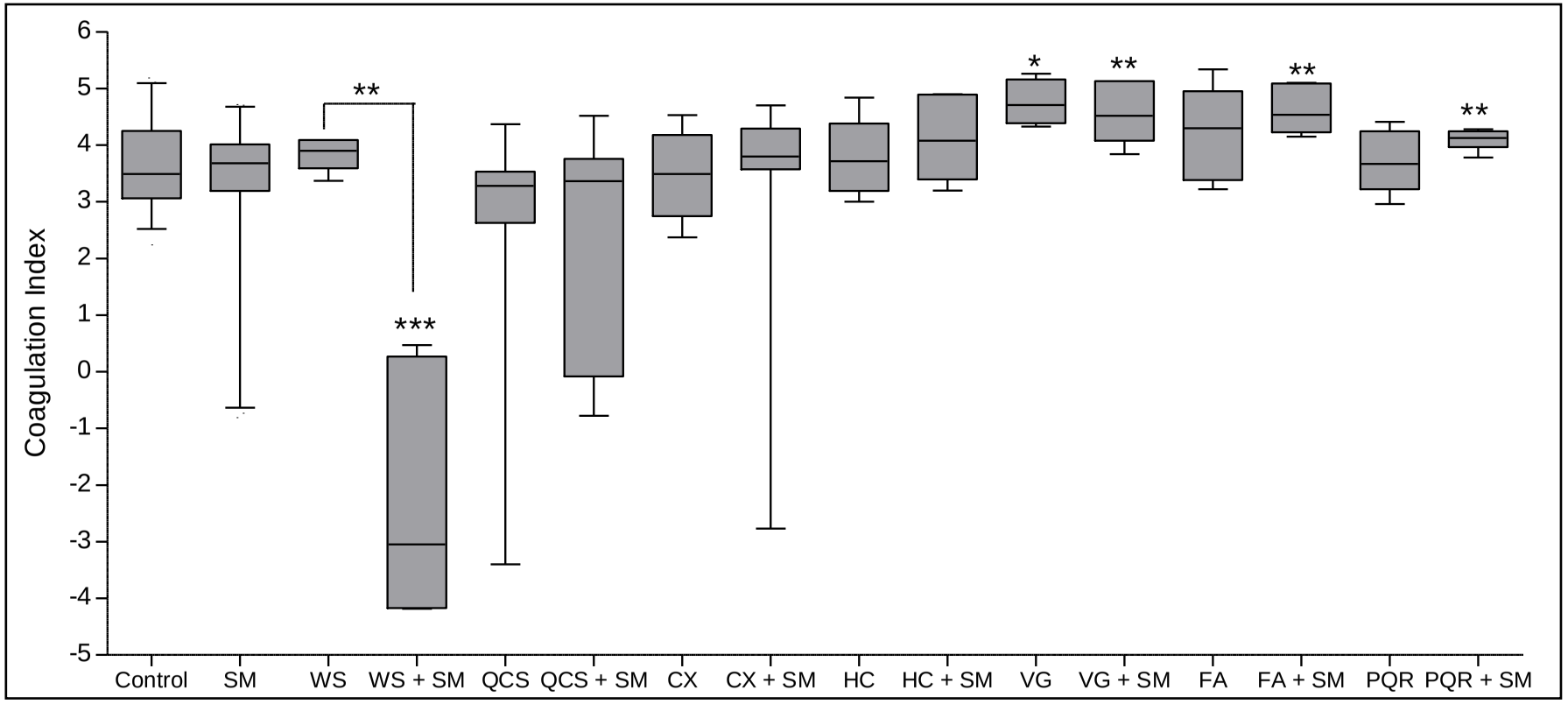

Figure 3.10: Overall assessment of coagulation (Coagulation Index; CI) of whole blood following addition of sulphur mustard and haemostatic products

*Haemostats were tested in combination with SM. Haemostats tested included: WoundStat™, VitaGel™, Celox™, FastAct®, ProQR®, HemCon®, and QuikClot ACS+®. Untreated blood and SM-exposed served as negative and positive controls, respectively. Black line represents significant difference between haemostat (naive blood) and haemostat (SM-contaminated blood) treatment groups. Significant differences between haemostat (SM-contaminated blood) and SM treatment groups are shown, where *, ** and *** represent a p value of <0.05, <0.01 and <0.001, respectively. Data are expressed as mean, 95% confidence intervals and inter-quartile range represented by the mid-line, outer lines and box, respectively (n= 6 to 45).*

Treatment Group	R Time	K Time	α angle	MA	G	CI
WS	+	+	+	0	0	0
WS + SM	+	0	0	-	-	-
VG	+	0	0	+	+	+
VG + SM	+	+	+	+	+	0
CX	0	0	0	0	0	0
CX + SM	0	0	0	0	0	0
FA	+	0	0	0	0	0
FA + SM	+	0	0	0	0	0
PQR	+	+		0	0	0
PQR + SM	0	+	+	0	0	0
HC	0	0	0	0	0	0
HC + SM	0	0	0	0	0	0
QCS	0	0	0	0	0	0
QCS + SM	0	0	0	0	0	0

Coagulation parameter significantly improved compared to control	+
No significant difference compared to control	0
Coagulation parameter significantly worse than control	-

Table 3-4: Thrombelastography parameters results for haemostat (naive blood) and haemostat (SM-contaminated blood) treatment groups presented as a "traffic-light chart".

The colours represent the clotting efficacy of each product; where a significant worsening (red; -), no significant difference (yellow; 0) or a significant improvement (green; +) in coagulation parameters measured compared to the control (untreated) is shown for each of the treatment groups.

The effect of sulphur mustard on blood coagulation *in vivo*

Thrombelastography parameters were also measured for animals challenged with a percutaneous SM challenge via superficially damaged skin with and without decontamination using WoundStat™. These measurements were conducted to investigate whether SM or WoundStat™ had an effect on systemic coagulation (when applied percutaneously to superficially damaged skin). Statistically significant differences in either R time, total clot strength or coagulation index were not observed between the two treatment groups (Figure 3.11 – 13). Additionally, no statistically significant difference was observed for the "SM-exposed" time points (60 – 360 min) compared to the unexposed baseline sample for either treatment group.

An area of concern identified by the *in vitro* studies was the decreased clot strength following treatment of blood with a combination of WoundStat™ and SM (Figure 3.9 and Table 3.4). However, WoundStat™ or SM treatment alone did not cause an adverse effect *in vitro*. No statistically significant difference was observed between SM only and SM + WoundStat™ treated animals in relation to clot strength. This study also measured clot lysis at 30 min (after the start of coagulation, R time). Clot lysis (30 min after R time) for both treatment groups was less than 1% at all time point measured.

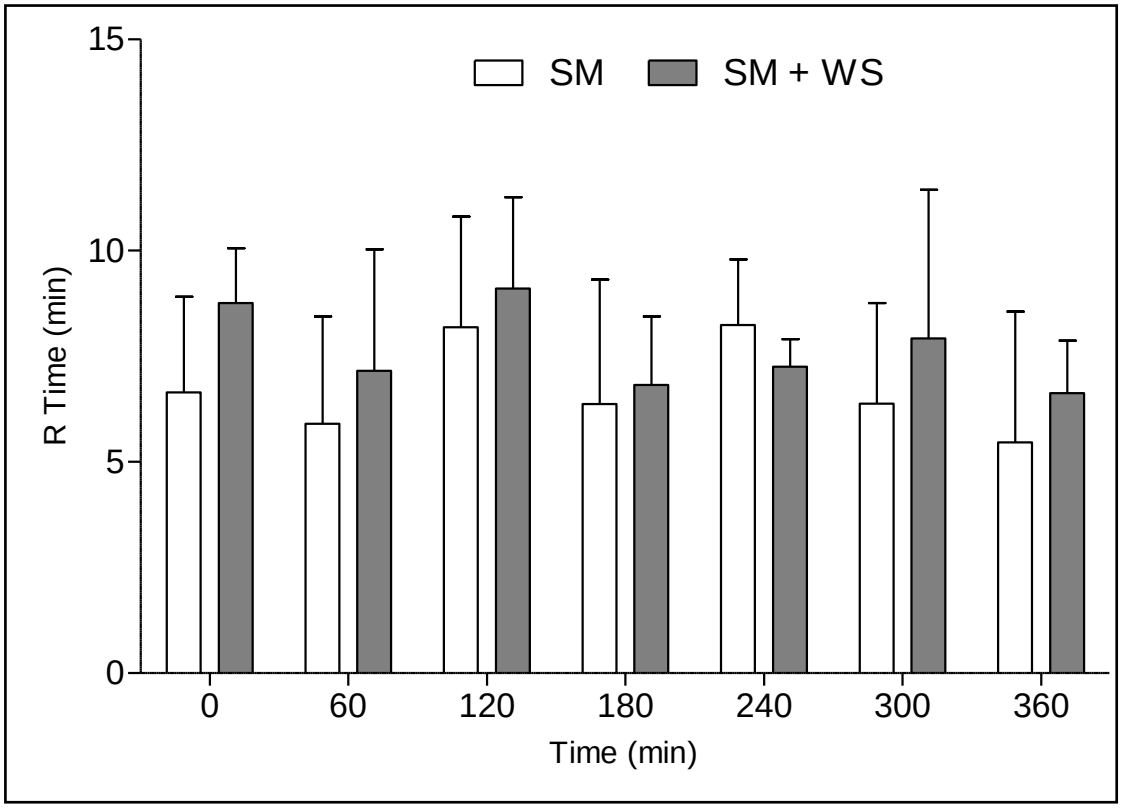

Figure 3.11: Initial fibrin formation (R Time; min) of whole blood (from systemic circulation) following percutaneous application of sulphur mustard (SM) and subsequent application of WoundStat™ (SM+WS) to superficially damaged skin.

Values are expressed as mean ± standard deviation (n=6).

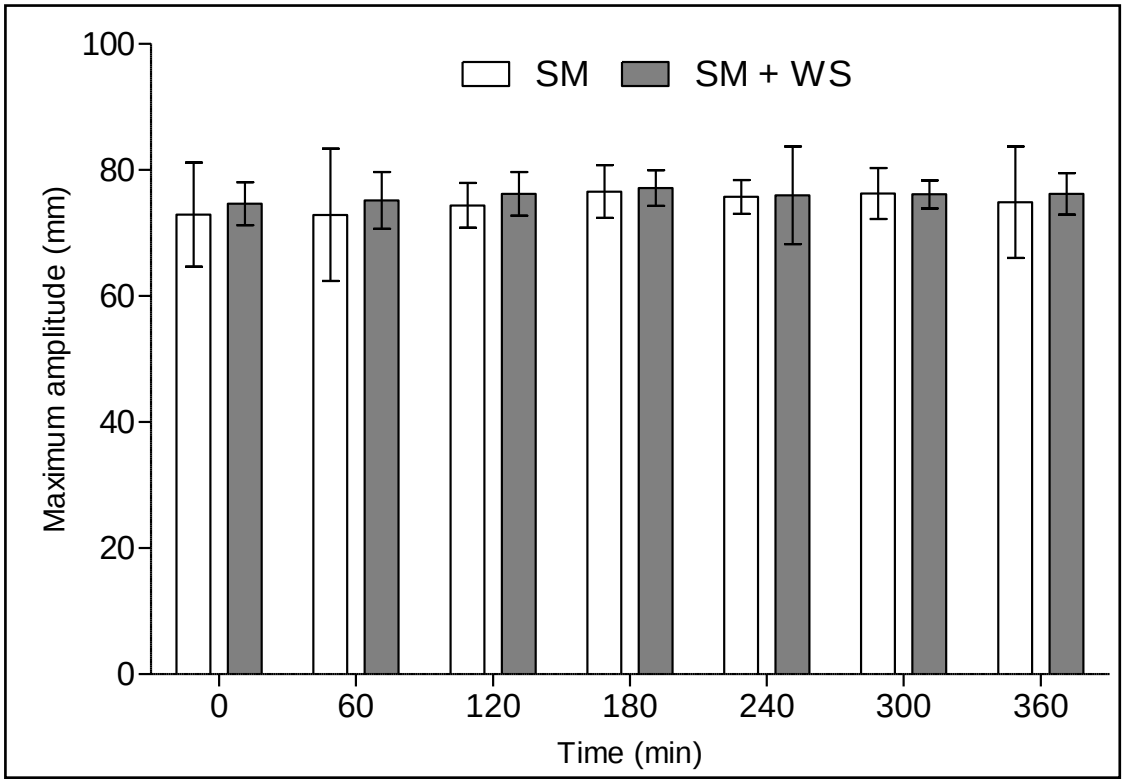

Figure 3.12: Total clot strength (maximum amplitude) of whole blood (from systemic circulation) following percutaneous application of sulphur mustard (SM) and subsequent application of WoundStat™ (SM+WS) to superficially damaged skin.

Values are expressed as mean ± standard deviation (n=6).

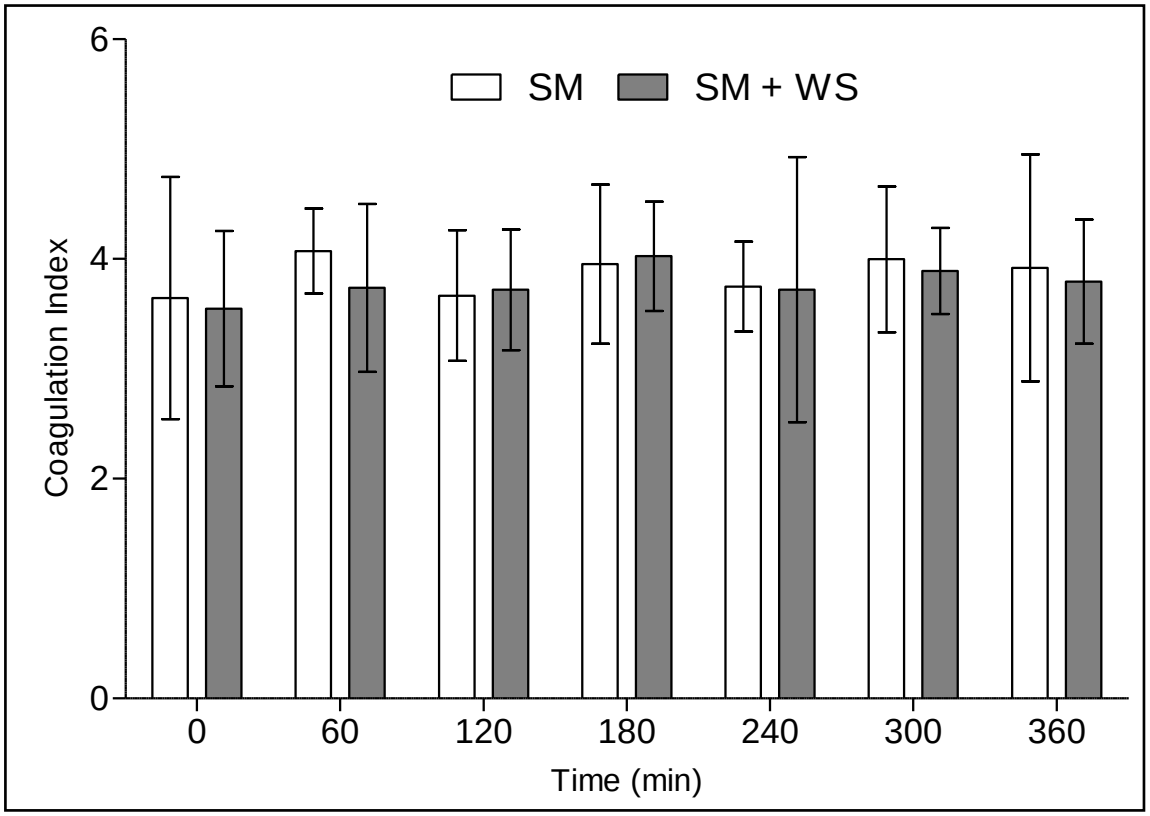

Figure 3.13: Overall assessment of coagulation (Coagulation Index; CI) of whole blood (from systemic circulation) following percutaneous application of sulphur mustard (SM) and subsequent application of WoundStat™ (SM+WS) to superficially damaged skin.

Values are expressed as mean ± standard deviation (n=6).

DISCUSSION

This study has shown that SM does not significantly affect coagulation *in vitro* and several haemostats have been identified that significantly enhance coagulation in SM-contaminated blood. Several parameters of performance for one effective haemostat, WoundStat™ was found to be adversely affected by SM-contaminated blood. However, this was not observed *in vivo.*

Thrombelastography has been previously validated for use as an *in vitro* method of monitoring coagulation and evaluating the efficacy of haemostats in whole blood (Kheirabadi*, et al*. 2009, Kheirabadi*, et al*. 2010, Ostomel*, et al*. 2006). However, there are a number of caveats that must be taken into consideration when interpreting and extrapolating the findings from this study.

Relevance of application of test products

Some of the test haemostats require sustained pressure to be applied in order to achieve cessation of haemorrhage (Pusateri*, et al*. 2003a, Pusateri*, et al*. 2003b, Ward*, et al*. 2007, Kheirabadi*, et al*. 2005). Chitosan-based haemostats also have mucoadhesive properties and can seal the vessel rupture (Sambasivan*, et al*. 2009). Clearly testing these mechanisms of action could not be achieved using TEG. Therefore, only the intrinsic haemostatic capacity of products was evaluated. This may have resulted in some products not performing as well as anticipated based on previous *in vivo* data (Pusateri*, et al*. 2003a, Kheirabadi*, et al*. 2009).

Suitability of pig blood as a model for human blood

The use of animal blood as a substitute for human blood has the potential limitation of not accurately modelling the response of human blood *in vivo* (Siller-Matula, *et al.* 2008). This could result in the selection of an ineffective product or elimination of products that would otherwise be suitable. The pig has been previously described as a suitable model for researching *in vitro* blood coagulation (Velik-Salchner*, et al*. 2006, Olsen*, et al*. 1999) although there are key differences. Notably, pig's blood coagulates more easily than human blood due to increased intrinsic coagulation pathway activity (Olsen*, et al*. 1999). Also, there are differences in the platelet surface protein $GPII_b/III_a$ between human and porcine blood which may affect total clot strength (Royo*, et al*. 1998). However, total clot strength measured by TEG was comparable between human and porcine blood (Kessler*, et al*. 2011). Ideally, the findings of this study should be further validated with human blood but the number of samples required may make this unfeasible.

Use of citrated blood

Sodium citrate is an effective anticoagulant (through chelation of calcium ions) and increases the viability window for use in coagulation studies (Mann et al. 2007). However, the blood must be reactivated using calcium chloride. Thrombelastography parameters for recalcified citrated blood differ significantly to those for native blood (Camenzind*, et al*. 2000). Therefore, it is possible that the haemostatic ability of some products may also be affected by recalcified citrated blood. In light of the potential limitations, the key findings of this study will be discussed.

Sulphur mustard did not have a significant effect on any of the coagulation parameters measured regardless of whether the blood was obtained from unexposed animals (and exposed to SM *in vitro*) or from animals exposed to SM percutaneously (10 µl via superficially damaged skin). This was surprising as SM is able to alkylate proteins found in blood (Black*, et al*. 1997, Noort*, et al*. 1996), thus it is reasonable to postulate that SM could alkylate proteins key to coagulation such as thrombin. However, if reactions with coagulation factors do occur they are not sufficient to adversely affect coagulation as measure by TEG. As the SM-treated blood was used exclusively on two TEG machines there is the possibility that this was due to machine or channel bias. However, no statistically significant difference in R time results for control blood were observed when individual channels were compared (Figure 3.2).

Sulphur mustard has also been shown to increase expression of uPA (Detheux*, et al*. 1997). This enzyme cleaves inactive plasminogen to produce the active serine protease, plasmin (Vasquez*, et al*. 1998). Plasmin cleaves the cross-linked fibrin mesh resulting in thrombolysis (Pryzdial*, et al*. 1999). Therefore, it is possible that SM could increase the rate of clot lysis through activation of uPA. In the TEG study in which blood was contaminated *in vitro*, clot viscosity was only measured until maximum amplitude was reached so observation of any subsequent effects on clot lysis was unlikely. However, clot lysis was also measured for whole blood obtained from animals exposed percutaneously to SM (via superficially damaged skin) *in vivo*. There were no statistically significant differences in clot lysis between the baseline (0 min; unexposed) samples and the samples obtained post SM challenge (60 – 360 min post challenge). Therefore, reported changes in haematology for SM exposure victims (Mahmoudi*, et al*.

2005) which could affect coagulation may occur at later time points to those measured in this study.

Four haemostats (WoundStat™, FastAct®, VitaGel™ and ProQR®) significantly increased the rate of coagulation (reduction in R Time) and overall clotting kinetics (K time and alpha-angle) compared to control blood. However, VitaGel™ was the only haemostat to significantly increase shear elastic modulus strength (SEMS) and overall coagulation index in untreated blood compared to control blood. The mechanisms of action for FastAct® and VitaGel™ are similar: both are liquid formulations which contain thrombin. Thrombin is a key clotting factor in the amplification and propagation phases of coagulation and cleaves fibrinogen to fibrin to produce a fibrin clot (Monroe*, et al*. 2002). This would be expected to result in a reduction in both R and K Time and an increase in α-angle (Kawasaki*, et al*. 2004, Johansson*, et al*. 2008, Rivard*, et al*. 2005). Thrombin is also a potent platelet agonist (Brass. 2003). Activated platelets provide a platform for the propagation phase of coagulation, as well as providing structural support to the fibrin clot mesh resulting in increased total clot strength (Monroe and Hoffman. 2006).

In general, SM did not have a significant effect on haemostat performance. One notable exception was the SEMS and coagulation index values for WoundStat™ plus SM treatment group which were significantly lower compared to both the control and WoundStat™ only treatment groups. The SEMS is derived from the maximum amplitude thrombelastography parameter and is representative of total clot elasticity. Clot strength is a direct function of the dynamic properties of fibrin and platelet binding via $GPII_b/III_a$ receptor (Mousa*, et al*. 2000). Therefore, the addition of SM in combination with WoundStat™ may cause a structural or functional change in

$GPII_b/III_a$ integrin, platelet or fibrin or a change in platelet number. As the full haemostatic mechanism of WoundStat™ has yet to be elucidated, it is difficult to postulate which particular aspect(s) of WoundStat™-induced coagulation was affected by SM. Although, it is likely that the propagation phase of coagulation is the affected phase of coagulation as R time, K time and alpha-angle were unaffected by SM in combination with WoundStat™. Samples were analysed in duplicate with all four treatment groups analysed at the same time using blood from the same animals. Therefore, it is unlikely that variations in fibrin concentration or platelet number between the test conditions were responsible for this effect. However, the coagulation parameters of blood obtained from animals treated with SM and WoundStat were measured and there was not a statistically significant difference in clot strength when compared to the baseline sample (unexposed; 0 min) or animals exposed to SM only (Figure 3.12 and 3.13). Therefore, the effects on clot strength seen *in vitro* may be related to SM or WoundStat™ dose, or due to direct interactions between SM/WoundStat™ and platelets.

Three haemostats (QuikClot ACS+®, HemCon® and Celox™) were not found to significantly enhance any of the coagulation parameters measured compared to the control. This was surprising, as the products are reported to be effective *in vivo* in the literature (Ahuja*, et al*. 2006, Pusateri*, et al*. 2003b, Arnaud*, et al*. 2007). However, Kheirabadi *et al.* (2009) also observed a lack of *in vitro* efficacy for HemCon® and Celox™. The poor performance of these products in this model could be due to the lack of physical compression that would normally be applied under conditions of actual use. Also, the mucoadhesive properties of chitosan-based haemostats (HemCon® and Celox™) play a key role in arresting bleeding by forming a seal at the site of vessel

rupture a mechanism that would be absent *in vitro*. Nevertheless, all three products are supposed to be able to clot blood via electrostatic interactions with red blood cells (Kozen*, et al*. 2008, Kozen*, et al*. 2007, Monroe and Hoffman. 2006, Najjar*, et al*. 2004, Hampton and Mitchell. 1966), and so this complete lack of efficacy was unexpected.

Conclusions

Thrombelastography provides a suitable *in vitro* model for the quantification of haemostat efficacy in untreated and SM-treated blood. This study has identified that SM had no measurable effect on TEG coagulation parameters. Subsequent studies using blood obtained from animals exposed to SM *in vivo* are in agreement with the *in vitro* findings. A number of haemostatic products have been identified which are able to significantly increase the rate of clotting and are not impeded by the presence of SM. These haemostats could be effective as haemostatic decontaminants and warrant further testing.

Recommendations for future work

- Haemostatic products should be assessed for ability to decontaminate skin (intact and damaged) *in vitro* (Chapter 4).
- The effect of SM on coagulation should be evaluated using human blood to establish whether there are species-specific effects.

Chapter 4

The effect of superficial damage on the percutaneous absorption of SM and efficacy of haemostats as decontaminants in vitro

INTRODUCTION

Damaged skin has been shown to have a higher permeability to hydrophobic compounds than undamaged skin *in vitro* (Borrás-Blasco*, et al*. 1997) and *in vivo* (Gunther*, et al*. 1998; Jakasa*, et al*. 2006). As previously described in Chapter 1, the primary barrier to dermal absorption is generally regarded to be the SC (Blank. 1965, Monash. 1958). If the SC were removed due to a penetrating injury or abrasion, it is reasonable to postulate that the penetration of SM would be increased and this could result in increased toxicity. However, there is little in the published literature to substantiate this hypothesis.

As described in Chapter 1, current in-service decontaminants fall into two broad categories; reactive decontaminants and adsorptive (passive) decontaminants. In this Thesis the adsorptive properties of some haemostats were exploited to investigate whether they would be suitable as decontaminants. In addition, liquid haemostats (containing activated clotting factors) were combined with a novel reactive decontaminant to assess efficacy as a decontaminant.

The static diffusion cell system is an established technique for measuring the dermal absorption of chemicals including SM (Chilcott*, et al*. 2005, Schmook*, et al*. 2001). This *ex vivo* approach is also in line with the "3 Rs" ethical framework as it significantly reduces the number of animals needed for the required screening study.

Aims

To utilise the static diffusion cell system to investigate;

- the effect of skin damage on the rate and extent of dermal absorption of SM *in vitro*,
- the efficacy of candidate haemostats as decontaminants for undamaged skin and damaged skin *in vitro*.

MATERIALS AND METHODS

Full details of methods employed in this study are described in Chapter 2. Briefly, the dermal absorption of ^{14}C-SM through split-thickness, intact or superficially damaged porcine skin was measured using a static diffusion cell system. Skin was superficially damaged by the removal of the upper skin layers (nominal 100 μm removed). This uniform damage was achieved using an electric dermatome (as described in Chapter 2). The decontamination efficacy of each test haemostatic products (Table 2.2) was evaluated, with standard military decontaminants (Table 2.3) used as to bench-mark efficacy. Up to 5 treatment groups (n=6) and a control group (untreated; n=6) were assessed per experiment. Table 4.1 outlines the treatment groups included in each experiment (study 1 – 4). Dermal absorption was measured over a 24 h period and the amount of ^{14}C-SM remaining in the test product, skin and receptor fluid was measured at the end of the study. Ineffective products were eliminated from further evaluation (*in vivo* damaged skin model; Chapter 6) as shown in Figure 4.1.

	Undamaged skin			Damaged skin
Study number	1	2	3	4
Treatment group	Control	Control	Control	Control
	WS	FA	FA + TOP	Damaged control
	QC	VG	VG + TOP	WS (damaged)
	PQR	HC	M291	QC (damaged)
	CX	TOP		PQR (damaged)
	FE	RSDL®		FE (damaged)

Table 4-1: Treatment group designation for the studies described in Chapter 4.

Up to 4 haemostats (n=6) were tested per experiment (WoundStat™; WS, QuikClot ACS+®; QC, ProQR®; PQR, Celox™; CX, HemCon®; HC, FastAct®; FA, VitaGel™; VG, tetraglyme, oxime and polyethyleneimine; TOP, FastAct® in combination with TOP; FA + TOP and VitaGel™ in combination with TOP; VG + TOP). The military decontaminants (fuller's earth; FE, Reactive Skin Decontamination Lotion®; RSDL® and M291) were included as a positive controls (n=6). Studies 1 – 3 measured SM penetration through undamaged (abdominal flank) skin and study 4 measured SM penetration through superficially damaged (dorsum) skin. Undamaged dorsal skin served as a validation control (as described in Chapter 2).

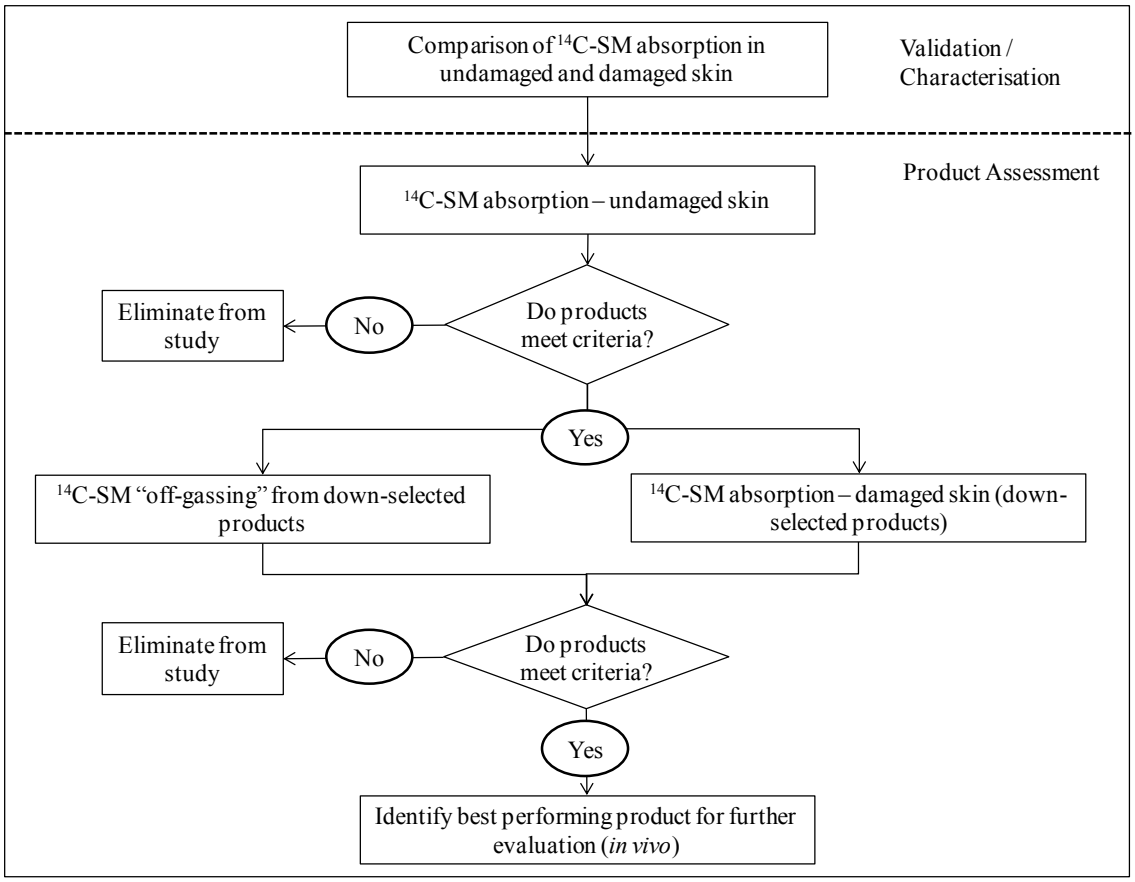

Figure 4.1: Decision process flow chart for haemostatic product down-selection to identify suitable product to test in vivo.

RESULTS

Penetration of SM – difference between damaged and undamaged skin

There was a significant (2 – 3 fold) increase in the maximum rate of absorption (J_{max}) of ^{14}C (derived from ^{14}C–SM) penetration through dorsal skin following damage ($p<0.05$; Figure 4.2 and Table 4.2). There were no significant differences in the absorption kinetics (J_{max}) or the total amount of ^{14}C (derived from ^{14}C–SM) penetrating through the skin neither between individual batches of abdominal skin nor between undamaged dorsal and abdominal skin (Table 4.2 and Figure 4.3). However, the recovery of ^{14}C-SM from one batch of abdominal skin (study 2; Figure 4.4) was significantly greater than the other abdominal skin samples.

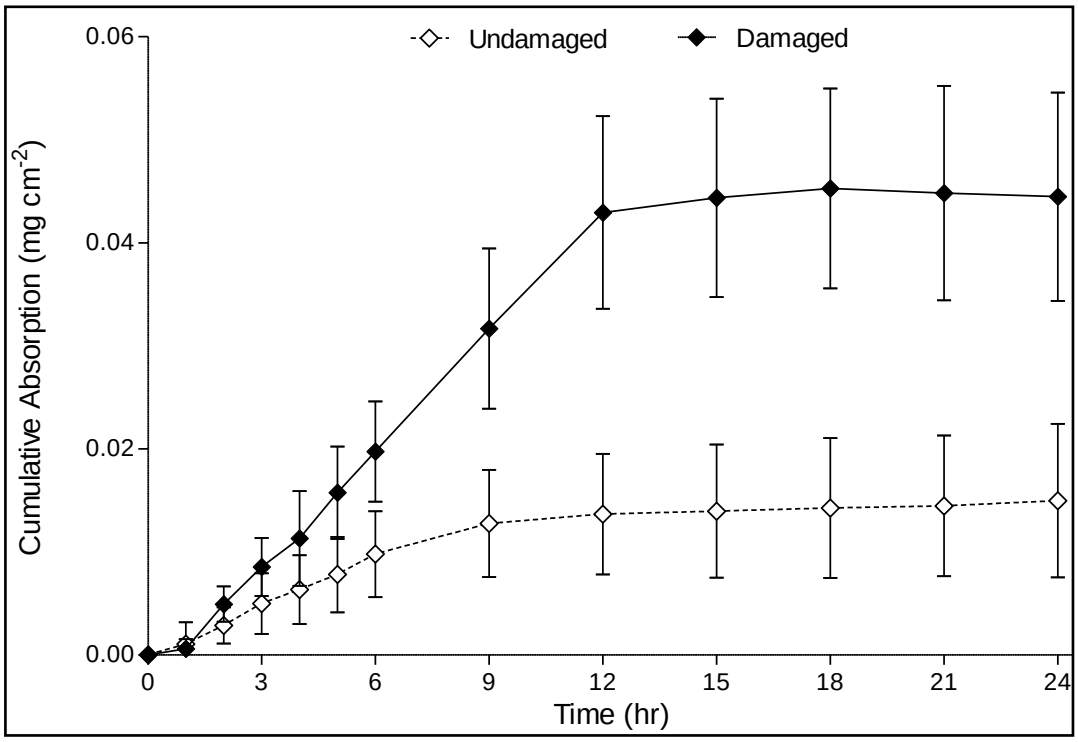

Figure 4.2: The cumulative absorption of ^{14}C (derived from ^{14}C-SM) into the receptor fluid through split thickness undamaged and damaged (top 100 µm removed) control, dorsal skin.

Values are expressed as mean ± 95% confidence intervals (n=6).

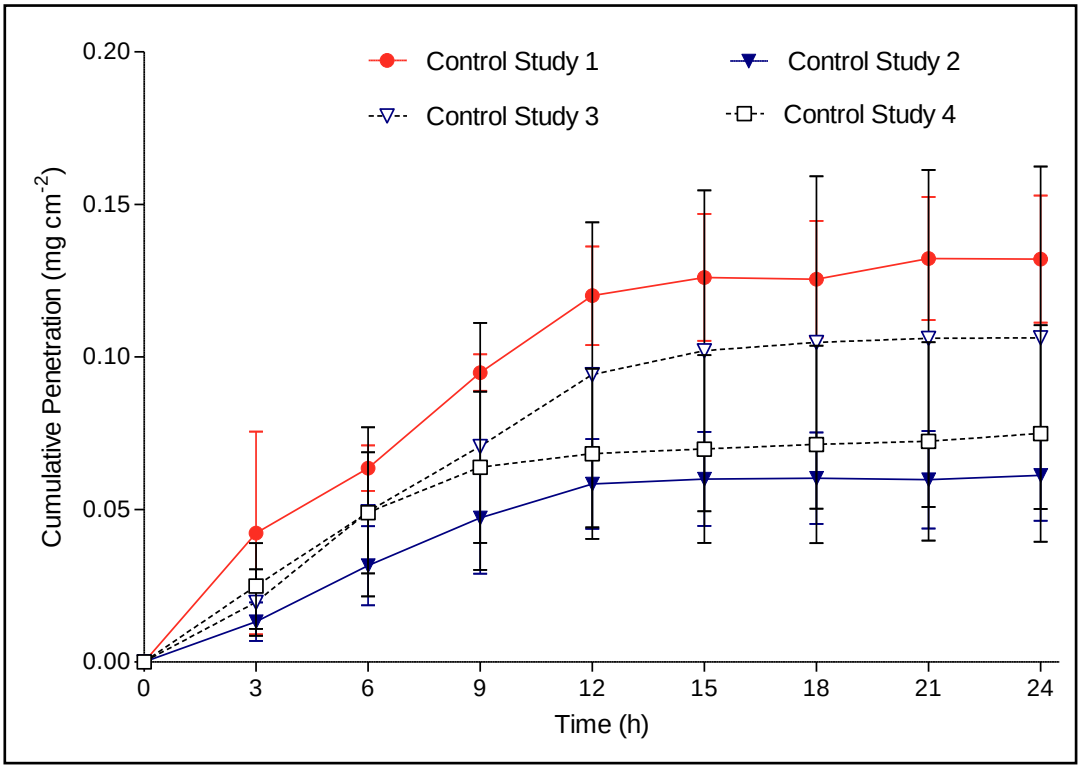

Figure 4.3: Cumulative absorption of ^{14}C (derived from ^{14}C–SM) penetrating split-thickness, undamaged abdominal and dorsal skin.

Values are expressed as mean ± S.D. (n=6) for studies 1 – 3 (undamaged; abdominal skin, solid line) and study 4 (undamaged; dorsal skin, dashed line).

		Maximum rate of absorption ($\mu g\ cm^{-2}\ h^{-1}$)	Total absorption at 24 h ($\mu g\ cm^{-2}$)
Undamaged Abdominal	Study 1	5.9 ± 3.2**	104.1 ± 57.4**
	Study 2	5.7 ± 2.3**	61.2 ± 14.9**
	Study 3	8.5 ± 4.9**	106.4 ± 56.1**
Undamaged Dorsum	Study 4	6.5 ± 2.6**	74.9 ± 35.5**
Damaged Dorsum	Study 4	18.5 ± 4.2	222.4 ± 48.2

Table 4-2: The maximum rate of absorption (J_{max}) and total absorption at 24 h of ^{14}C (derived from ^{14}C–SM) through split-thickness undamaged and damaged skin.

*Average values (mean ± S.D.) are shown for control treatment group for each study (n=6). Studies 1 – 3 used undamaged abdominal flank skin, whilst study 4 used undamaged and damaged dorsal skin. Statistically significant differences between undamaged and damaged skin are indicated, where ** represents a p-value of <0.01.*

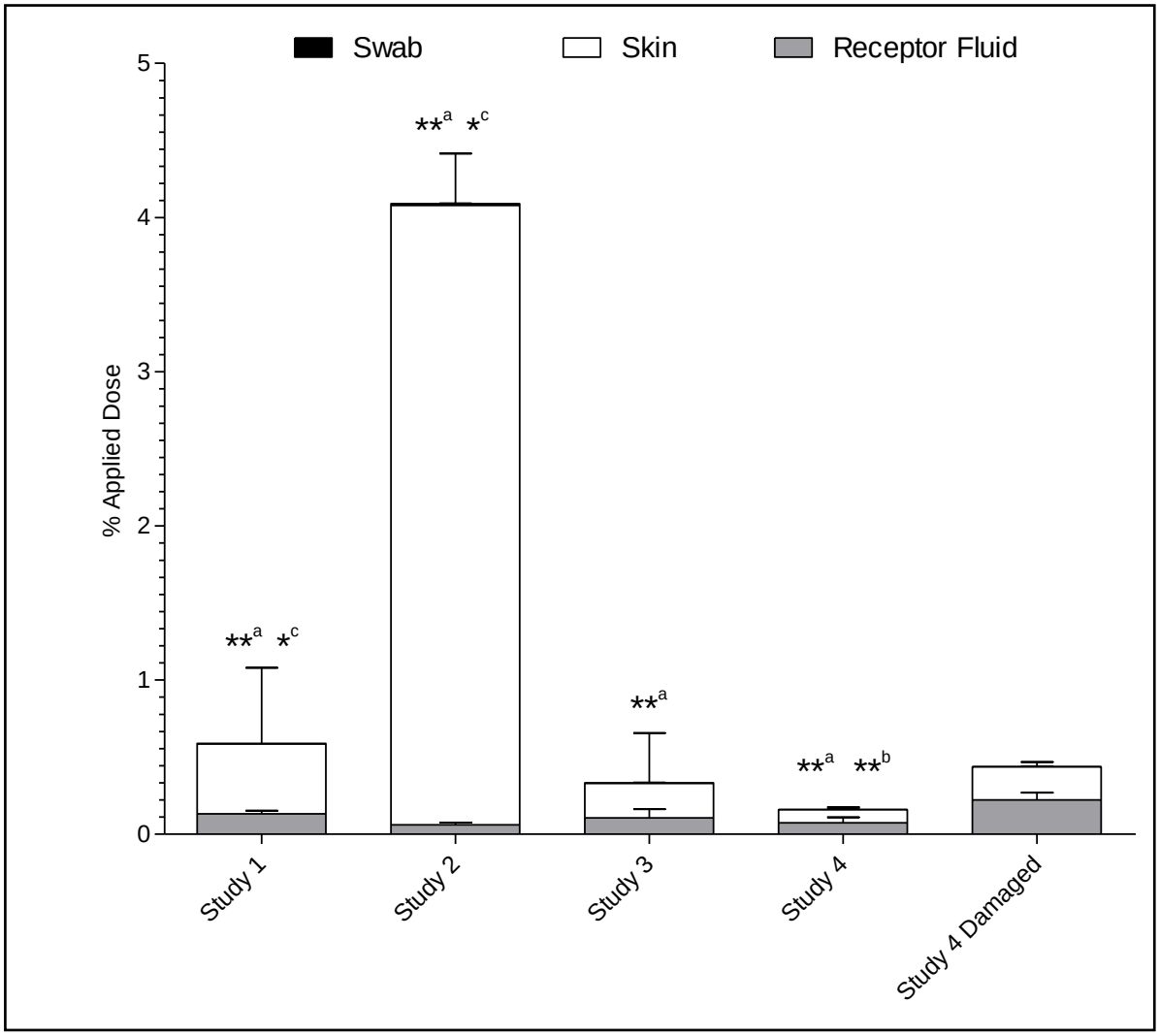

Figure 4.4: The distribution of ^{14}C (derived from ^{14}C–SM) recovered from the skin surface (swab), within the skin and receptor chamber fluid 24 h post exposure

*Data are expressed as logged mean ± S.D. (n=6). Studies 1 – 3 used undamaged abdominal flank skin, whilst study 4 used undamaged and damaged dorsal skin. Statistical significance differences between undamaged and damaged skin are shown, where * and ** represents p-values of <0.05 and <0.01, respectively for swab[a], skin[b] and receptor fluid[c].*

Effectiveness of haemostatic products as decontaminants for sulphur mustard – undamaged skin

WoundStat™ and fuller's earth both significantly reduced the dermal absorption ($p<0.01$; rate and extent) of ^{14}C (derived from ^{14}C–SM) through undamaged skin over a 24 h period (Table 4.3 and Figure 4.5). In comparison with untreated (control) skin, the total amount penetrating into the receptor fluid over 24 h was reduced by 92 ± 2.7% (83.6 ± 54.7 μg cm^{-2} vs. 7.1 ± 2.3 μg cm^{-2}) and 90 ± 5.1% (83.6 ± 54.7 μg cm^{-2} vs. 8.7 ± 4.3 μg cm^{-2}) following treatment with fuller's earth and WoundStat™, respectively. There was not a statistically significant difference in total dermal absorption for cells treated with QuikClot ACS+®, Celox™ or ProQR® compared to the control group (Table 4.3).

The amount of ^{14}C (derived from ^{14}C–SM) recovered from the skin after 24 h was significantly reduced for diffusion cells treated with WoundStat™ or fuller's earth compared to control diffusion cells ($p<0.01$; Figure 4.6). There was no significant difference in the amount of ^{14}C (derived from ^{14}C–SM) recovered from skin treated with QuikClot ACS+®, ProQR® or Celox™ and control (untreated) (Figure 4.6). Significant increases in the amount recovered from the skin surface (swab) were seen for ProQR® (14-fold) and fuller's earth (109-fold) compared to control values ($p<0.01$). The amount recovered from the haemostat was significantly higher for WoundStat™ compared to Celox™ ($p<0.001$) and QuikClot ACS+® ($p<0.05$) and fuller's earth compared to Celox™ ($p<0.01$; Figure 4.6).

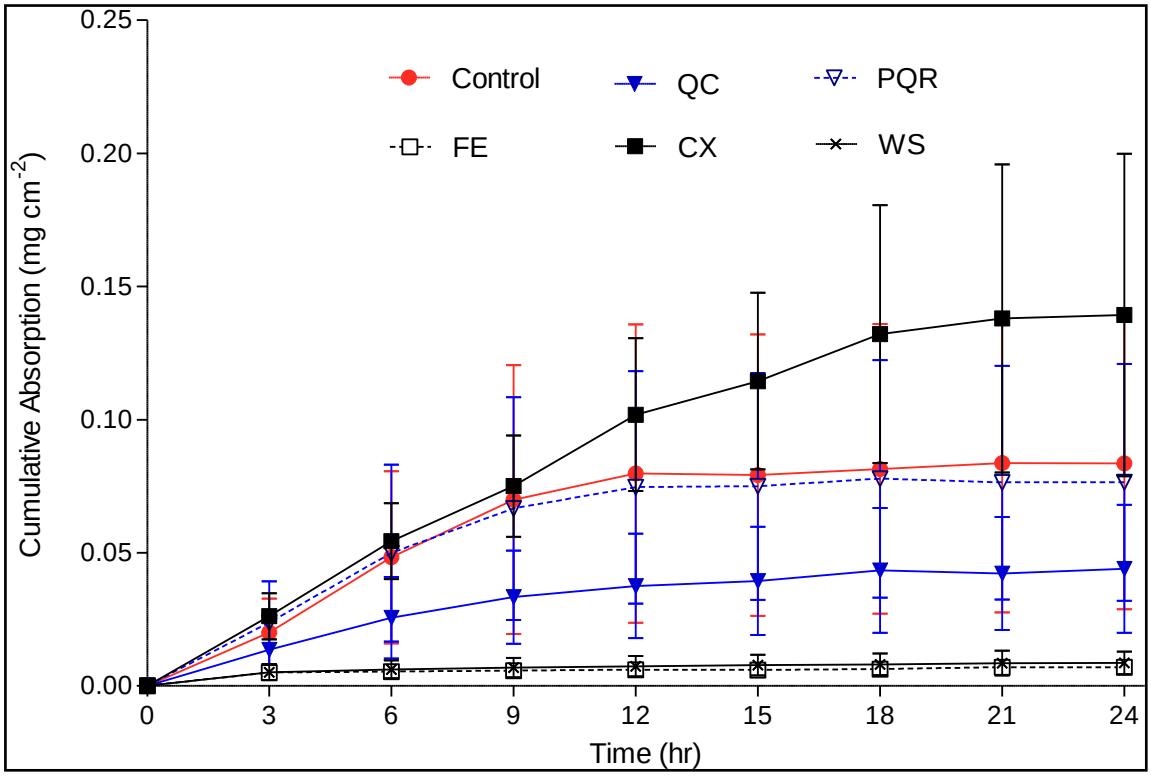

Figure 4.5: Cumulative absorption of ^{14}C (derived from ^{14}C–SM) penetrating undamaged skin following application of haemostatic products

Haemostats tested included: WoundStat™; WS, QuikClot ACS+®; QC, ProQR®; PQR and Celox™; CX. A standard military decontaminant (fuller's earth; FE) was included as a positive control. Values are expressed as mean ± S.D. (n=6).

Treatment Group	Maximum rate of absorption ($\mu g\ cm^{-2}\ h^{-1}$)	Total absorption at 24 h ($\mu g\ cm^{-2}$)
Control	5.9 ± 3.2	104.1 ± 57.4
WS	0.3 ± 0.1**	8.9 ± 4.3**
FE	0.1 ± 0.09**	7.1 ± 2.3**
QC	3.3 ± 1.6	44.0 ± 24.0
PQR	7.1 ± 4.4	76.5 ± 44.5
CX	8.2 ± 1.9	139.3 ± 60.6

Table 4-3: The maximum rate of absorption (J_{max}) and total absorption at 24 h of ^{14}C (derived from ^{14}C–SM) through split thickness undamaged skin following application of haemostatic products.

*Average values (mean ± S.D.) are shown for control and treatment groups (n=6). Statistically significant differences between control and decontaminated skin are indicated, where ** represents a p-value of <0.01.*

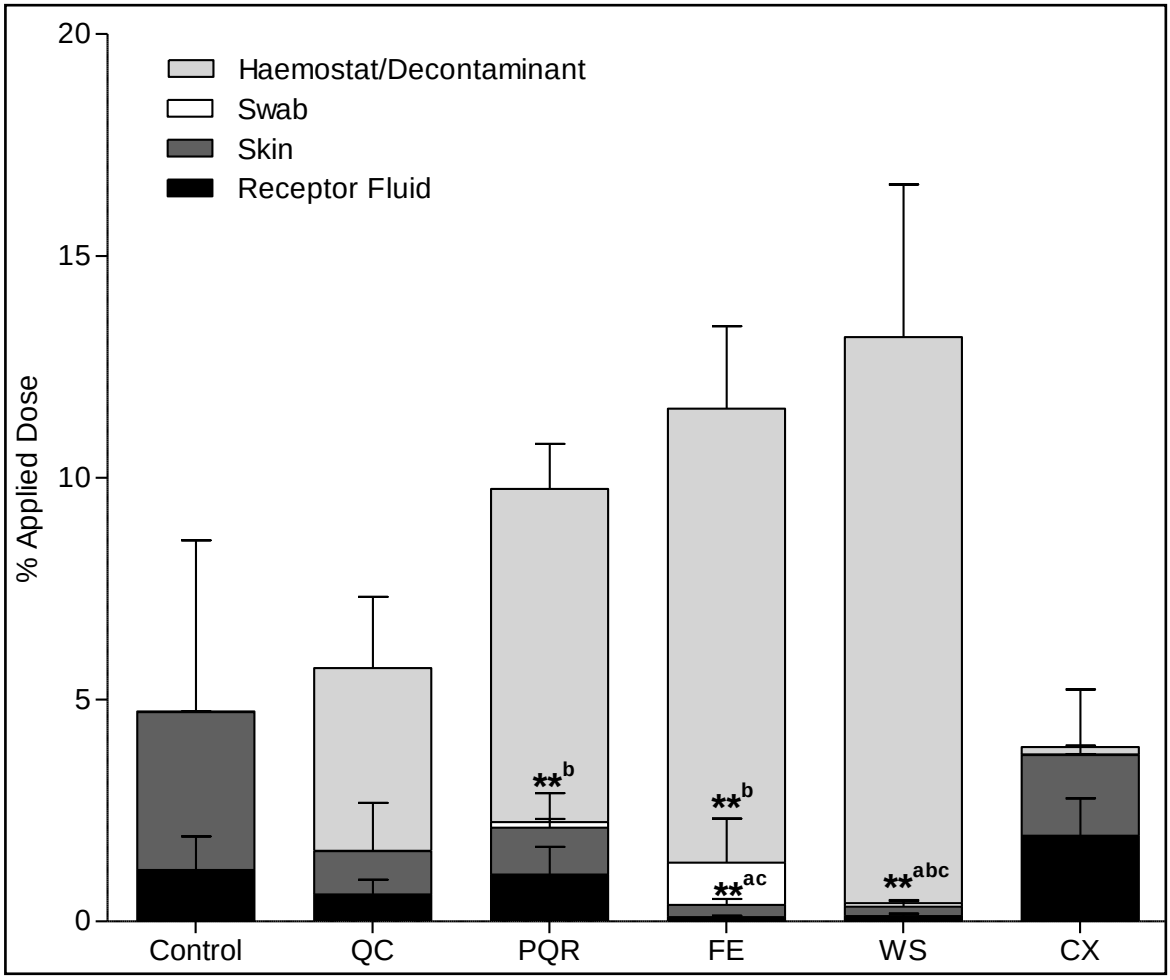

Figure 4.6: The distribution of ^{14}C (derived from ^{14}C–SM) recovered from undamaged skin at 24 h post-exposure following application of haemostatic products.

*Haemostats tested included: WoundStat™; WS, QuikClot ACS+®; QC, ProQR®; PQR and Celox™; CX. A standard military decontaminant (fuller's earth; FE) was included as a positive control. Individual values are mean ± S.D. (n=6). Statistically significant differences between control and treated cells are shown, where ** represents a p-value of <0.01 for skin[a], swab[b] and receptor fluid[c].*

VitaGel™ and FastAct® both significantly increased the rate and extent of ^{14}C (derived from ^{14}C–SM) dermal absorption over a 24 h period compared to the control group ($p<0.01$; Figure 4.7 and Table 4.4). In comparison with the control group, the total amount penetrating into the receptor fluid over 24 h was increased by 657% (61.2 ± 14.9 μg cm^{-2} vs. 401.9 ± 115.4 μg cm^{-2}) and 512% (61.2 ± 14.9 μg cm^{-2} vs. 313.2 ± 75.6 μg cm^{-2}) for VitaGel™ and FastAct®, respectively. Following treatment with HemCon®, there was a significant increase in the total amount of ^{14}C (derived from ^{14}C–SM) penetrating the skin ($p<0.05$; Figure 4.7 and Table 4.4). The rate of absorption was also significantly higher following treatment with HemCon® ($p<0.01$). The rate of absorption was significantly reduced ($p<0.05$) following application of Reactive Skin Decontamination Lotion® (RSDL®) or tetraglyme, oxime and polyethyleneimine (TOP). However, there was no significant difference in the total amount absorbed through the skin at 24 h (Table 4.4) in these treatment groups.

Statistically significant reductions in the amount of ^{14}C (derived from ^{14}C–SM) recovered within the skin compared to the control group were observed for diffusion cells treated with FastAct® and VitaGel™ ($p<0.01$; Figure 4.8). Significant increases in the amount recovered from the skin surface (swab) were seen for RSDL® and TOP treatment groups compared to the control group (Figure 4.8). The amount of recoverable ^{14}C (derived from ^{14}C–SM) remaining in the test products, HemCon® and RSDL® was significantly higher than the amount of ^{14}C (derived from ^{14}C–SM) recovered from the novel decontaminant, TOP and the liquid haemostats; FastAct® and VitaGel™ (Figure 4.8).

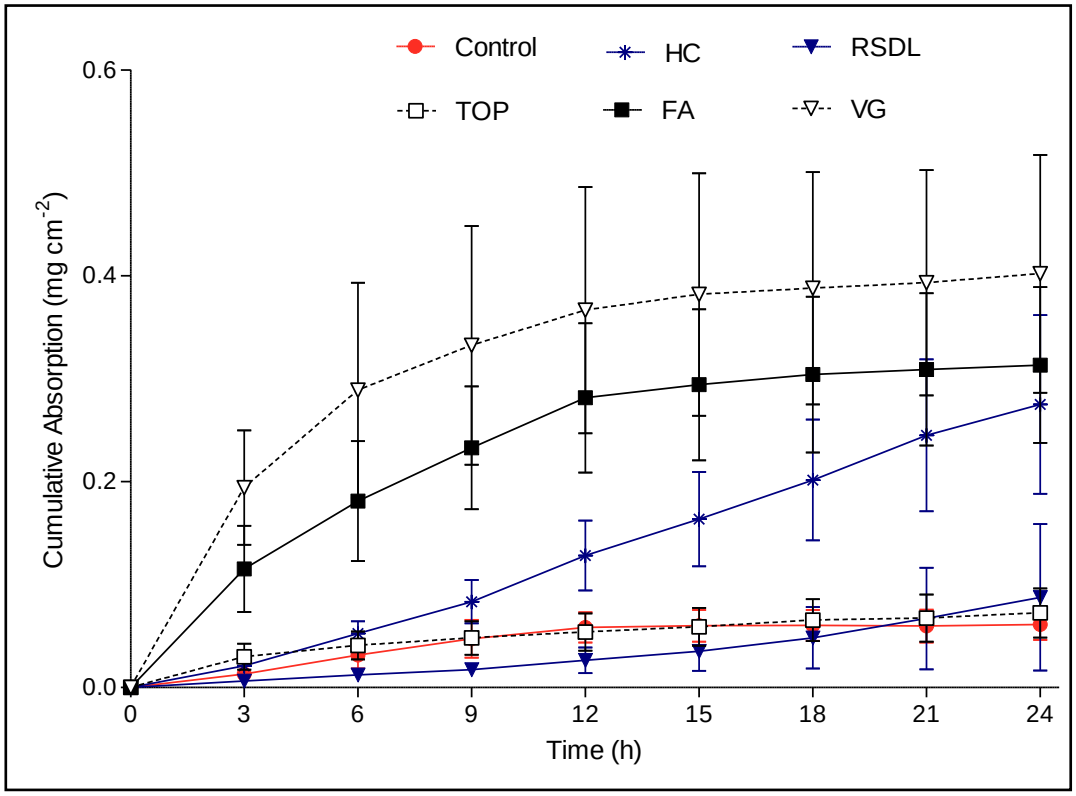

Figure 4.7: Cumulative absorption of ^{14}C (derived from ^{14}C–SM) penetrating undamaged skin following application of haemostatic products.

Haemostats tested included: HemCon®; HC, FastAct®; FA and VitaGel™; VG. A novel reactive decontaminant (tetraglyme, oxime and polyethyleneimine; TOP) was also evaluated. A standard military decontaminant (Reactive Skin Decontamination Liquid®; RSDL®) was included as a positive control. Individual values are mean ± S.D. (n=6)

Treatment Group	Maximum rate of absorption ($\mu g\ cm^{-2}\ h^{-1}$)	Total absorption at 24 h ($\mu g\ cm^{-2}$)
Control	5.7 ± 2.3	61.2 ± 14.9
HC	10.4 ± 2.3*	275 ± 83.9**
RSDL	1.7 ± 1.0**	87.6 ± 71.2
TOP	3.0 ± 0.9*	72.4 ± 23.8
FA	19.6 ± 6.6**	313.2 ± 75.7**5
VG	23.0 ± 12.2**	401.8 ± 115.4**

Table 4-4: The maximum rate of absorption (J_{max}) and total absorption at 24 h of ^{14}C (derived from ^{14}C–SM) through split-thickness, undamaged skin following application of haemostatic products.

*Average values (mean ± S.D.) are shown for control and treatment groups (n=6). Statistically significant differences between control and decontaminated skin are indicated, where * and ** represents a p-value of <0.05 and <0.01, respectively.*

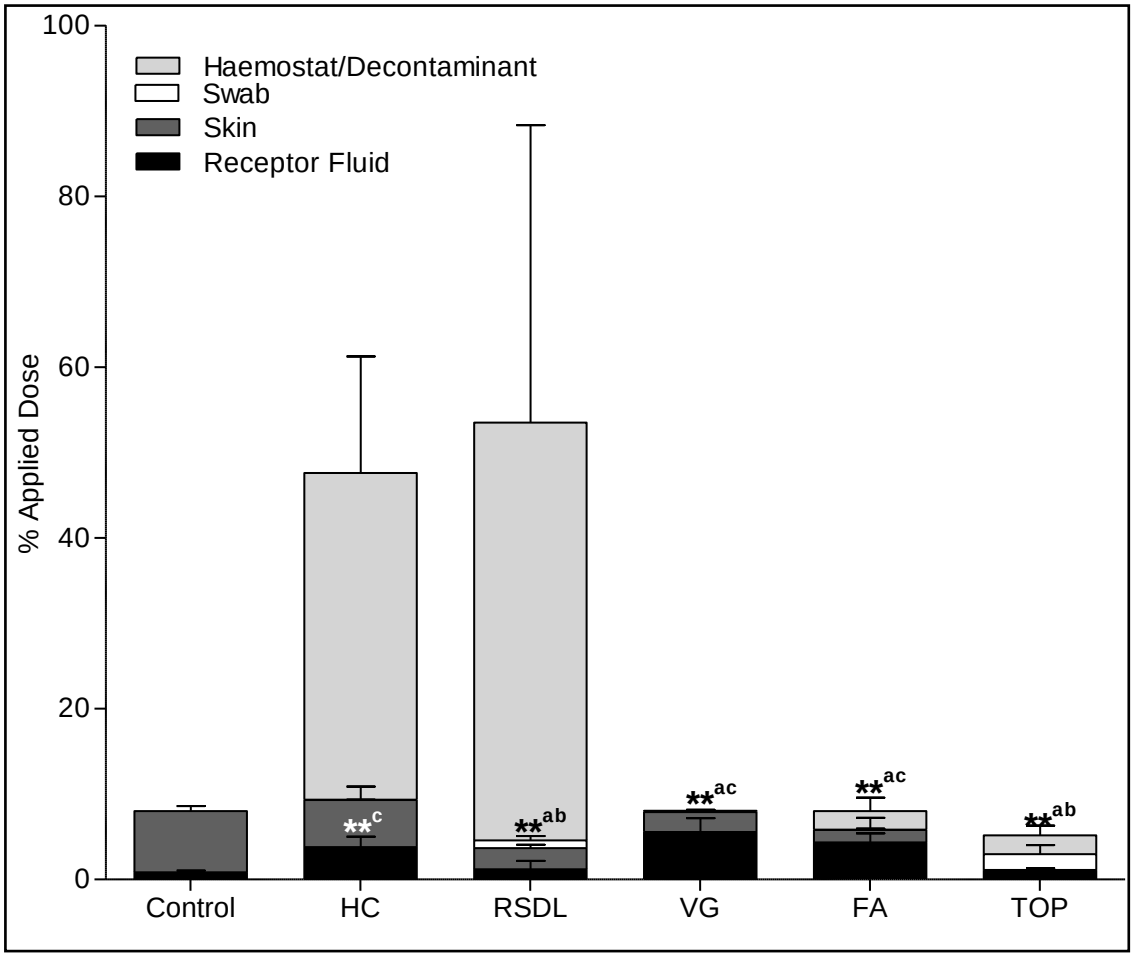

Figure 4.8: The distribution of ^{14}C (derived from ^{14}C–SM) recovered from undamaged skin at 24 h post-exposure following application of haemostatic products.

*Haemostats tested included: HemCon®; HC, FastAct®; FA and VitaGel™; VG. A novel reactive decontaminant (tetraglyme, oxime and polyethyleneimine; TOP) was also evaluated. A standard military decontaminant (Reactive Skin Decontamination Liquid®; RSDL®) was included as a positive control. Values are expressed as mean ± S.D. (n=6). Statistically significant differences between control and treated cells are shown, where ** represents a p-value of <0.01 for skin[a], swab[b] and receptor fluid[c].*

The significant enhancement in dermal absorption of ^{14}C (derived from ^{14}C–SM) observed following treatment with FastAct® and VitaGel™ (Figure 4.7) was absent when these products were applied to contaminated skin in combination with TOP (Figure 4.9). However, the maximum rate and total absorption of ^{14}C-SM following FastAct® + TOP and VitaGel™ + TOP treatments were not statistically different to control (untreated) skin (Table 4.5).

The military decontaminant (M291) significantly reduced the amount of ^{14}C (derived from ^{14}C–SM) absorbed through undamaged skin over a 24 h period ($p<0.01$; Table 4.5 and Figure 4.9). The amount of ^{14}C-SM recovered from the skin was significantly lower in the M291 treatment group (9-fold decrease) compared to the control group ($p<0.01$; Figure 4.10). Significant increases in the amount recovered from the skin surface (swab) were seen for all treatment groups compared to control group ($p<0.01$; Figure 4.10). The amount of ^{14}C (derived from ^{14}C–SM) recovered from M291 was significantly higher than amount retained in either the FastAct® + TOP or VitaGel™ + TOP treatment groups (Figure 4.10).

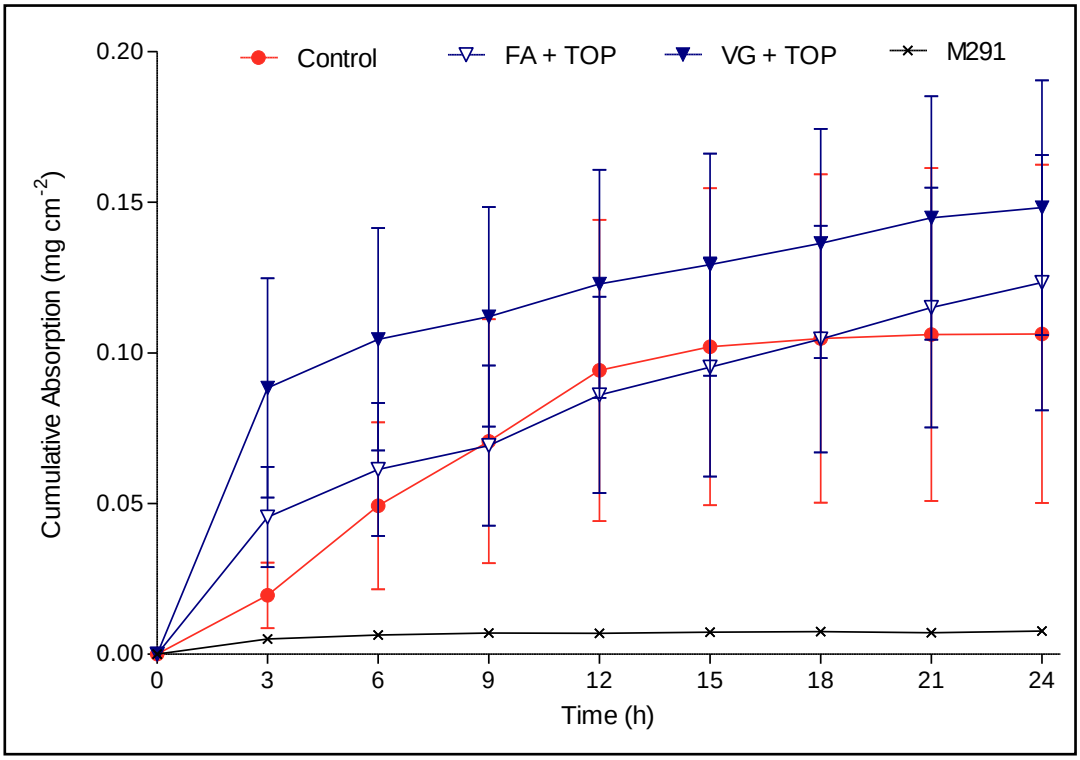

Figure 4.9: Cumulative absorption of ^{14}C (derived from ^{14}C–SM) penetrating undamaged skin following application of haemostatic products.

Haemostats tested included: FastAct® in combination with TOP; FA + TOP and VitaGel™ in combination with TOP; VG + TOP. A military decontaminant (M291) was included as a positive control. Individual values are mean ± S.D. (n=6).

Treatment Group	Maximum rate of absorption ($\mu g\ cm^{-2}\ h^{-1}$)	Total absorption at 24 h ($\mu g\ cm^{-2}$)
Control	8.5 ± 4.9	106.3 ± 56.1
FA + TOP	4.0 ± 2.0	123.3 ± 42.3
VG + TOP	4.0 ± 0.5	148.2 ± 42.3
M291	0.3 ± 0.1**	7.7 ± 1.3**

Table 4-5: The maximum rate of absorption (J_{max}) and total absorption at 24 h of ^{14}C (derived from ^{14}C–SM) through split-thickness, undamaged skin following application of haemostatic products.

*Average values (mean ± S.D.) are shown for control and treatment groups (n=6). Statistically significant differences between control and decontaminated skin are indicated, where ** represents a p-value of <0.01.*

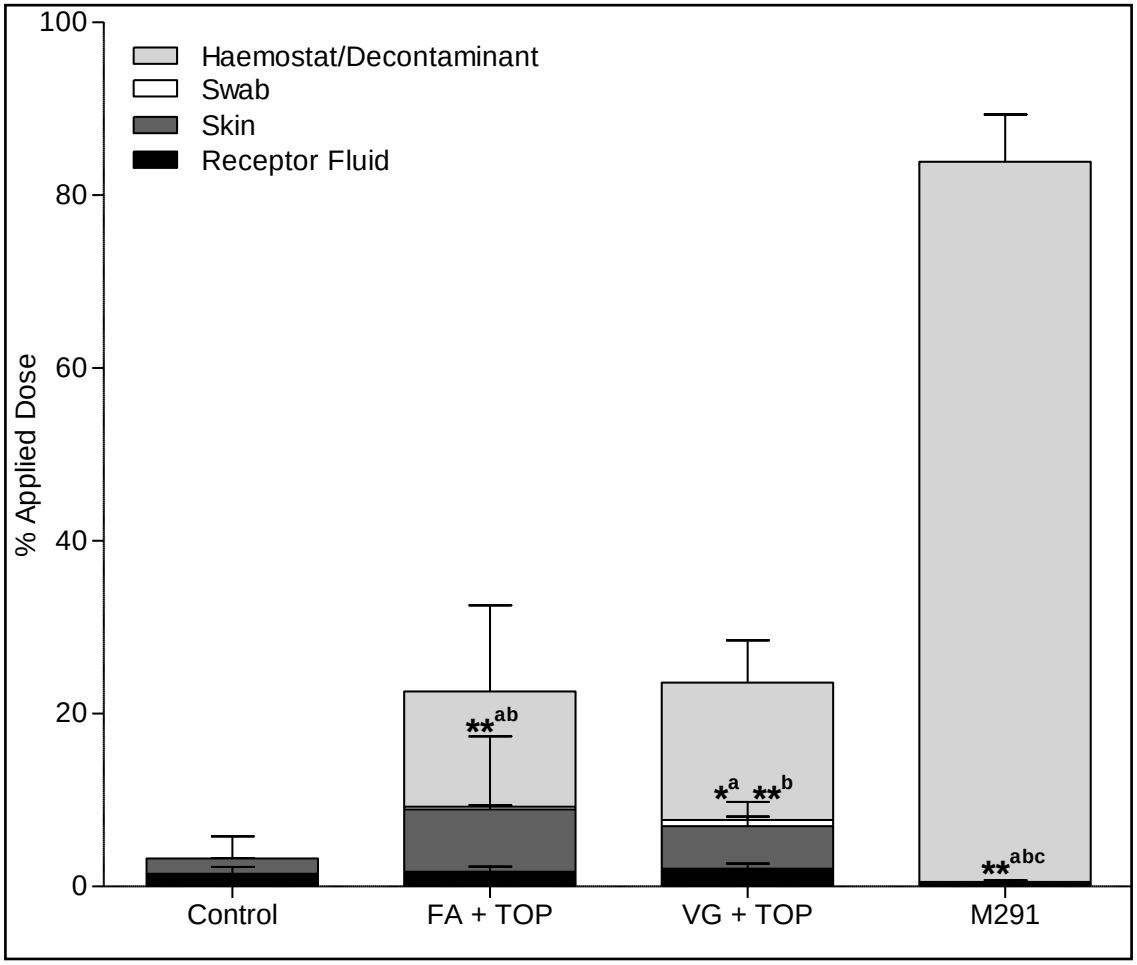

Figure 4.10: The distribution of ^{14}C (derived from ^{14}C–SM) recovered from undamaged skin at 24 h post-exposure following application of haemostatic products.

*Haemostats tested included: FastAct® in combination with TOP; FA + TOP and VitaGel™ in combination with TOP; VG + TOP. A military decontaminant (M291) was included as a positive control. Individual values are mean ± S.D. (n=6). Statistically significant differences between control and treated cells are shown, where * and ** represents p-values of <0.05 and <0.01 for skin[a], swab[b] and receptor fluid[c].*

Summary of results using undamaged skin

A summary of data from studies 1 – 3 is presented in Figure 4.11 and Table 4.6. WoundStat™ was the only haemostat tested that was consistently comparable in efficacy to the "benchmark" military products (fuller's earth and M291). Moreover, three products (HemCon®, VitaGel™ and FastAct®) caused a significant increase in the total absorbed dose of ^{14}C (derived from ^{14}C–SM). Therefore, the products selected for further evaluation using superficially damaged skin *in vitro* were WoundStat™, QuikClot ACS+® and ProQR®.

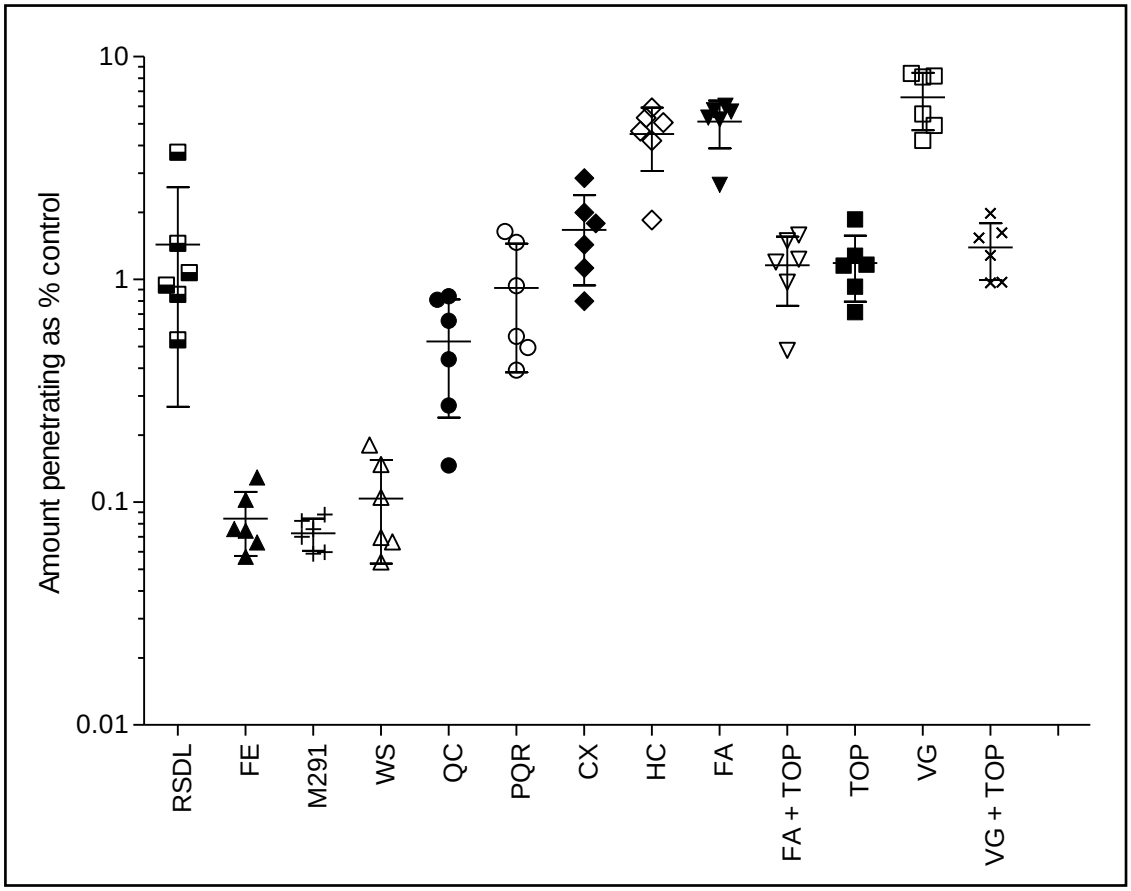

Figure 4.11: The total amount of ^{14}C (derived from ^{14}C–SM) penetrating undamaged skin 24 h post-exposure following application of haemostatic products.

Haemostats tested included: WoundStat™; WS, QuikClot ACS+®; QC, ProQR®; PQR, Celox™; CX, HemCon®; HC, FastAct®; FA, VitaGel™; VG, tetraglyme, oxime and polyethyleneimine; TOP, FastAct® in combination with TOP; FA + TOP and VitaGel™ in combination with TOP; VG + TOP. The military decontaminants (fuller's earth; FE, Reactive Skin Decontamination Lotion®; RSDL® and M291) were included as a positive controls. Penetration values have been normalised to control values for their respective study. Individual values are shown as well as mean (central line; n=6) and S.D. (outermost lines).

Treatment Group	Rate of Absorption	Extent of absorption
WS	-	-
QCS	0	0
PQR	0	0
VG	+	+
FA	+	+
TOP	-	0
FA + TOP	0	0
VG + TOP	0	0
CX	0	0
HC	+	+
FE	-	-
RSDL	0	0
M291	-	-

Significant increase compared to control	+
No significant difference compared to control	0
Significant decrease compared to control	-

Table 4-6: Dermal absorption of ^{14}C (derived from ^{14}C–SM), rate and extent at 24 h presented as a "traffic-light chart" following application of haemostatic products.

Haemostats tested included: WoundStat™; WS, QuikClot ACS+®; QC, ProQR®; PQR, Celox™; CX, HemCon®; HC, FastAct®; FA, VitaGel™; VG, tetraglyme, oxime and polyethyleneimine; TOP, FastAct® in combination with TOP; FA + TOP and VitaGel™ in combination with TOP; VG + TOP. The military decontaminants (fuller's earth; FE, Reactive Skin Decontamination Lotion®; RSDL® and M291) were included as a positive controls. The colours represent the efficacy of each product; where a significant increase (red; +), no significant difference (yellow; 0) or a significant decrease (green; -) in either rate or extent of absorption compared to the control is shown for each of the treatment groups.

Effectiveness of haemostatic products as decontaminants for sulphur mustard – damaged skin

Decontamination of damaged skin with WoundStat™, QuikClot ACS+® and fuller's earth consistently led to a significant reduction in the amount of ^{14}C (derived from ^{14}C–SM) absorbed through damaged skin over a 24 h period ($p<0.01$; Figure 4.12 and Table 4.7). However, there was no significant difference in total ^{14}C (derived from ^{14}C–SM) penetrating through the skin between controls and skin treated with ProQR®.

The amount of ^{14}C (derived from ^{14}C–SM) recovered from the skin was significantly lower following treatment with WoundStat™, QuikClot ACS+® or fuller's earth compared to control diffusion cells ($p<0.01$; Figure 4.13). The amount within the skin was not reduced for diffusion cells treated with ProQR®. Significantly more ^{14}C (derived from ^{14}C–SM) was recovered from the skin surface (swab) for cells treated with either fuller's earth or ProQR® compared to the control group. Significantly less ^{14}C-SM was distributed within the haemostat for the QuikClot ACS+® treatment group compared to ProQR® ($p<0.001$) and fuller's earth ($p<0.05$). There was also a significant difference in the amount recovered from the haemostat between the ProQR® and WoundStat™ treatment groups.

Fuller's earth was the only treatment less effective in decreasing ^{14}C-SM penetration through damaged skin compared to undamaged skin (Figure 4.14). WoundStat™ was the only candidate haemostat to significantly reduce the penetration of ^{14}C (derived from ^{14}C–SM) through both undamaged and damaged skin (Table 4.8).

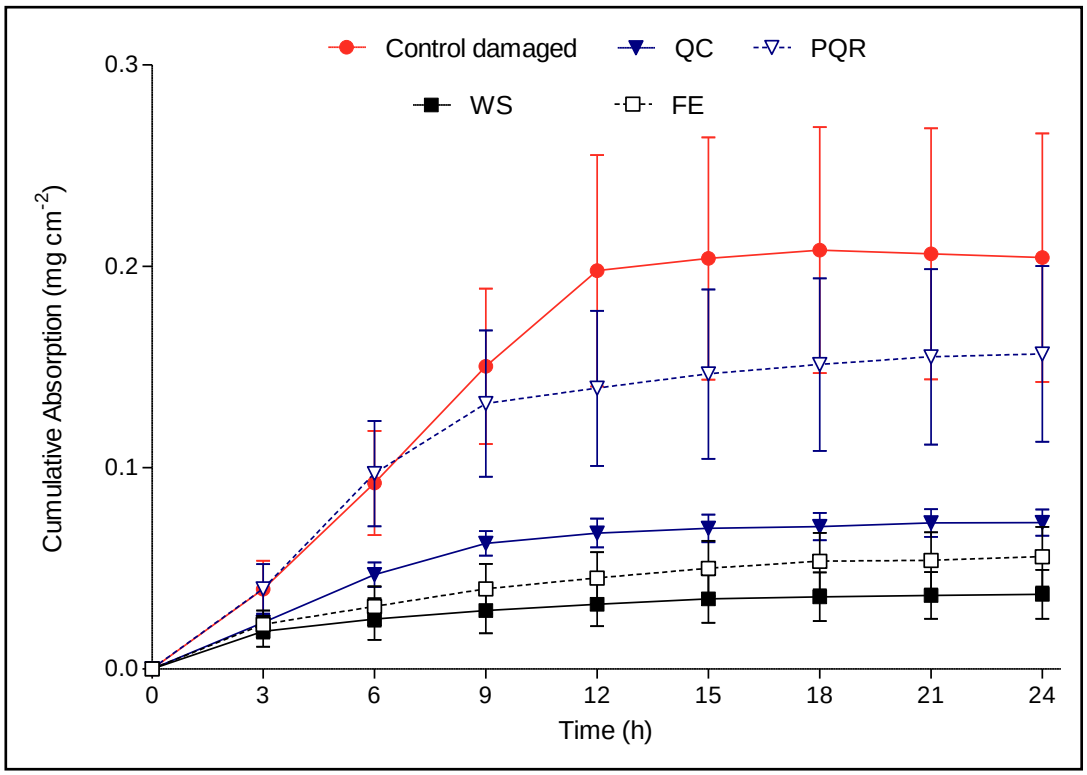

Figure 4.12: Cumulative absorption of ^{14}C (derived from ^{14}C–SM) through damaged skin following application of haemostatic products.

Haemostats tested included: WoundStat™; WS, QuikClot ACS+®; QC and ProQR®; PQR. A standard military decontaminant (fuller's earth; FE) was included as a positive control. All values are mean ± S.D. (n=6).

Treatment Group	Maximum rate of absorption ($\mu g\ cm^{-2}\ h^{-1}$)	Total Absorption at 24 h ($\mu g\ cm^{-2}$)
Control damaged	18.5 ± 4.2	222.4 ± 48.2
QC	6.5 ± 0.7**	72.8 ± 6.5**
PQR	15.4 ± 4.1	156.5 ± 43.6
WS	1.7 ± 0.7**	37.2 ± 12.2**
FE	2.9 ± 1.0**	55.7 ± 14.9**

Table 4-7: The maximum rate of absorption (J_{max}) and total absorption at 24 h of ^{14}C (derived from ^{14}C–SM) for damaged skin following application of test haemostatic decontaminants.

*Average values (mean ± S.D.) are shown for control and treatment groups (n=6). Statistically significant differences between undamaged and damaged skin are indicated, where ** represents a p-value of <0.01.*

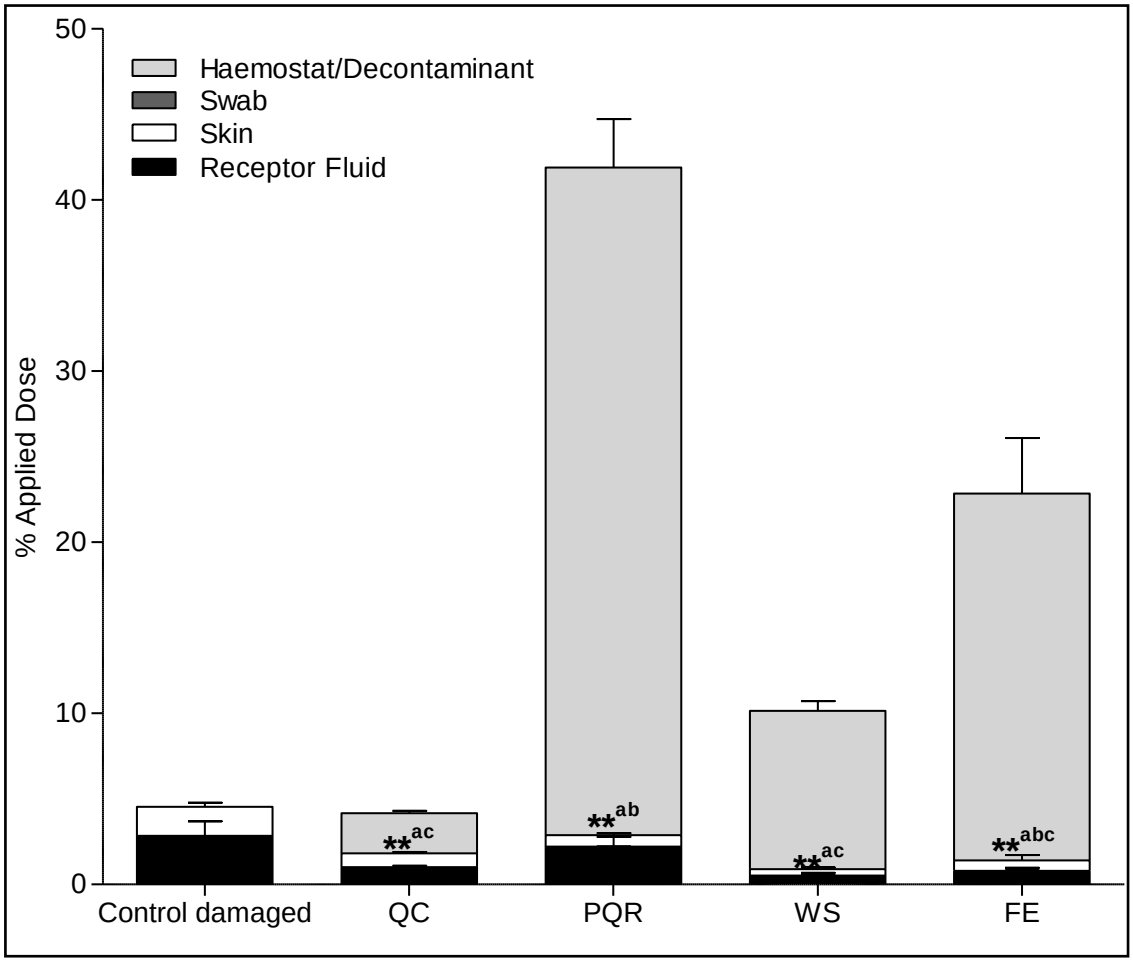

Figure 4.13: The distribution of ^{14}C (derived from ^{14}C–SM) recovered from damaged skin at 24 h post-exposure following application of haemostatic products.

*Haemostats tested included: WoundStat™; WS, QuikClot ACS+®; QC and ProQR®; PQR. A standard military decontaminant (fuller's earth; FE) was included as a positive control. Individual values are mean ± S.D. (n=6). Statistically significant differences between damaged control and treated cells are shown, where ** represents a p-value of <0.01 for skin[a], swab[b] and receptor fluid[c].*

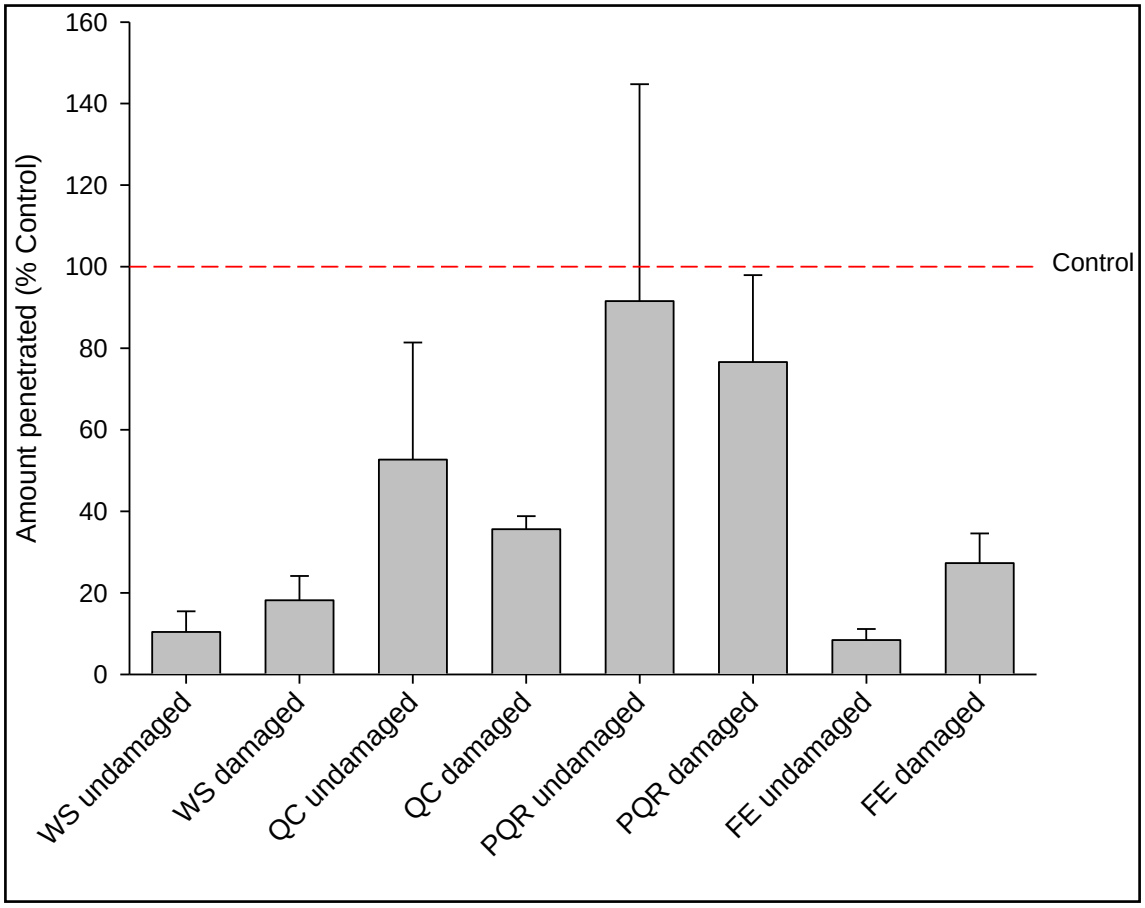

Figure 4.14: The total amount of ^{14}C (derived from ^{14}C–SM) penetrated through undamaged and damaged porcine skin at 24 h post-exposure following application of haemostatic products.

Haemostats tested included: WoundStat™; WS, QuikClot ACS+®; QC and ProQR®; PQR. A standard military decontaminant (fuller's earth; FE) was included as a positive control. Penetration values are expressed as a percentage of control values for their respective study. Individual values are mean ± S.D. (n=6).

Treatment group		Rate of Absorption	Extent of absorption
WoundStat™	Undamaged	-	-
	Damaged	-	-
QuikClot ACS+®	Undamaged	0	0
	Damaged	-	-
ProQR®	Undamaged	0	0
	Damaged	0	0
Fuller's earth	Undamaged	-	-
	Damaged	-	-

Significant increase compared to control	+
No significant difference compared to control	0
Significant decrease compared to control	-

Table 4-8: Dermal absorption (rate and extent at 24 h) of ^{14}C (derived from ^{14}C–SM) through damaged and undamaged skin following application of haemostatic products.

Haemostats tested included: WoundStat™; WS, QuikClot ACS+®; QC and Pro QR®; PQR. The military decontaminant (fuller's earth; FE) was included as a positive control. The colours represent the efficacy of each product; where a significant increase (red; +), no significant difference (yellow; 0) or a significant decrease (green; -) in either rate or extent of absorption compared to the control is shown for each of the treatment groups.

Desorption characteristics of the test products at ambient temperatures

Statistically significant differences in the amount of ^{14}C (derived from ^{14}C–SM) recovered between unoccluded and occluded groups were observed for the haemostats ProQR® and QuikClot ACS+® at ambient temperatures ($p<0.01$; Figure 4.15). There was no reduction in the amount of ^{14}C (derived from ^{14}C–SM) recovered from the unoccluded group for the haemostat, WoundStat™ or the "bench-mark" decontaminant fuller's earth compared to the occluded product controls.

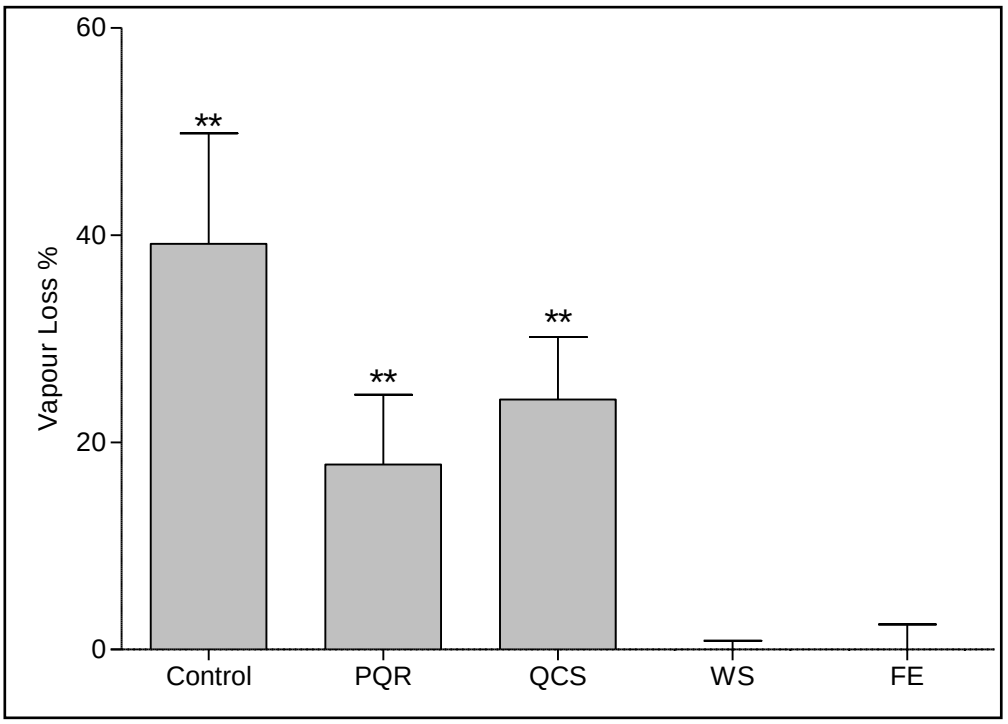

Figure 4.15: Desorption of ^{14}C (derived from ^{14}C–SM) at ambient temperatures (21°C) at 3 h post-exposure following application of haemostatic products.

*Haemostats tested included: WoundStat™; WS, QuikClot ACS+®; QC and ProQR®; PQR. A standard military decontaminant (fuller's earth; FE) was included as a positive control. Data are expressed as the percentage loss in recovery for unoccluded cells compared to occluded cells. Individual values are mean ± S.D. (n=6). Statistically significant differences between unoccluded and occluded cells are shown where ** represents a p-value of <0.01.*

DISCUSSION

This study has shown that defined, superficial skin damage leads to a significant loss of barrier function (as demonstrated by enhanced dermal absorption of ^{14}C derived from ^{14}C–SM) which can be effectively mitigated by the timely application of certain haemostatic products.

It is important to consider the limitations of experimental models to avoid erroneous interpretation of the results. Whilst the use of static diffusion cells has been subject to extensive validation (Franz. 1978, Chilcott*, et al*. 2007, Chilcott*, et al*. 2001, Ng*, et al*. 2010), the following factors need consideration.

Suitability of pig skin as a model for human skin

The use of *ex vivo* animal skin has the potential limitation of not accurately predicting human absorption *in vivo* (Bartek*, et al*. 1972). Obtaining human skin from elective surgical procedures would eliminate the need for using alternative species, but obtaining enough suitable human skin (free from overt pathology) is subject to many practical issues and so availability is poor. However, dermal absorption through pig skin has been shown to correlate well with human skin for a number of chemicals (Bartek*, et al*. 1972, Hawkins and Reifenrath. 1986, Reifenrath*, et al*. 1991, Reifenrath*, et al*. 1984) including SM (Hawkins and Reifenrath. 1986, Chilcott*, et al*. 2001, Reifenrath*, et al*. 1991). Moreover, use of pig skin *in vitro* facilitates a direct comparison with *in vivo* models of superficial skin damage (see Chapter 5). Additional *in vitro* studies with human skin could be conducted to further validate the findings of this present study.

Suitability of frozen skin tissue

Although the physical barrier properties of skin have been shown to be unaffected by freezing at -20°C (Harrison*, et al*. 1984, Nakai*, et al*. 1999), skin enzymatic function is likely to be compromised (Wester*, et al*. 1998). Glutathione S-transferases catalyse conjugation of SM with glutathione to detoxify the cell in a phase II reaction (Black*, et al*. 2010). The conjugation reaction increases the solubility of SM and thus may have an effect on the rate of dermal absorption. Sulphur mustard and its analog (2-chloroethyl ethyl sulphide; CEES) have been shown to interact with both CYPs and lactate dehydrogenase (Mol and De Vries-Van de Ruit. 1992, Gray*, et al*. 2010, Pons*, et al*. 2001). Sulphur mustard analog, 2-chloroethyl ethyl sulphide (CEES) has been shown to inhibit CYPs resulting in increased reactive oxygen species (ROS) production and potentially increased ROS-dependent cell death (Gray*, et al*. 2010). Therefore, biotransformations which occur *in vivo* that could potentially affect toxicity (local or systemic) may not be present *in vitro*. This could be resolved by the use of viable, unfrozen skin. Viability of the skin tissue would need to be maintained with the continual replacement of a physiological compatible receptor medium such as tissue culture medium (Collier*, et al*. 1989). However, SM must have sufficient solubility in the receptor fluid used to ensure sink conditions are maintained. Good correlation between *in vitro* and *in vivo* absorption rates of SM (Chilcott*, et al*. 2007, Nagy*, et al*. 1946, Chilcott*, et al*. 2001) suggests that the absence of any active transport mechanisms does not significantly impact on dermal absorption of SM.

Speciation of ^{14}C-moieties

In this study, liquid scintillation counting was used to measure the quantity of the ^{14}C-radioisotope derived from ^{14}C-SM present in the samples. This analytical method does not differentiate between the original compound (SM) and any subsequent breakdown products. Therefore, it is assumed that the amount of ^{14}C-radiolabel detected is equivalent to the corresponding amount of SM (determined by reference to standard solutions prepared and analysed simultaneously). Degradation of ^{14}C-SM by the test product may occur (particularly with the reactive decontaminants e.g. RSDL®) or by hydrolysis on the skin surface or in the dermal layers. This could mean that ^{14}C detected in the skin or in the skin surface (swab) is in fact a hydrolysis breakdown product e.g. thiodiglycol or thiodiglycol sulfoxide. To address this problem, speciation of the ^{14}C-label would be required. Previously, liquid chromatography combined with mass spectrometry (LC-MS) has been used to speciation SM and its metabolites (Noort, *et al*. 2004, Noort, *et al*. 2000). These may include TDG and protein adducts or conjugates. However, prior *in vitro* studies by Chilcott *et al.* (2001) have noted that there is little hydrolysis of SM within the epidermal layers (Chilcott, *et al*. 2001). This is presumably due to the fact that SM can partition into the lipid environment of the SC and is "protected" from the more aqueous environment of the epidermis and dermis. Therefore, ^{14}C detected on the skin surface (swab) or within the skin is possibly intact SM.

Receptor chamber fluid

An important caveat of the static diffusion cell system is the lack of a functioning cutaneous circulation and thus potential for accumulation of penetrant in the receptor fluid medium (Bronaugh and Stewart. 1985, Cooper and Berner. 1985, Grummer and Maibach. 1991). Therefore, the penetrant must be sufficiently soluble in the receptor fluid medium to ensure the rate of absorption is not limited (Wester and Maibach. 1992). A decrease in the thermodynamic activity gradient between donor and receptor chambers could result in underestimation of the absorption of the chemical *in vitro*. The presence of ethanol in the receptor fluid (50% aqueous ethanol) increases the solubility of SM and allows rapid hydrolysis (half-life = 30 s) (Chilcott 2000). Therefore, infinite sink conditions in the receptor chamber should be maintained. However, aqueous ethanol has its own limitations as it is clearly not a direct physiological representation of blood. Nonetheless, SM absorption studies (porcine skin) using aqueous ethanol as a receptor medium have shown good *in vitro-in vivo* correlation (Chilcott*, et al*. 2007, Chilcott*, et al*. 2001). Furthermore, the dermal absorption rates measured *in vitro* with human skin (79 and 294 μg cm^{-2} h^{-1} for full thickness skin and epidermal membranes, respectively) are in agreement with reported penetration rates using human volunteers (60 – 240 μg cm^{-2} h^{-1}) (Chilcott*, et al*. 2000, Renshaw. 1946). Aqueous ethanol has also been shown to more accurately model *in vivo* dermal absorption of lipophilic chemicals than physiological saline solution (with and without the addition of bovine serum albumin) (Kasting*, et al*. 1997).

Relevance of topical product application

Generally, topical "in-service" decontaminants are not left *in situ* for 24 hours: current doctrine dictates that users remove any residual decontaminant after use. Previous decontamination studies with RSDL® and fuller's earth were performed under more realistic conditions where the decontaminants were removed after two minutes of dermal contact (Taysse*, et al*. 2007). Therefore, the extended time the products were left in contact in the skin could result in desorption of SM (or SM degradation products; Chapter 1; Figure 1.8) from the test product and ultimately enhanced absorption of SM. However, the aim of the study was to identify a haemostatic decontaminant which can safely remain within a wound for a minimum of several hours. Furthermore, it is critical that SM does not undergo desorption from the product to present a secondary exposure hazard. Thus, whilst the duration over which each decontamination production was in contact with the skin is not in alignment with supplier's instructions for use, this approach represents a "worst case scenario" and represents a highly conservative approach to the assessment of product efficacy.

In "real-life" situations, haemostats are applied within a wound with sustained pressure to help arrest bleeding. Correspondingly, *in vivo* efficacy studies have incorporated continuous pressure at the site of application for up to four minutes (Pusateri*, et al*. 2003a, Pusateri*, et al*. 2003b, Ward*, et al*. 2007, Kheirabadi*, et al*. 2005). Furthermore, haemostats whose mechanism of action is via absorption of plasma may create a tamponade effect within the wound. This may increase pressure in the wound and enhance absorption of SM in the wound. In this present *in vitro* study, no additional pressure was applied to the skin. Therefore, it would desirable to develop a

method of applying uniform, sustained pressure to a haemostat to assess whether this has an effect on dermal absorption of ^{14}C-SM.

There are a number of published studies which have investigated the penetration of SM through undamaged human and porcine skin (Hattersley*, et al*. 2008, Chilcott*, et al*. 2000, Chilcott*, et al*. 2001). However, this is the first study to investigate the penetration of SM through superficially damaged skin. Taking account of the limitations noted above, the main findings of this study are discussed below:

Superficial damage to the skin was found to significantly increase both the rate and extent of dermal absorption of ^{14}C (derived from ^{14}C–SM). This was anticipated, as the 100 µm layer removed corresponds to the SC and majority of the epidermal layer in swine (Qvist*, et al*. 2000) and the SC is generally regarded as the main barrier to percutaneous permeation (Blank. 1965). However, SM is a hydrophobic chemical (Log P 1.37) which can rapidly partition into the lipid-rich SC layer of the skin (Chilcott*, et al*. 2000, Rosenblatt*, et al*. 1996, Cullumbine. 1947). Therefore, the more aqueous dermal layer may provide a less favourable environment for the partitioning of SM. This could potentially reduce the rate and extent of absorption of lipophilic chemicals by reducing permeability, as previously described (Cross*, et al*. 2003). This was not observed in the present study.

A statistically significant increase in the amount of ^{14}C (derived from ^{14}C–SM) recovered from within one batch of abdominal skin was observed (Figure 4.4). However, the difference in recovery equated to 3% of the applied dose and thus was a relatively small difference. This apparent discrepancy is likely to be a reflection of inherent inter-individual variation in barrier function and is within the range of reported variation (2 – 6 fold) (Southwell*, et al*. 1984, Schaefer and Redelmeier. 1996). Inter-

individual differences in percutaneous penetration have been, in part, attributed to filaggrin and SC lipids in man. Filaggrin has also been identified in pig skin as contributing to SC permeability (Liu, *et al*. 2010) and difference in filaggrin and SC lipids may account for the apparent discrepancy in the data. This does also highlight the potential for decontaminants to have variable efficacy due to inter-individual differences. Each study was conducted with skin from one animal to try to limit variation between treatment groups in each study. Moreover, inter-study comparisons were conducted using values that were relative-to-control to account for inter-study variation due to skin from different animals. Therefore, this apparently anomalous result doesn't reduce confidence in interpreting these data.

WoundStat™ was found to significantly reduce the rate and extent of dermal absorption through both intact and superficially damaged skin. Both WoundStat™ and fuller's earth are comprised of hydrous montmorillonite or smectite granules (Ward, *et al*. 2007). Smectites are mineral clays with an expanding crystal lattice structure that has a high ion-exchange capacity and can absorb organic molecules into the interlayer space (Liu and Zhang. 2007). This allows WoundStat™ to absorb plasma to locally increase clotting factor concentrations and promote coagulation (Carraway, *et al*. 2008, Ward, *et al*. 2007). This has also been attributed to fuller's earth decontaminating properties (Wattana and Bey. 2009). Fuller's earth has shown efficacy against SM *in vitro* and *in vivo* (Chilcott, *et al*. 2001, Taysse, *et al*. 2007, Taysse, *et al*. 2011). Presumably the ability of WoundStat™ to decontaminant undamaged and damaged skin with an equivalent efficacy to fuller's earth is due to their similar structures that allow the passive adsorption and sequestering of SM.

Fuller's earth (FE) was the only treatment less effective in decreasing ^{14}C-SM

penetration through damaged skin compared to undamaged skin. Reduced decontamination efficacy of FE in damaged skin has also been observed *in vivo* (Bjarnason, *et al*. 2008). The decrease in efficacy could potentially be due to increased TEWL following the removal of the SC. Increased water vapour at the skin surface could result in formation of a FE solution. This could allow the SM to be mobilised from FE and be potentially available for dermal absorption. A similar discrepancy in decontamination efficacy between dry FE and FE solutions has been previously reported *in vivo* (Bjarnason, *et al*. 2008).

QuikClot ACS+® was shown to be ineffective in reducing the rate or extent of ^{14}C-SM permeation through intact skin. However, it was found to significantly reduce the rate and extent of ^{14}C-SM absorption through superficially damaged skin. ProQR® was shown to be ineffective in both intact and superficially damaged skin. Surprisingly, both haemostats are thought to share the same mechanism of action as WoundStat™ (passive absorption of liquid into the interlayer space) (Kheirabadi, *et al*. 2009). Thus it is possible that the differences in efficacy are due to different binding capacities for hydrophobic chemicals: ProQR® contains a hydrophilic polymer (Ho and Hruza. 2007) whilst QuikClot ACS+® is comprised of partially-hydrated zeolite beads (Ostomel, *et al*. 2006). Thus product design features that assist in absorption of water from blood may actually inhibit the absorption of hydrophobic chemicals. Although QuikClot ACS+® did significantly reduce dermal absorption; it was not found to successfully sequester ^{14}C-SM; the significant "off-gassing" of the SM-contaminated product could present a secondary exposure hazard. QuikClot ACS+® has been reported to generate heat when binding water. Thus, it is conceivable that a similar, exothermic reaction may be responsible for promoting volatilisation of SM (Arnaud, *et al*. 2007). Infrared

thermography could be used to measure the surface temperature of QuikClot ACS+® when in contact with SM to establish whether an exothermic reaction is the cause of the volatilisation.

Reactive Skin Decontamination Liquid® (RSDL®) and the novel decontaminant TOP (comprised of tetraglyme, oxime and poly(ethyleneimine)) were not found to significantly reduce the extent of ^{14}C-SM dermal absorption through intact skin. Both products are reactive decontaminants and enhance the hydrolysis of SM to produce non-toxic degradation products including TDG (Sawyer et al. 1991). The ineffectiveness of RSDL® was unexpected as it has previously been shown to be effective as a decontaminant *in vivo* (Taysse*, et al*. 2007). This apparent lack of efficacy could be due to the combination of occlusion and lack of ^{14}C speciation.

Both RSDL® and TOP are viscous liquids and it is probable that they form an occlusive layer on the skin. This could potentially increase dermal absorption by reducing evaporation of SM from the skin surface. It has been previously reported that 80% of the applied dose evaporates under unoccluded conditions, thus occlusion would increase the amount available for dermal absorption (Renshaw. 1946, Chilcott*, et al*. 2001). Moreover, occlusion of the skin has been shown to disrupt barrier function of the SC via increased hydration in the skin layer (Ryatt*, et al*. 1988, Zhai and Maibach. 2002). Increases in dermal absorption of certain chemicals (dependent on partition coefficient) have been observed following occlusion (Ryatt*, et al*. 1988). One degradation product of SM (TDG) is much less hydrophobic than SM (log P value -0.77) (Reddy*, et al*. 2005). Therefore hydration-dependent barrier disruption is likely to enhance the permeation of TDG and may result in increased ^{14}C-label detected in the receptor fluid. Moreover, the lack of speciation of radiolabelled products means the ^{14}C

radiolabel detected in the receptor fluid could be attributed to a ^{14}C radiolabelled-degradation product and not ^{14}C-SM. This may not be a cause for concern for non-toxic SM degradation products. However, the overall project objective is to identify a product which is suitable for decontaminating SM- or organophosphate-contaminated wounds. Therefore, a conservative approach is taken as some organophosphate degradation products are toxic and so irreversible sequestration is desirable (Munro*, et al*. 1999).

Liquid haemostats (FastAct® and VitaGel™) significantly increased both the extent and rate of dermal absorption of ^{14}C-SM through intact skin. This is possibly due to the formation of an occlusive barrier which reduces evaporative loss, as seen for the reactive decontaminants; RSDL® and TOP. However, the formation of a SM-haemostat (aqueous) solution may also have an effect on the rate of absorption. The presence of a hydrophobe such as SM in an aqueous solution results in disruption of the hydrogen bonding network between water molecules in the solution. The inability of SM to form hydrogen bonds with water molecules in the aqueous haemostat results in the formation of a solvation or hydration shell around the SM molecule. This reduces the translational and rotational entropy of the water molecules and thus is unfavourable in terms of free energy within the system. Therefore, it is more thermodynamically favourable for SM to partition from the aqueous haemostat into the less aqueous SC. This could partially account for the increase in the amount and rate at which SM is absorbed into the skin layers. Increased penetration (resulting in increased lesion severity) has been observed *in vivo* following pre-wetting of the skin (Renshaw. 1947). Interestingly, there was a correlation between enhancement of ^{14}C-SM absorption and decreased recovery from the skin following FastAct® and VitaGel™ treatment. One conceivable explanation is that the occlusive layer also reduces TEWL which eventually results in increased

hydration status of the SC. Conversely, this may provide a less thermodynamically favourable environment for lipophilic chemicals such as SM as the SC may become a more aqueous environment. Therefore, SM could preferentially partition into the receptor fluid rather than remaining within the SC, forming a reservoir as previously described (Hattersley*, et al*. 2008). This could potentially account for the enhanced dermal absorption (rate and extent) as well as the reduced skin recovery at 24 h post-exposure.

Interestingly, the penetration enhancement effect of FastAct® and VitaGel™ was diminished when used in combination with TOP. Two components of TOP tetraglyme (tetraethylene glycol dimethyl ether) and oxime have been shown to degrade SM and reduce percutaneous absorption (Gordon *et al* 2002). Therefore, it is possible that TOP in combination with either FastAct® and VitaGel™ is relatively efficacious in sequestering and detoxifying SM thus reducing the amount available for absorption.

Significant increases in the rate and extent of absorption of ^{14}C-SM were also observed for the chitosan-based haemostat, HemCon®. The other chitosan-based haemostat Celox™ was ineffective in reducing dermal absorption. The formulation of the products may have contributed to their poor performance as decontaminants as HemCon® (bandage) and Celox™ (flake-like haemostat) could potentially form an occlusive layer, reducing evaporative loss of SM and thus increasing the dose available for dermal absorption.

Chitosan-based haemostats promote coagulation via electrostatic interactions between positive-surface charges of the polysaccharide and the negative-surface charges of erythrocytes, resulting in aggregation of platelets and erythrocytes (Najjar*, et al*. 2004). Sulphur mustard has been shown to form degradation products which have a

positively-charged sulphonium ion and therefore may not bind to chitosan-based haemostats.

Conclusions

The Franz-type static diffusion cell system provides an *in vitro* method for measuring the ability of haemostats to decontaminant undamaged and damaged skin exposed to SM. The dermal absorption of SM is significantly increased in damaged skin. This study has identified a haemostat, WoundStat™, which can significantly reduce the dermal absorption of SM through both intact and superficially damaged porcine skin. This is most probably due to the high ion-exchange capacity and expanding nature of the smectite-based product which allows the adsorption and sequestration of SM in the interlayer space. The decontamination efficacy of WoundStat™ in this study is comparable with the military decontaminants fuller's earth and M291.

Recommendations for future work

- WoundStat™ should be evaluated in an *in vivo* superficial wound pig model to test its ability to reduce SM lesion severity (Chapter 5)
- The vapour-phase and contact desorption characteristics for the haemostats should be evaluated using gas-chromatography and mass-spectrometry.
- Liquid-chromatography should be used for the speciation of ^{14}C-labelled products permeating into the receptor fluid and those recovered from within the skin layers, to establish whether they are breakdown products or parent compound (SM).
- The binding capacity for the haemostats should be assessed using an Enslinn test (Thorps. 1963) to measure the maximum binding capacity for SM.

Chapter 5

The toxic effects of sulphur mustard (SM) when applied via superficial damaged skin with respect to early time-point sequelae of gross clinical signs, microscopic and gene expression changes and toxicokinetics

INTRODUCTION

Superficial damage to the skin increases both the rate and total amount of SM penetrating through the skin *in vitro* (Chapter 4). Thus it is reasonable to postulate that removal of the upper skin layers (SC and epidermis) will also increase dermal absorption *in vivo*. This poses a substantial problem when treating or decontaminating individuals who have sustained injuries potentially contaminated with toxic chemicals such as SM. However, there are limited *in vivo* toxicokinetic data when SM is applied percutaneously (Clemedson*, et al*. 1963, Zhang and Wu. 1987, Tripathi*, et al*. 1995). No measurable SM was detectable in the circulation when applied percutaneously to undamaged pig skin (Brown and Rice. 1997, Zhang and Wu. 1987) . This study is the first to investigate the effect of skin damage on the toxicokinetics and distribution of ^{14}C-SM.

Microscopic changes 24 h after SM exposure in undamaged pig skin are characterised by significant neutrophil infiltrate, collagen degeneration, severe capillary necrosis and congestion and microblister formation at the epidermal/dermal junction (Brown and Rice. 1997). Few definite structural changes have been described at early time points (6 h post exposure) in undamaged skin (Brown and Rice. 1997). The removal of the SC and epidermis is likely to result in an increase in the rate of absorption but the effect on lesion progression is unclear. It would be reasonable to postulate that removal of the skin barrier is likely to result in a more severe injury. However, the primary cytotoxic target for SM is basal keratinocytes (Black*, et al*. 2011) and thus the removal of the layer may reduce the skin lesion. Gold *et al.* (1994) observed slight-moderate erythema and slight necrosis at 48 h post exposure when SM was applied to a full-thickness skin injury in hairless guinea pig. However, lesion

severity was based on clinical observations and was not histologically scored thus the microscopic effects are largely undefined. This study aims to identify early time-point microscopic changes associated with SM exposure to superficial damaged skin.

Changes in gene expression following percutaneous exposure to SM have been reported for undamaged skin. Major gene categories activated by SM include apoptosis, inflammation, cell cycle regulation, cytoskeleton regulation and oncogenes (Vallet, *et al*. 2012, Gerecke, *et al*. 2009, Dillman III, *et al*. 2006, Sabourin, *et al*. 2004, Sabourin, *et al*. 2002, Rogers, *et al*. 2004). However, the use of a murine model in such studies may not accurately model percutaneous absorption of SM in human skin, which is of particular concern when investigating early time point expression changes. At present there are no published gene expression studies for SM-exposed damaged skin. The aim of this study is to establish the early time point (6 h) effects of SM toxicity to gain understanding of any additional mechanisms involved when SM is applied to superficially damaged skin.

The domestic pig (*Sus scrofa domestica*) is an established model for evaluating SM-induced cutaneous lesions (Price, *et al*. 2009, Chilcott, *et al*. 2007, Reid, *et al*. 2001). Sulphur mustard has been shown to induce microblistering in pig which is comparable with the blistering seen in humans (Brown and Rice. 1997, Mitcheltree, *et al*. 1989). Therefore the pig is considered a suitable model for characterising SM lesion development and SM distribution when applied to damaged skin.

Aims

The purpose of this study was to investigate *in vivo*;

- the toxicokinetics of SM when applied to superficially damaged skin
- SM lesion development in damaged skin and
- the effect of SM on relative gene expression in damaged skin.

MATERIALS AND METHODS

Full details of methods employed in this study are described in Chapter 2. Briefly, dermal absorption of ^{14}C-SM through superficially damaged porcine skin was measured *in vivo* (Figure 5.1). The distribution of ^{14}C-SM in the blood, dosing site and organs was measured by liquid scintillation counting. The SM lesion progression was measured using a range of biophysical instruments (LDI, SRS and TEWL) and lesion severity was assessed by histopathology. Sulphur mustard-induced changes in gene expression were investigated using oligonucleotide microarrays.

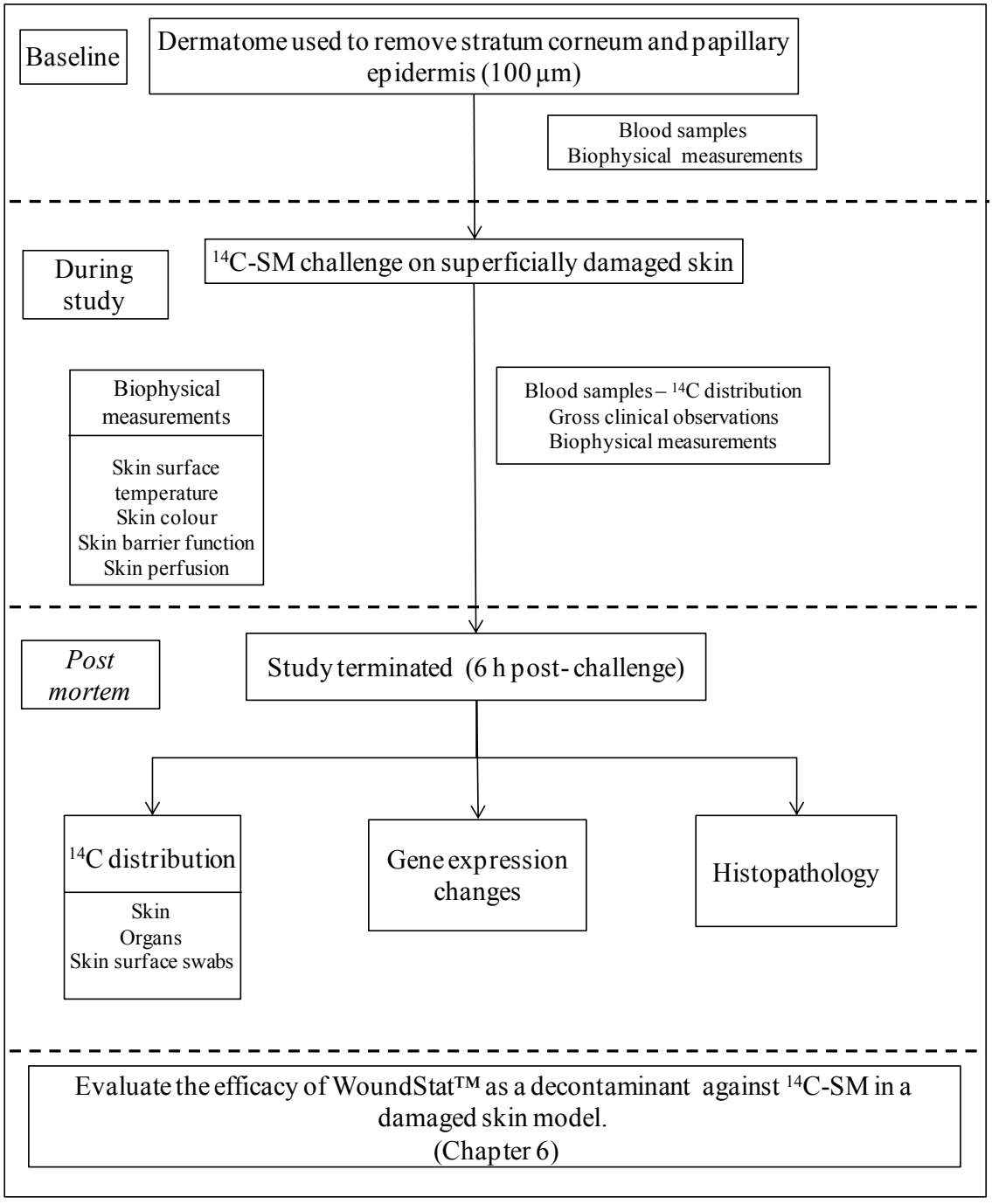

Figure 5.1: Experiment flow chart for characterisation of SM dermal toxicity and toxicokinetics when applied to superficially damaged skin.

RESULTS

Gross clinical observations (digital photography):

There were no remarkable visual changes seen over the 6 h study period for the control (undamaged skin) site and damaged skin site.

Blanching at the exposure site was observed at 60 min for all animals (n=6; Table 5.1 and Figure 5.2a). Erythema was only observed in four out of six animals with the median time to observable erythema at the exposure site being 120 min (Table 5.1 and Figure 5.2b). All animals developed an ulcerated area or skin erosion directly below the SM droplet with 6 h (Table 5.1 and Figure 5.2c). Oedema at the exposure site was noted in five out of six animals (median time; 60 min).

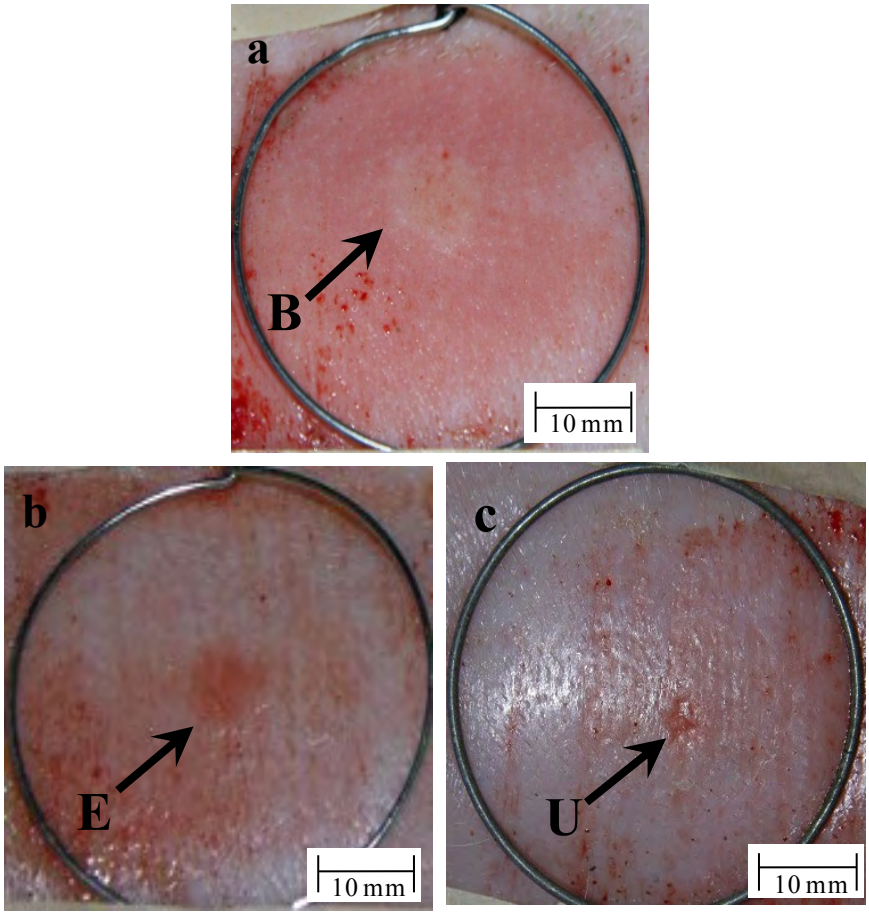

Figure 5.2: Representative photographs of skin exposure sites.

Doughnut-shaped blanching (B) 1 h post challenge (a), development of erythema (E) 2 h post challenge (b), and ulceration of skin (U) 5 h post challenge (c).

	Onset and occurrence of visual signs of dermal toxicity			
Time point (min)	Erythema	Blanching	Ulceration	Oedema
Baseline	(0/6)	(0/6)	(0/6)	(0/6)
60	(0/6)	*6* (6/6)	(0/6)	*3* (3/6)
120	*3* (3/6)	(1/6)	(0/6)	*2* (4/6)
180	*1* (3/6)	(1/6)	*2* (2/6)	*1* (3/6)
240	(3/6)	(0/6)	*3* (5/6)	(3/6)
300	(1/6)	(0/6)	(5/6)	(2/6)
360	(1/6)	(0/6)	*1*(6/6)	(2/6)

Table 5-1: The time to onset and occurrence of gross clinical signs of toxicity following the application of SM to superficially damaged skin.

Physical changes to the skin (oedema and ulceration) and skin colour changes (reddening; erythema or blanching) at the exposure site were scored by one individual. Numbers shown in italics indicates the number of animals first presenting with clinical sign. The numbers in brackets indicate number of animals presenting with this clinical sign at specific time points (n=6).

Biophysical Measurements

Skin colour (skin reflectance spectroscopy)

Values for all three CIELAB parameters (L*a*b*) for control (undamaged skin) showed no statistically significant change over the 6 h study period (Figures 5.3 – 5.5). Removal of the SC and epidermis resulted in statistically significant increases in skin redness and hue ($p<0.05$; Figures 5.4 and 5.5). Increases in skin hue (b*) correspond to increases in yellowness of the skin. However, removal of the upper skin layers did not result in a statistically significant difference in skin brightness (L*) compared to control (untreated) sites (Figure 5.3). Liquid SM exposure did not result in statistically significant differences in skin colour or brightness parameters compared to unexposed damaged skin (Figures 5.3 – 5.5).

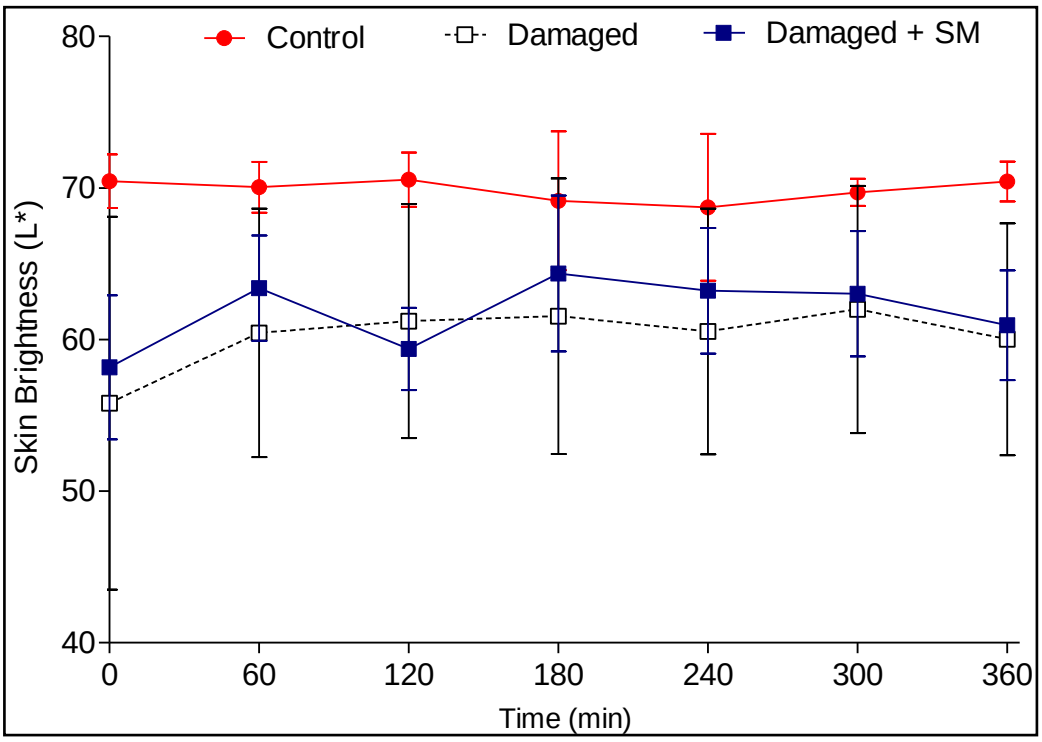

Figure 5.3: Skin lightness (expressed as the CIELAB colour scale parameter, L*) following superficial damage with and without exposure to SM compared to undamaged control site.

All values are expressed as mean ± 95% confidence intervals (n=6).

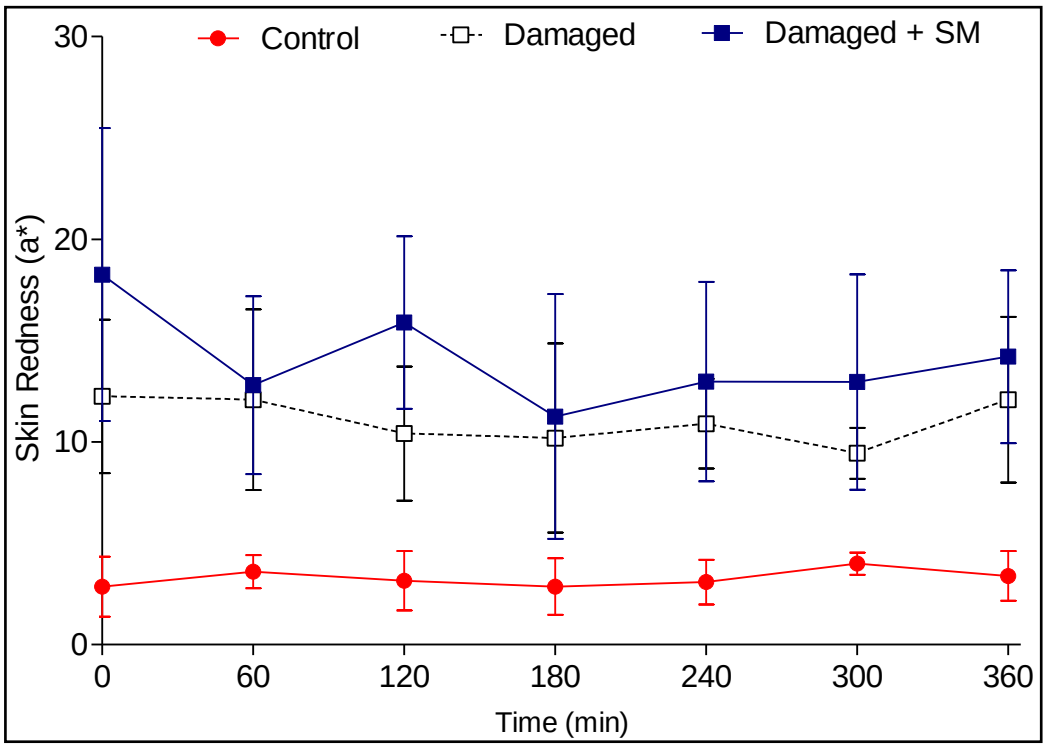

Figure 5.4: Skin erythema (expressed as the CIELAB colour scale parameter, a*) following superficial damage with and without exposure to SM compared to undamaged control site.

All values are expressed as mean ± 95% confidence intervals (n=6).

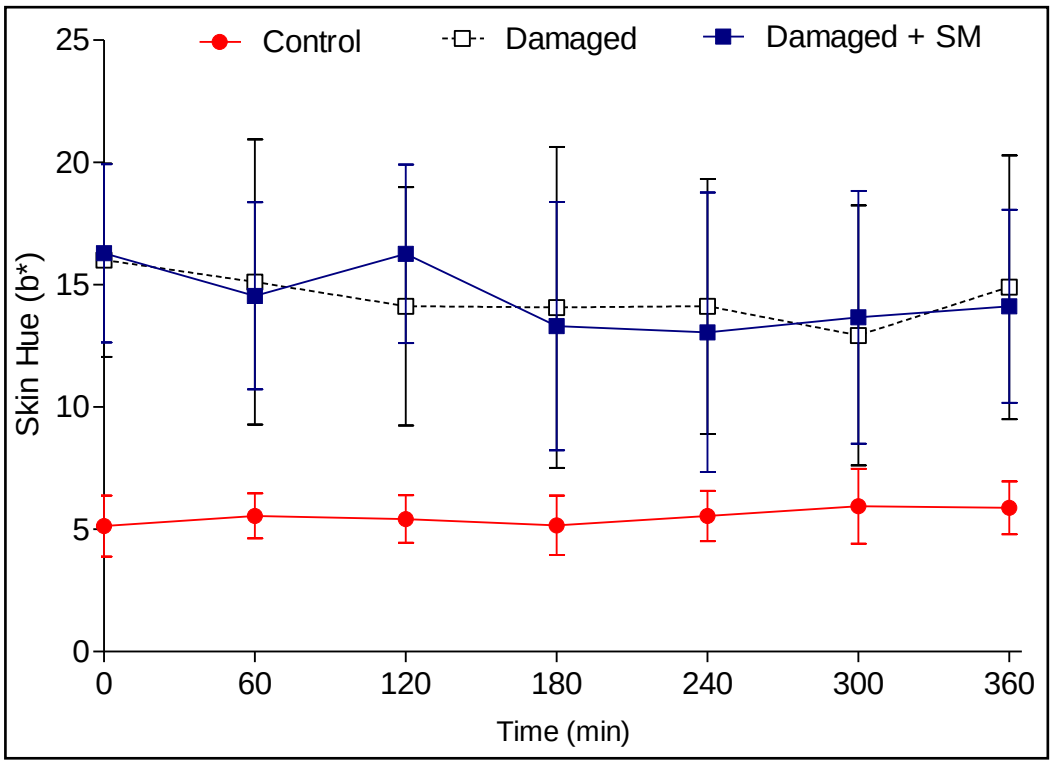

Figure 5.5: Skin hue (expressed as the CIELAB colour scale parameter, b*) following superficial damage with and without exposure to SM compared to undamaged control site.

All values are expressed as mean ± 95% confidence intervals (n=6).

Skin surface temperature (infrared thermography)

Skin surface temperature for control (undamaged skin) site remained constant throughout the 6 h study period. A statistically significant decrease in average skin surface temperature was observed following superficial damage to the skin (removal of SC and epidermis; Figure 5.6). However, there were no statistically significant differences in skin surface temperatures between the damaged skin treatment groups for the remainder of the study. Sulphur mustard exposure did not produce any obvious visual changes in the thermographs when applied to damaged skin (Figure 5.7).

Cutaneous blood perfusion (laser Doppler imaging)

Sulphur mustard significantly reduced dermal blood flow at the exposure site 120 min post application of ^{14}C-SM. A statistically significant reduction in maximal perfusion unit was observed for the SM exposed site compared to the damaged (unexposed) site ($p<0.05$; Figure 5.8). This reduction in perfusion unit corresponded with the appearance of a distinct low flux area (blue-purple) (Figure 5.7).

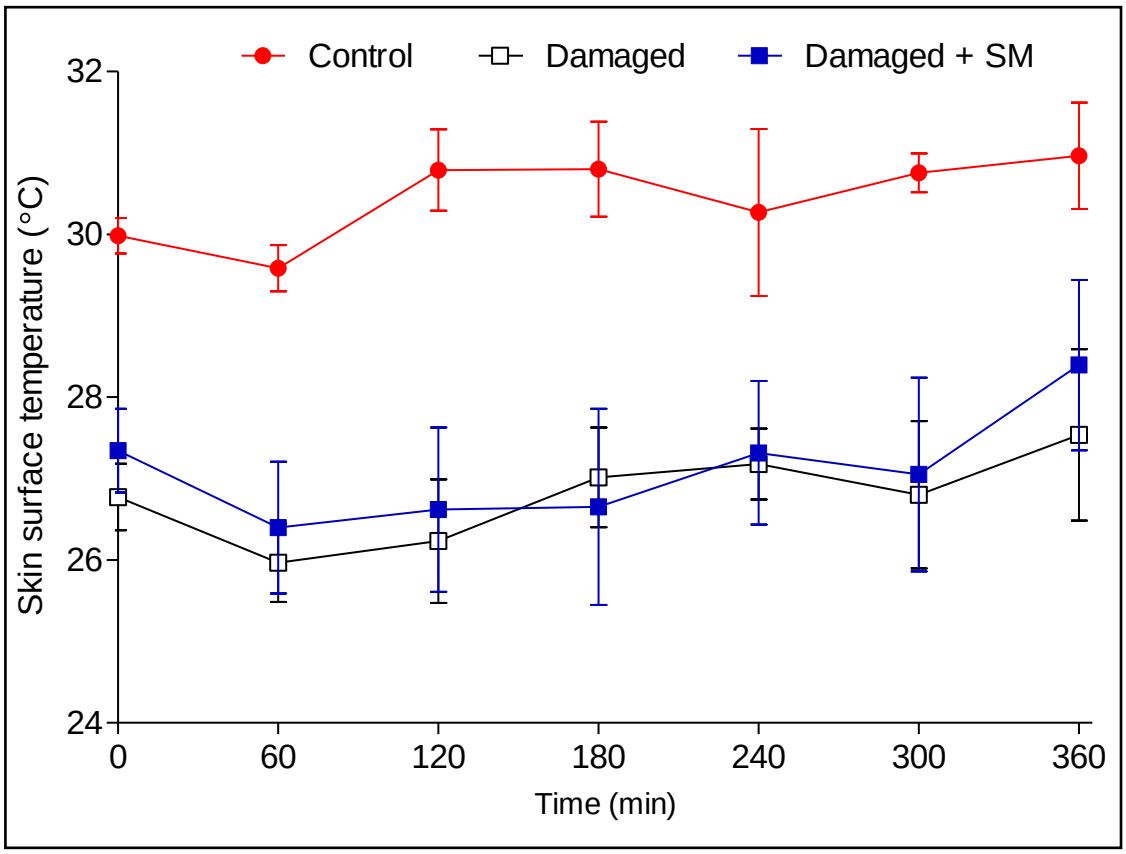

Figure 5.6: Skin surface temperature following superficial damage with and without exposure to SM compared to undamaged control site.

All values are expressed as mean ± S.D. (n=6).

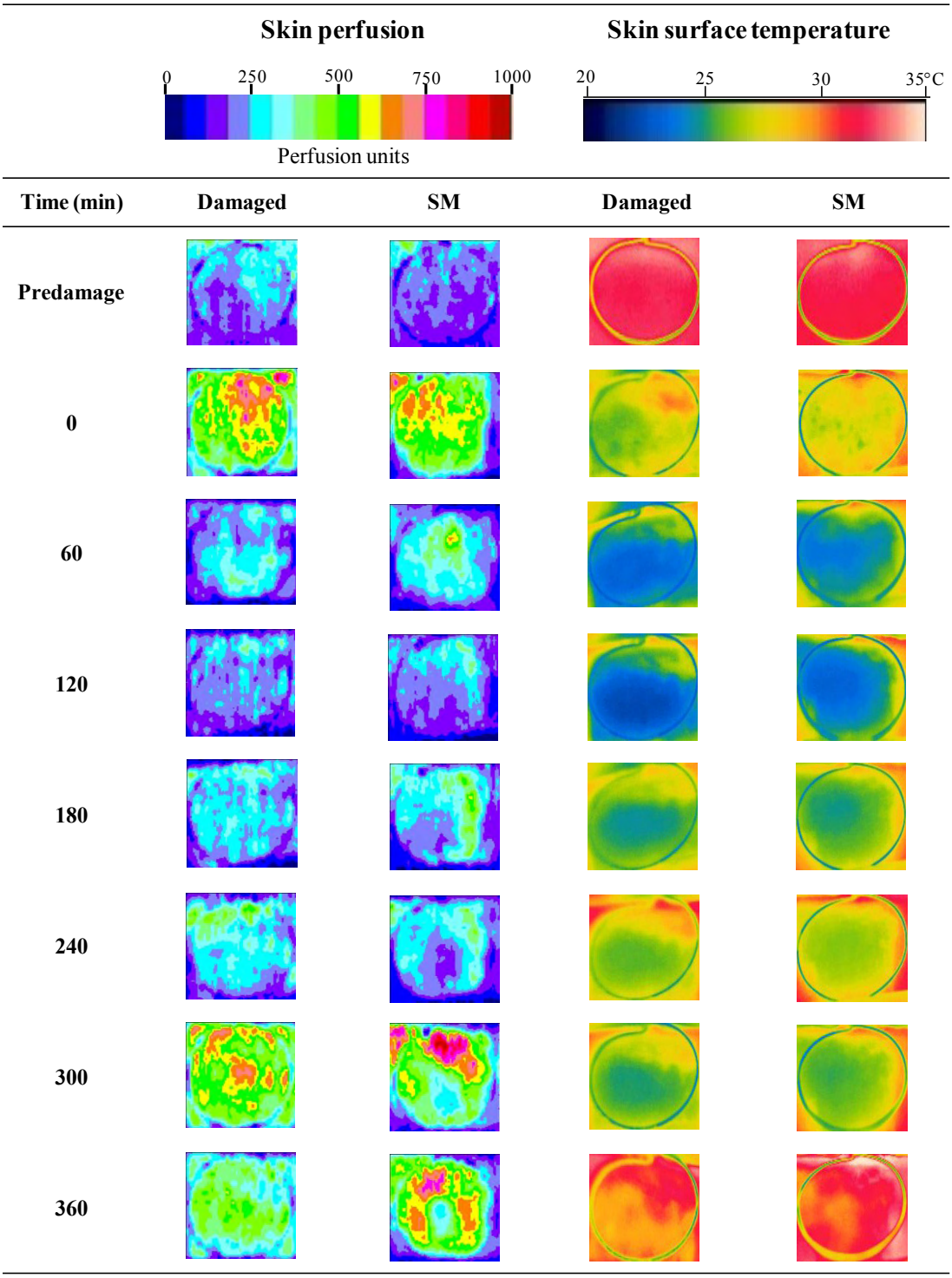

Figure 5.7: Representative skin perfusion images (laser Doppler imaging) and thermographs (infrared thermography) following superficial damage with (SM) and without (damaged) exposure to SM.

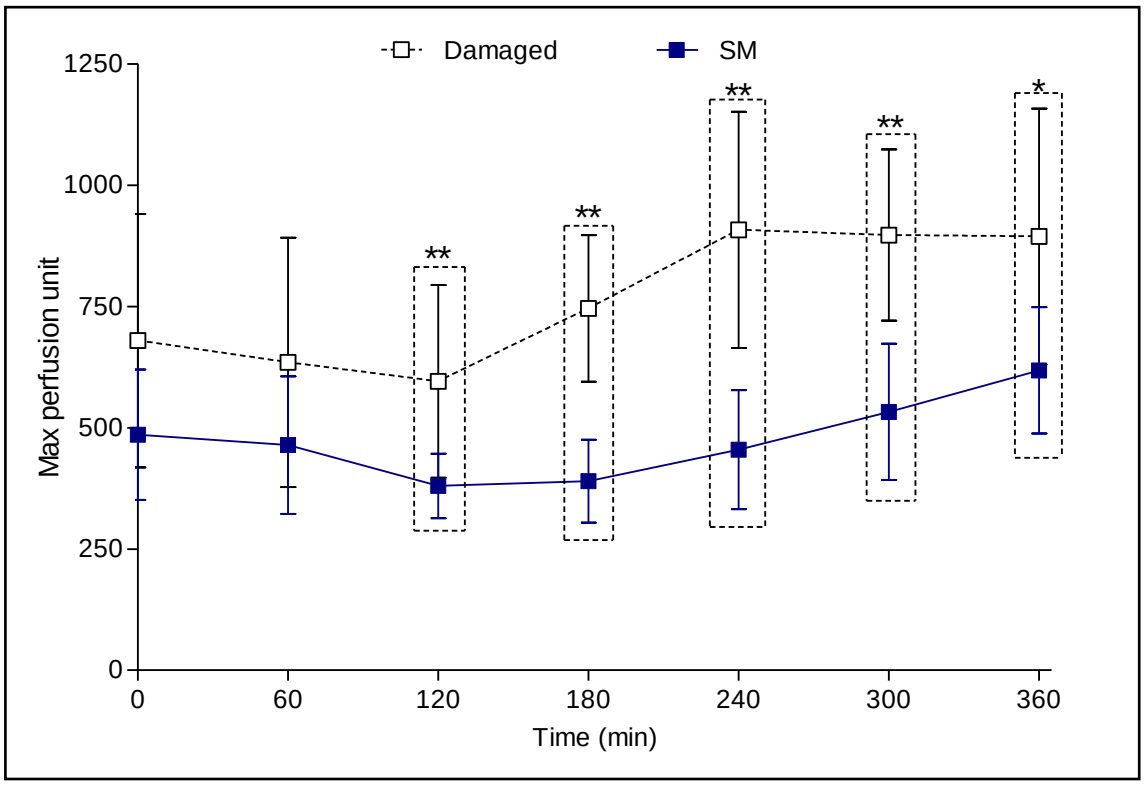

Figure 5.8: Maximum blood perfusion at treatment sites following superficial damage with and without exposure to SM expressed as perfusion units.

*All values are expressed as mean ± 95% confidence intervals (n=6). Dashed box represents a statistically significant difference between the treatment sites where * and ** represent a p-value of <0.05 and <0.01, respectively.*

Skin barrier integrity (transepidermal water loss)

Superficial damage to the skin surface resulted in significantly increased TEWL compared to control (undamaged) values (Figure 5.9). However, SM exposure did not have a significant effect on TEWL during the six hour study period (Figure 5.9). A significant increase in TEWL over the six hour study period was observed for control (undamaged) skin ($p<0.002$; Figure 5.9).

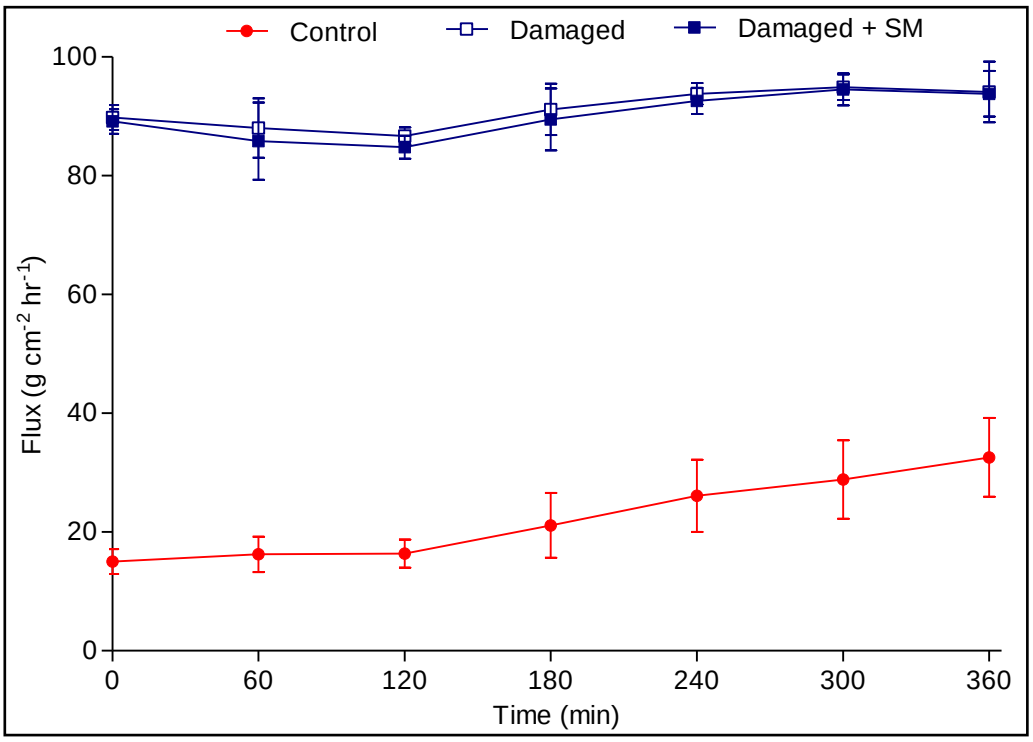

Figure 5.9: Transepidermal water loss (TEWL) following superficial damage to skin with and without exposure to SM.

Control (undamaged) TEWL values are also shown. All values are expressed as mean ± 95% confidence intervals (n=6).

Radiometric Analysis

Maximum blood concentrations of ^{14}C derived from ^{14}C-SM were attained 120 minutes post exposure (Figure 5.10). Elimination kinetics derived from these data are summarised in Table. 5.2. The results shown are an estimation of the elimination kinetics, which appear to fit a first order kinetic model. Further time-points would be required to provide a more accurate estimation.

Overall, 6.3 ± 1.6% of the applied dose of ^{14}C-SM was recovered from the skin, skin surface swabs, organs and blood samples. The total amount of ^{14}C derived from ^{14}C-SM in the systemic circulation was estimated from the 360 min blood sample and the estimated total blood volume, assuming even distribution of ^{14}C throughout the blood. The skin surface swabs and skin accounted for the largest percentage of ^{14}C derived from ^{14}C-SM recovered (45.9 ± 9.6% and 35.3 ± 7.5%, respectively; Figure 5.11).

The amounts of ^{14}C derived from ^{14}C-SM recovered from internal organs (6 hours post-challenge) totalled 1327 ± 297 ng. Predominant distribution was in the kidney, followed by liver and small intestine when the data were expressed as ng of ^{14}C-SM per g of organ weight (Figure 5.12).

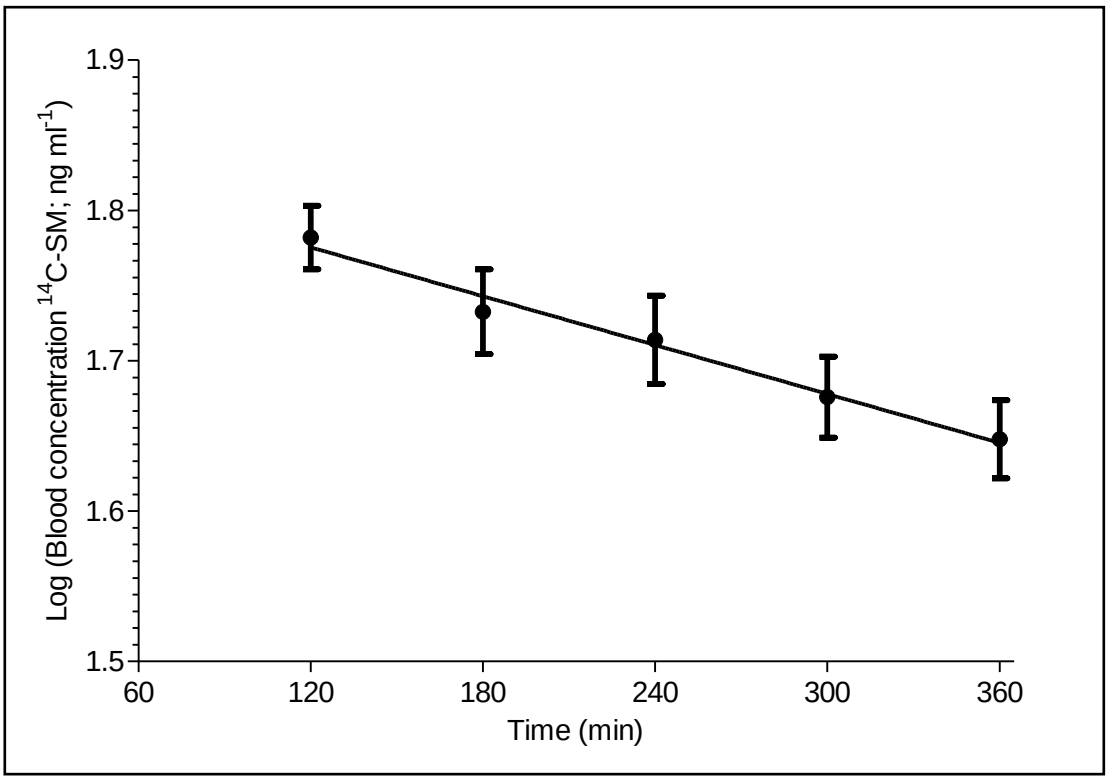

Figure 5.10: Semi-logarithmic plot of blood concentration against time for calculation of elimination kinetic parameters of ^{14}C (derived from ^{14}C-SM) from whole blood following application of 10 µL droplet of ^{14}C-SM via superficially damaged skin.

All values are expressed as mean ± S.D. (n=6). Kinetic parameters were subsequently calculated using equation described in Chapter 2.

Elimination Parameters	
$T_{½}$ (min)	425 ± 60
C_{max} (ng ml^{-1})	60.8 ± 64
Slope (pg ml^{-1} min^{-1})	-64.7 ± 9.0
K_{el} (pg ml^{-1} min^{-1})	149 ± 21
C_0 (ng ml^{-1})	67.5 ± 7.0
V_d (L)	190 ± 22
D (mg)	11.5 ± 0.5

Table 5-2: Elimination kinetic parameters following ^{14}C-SM challenge via damaged skin.

Values are expressed as mean ± S.D. of n=6 animals and are derived from linear regression analysis of a semi-logarithmic plot of whole blood concentration against time. Equations used as described in Chapter 2. Half life ($T_{½}$) was calculated from the Equation 2.8. The value of C_0 was calculated as the y-intercept of the line of best fit (and so is equal to the theoretical whole blood concentration at time of challenge). The peak concentration (C_{max}) was the largest concentration measured directly from whole blood samples. The elimination constant (K_{el}) was calculated by multiplying the slope by -2.303 (Equation 2.9). The apparent volume of distribution (V_d) was calculated from Equation 2.10. The apparent dose ("D") was subsequently calculated from Equation 2.11, using V_d and C_{max} values; the actual applied dose was 11.5 mg.

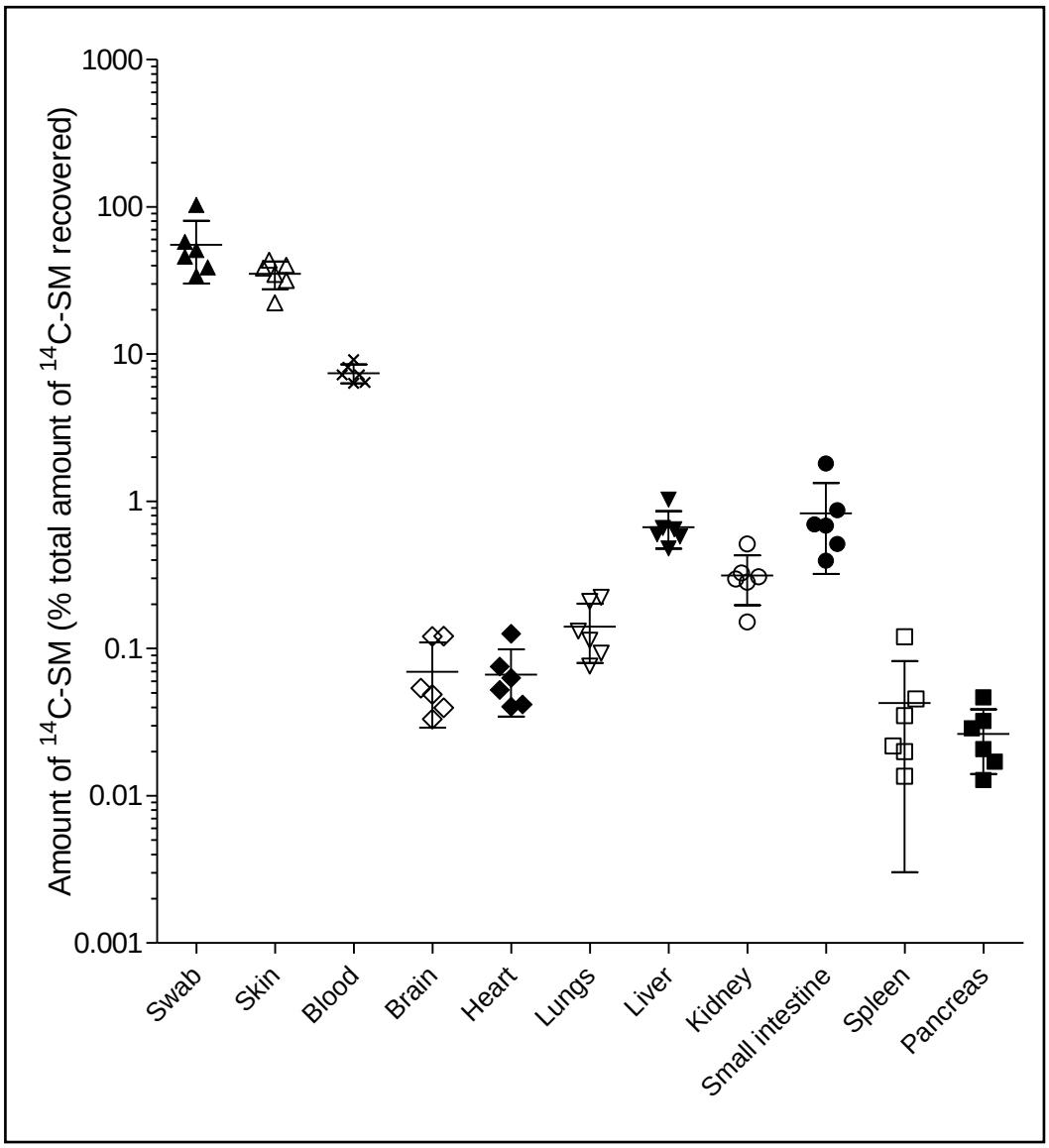

Figure 5.11: Recovery of ^{14}C derived from ^{14}C-SM from skin surface swabs, skin, blood and organs expressed as a log percentage of the total amount of ^{14}C recovered.

Individual values (n=6) are shown in addition to the mean (central line; n=6) and S.D. (outermost lines).

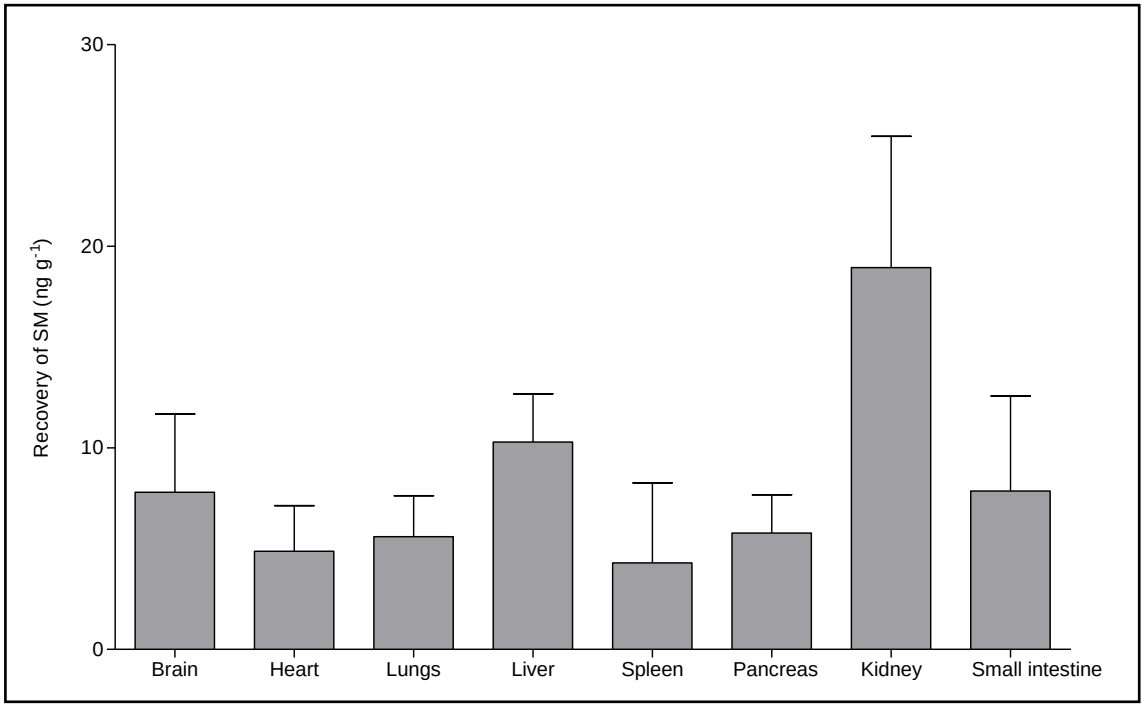

Figure 5.12: Recovery of ^{14}C derived from ^{14}C-SM in internal organs expressed as ng (SM) per g (organ weight).

All values are expressed as mean ± S.D. (n=6).

Histology

The occurrence and severity of histopathological changes are summarised in Table 5.3. Histological examination confirmed that the use of a dermatome achieved complete removal of the SC and epidermis (Figure 5.13 and 5.14). The remaining intact epithelium (at the edge of the treatment site) was histologically normal, as were the hair follicles and other adnexal structures (Figure 5.13). All control (intact skin) slides appeared normal.

There were no significant microscopic changes between the unexposed and SM-exposed damaged skin sites. Both groups showed mild, perivascular, polymorphonuclear neutrophil (PMN) infiltrate in the dermis as well as increased PMNs within the capillary lumen (Figure 5.14 – 5.16).

The changes noted in both the SM-exposed and unexposed damaged skin sites were consistent with an acute, inflammatory response, secondary to the tissue damage caused by the dermatome. The changes included escharification, variable haemorrhage, and a mild, perivascular to diffuse, PMN infiltrate with degenerate PMNs on the exposed, damaged surface. Hyper-eosinophilic, dermal collagen (degenerate) at the surface of the exposed dermis was also present.

Lesion		Treatment Group		
		Control (n=6)	Damaged (n=6)	Damaged + SM (n=6)
Surface and follicular keratinocyte degeneration/necrosis	Occurrence	0	0	0
	Severity	Normal (6)	Normal (6)	Normal (6)
Subepidemal separation/vesiculation	Occurrence	0	0	0
	Severity	Normal (6)	Normal (6)	Normal (6)
Blood vessel dilation-dermal	Occurrence	0	2	4
	Severity	Normal (6)	Normal (4) Minimal (2)	Normal (2) Minimal (4)
Perivascular to diffuse, neutrophilic cell infiltrate-dermal	Occurrence	0	6	6
	Severity	Normal (6)	Mild (6)	Mild (6)
Sero-cellular crusting-surface (Escharification)	Occurrence	0	6	6
	Severity	Normal (6)	Mild (1) Moderate (5)	Minimal (2) Mild (4)

Table 5-3: Occurrence and severity of histopathological findings for control (untreated) and damaged skin with and without SM exposure.

Lesions were histopathologically scored where; marked> moderate> mild> minimal> normal indicates the severity of the lesion. Number in brackets indicates number of animals in each severity group (n=6).

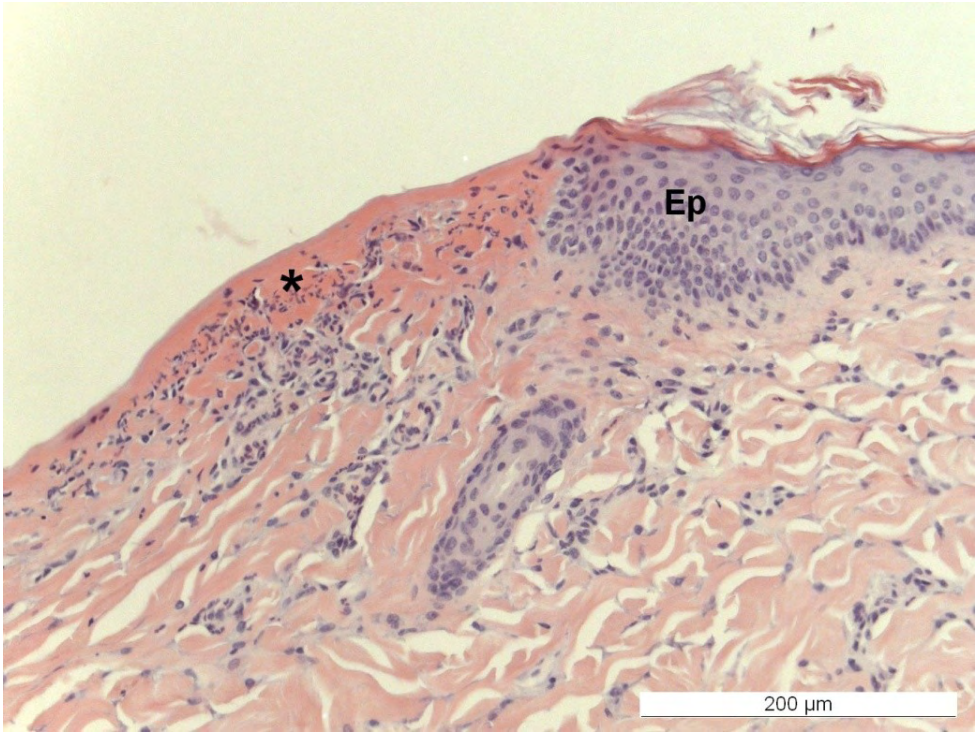

Figure 5.13: Histopathology of superficially damaged skin showing junction of intact and damaged epidermis.

Escharification (*) and a mild, PMN infiltrate are seen. The adjacent, intact epidermis is normal (Ep). The haematoxylin and eosin stained section was viewed by light microscopy with bright field illumination at 20x zoom objective lens.

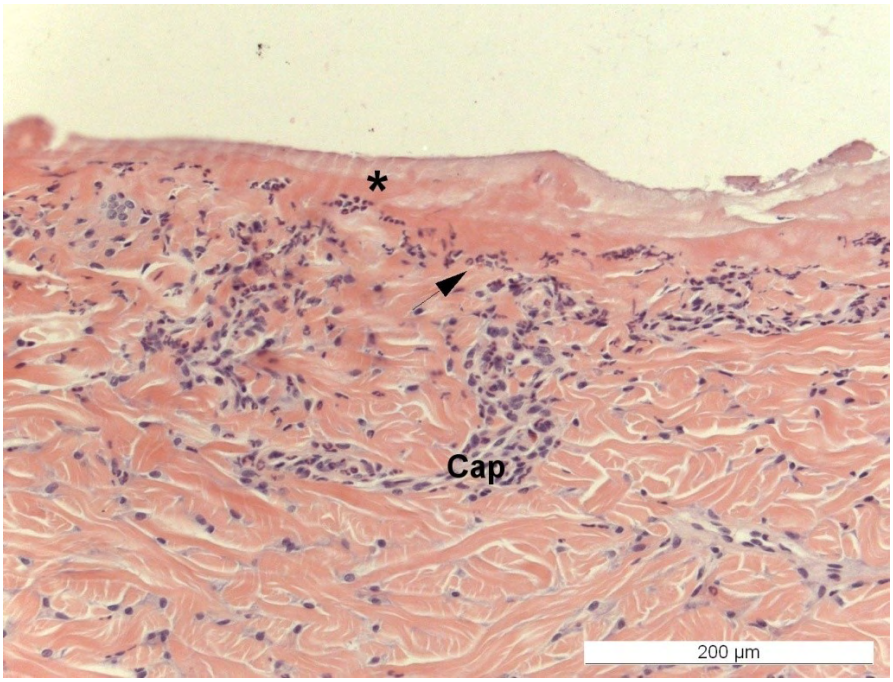

Figure 5.14: Histopathology of superficially damaged skin showing complete loss of epidermis and replacement with an eschar and exposed, dermal collagen (*).

A mild, PMN infiltrate (arrow) is present associated with superficial blood vessels (Cap). The haematoxylin and eosin stained section was viewed by light microscopy with bright field illumination at 20x zoom objective lens.

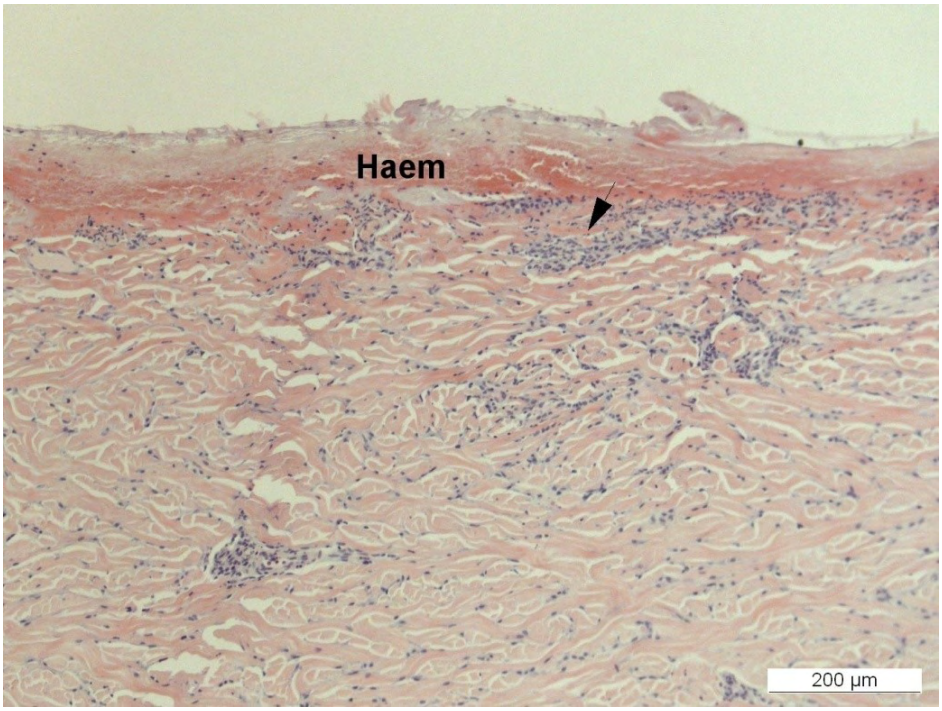

Figure 5.15: Histopathology of superficially damaged skin showing epidermal loss, marked surface haemorrhage (Haem) with fibrin and cellular debris.

Neutrophilic cell infiltrate is also shown (arrow). The haematoxylin and eosin stained section was viewed by light microscopy with bright field illumination at 10x zoom objective lens.

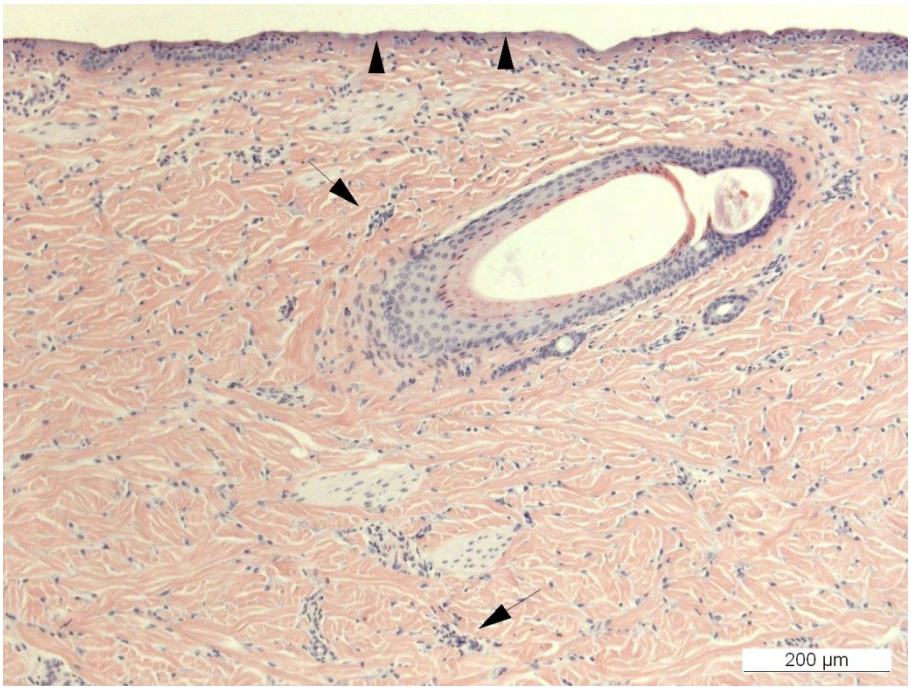

Figure 5.16: Histopathology of superficially damaged skin following SM exposure.

Partial to complete loss of the epidermis observed. Neutrophilic cell infiltrate are present (arrow). The haematoxylin and eosin stained section was viewed by light microscopy with bright field illumination at 10x zoom objective lens.

Genomic Analysis

Relative mRNA levels for gene transcripts for the different treatment sites were compared to identify up-regulated or down-regulated genes (as described in Chapter 2). Differential expression was defined as a false discovery rate (FDR) corrected p value <0.05 and ≥ 2-fold change in relative mRNA levels. Approximately 1.4% of total transcripts (43663 probes) were found to have an altered expression pattern. Damaged (unexposed) skin had 397 transcripts whose relative mRNA levels were statistically different to control (untreated) skin. Sulphur mustard-exposed damaged skin had 206 transcripts whose relative mRNA levels statistically significantly differed to control (untreated) skin. Of these differentially expressed transcripts, 136 were shared by both unexposed and SM exposed damaged skin.

There were 118 differentially expressed transcripts in SM treated animals (unexposed vs. SM-exposed, damaged skin). Sequences that did not match any genes currently registered on GenBank or Unigene were listed as unknowns. Sequences that did not have a characterised gene product (based on GenBank Accession number and Unigene identifier) were excluded from further *in silico* validation analysis. However, a full list of differently expressed gene transcripts (≥1.5-fold change); including those with uncharacterised or predicted gene products is provided in Appendix 1 (Table 2 and 3). From the genes that met these criteria (≥2-fold change), 1 gene transcript was found to be up-regulated (Table 5.4) and 36 gene transcripts were found to be down-regulated (Table 5.6).

Gene product	GenBank accession number	Fold change	Corrected p-value
Thioredoxin interacting protein	NM_001044614	2.2	0.0002

Table 5-4: Differentially up-regulated gene transcripts in the skin following ^{14}C-SM percutaneous challenge via superficially damaged skin.

Fold changes were determined by the mean expression ratio of SM exposed: unexposed damaged skin. Statistically significance differences in relative gene expression were identified by parametric t-test with a Benjamini and Hochberg False Discovery Rate (FDR) multiple-testing correction applied. Statistical significance was predefined as corrected p-value ≤0.05.

Gene product	GenBank accession number	Fold change	Corrected p-value
S-antigen (arrestin)	NM_214079	6.6	0.01
methionine adenosyltransferase I, alpha	NM_001243187	6.6	0.01
Dual oxidase 2	NM_213999	4.5	0.01
Uroplakin 2	NM_214012	4.4	0.002
Fc fragment of IgA, receptor for	NM_001123112	4.3	0.0007
Adrenergic alpha-1D receptor	NM_001123073	3.9	0.008
Chromogranin B	NM_214081	3.9	0.04
Nitric oxide synthase 2 (inducible)	NM_001143690	3.5	0.01
Mucin 13, cell surface associated	NM_001105293	3.5	0.006
Progesterone receptor membrane component 2	NM_001097521	3.5	0.03
Prostaglandin G/H synthase 2	NM_214321	3.4	0.002
immunoglobulin superfamily, member 1	AK349537	3.4	0.004
outer dense fibre protein 2-like	EW159310	3.2	0.02
prostaglandin-endoperoxide synthase 2 (prostaglandin G/H synthase and cyclooxygenase)	NM_214321	3.2	0.002
NADH dehydrogenase (ubiquinone) 1 beta subcomplex, 8, 19kDa	AK236557	3.1	0.0003
albumin	NM_001005208	2.9	0.009
PR domain containing 10	AK239583	2.9	0.004
progestin and adipoQ receptor family member VIII	NM_213740	2.7	0.01
adenosine monophosphate deaminase 1	NM_001123076	2.7	0.0003
retrotransposon-like 1	NM_001134358	2.6	0.0005
gastrin	NM_001004036	2.6	0.01

pancreatic lipase-related protein 1	NM_001142897	2.5	0.004
steroid sulfatase (microsomal), isozyme S	DN129273	2.5	0.02
CHD3-like protein	EU780792	2.5	0.003
MARC 2PIG Sus scrofa cDNA 5', mRNA sequence	BF190050	2.3	0.02
multicatalytic proteinase subunit K	AY610111	2.3	0.002
hepatocyte nuclear factor 4, alpha	NM_001044571	2.3	0.0002
WD repeat domain 46	AK348376	2.2	0.007
cytochrome P450 2C33	NM_214414	2.2	0.008
tumour necrosis factor, alpha-induced protein 8-like 2	NM_001204370	2.2	<0.0001
annexin A9	NM_001243348	2.2	<0.0001
carnitine palmitoyltransferase 1B (muscle)	NM_001007191	2.1	0.004
MARC 2PIG Sus scrofa cDNA 5', mRNA sequence	BI360438	2.0	0.03
creatine kinase, muscle	NM_001129949	2.0	0.02
kinesin family member C1	AK233842	2.0	0.03

Table 5-5: Differentially down-regulated gene transcripts in the skin following ^{14}C-SM percutaneous challenge via superficially damaged skin.

Fold changes were determined by the mean expression ratio of SM exposed: unexposed damaged skin. Statistically significance differences in relative gene expression were identified by parametric t-test with a Benjamini and Hochberg False Discovery Rate (FDR) multiple-testing correction applied. Statistical significance was predefined as corrected p-value ≤0.05.

DISCUSSION

This study has demonstrated that direct application of SM to superficial wounds results in rapid onset of erythema and ulceration and a significant decrease in perfusion at the skin exposure site. The pig is an established model for investigating the effects of SM *in vivo* (Price*, et al*. 2009, Chilcott*, et al*. 2007, Renshaw. 1946, Reid*, et al*. 2001). However, use of this model has the following limitations.

Relevance of animal model

The human dermal response to SM is unique in the fact that currently used animal models do not typically produce the classical gross, bullous blister (Renshaw. 1946, Mcadams. 1956). This could potentially mean that decontaminants that are effective in animal models may not have sufficient efficacy in humans. However, dermal/epidermal separation resulting in microblistering has been observed in porcine skin in response to SM exposure (Brown and Rice. 1997, Mitcheltree*, et al*. 1989). As previously described the structure of pig skin closely resembles that of human skin (Bartek*, et al*. 1972) and penetration rates of SM through intact skin *in vitro* are akin to human skin (Reifenrath*, et al*. 1991). Therefore, the pig provides a suitable model for decontaminant efficacy testing.

Length of study period

Previous studies have followed lesion development over a considerably longer time period (>24 h) than this study (Graham*, et al*. 2000, Reid*, et al*. 2000). This study investigated early time point (up to 6 h) effects of SM which negated the need to recover the animals. The use of terminal anaesthesia was considered a substantial

refinement to experimental animal welfare. Previous studies reporting histopathology conducted at early time points (≤ 6 h) following SM exposure via undamaged skin showed few definite structural alterations (Brown and Rice. 1997). However, the time course for cutaneous lesion progression following SM exposure via superficially damaged skin was unknown. Therefore, the absence of significant differences between the unexposed and SM-exposed damaged skin observed in this study are consistent with previous investigations.

Influence of SM-induced systemic effects on unexposed skin

As SM was applied to damaged skin, a damaged (unexposed) skin site from each animal served as the untreated control for differential gene expression analysis and histopathology. This has the potential limitation of being influenced by SM via the systemic circulation (Elsayed and Omaye. 2004). However, there was no detectable ^{14}C-SM present at this site (damaged, unexposed skin), although it is feasible that SM may have caused systemic inflammatory changes which may have altered dermal gene expression at unexposed sites. Use of an unexposed site on the same animal is consistent with previous studies investigating SM effects on cutaneous gene expression where systemic effects due to dermal SM exposure were not reported (Dillman III*, et al*. 2006, Rogers*, et al*. 2004).

Differences in microarray slide annotation

A manufacturing fault with the microarray gasket slides resulted in some arrays having to be repeated using a new batch of oligonucleotide microarray slides. However, the new batch of slides was subsequently identified as a different technology during analysis using GeneSpring software. This required a custom technology file to be

created and translation from one slide version to another to allow sample comparison between the different versions. However, differences in annotations between the two versions could have resulted in some probes becoming redundant. This may have impacted on the number or identity of genes that were differentially expressed following SM exposure. The effect of translating the data between different slide versions was assessed by comparing the differentially expressed gene list using each version of the array slide as the primary template for translation of the other slide version. Fold-change and statistical analysis were then conducted on both data sets. No differences in the identity or number of genes differentially expressed were found between the data sets.

Quantification of gene expression changes

Quantitative real-time polymerase chain reaction (qRT-PCR) is considered the "gold standard" for validation of results obtained from microarray experiments (Wang, *et al*. 2006). Due to time constraints, qRT-PCR could not be performed on gene transcripts identified as differentially expressed using the microarray platform. Therefore, the reported differences in gene expression between treatment groups are relative and use of qRT-PCR would be desirable to quantify and validate gene transcript expression changes reported in this Thesis.

Speciation of ^{14}C radiolabelled products

As discussed earlier (Chapter 4) the use of liquid scintillation counting to quantify the amount of ^{14}C-SM does not allow for speciation of the ^{14}C-radiolabel isotope. Therefore, this approach assumes that the amount of ^{14}C-SM present is equivalent to the amount of ^{14}C isotope measured. It has been previously shown that SM is conjugated or

hydrolysed *in vivo* (Black, *et al*. 1993, Capacio, *et al*. 2004) so the ^{14}C isotope could be attributed to a conjugate or hydrolysis product. Speciation of radiolabelled compounds using chromatography (gas or liquid) and mass spectrometry would determine if these compounds were the SM parent molecule or a hydrolysis product/conjugate. These techniques have been previously used to identify SM metabolites (Noort, *et al*. 2004, Noort, *et al*. 2000). Although these limitations should be considered when interpreting and extrapolating data to human SM injuries they do not negate the usefulness of this model and the findings described below.

Removal of the skin barrier layer (SC and epidermis) greatly reduced the lag time between SM challenge and the appearance of advanced signs of exposure compared to published data for undamaged skin (Smith, *et al*. 1997, Graham, *et al*. 2000, Reid, *et al*. 2000). Skin erosions or ulcerations were observed in all animals (4 h median time) within 6 h compared to previously reported delay of up to 24 h. Thus, one speculative conclusion from this study is that the latency period seen for SM injuries could be in part due to delayed absorption and not exclusively due to delays caused by cellular processes described in Chapter 1, such as DNA damage or inflammatory-mediated responses (Papirmeister, *et al*. 1985, Arroyo, *et al*. 2001a).

Blanching of the skin surrounding the SM droplet was noted in all animals within 60 min of exposure. Maximal blood flow, as measured by LDI, in the skin was also significantly reduced following SM exposure. Reduced perfusion at the exposure site could be attributable to either SM-induced necrotic capillary congestion or vasoconstriction of the blood vessels in the dermis. Histopathological analysis revealed capillary dilation and congestion of subepidermal capillaries with perivascular

inflammatory cell infiltrate. This is consistent with previous studies which also observed significantly reduced skin perfusion at the lesion site (Brown*, et al*. 1998).

Sulphur mustard has been shown to cause significant changes in vascular permeability in a dose-dependent manner (Zhang*, et al*. 1995b). It has been postulated that this may be mediated by SM-induced prostaglandin release (Zhang*, et al*. 1995b). Oedema at the exposure site was also observed in two thirds of the animals. Therefore, SM may cause inflammatory-mediated, extra-vascularisation of fluid resulting in localised oedema and reduced perfusion at the exposure site. There was evidence of oedema in the histology sections of SM exposed skin although, the SM-exposed, damaged skin was not overtly different to the unexposed damaged skin.

Skin reflectance spectroscopy has been previously used to assess SM and thermal burn progression and severity (Chilcott. 2000). Removal of the SC and epidermis resulted in statistically significant increases in both skin redness (a*) and hue (b*). The increase in the two parameters can be attributed to punctate haemorrhage and inflammation (skin redness) and sero-cellular crusting or escharification (skin yellowness) following the removal of the upper skin layers. These observations were confirmed by histopathology. Sulphur mustard did not have a statistically significant effect on CIELAB (L*a*b*) parameters compared to damaged (unexposed) skin. This was unexpected as erythema was visible in half the animals at 2 h post challenge. Previous studies have observed statistically significant changes in skin redness (a*) at 1 h post challenge (Chilcott. 2000). However, removal of the upper skin layers resulted in the unexposed skin becoming erythematous. Therefore, although a qualitative difference in skin redness was observed between the SM-exposed and unexposed skin it was not deemed statistically significant in terms of a* value.

Transepidermal water loss has been previously been used as a measure of skin barrier function (Chilcott. 2000). Unsurprisingly, removal of the upper (100 μm) skin layers (equating to loss of SC and epidermis) with a dermatome resulted in significantly increased TEWL rates compared to undamaged control values. Over the 6 h study period no statistically significant differences were observed between either of the damaged groups regardless of SM exposure. This is consistent with findings from previous studies using undamaged skin porcine models (Chilcott. 2000). A significant increase in TEWL was observed for the control (untreated) skin ($p<0.002$). This may possibly be attributed to combined effects of constant air flow (>0.5 m s^{-1}) and low humidity within the chemical fume hood resulting in an increase water gradient between the skin and the surrounding air. Alternatively, it could be due to diurnal variation or changes in skin physiology resulting from cumulative effects of anaesthesia.

Histopathology confirmed that the use of an electric dermatome achieved complete removal of the SC and epidermis. One concern with skin from the same animal serving as a control was that SM could induce a systemic inflammatory response which could affect the surrounding dorsal skin. However, no significant microscopic changes in control (untreated) gross skin structure were observed. There were no significant difference in microscopic findings between SM-exposed and unexposed damaged skin groups. This was unexpected as there were significant differences in both blood perfusion and the amount of ^{14}C derived from ^{14}C-SM within the skin between the two sites. However, the presence of a few definite structural alterations at 6 h post exposure is in agreement with previous SM studies using undamaged skin (Brown and Rice. 1997, Greenberg*, et al*. 2006). Work by Brown et al. (1997) also observed

perivascular PMN infiltrate, seen in this study. Focal vacuolation and limited pyknotic nuclei in basal keratinocytes have also been reported (Brown and Rice. 1997, Greenberg*, et al*. 2006, Kan*, et al*. 2003). Removal of the epidermis in this study would prevent this being observed and the acute inflammatory response resulting from the initial tissue damage (removal of skin layers) may mask any additional histopathological changes caused by SM at this early time point.

Radiolabelled (^{14}C) SM was rapidly absorbed through superficial damaged skin into the circulation. Total recovery from the skin, skin surface swabs, blood and internal organs samples equated to 6.2 ± 1.6% of the applied dose. This corresponds to the percentage dose penetrated in the *ex vivo* isolated perfused porcine skin flap (IPPSF) model at a comparable time-point (Riviere*, et al*. 1995). The largest proportion of ^{14}C derived from ^{14}C-SM recovered 6 h post-challenge was from the skin surface swabs and the skin at the exposure site (3.5 ± 1.6% and 2.2 ± 0.5% of applied dose, respectively). Once absorbed, the majority of the ^{14}C resided within the skin or blood which is in agreement with previous studies (Hambrook*, et al*. 1992). At early time-points, a large fraction of SM within the skin is still mobile but there is debate as to whether it is conjugate/hydrolysis product (Hambrook*, et al*. 1992, Spoo*, et al*. 1995) or the parent compound, SM (Hattersley*, et al*. 2008).

Toxicokinetics of SM in the blood appeared to fit a first-order elimination model. This was in agreement with Zhang and Wu (1987) for SM exposure via subcutaneous route. Blood concentrations of ^{14}C derived from ^{14}C-SM peaked at 120 min post-exposure with a calculated half-life of 460 ± 62 min. However, the previous study did not detect any SM in the blood via the percutaneous route (Zhang and Wu. 1987). This could be attributed to the difference in absorption between superficially

damaged and undamaged skin. However, the previous study quantified SM by flame photometric gas chromatography (GC-FP) detection where as this study used liquid scintillation counting to quantify ^{14}C-isotope. Thus the ^{14}C-isotope detected could be a conjugate or hydrolysis product of SM and not intact SM. Alternatively GC-FP may not be sensitive enough to detect these changes.

The distribution of radioactivity within internal organs tends to suggest that the main route of excretion is in the urine followed by the faecal route. Accumulation of radiolabelled SM in the kidneys and small intestine has also been shown in rodent models (Hambrook*, et al*. 1992). Hepatic metabolism of SM has previously been documented (Davison*, et al*. 1961) and both conjugates and hydrolysis products of SM have previously been detected in the urine of exposed subjects or animals (Black*, et al*. 1992, Maisonneuve*, et al*. 1993).

The aim of the microarray studies was to identify potential genes of interest affected by SM exposure which warrant further investigation. Overall, only one gene transcript, thioredoxin interacting protein (TXNIP), met the 2-fold increase in relative gene expression threshold following SM exposure. However, seven out of the top ten up-regulated gene transcripts (≥ 1.5-fold change) were TXNIP. Thioredoxin interacting protein (also known as Vitamin D3 up-regulated protein 1) is a pro-apoptotic member of the α-arrestin family (Kim*, et al*. 2012, Patwari*, et al*. 2009) but has not previously been identified as being up-regulated following SM exposure (Dillman III*, et al*. 2006, Sabourin*, et al*. 2004, Rogers*, et al*. 2004). Thioredoxin interacting protein is thought to be involved in the regulation of keratinocyte differentiation (Zhou*, et al*. 2010, Champliaud*, et al*. 2003). Sulphur mustard is known to promote keratinocyte terminal

differentiation via intracellular calcium influx which promotes cornified envelope development (Rosenthal, *et al*. 1998, Popp, *et al*. 2011, Eckert, *et al*. 1993).

Thioredoxin interacting protein has also been shown to be involved in NLRP3 inflammasome activation and subsequently interleukin-1beta (IL-1β) production (Zhou, *et al*. 2010) and has been shown to be induced by oxidative stress mediated by an influx of calcium into the cytoplasm (Kim, *et al*. 2012). Interleukin-1β mRNA levels have been shown to be increased as early as 6 h post SM exposure (Sabourin, *et al*. 2000, Vallet, *et al*. 2012, Sabourin, *et al*. 2002). Therefore, TXNIP could provide a potential therapeutic target for reducing inflammation caused by SM exposure and warrants validation and further investigation.

Down regulated gene transcripts indentified were mostly involved in inflammatory/immune response, oxidative stress response, cell signalling or cell differentiation/proliferation. Dual oxidase 2 is a member of the NADP oxidase family and has NADPH/Ca^{2+}-dependent hydrogen peroxide-generating activity in the airway epithelium (Ameziane-El-Hassani, *et al*. 2005).

Prostaglandin G/H synthase 2 also known as cyclooxygenase-2 (COX-2) has been previously been shown to be up-regulated in response to SM exposure and is involved in the acute phase inflammatory response caused by SM (Gerecke, *et al*. 2009, Wormser, *et al*. 2004) which is in direct contrast to the findings of this present study. The previous studies investigated the effects at later time points to this study. Therefore, it is conceivable that SM-induced COX-2 expression may be time-dependent.

Calcium plays a key role in SM-induced cytotoxicity and terminal differentiation of keratinocytes (Rosenthal, *et al*. 1998). Chromogranin B interacts with inositol 1,4,5-triphosphate receptors (IP_3R) to modulate Ca^{2+} release from intracellular

stores and subsequent Nuclear Factor κB (NF κB) activity (Heidrich, *et al*. 2008). Calcium via CaM can also induce intrinsic mitochondrial pathways of apoptosis (Simbulan-Rosenthal, *et al*. 2006). Calcium and CaM are also thought to induce nitric oxide production via nitric oxide synthase (Spratt, *et al*. 2007).

Relative mRNA expression of inducible nitric oxide synthase (iNOS) was found to be down-regulated following SM exposure. This is in disagreement with other published studies where increases in iNOS function following SM exposure were observed (Gao, *et al*. 2008, Steinritz, *et al*. 2009). However, in a keratinocyte wound model, SM exposure was found to decrease iNOS expression (Ishida, *et al*. 2008). Nitric oxide (NO), produced by iNOS, has a role in wound healing (Schwentker, *et al*. 2002) and SM-induced iNOS inhibition has been attributed to delayed wound healing (Ishida, *et al*. 2008). This apparent disagreement between studies could be dependent on SM dose, the use of immortalised keratinocytes versus normal human epithelial keratinocytes or due to the relative increase in iNOS as a result of wounding.

Interestingly, SM-induced down-regulation of gene transcripts which do not appear to have a defined role in the skin was observed. One potential explanation is that the dermal layers contain a large number of cells with distinct functions e.g. vascular endothelial cells in papillary capillaries or neutrophils. Microarrays were performed with total RNA pooled from many cell types in whole skin and reflect the global response to SM in the tissue. Therefore, SM-induced down-regulation of adrenergic alpha-1D receptor observed could be associated with vascular cells in the sample and not directly involved in keratinocyte response to SM. Likewise down-regulation of IgA Fc receptors is likely to be associated with the PMN infiltrate observed in the dermis.

Uroplakin II (UPK2) is a membrane-associated protein that is critical for barrier function in the urothelium. Uroplakin II has also been associated with the transcriptional regulator, interferon regulatory factor-1 (IRF-1), which promotes terminal cell differentiation in the urothelium (Varley, *et al*. 2008). Interferon regulatory factor-1 is believed to have a role in the regulation of cornified envelope genes during keratinocyte terminal differentiation (Nakanishi, *et al*. 1997) and DNA damage-induced apoptosis (Tamura, *et al*. 1995). Aberrant expression of IRF-1 has been attributed to the development of bullous pemphigoid which is characterised by subepidermal blistering (Odanagi, *et al*. 2004). Therefore, UPK2 may have an additional role in skin epithelium barrier function that has yet to be characterised.

S-antigen, a member of the arrestin/β-arrestin protein family has been previously identified as down-regulated in response to SM exposure (Rogers, *et al*. 2004). This protein is normally associated with regulation of light activated phosphorylated rhodopsin (Brown, *et al*. 2010). S-antigen may also be involved in regulation of oxidative stress and inflammation although its role has yet to be fully elucidated (Brown, *et al*. 2010, Khurana, *et al*. 2008). Mucin 13 is a membrane-bound, O-linked glycoprotein localised in the epithelium (Singh and Hollingsworth. 2006). Whilst a defined function for mucin 13 in the skin is currently unknown, other members of the mucin family are associated with cell adhesion and immune modulation (Rounds, *et al*. 1999).

Lack of protein and gene function characterisation is a major disadvantage of using the pig compared with the mouse. However, pig skin provides a more accurate representation of human skin in terms of dermal absorption compared to mouse skin (Bartek, *et al*. 1972). Therefore, further work to characterise the biological function of

porcine genes would be advantageous and could expand the use of the pig to study the genomic effects of SM. However, it is worth noting that when SM is applied to damaged skin, differentially expressed genes are predominantly down regulated in the skin. This is in contrast with the predominant upregulation of gene expression in the skin in response to SM applied to undamaged skin at similar time points (Gerecke*, et al*. 2009). Moreover, it is unlikely the predominate down regulation observed is non-specific as the expression of house-keeping genes such as calnexin and β-catenin was unaffected by SM exposure. Therefore, further investigations are needed to establish if there are differences in SM-induced toxicity between damaged and undamaged skin, to allow further development of medical countermeasures for SM-exposed damaged skin injuries.

Conclusions

The pig is an established model for investigating the progression of SM cutaneous lesion *in vivo.* This study has shown that removal of the SC and epidermis reduces the lag time between SM exposure and the appearance of advanced signs of toxicity. Sulphur mustard also significantly reduced perfusion rates at the exposure site within 6 hours. However, no significant changes in skin colour, barrier function to water loss, or skin surface temperature were observed between SM-exposed and unexposed damaged skin. Furthermore, no significant microscopic changes were observed in SM-exposed skin compared to unexposed skin. Damaged associated with removal of the upper skin layers could potentially account for this. Sulphur mustard induced changes in relative mRNA levels in gene transcripts were primarily associated with oxidative stress, inflammatory response and keratinocyte terminal differentiation.

Recommendations for future work

- This pig model should be used to assess the decontaminant efficacy of WoundStat™ *in vivo* (Chapter 6).
- Liquid-chromatography should be used for the speciation of sample containing ^{14}C-isotope to determine whether they contain the parent compound (SM) or a conjugate/hydrolysis product.
- Relative changes in mRNA levels observed using microanalysis should be quantified and validated using qRT-PCR.

Chapter 6

WoundStat™ is effective in reducing SM-induced toxicity when applied to superficially damaged skin in vivo

INTRODUCTION

WoundStat™ has been shown to significantly reduce the penetration of ^{14}C-SM through superficially damaged skin *in vitro* (Chapter 4). However, superficial damage to the skin has been shown to reduce the time to appearance of advanced signs of toxicity and allows rapid systemic distribution *in vivo* of SM (Chapter 5). Changes in blood flow following SM exposure were apparent at an early time point and this may provide a useful measure by which the efficacy of WoundStat™ can be measured. Changes in relative expression of a number of genes including: iNOS, TXNIP and DUOX2 were also observed. The down-regulation in gene expression observed for iNOS was in agreement with previous *in vitro* wounded skin studies (Ishida*, et al*. 2008). However, other *in vivo* studies using undamaged skin have observed an increase in iNOS gene expression following SM exposure (Steinritz*, et al*. 2009). This suggests that the combined physical injury (removal of upper skin layers) and SM exposure may result in gene expression changes which have not be previously described by other *in vivo* studies. Therefore, SM therapeutic targets identified for undamaged skin may not be suitable for damaged skin.

A number of *in vivo* studies have evaluated decontamination of SM using undamaged skin (Chilcott*, et al*. 2007, Taysse*, et al*. 2007, Taysse*, et al*. 2011, Wormser*, et al*. 2002). However, there is only one published study examining the efficacy of decontamination regimes *in vivo* when SM is applied to hairless guinea pigs via damaged skin (Gold*, et al*. 1994). Furthermore, this study used limited endpoints, namely gross clinical observations at 48 h, by which to determine the efficacy of decontamination. Therefore, conclusions drawn solely on these data are likely to be relatively subjective.

Whilst both the pig and the hairless guinea-pig are thought to provide good animal models of percutaneous penetration (Barbero and Frasch. 2009, Simon and Maibach. 2000) the smaller blood volume of the guinea pig would prevent extensive acquisition of blood samples. This would limit the number of samples available for radiometric and genomic analyses. The pig has been shown to be a suitable animal model for characterising SM-induced cutaneous lesions (Chapter 5). Therefore, this model was used to evaluate the efficacy of WoundStat™ as a decontaminant.

Aims

The purpose of this study was to evaluate the decontamination efficacy of WoundStat™ *in vivo*. The efficacy of WoundStat™ was assessed by measuring;

- the toxicokinetics and distribution of ^{14}C-SM,
- SM lesion development and,
- the effect of WoundStat™ decontamination of SM-exposed skin on gene expression.

MATERIALS AND METHODS

Full details of methods employed in this study are described in Chapter 2. Briefly, the efficacy of WoundStat™ to reduce the severity of SM lesions and dermal absorption of ^{14}C-SM through superficially damaged porcine skin was measured *in vivo* (Figure 6.1). A 2 g bolus of WoundStat™ was applied to two damaged skin treatment sites: SM-exposed and unexposed at 30 s post-challenge. WoundStat™ remained *in situ* for 60 min before removal and was retained for radiometric analysis. The decontaminant was

removed for two reasons; (i) to allow biophysical measurements to be taken and (ii) to simulate a potential real-life scenario in which any haemostat/decontaminant would be removed once an appropriate medical facility was reached.

As described for Chapter 5, the distribution of ^{14}C derived from ^{14}C-SM (blood, dosing site and organs), lesion severity and progression and genomic changes were measured to evaluate decontamination efficacy of WoundStat™.

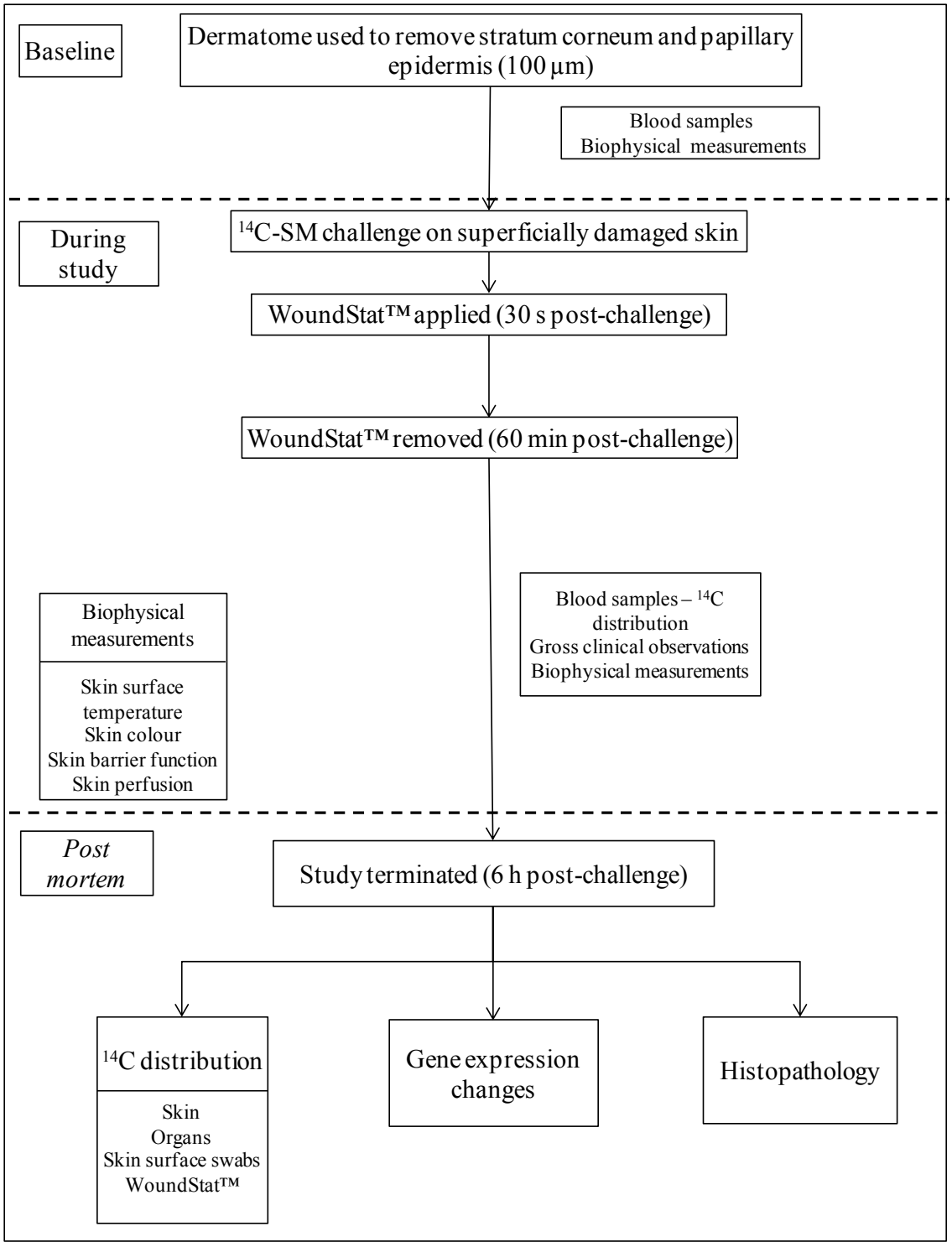

Figure 6.1: Experiment flow chart for evaluating WoundStat™ as a decontaminant against SM applied to superficially damaged skin.

RESULTS

Gross clinical observations (digital photography)

There were no remarkable visual changes seen over the 6 hour study period for the control (undamaged skin) site or damaged skin sites with and without WoundStat™. WoundStat™ reduced the appearance of skin blanching at the exposure site: 2 animals exhibited blanching at 60 min (Table 6.1) compared to all of the animals not receiving decontamination (n=6; Chapter 5, Table 5.1).

Erythema was observed in three out of six animals with the median time to observable erythema at the exposure site being 120 min (Table 6.1 and Figure 6.2). In two animals the erythematous area was surrounded by ring-like blanching. One animal had a considerable amount of dried blood at the exposure site and thus it was difficult to observe blanching or any additional erythema (Figure 6.2).

WoundStat™ also prevented the appearance of ulceration at the exposure site (n=6; Table 6.1) which was observed in all of the animals not receiving decontamination (n=6; Chapter 5, Table 5.1). The frequency of oedema at the exposure site following WoundStat™ treatment was half that of the control group (2 out of 6 animals; Table 6.1) and the mean time between SM challenge and the appearance of oedema was increased from 100 min to 180 min (Tables 5.1 and 6.1).

In two of the animals, wetting on the surface of the WoundStat™ was evident within 1 min of application to the SM-exposed site (Figure 6.2). The area on the surface corresponded to the location at which the SM droplet was applied so presumably represented SM absorbed into the product.

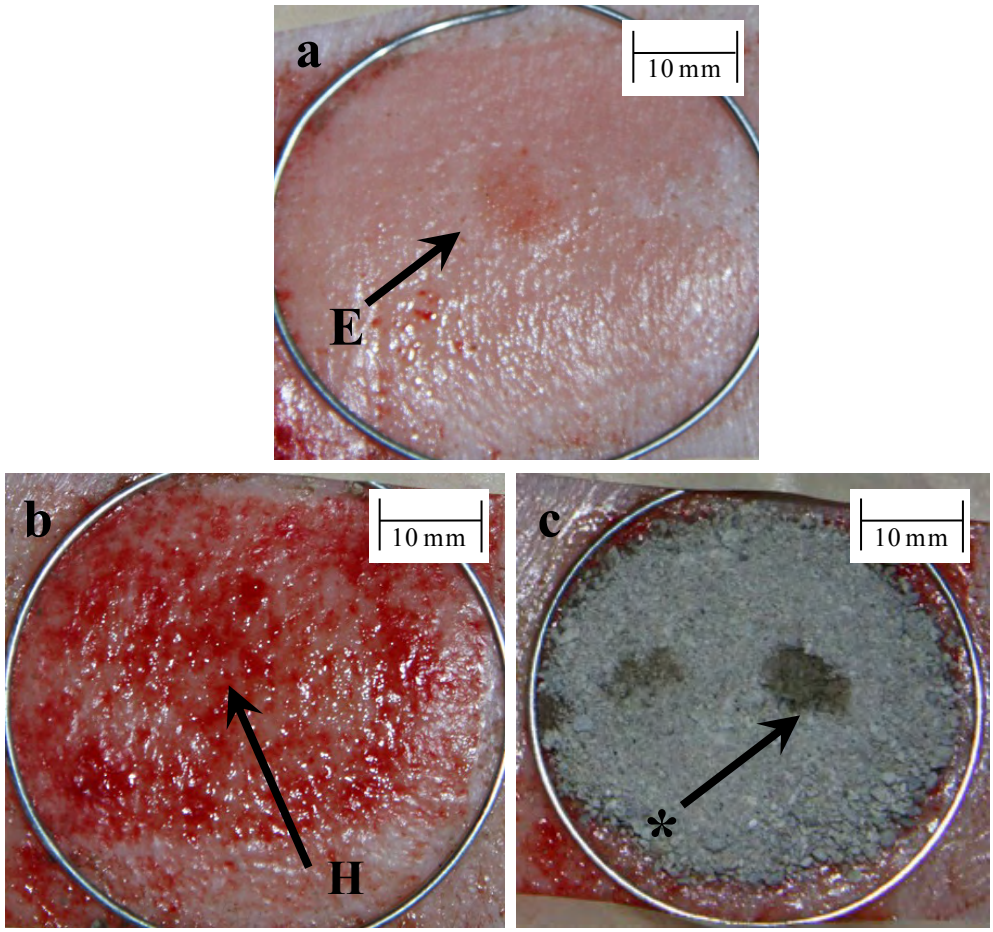

Figure 6.2: Representative photographs of skin exposure sites.

Development of erythema (E) 2 h post challenge (a),evidence of haemorrhage (H) at the skin surface 4 h post challenge (b), evidence of wetting on the surface of WoundStat™ (*) possibly SM (c).

	Onset and occurrence of visual signs of dermal toxicity			
Time point (min)	Erythema	Blanching	Ulceration	Oedema
Baseline	(0/6)	(0/6)	(0/6)	(0/6)
60	(0/6)	*2* (2/6)	(0/6)	(0/6)
120	*3* (3/6)	(0/6)	(0/6)	*1* (1/6)
180	(2/6)	(0/6)	(0/6)	(1/6)
240	(2/6)	(0/6)	(0/6)	*1* (2/6)
300	(2/6)	(0/6)	(0/6)	(1/6)
360	(2/6)	(0/6)	(0/6)	(0/6)

Table 6-1: Onset and occurrence of visual signs of SM dermal toxicity following WoundStat™ decontamination of SM-exposed, superficially damaged skin.

Physical changes to the skin (oedema and ulceration) and skin colour changes (reddening; erythema or blanching) at the exposure site were scored by one individual. Numbers shown in italics indicates the number of animals first presenting with clinical sign. The numbers in brackets indicate number of animals presenting with this clinical sign at specific time points (n=6).

Biophysical Measurements

Skin colour (skin reflectance spectroscopy)

Values for all three CIELAB parameters (L*a*b*) for control (undamaged) skin showed no statistically significant change over the 6 h study period (Figures 6.3 – 6.5). There was also no significant difference in CIELAB values for control (untreated) sites between the two groups of animals (p-value>0.05 for L*, a* and b* values; Figures 5.3 – 5 and 6.3 – 5). As previously described, the removal of the SC and epidermis resulted in statistically significant increases in skin redness and hue ($p<0.05$; Figures 6.4 and 6.5).

However, treatment with WoundStat™ resulted in a statistically significant decrease in skin brightness (L*) compared to control (undamaged) skin at all time points measured post-challenge ($p<0.05$; Figure 6.3). There was no significant difference between sites receiving SM challenge and WoundStat™ decontamination and those receiving only WoundStat™ for skin colour or brightness parameters measured (Figures 6.3 – 6.5).

Overall, there was not a statistically significant difference in skin brightness between SM-exposed skin with and without decontamination with WoundStat™ (Figure 6.6). However, there was a statistically significant difference between the two groups at 300 min post-challenge ($p<0.05$; Figure 6.6). No statistically significant difference in skin colour (a* and b*) was observed between SM-exposed skin with and without decontamination with WoundStat™ (Figures 6.7 – 6.8).

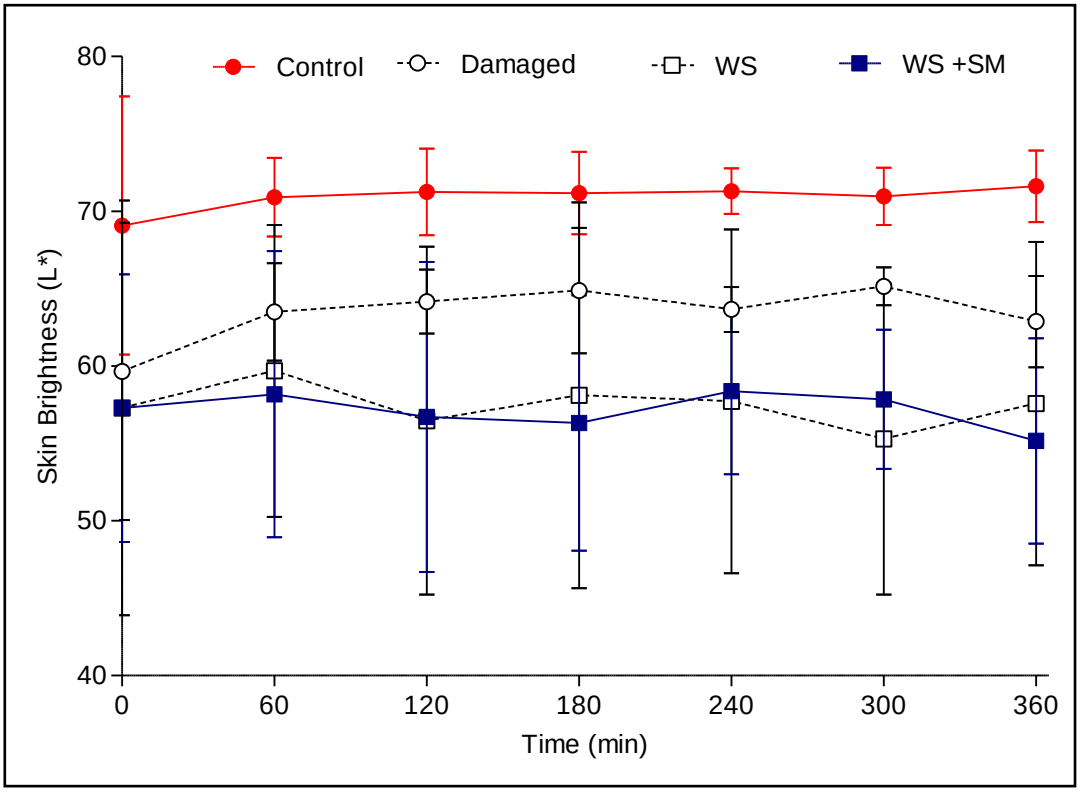

Figure 6.3: Skin lightness (expressed as the CIELAB colour scale parameter, L*) following superficial damage and treatment with WoundStat™ with (WS + SM) and without (WS) prior exposure to SM.

Undamaged (control) and damaged unexposed sites provided a negative and positive control, respectively. All values are expressed as mean ± 95% confidence intervals (n=6).

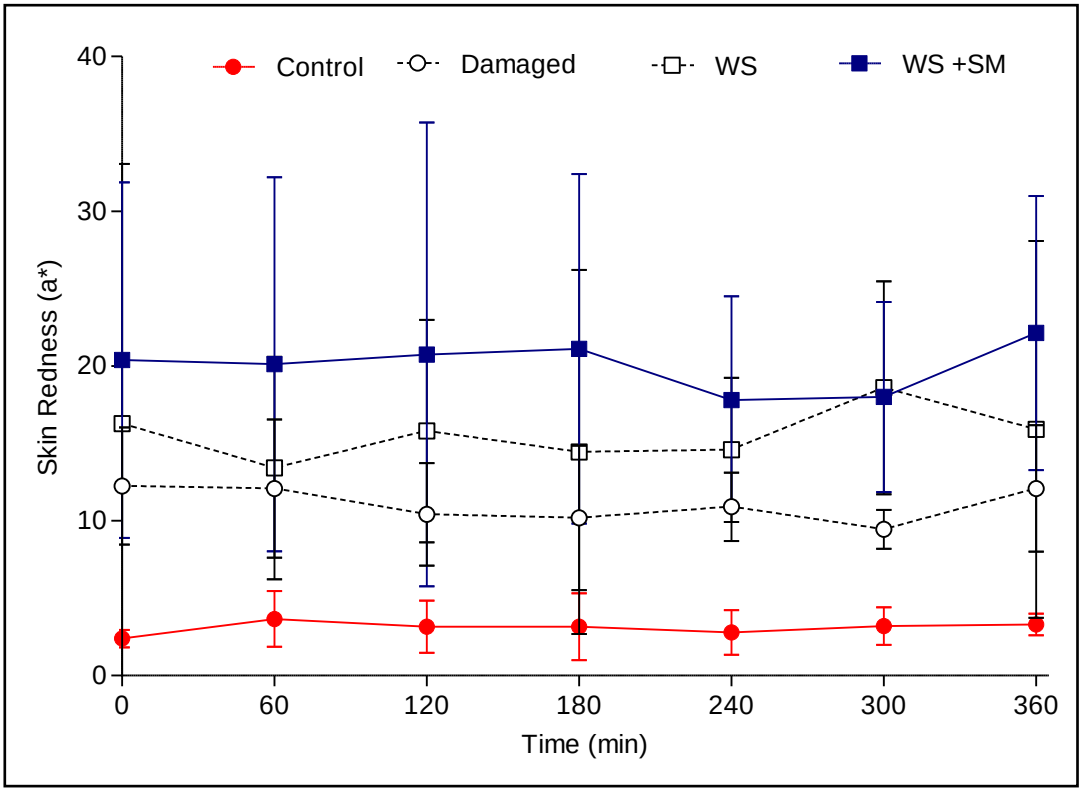

Figure 6.4: Skin erythema (expressed as the CIELAB colour scale parameter, a*) following superficial damage and treatment with WoundStat™ with (WS + SM) and without (WS) prior exposure to SM.

Undamaged (control) and damaged unexposed sites provided a negative and positive control, respectively. All values are expressed as mean ± 95% confidence intervals (n=6).

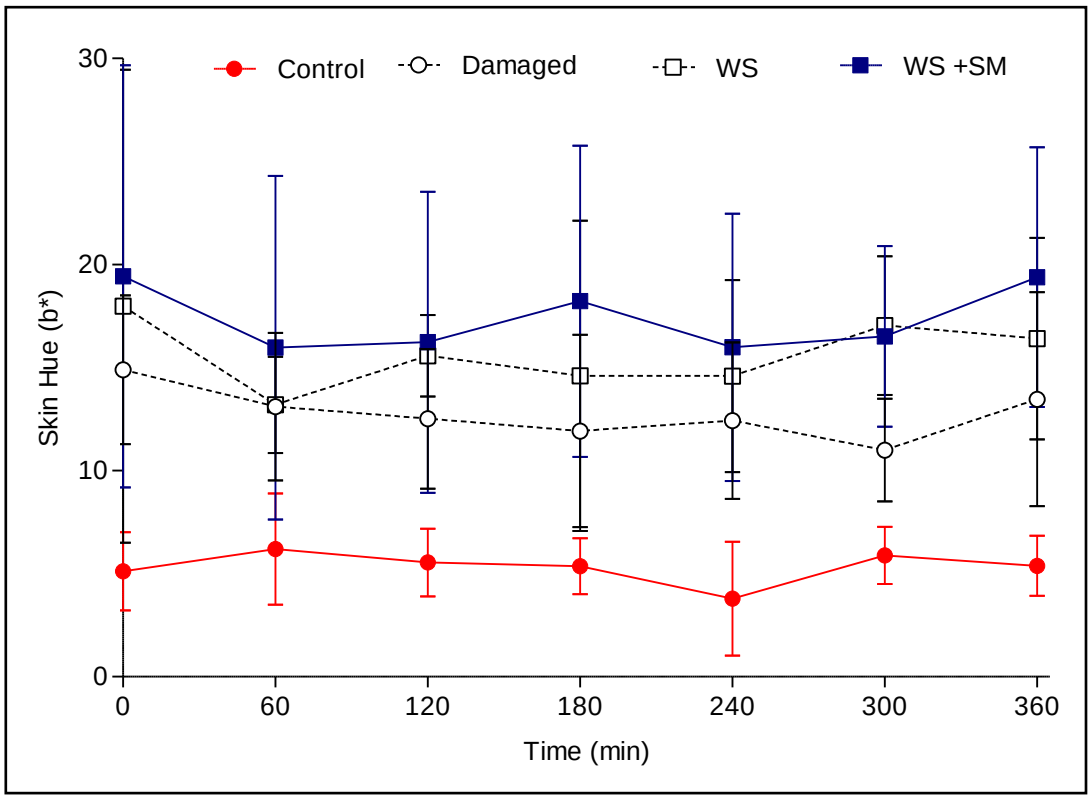

Figure 6.5: Skin hue (expressed as the CIELAB colour scale parameter, b*) following superficial damage and treatment with WoundStat™ with (WS + SM) and without (WS) prior exposure to SM.

Undamaged (control) and damaged unexposed sites provided a negative and positive control, respectively. All values are expressed as mean ± 95% confidence intervals (n=6).

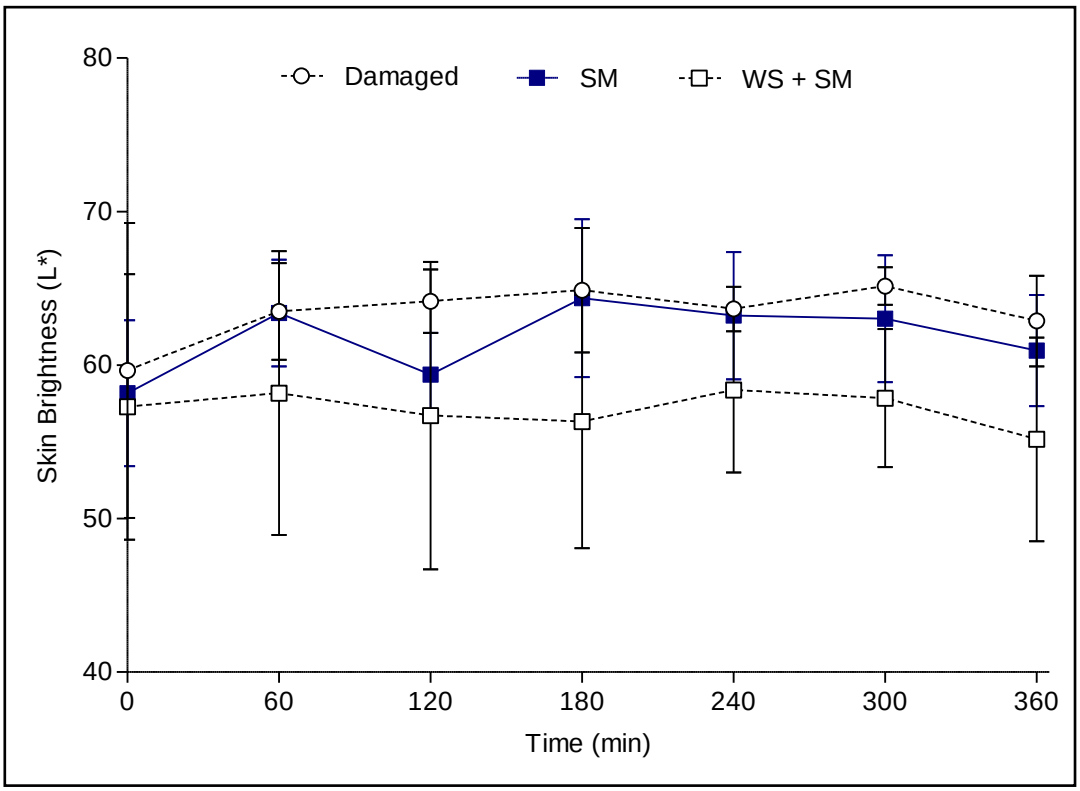

Figure 6.6: Skin lightness (expressed as the CIELAB colour scale parameter, L*) for the two treatment groups: superficial damage and SM challenge with decontamination with WoundStat™ (WS + SM) and without (SM; Chapter 5).

Damaged unexposed sites provided a positive control. All values are expressed as mean ± 95% confidence intervals (n=6).

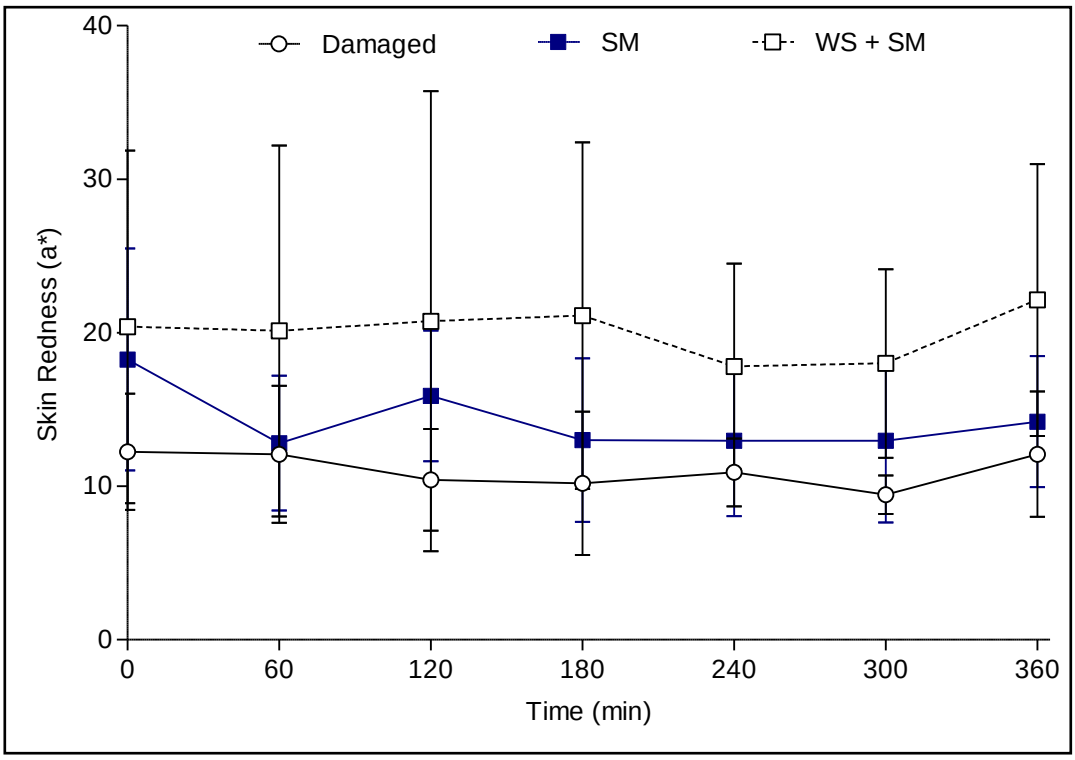

Figure 6.7: Skin erythema (expressed as the CIELAB colour scale parameter, a*) for the two treatment groups: superficial damage and SM challenge with decontamination with WoundStat™ (WS + SM) and without (SM; Chapter 5).

Damaged unexposed sites provided a positive control. All values are expressed as mean ± 95% confidence intervals (n=6).

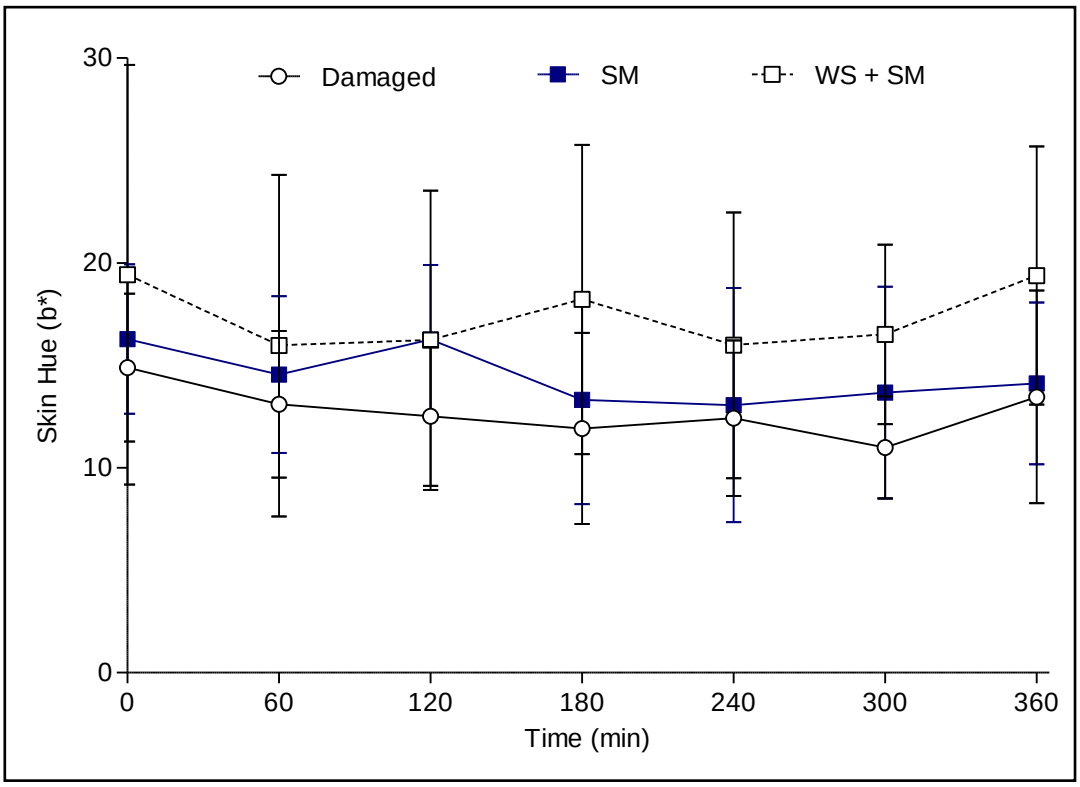

Figure 6.8: Skin hue (expressed as the CIELAB colour scale parameter, b*) for the two treatment groups: superficial damage and SM challenge with decontamination with WoundStat™ (WS + SM) and without (SM; Chapter 5).

Damaged unexposed sites provided a positive control. All values are expressed as mean ± 95% confidence intervals (n=6).

Skin surface temperature (infrared thermography)

There was not a statistically significant change in skin surface temperature for control (undamaged) skin over the 6 h study period ($p>0.05$; Figure 6.9). As previously described, a statistically significant decrease in average surface skin temperature was observed following superficial damage to the skin (removal of SC and epidermis) for all but two time points (240 and 300 min; Figure 6.9). However, there was not a statistically significant difference in skin surface temperature between the damaged skin and WoundStat™ (+/- SM) treatment groups (Figure 6.9) and SM did not produce any obvious visual changes in the thermographs (Figure 6.10). Decontamination with WoundStat™ did not result in a statistically significant change in skin surface temperature compared to SM-exposed non-decontaminated skin (Figure 6.11)

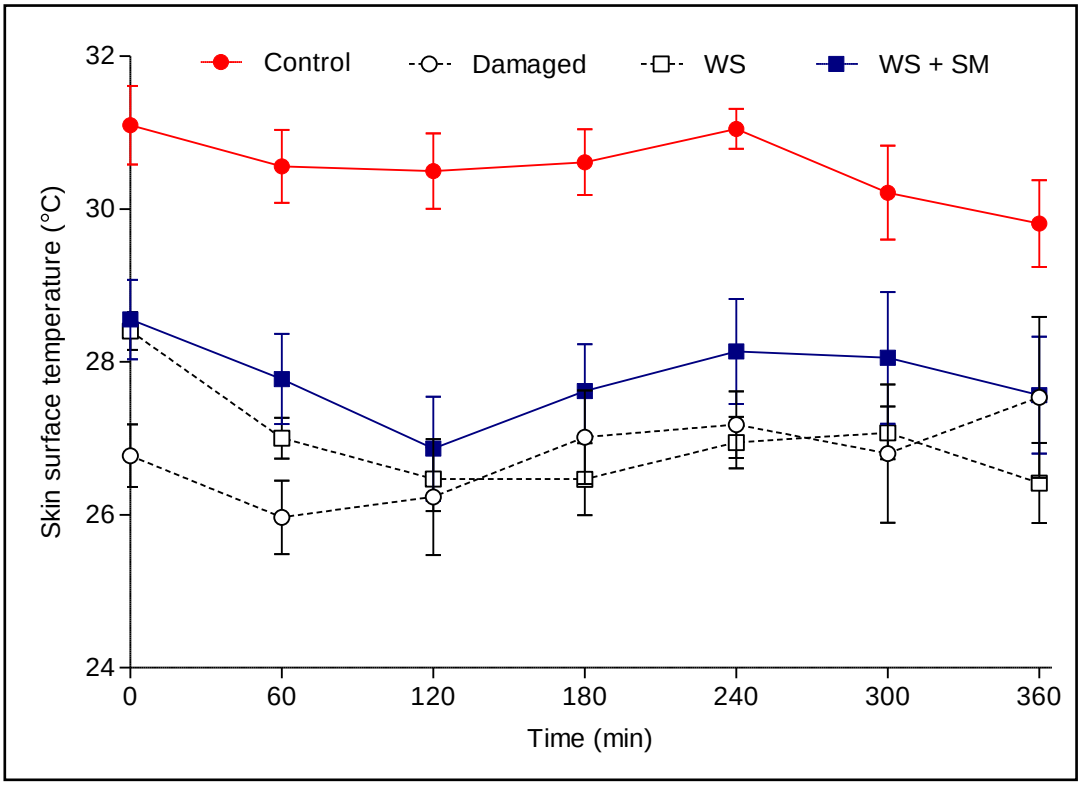

Figure 6.9: Skin surface temperature following superficial damage and treatment with WoundStat™ with (WS + SM) and without (WS) prior exposure to SM.

Undamaged (control) and damaged unexposed sites provided a negative and positive control, respectively. All values are expressed as mean ± S.D. (n=6).

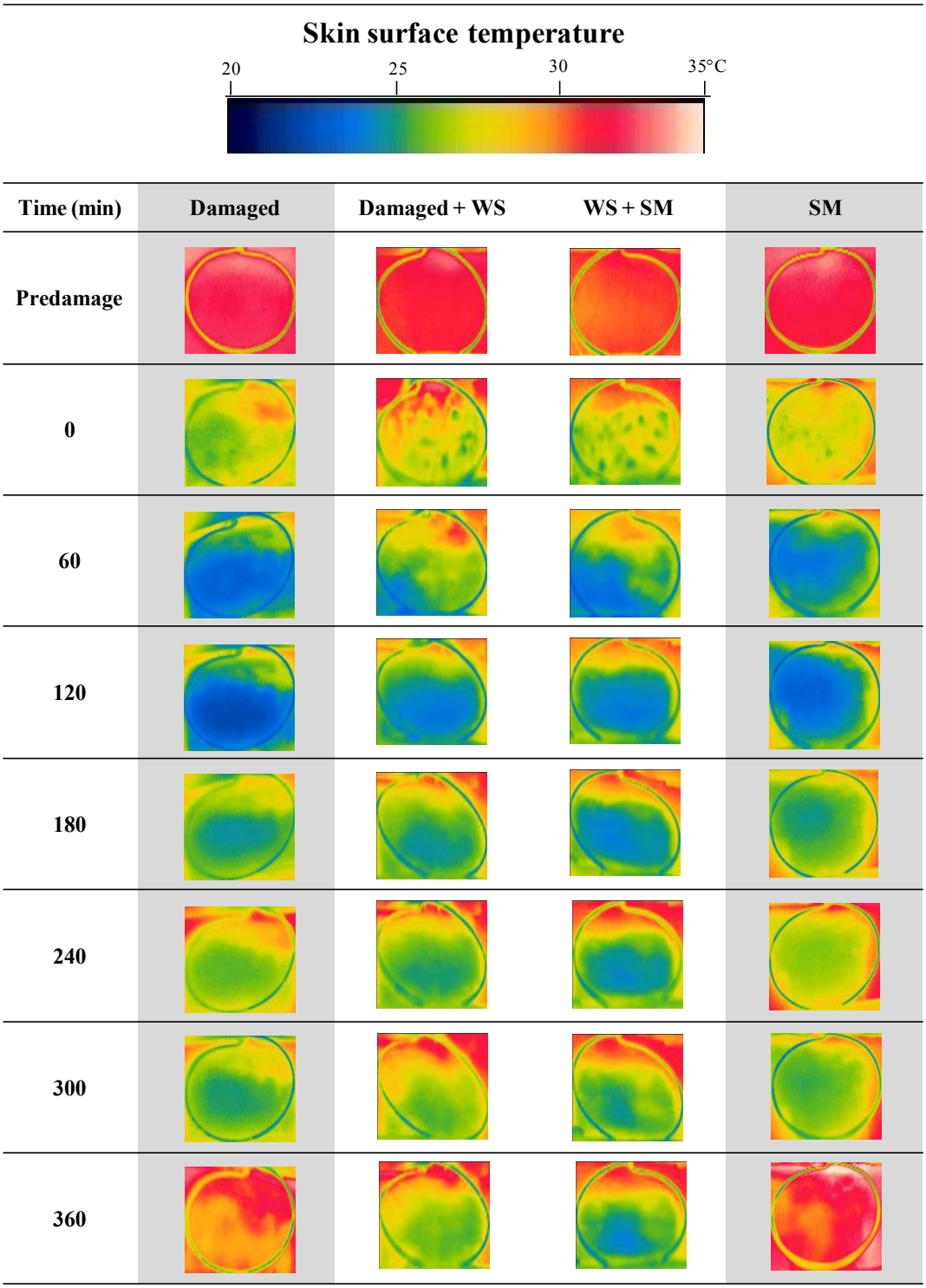

Figure 6.10: Representative skin surface thermographs (infrared thermography) following superficial damage and application of WoundStat™ with (WS + SM) and without (damaged + WS) exposure to SM.

Thermographs of damaged skin with and without SM exposure (but no WoundStat™ treatment) are shown for comparison (shaded in gray). Damaged skin (without SM) thermographs were from the same animal. Damaged and SM exposed skin (SM) thermographs are from Chapter 5.

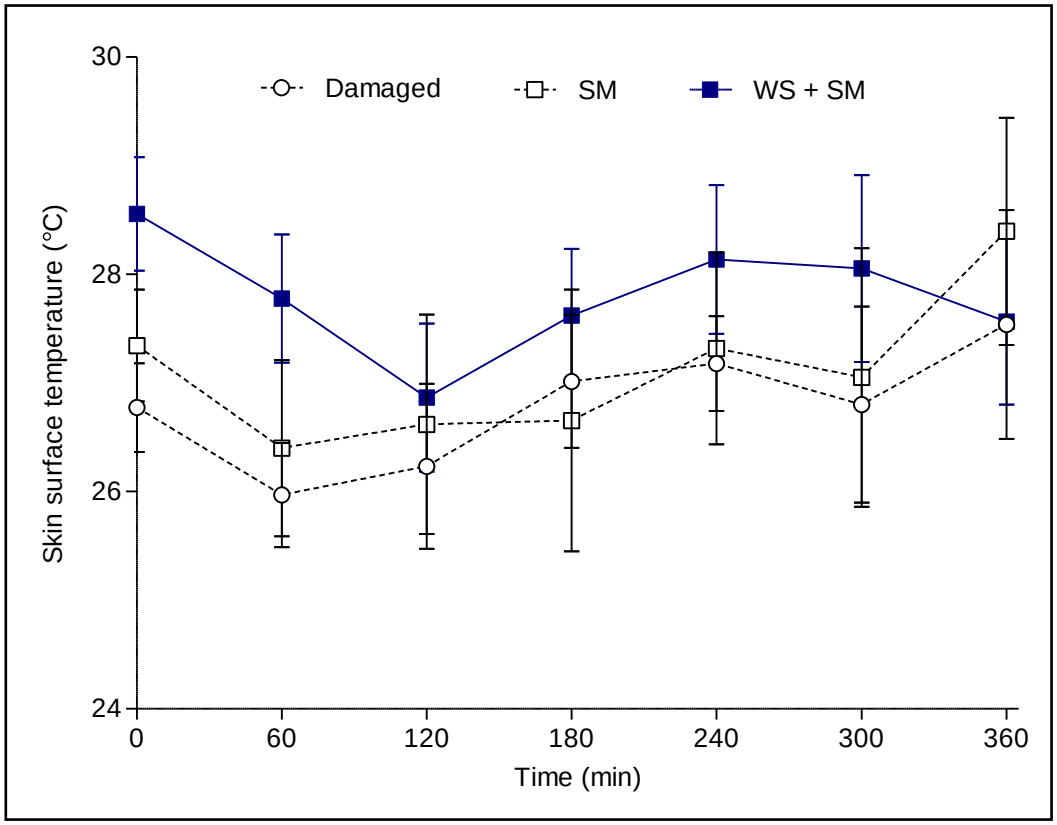

Figure 6.11: Skin surface temperature for the two treatment groups: superficial damage and SM challenge with decontamination with WoundStat™ (WS + SM) and without (SM; Chapter 5).

Damaged unexposed sites provided a positive control. All values are expressed as mean ± S.D. (n=6).

Cutaneous blood perfusion (laser Doppler imaging)

A statistically significant difference between WoundStat™ treated damaged skin (with and without SM exposure) was observed at 180 and 240 min post exposure ($p<0.05$; Figure 6.12). However, this decrease was transient and blood flow (measured as perfusion units) was not significantly different at 300 min onwards.

Decontamination with WoundStat™ significantly increased blood flow at the exposure site compared to SM only treatment site for all time points except 360 min post-challenge (Figure 6.13). Furthermore, the distinct area of low flux observed for SM-exposed skin not receiving decontamination was not present in WoundStat™ treated animals (Figure 6.14).

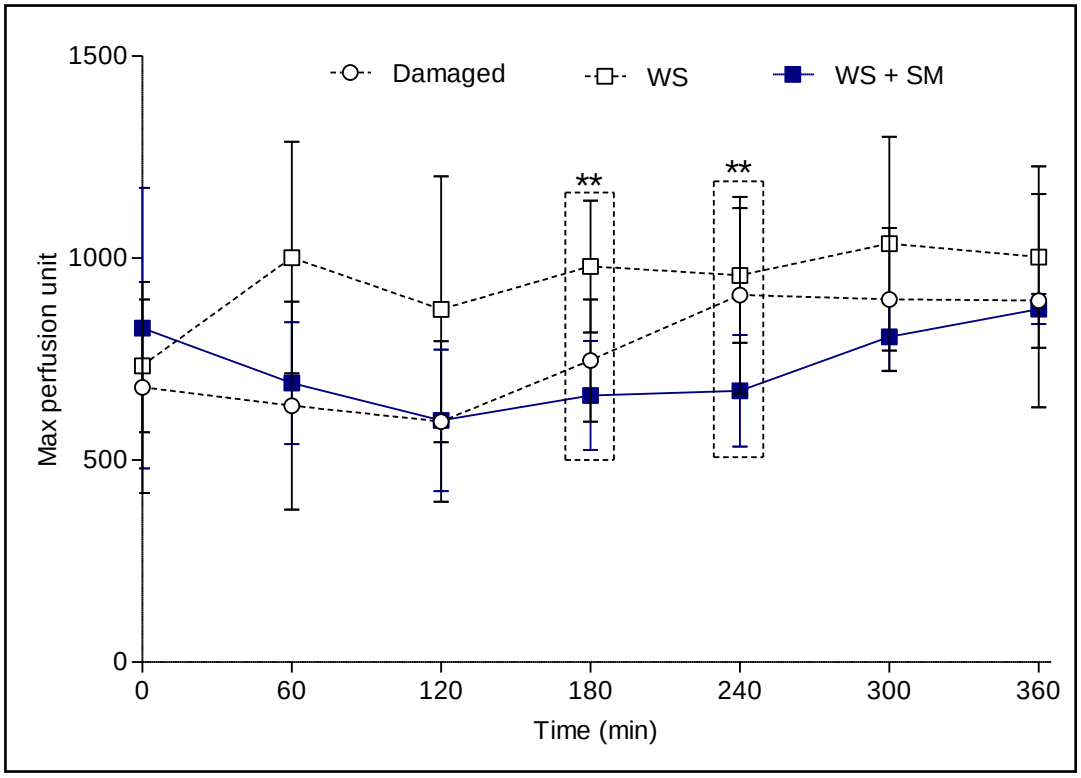

Figure 6.12: Maximum blood perfusion at the treatment site following superficial damage and treatment with WoundStat™ with (WS + SM) and without (WS) prior exposure to SM expressed as perfusion units.

*Damaged unexposed sites provided a positive control. All values are expressed as mean ± 95% confidence intervals (n=6). Dashed box represents a statistically significant difference between WoundStat™ only (WS) and SM and WoundStat™ (WS + SM) treatment sites where ** represent a p-value of <0.01.*

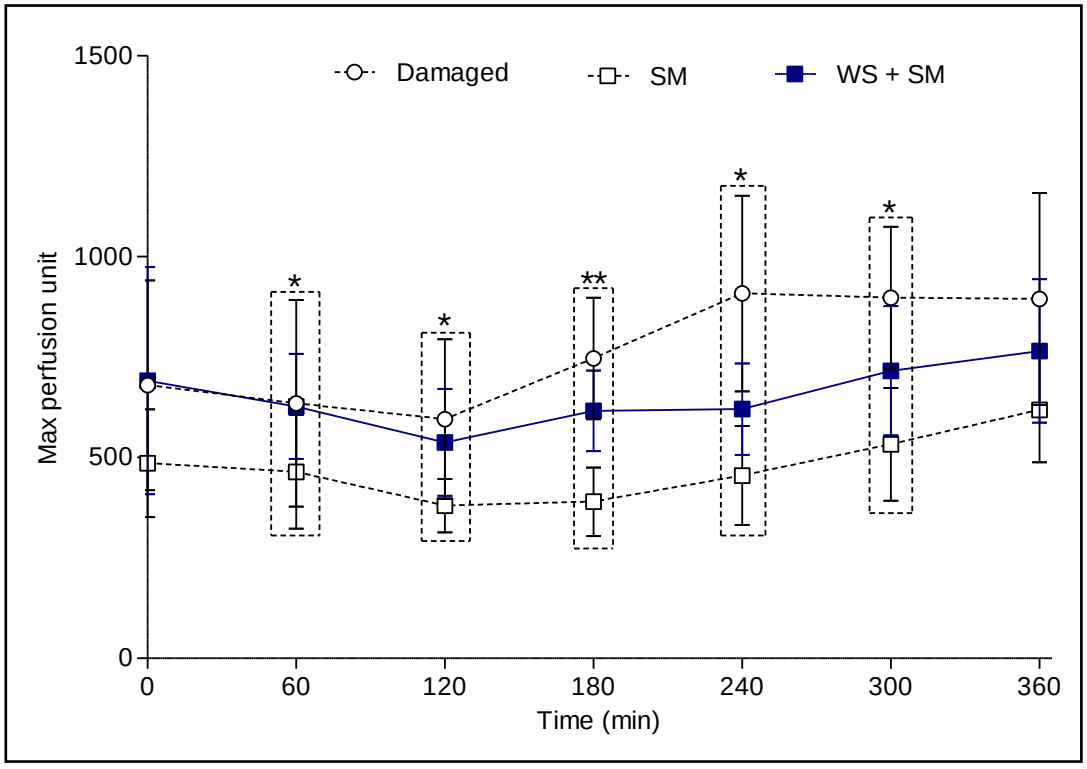

Figure 6.13: Maximum blood perfusion at the treatment site for the two treatment groups: superficial damage and SM challenge with decontamination with WoundStat™ (WS + SM) and without (SM; Chapter 5).

*Damaged unexposed sites provided a positive control. All values are expressed as mean ± 95% confidence intervals (n=6). Dashed box represents a statistically significant difference between the treatment groups (SM vs. WS + SM) sites where * and ** represent a p-value of <0.05 and <0.01, respectively.*

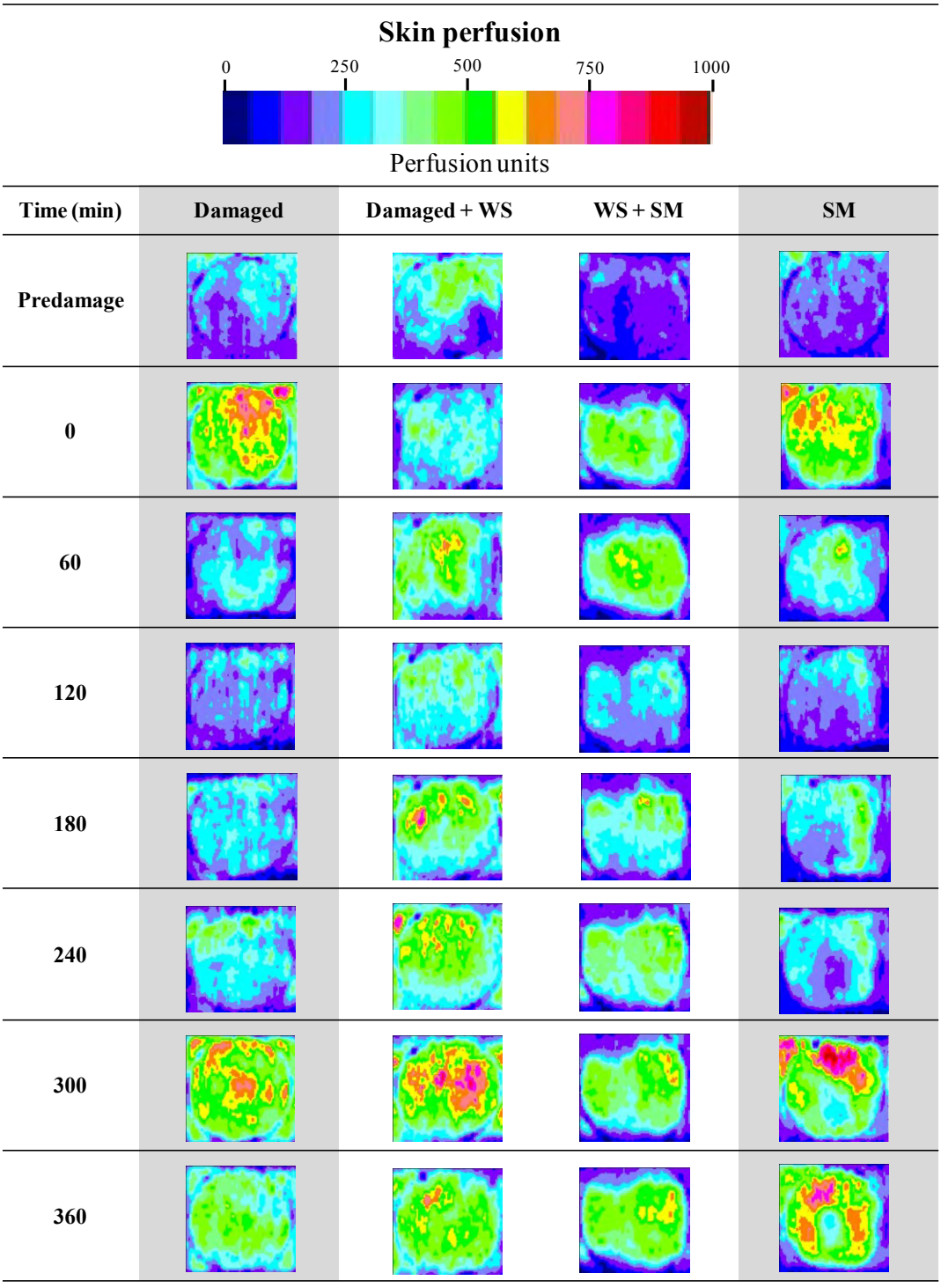

Figure 6.14: Representative skin perfusion images (laser Doppler imaging) following superficial damage and application of WoundStat™ with (WS + SM) and without (damaged + WS) exposure to SM.

Laser Doppler images of skin with and without SM exposure (but no WoundStat™ treatment) are shown for comparison (shaded in gray). Damaged skin (without SM) images were from the same animal. Damaged and SM exposed skin (SM) images are from Chapter 5.

Skin barrier integrity (transepidermal water loss)

Removal of the SC and epidermis regardless of additional treatment (WoundStat™ and/or SM) resulted in a statistically significant increase in TEWL compared to control (undamaged) values ($p<0.01$; Figure 6.15). There was not a statistically significant difference between WoundStat™ treated skin with or without prior SM-exposure (Figure 6.15). Decontamination of SM-exposed skin significantly increased TEWL over the 6 h study period, the one exception being 5 h post SM challenge (Figure 6.16).

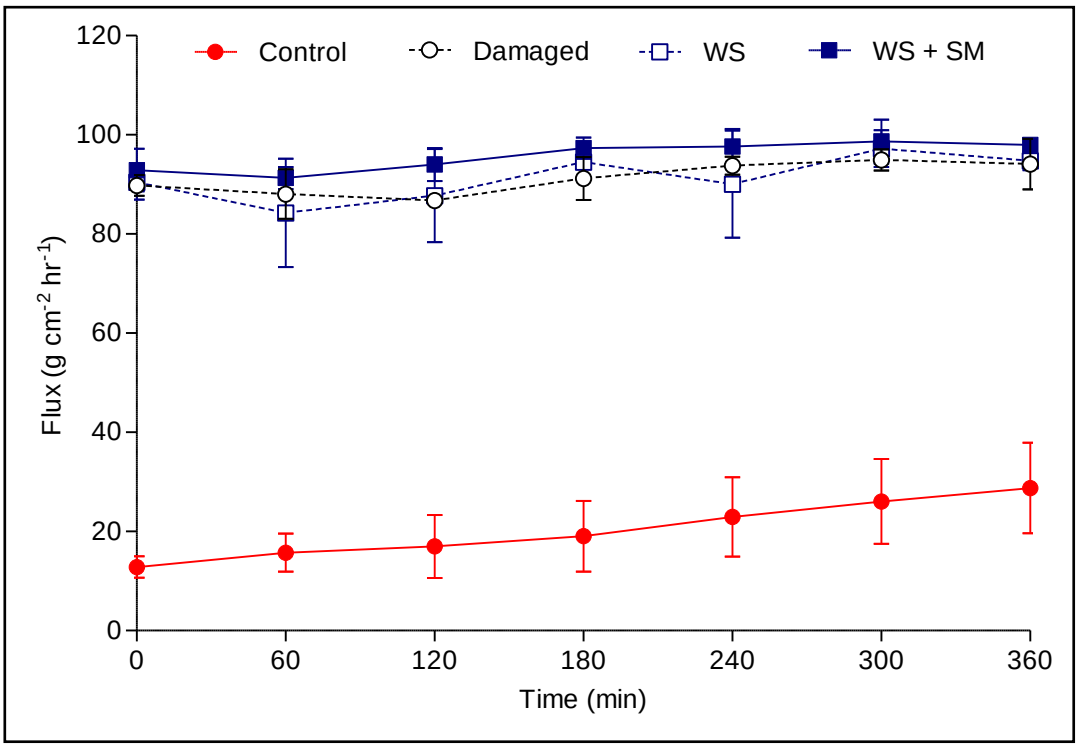

Figure 6.15: Transepidermal water loss (TEWL) following superficial damage and treatment with WoundStat™ with (WS + SM) and without (WS) prior exposure to SM.

Undamaged (control) and damaged unexposed sites provided a negative and positive control, respectively. All values are expressed as mean ±95% confidence intervals (n=6).

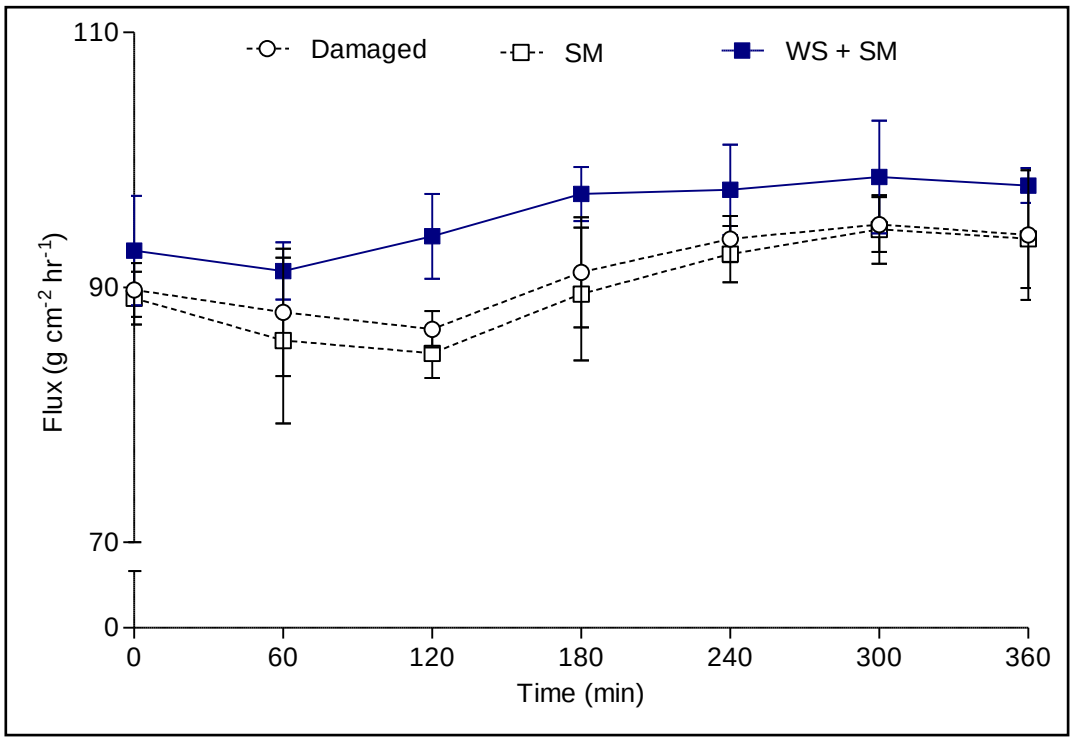

Figure 6.16: Transepidermal water loss (TEWL) following superficial damage and SM challenge with and without decontamination with WoundStat™.

Damaged unexposed sites provided a positive control. All values are expressed as mean ± 95% confidence intervals (n=6).

Radiometric Analysis

Concentrations of ^{14}C derived from ^{14}C-SM in the blood peaked 120 min post-challenge for both WoundStat™ treated and untreated groups (Figure 6.17). However, WoundStat™ treatment post-exposure significantly reduced the amount of ^{14}C derived from ^{14}C-SM measured in the blood at all time points measured ($p<0.001$; Figure 6.16). Elimination kinetics derived from a semi-logarithmic plot of the ^{14}C-SM blood concentrations are summarised in Table. 6.2. The results shown are an estimation of the elimination kinetics, which appear to fit a first order kinetic model. Further time-points would be required to provide a more accurate estimation. Elimination parameters measured including; peak concentration, slope and elimination constant were significantly reduced whilst the volume of distribution was significantly increased in WoundStat™- treated animals (Table 6.2). However, there was not a significant difference in either the half-life of ^{14}C-SM or calculated SM dose (from the semi-logarithmic plot) between the animal treatment groups.

Overall, 101 ± 8.4% of the applied ^{14}C-SM dose was recovered from the combined ^{14}C derived from ^{14}C-SM totals for the skin, skin surface swabs, organs and blood samples. The amount of ^{14}C derived from ^{14}C-SM in the total systemic circulation was estimated from the 360 min blood sample and the estimated total blood volume, assuming even distribution of ^{14}C throughout the blood. Recovery from WoundStat™ accounted for the largest percentage of total amount recovered (99.9 ± 8.6%; Figure 6.18). Use of WoundStat™ as a decontaminant significantly reduced the amount of ^{14}C-SM recovered from the skin and skin surface swabs compared to non-decontaminated animals ($p<0.001$; Figure 6.19).

The total amount of ^{14}C-SM (calculated from ^{14}C recovery) distributed in the internal organs (6 h post-challenge) on average was 886 ± 280 ng (Figure 6.20). In the WoundStat™-treated animals the predominant distribution in the organs when expressed as ng ^{14}C-SM per g organ weight, was the same non-decontaminated animals; primarily the kidneys, followed by the liver and small intestine (Figure 6.20).

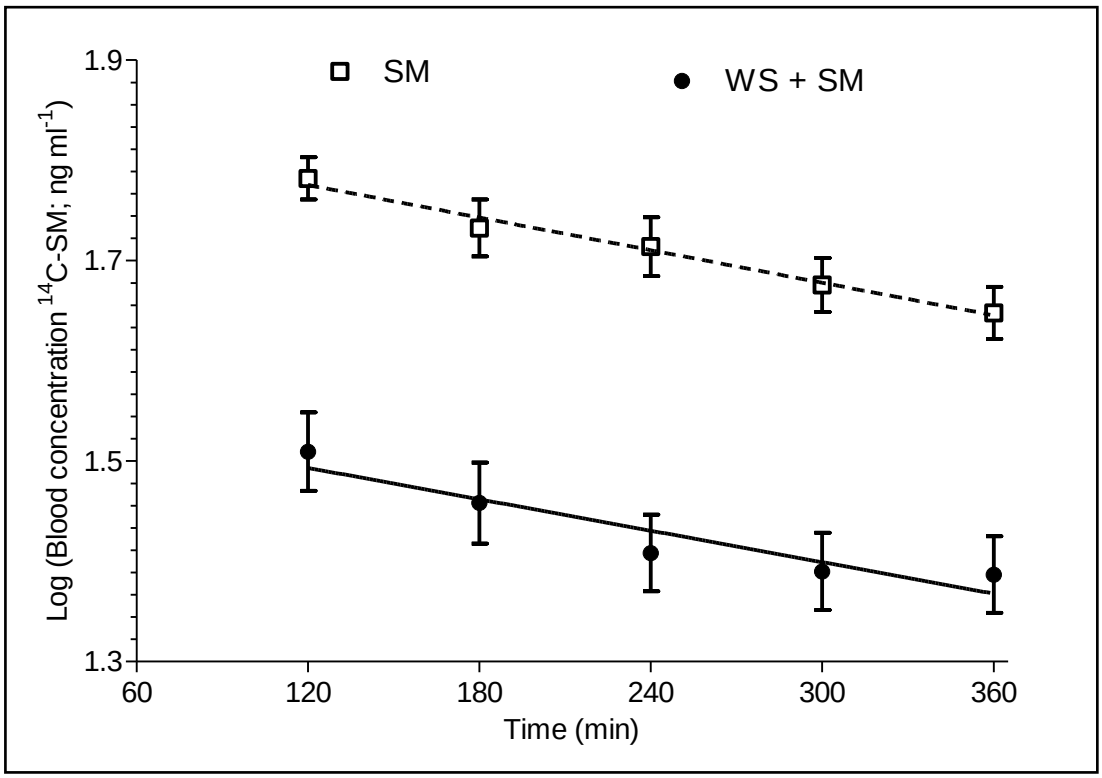

Figure 6.17: Semi-logarithmic plot of blood concentration against time for calculation of elimination kinetic parameters of ^{14}C (derived from ^{14}C-SM) from whole blood following application of 10 µL droplet of ^{14}C-SM via superficially damaged skin with (WS + SM) and without (SM) decontamition with WoundStat™.

All values are expressed as mean ± S.D. (n=6).

Elimination Parameters		
	WS + SM	SM (Chapter 5)
$T_{½}$ (min)	468 ± 121	425 ± 60
C_{max} (ng ml^{-1})	**33.0 ± 7.4	60.8 ± 64
Slope (pg ml^{-1} min^{-1})	*-34.4 ± 13.3	-64.7 ± 9.0
K_{el} (pg ml^{-1} min^{-1})	*79.1 ± 30.7	149 ± 21
C_0 (ng ml^{-1})	**35.9 ± 8.7	67.5 ± 7.0
V_d (L)	**371 ± 83	190 ± 22
D (mg)	11.7 ± 0.3	11.5 ± 0.5

Table 6-2: Elimination kinetic parameters following ^{14}C-SM challenge via damaged skin with and without WoundStat™ treatment.

*Individual values are average ± S.D. of n=6 animals and are derived from linear regression analysis of a semi-logarithmic plot of whole blood concentration against time. Equations used as described in Chapter 2. Half life ($T_{½}$) was calculated from Equation 2.8. The value of C_0 was calculated as the y-intercept of the line of best fit (and so is equal to the theoretical whole blood concentration at time of challenge). The peak concentration (C_{max}) was the largest concentration measured directly from whole blood samples. The elimination constant (K_{el}) was calculated by multiplying the slope by -2.303 (Equation 2.9). The apparent volume of distribution (V_d) was calculated from Equation 2.10. The apparent dose ("D") was subsequently calculated from Equation 2.11, using V_d and C_{max} values; the actual applied dose was 11.7 mg. Statistically significant differences between the SM only and WS + SM treatment groups are shown, where * and ** represent a p-value of 0.05 and 0.01, respectively.*

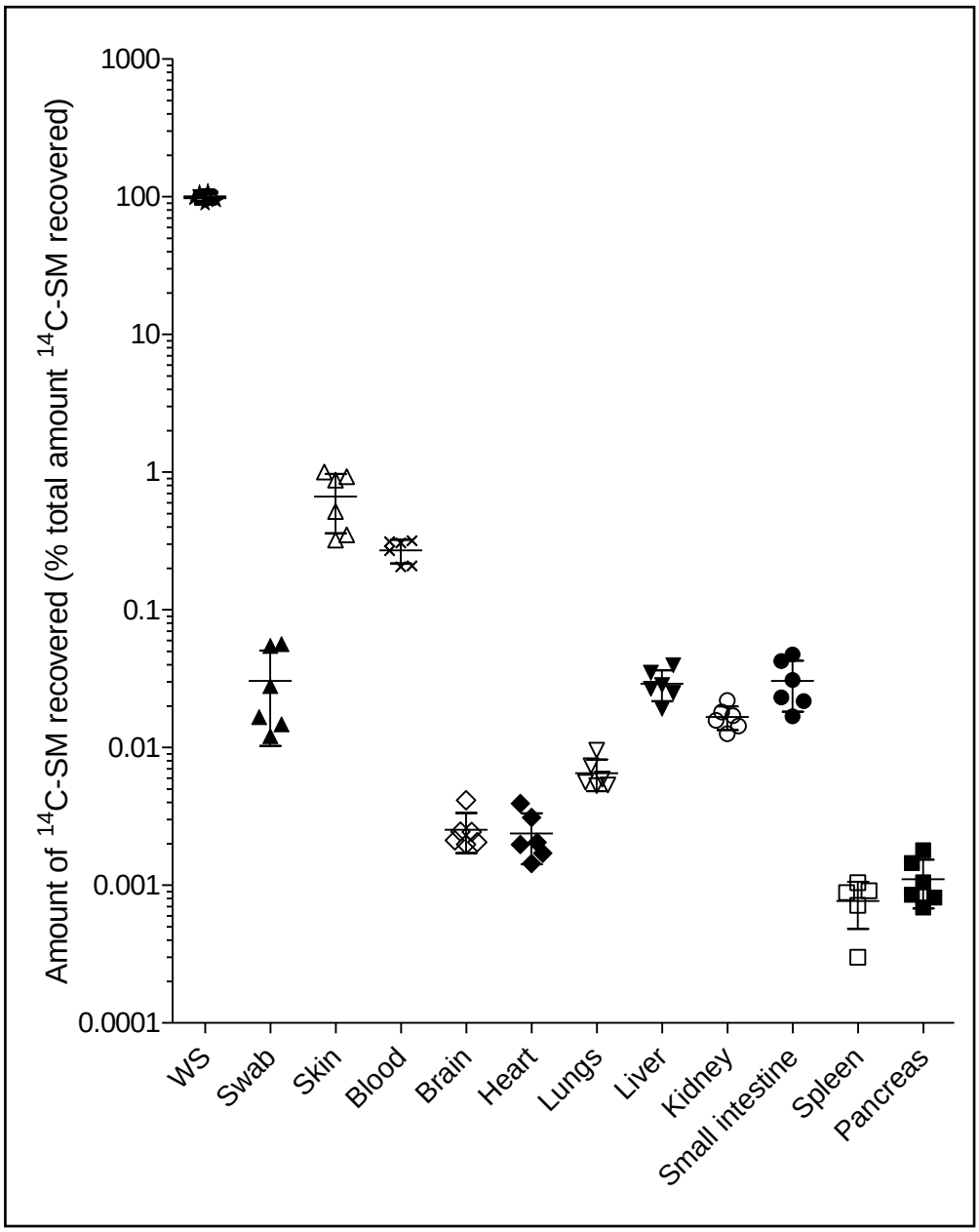

Figure 6.18: Recovery of ^{14}C-SM from the samples (WoundStat™; WS, skin surface swabs; swab, skin, blood and organs) expressed as a log percentage of the total amount of ^{14}C-SM recovered.

Individual values (n=6) are shown as well as mean (central line; n=6) and S.D. (outermost lines).

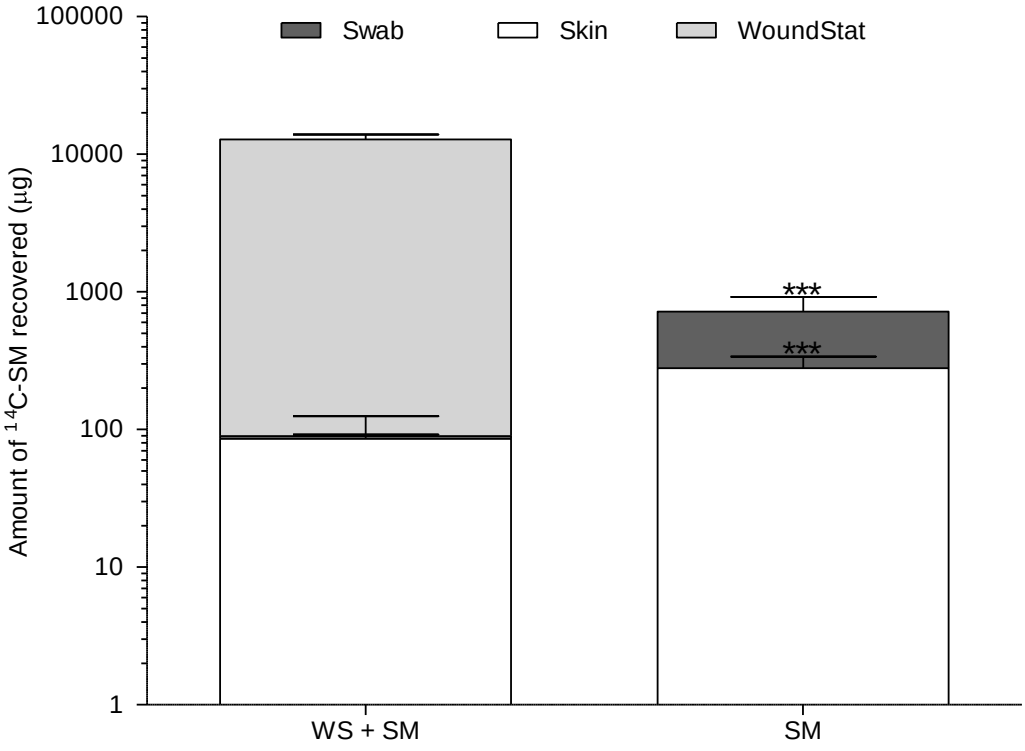

Figure 6.19: Recovery of ^{14}C-SM from the samples (WoundStat™, skin surface swabs and skin) expressed as a log amount of ^{14}C-SM (µg) recovered for decontaminated (WS + SM) and non-decontaminated (SM) animals.

*All values are mean ± standard deviation (n=6). Significant differences between the treatment groups (WS + SM vs. SM) are shown where *** represents a p-value of <0.001.*

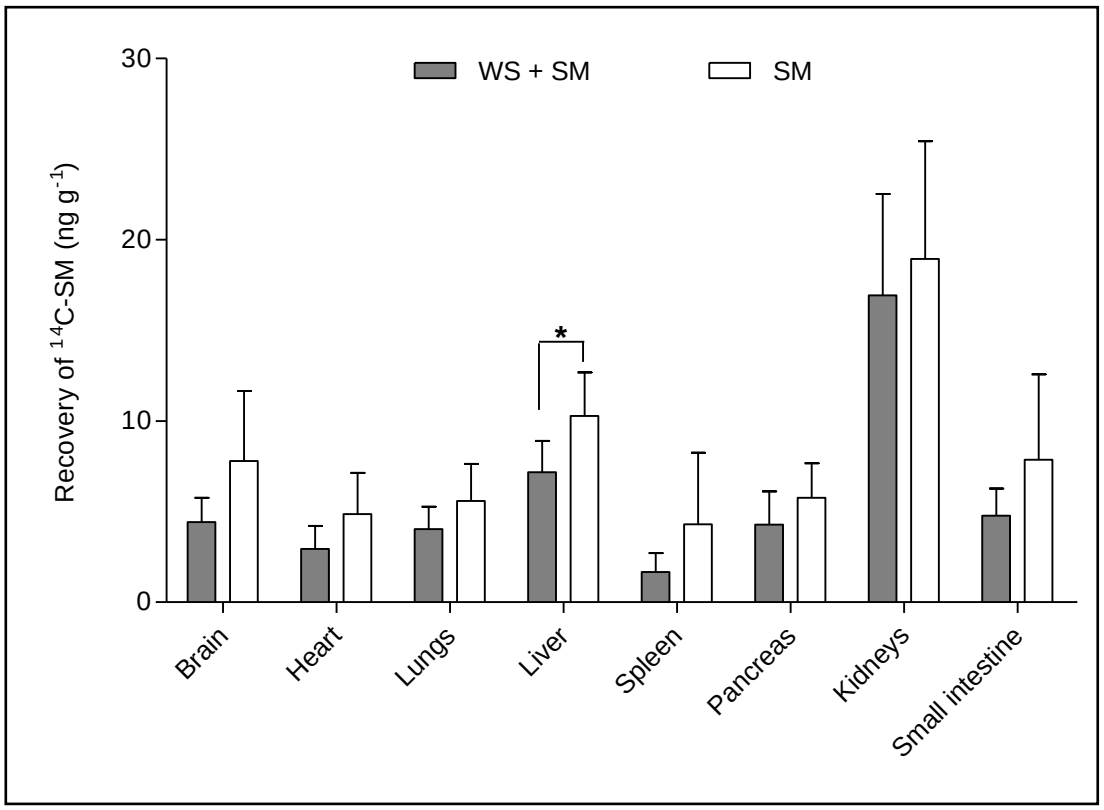

Figure 6.20: Recovery of ^{14}C-SM from internal organs expressed as ng (SM) per g (organ weight) for decontaminated (WS + SM) and non-decontaminated (SM) animals.

*All values are expressed as mean ± S.D. (n=6).Statistically significant differences between the treatment groups (WS + SM vs. SM) are shown are shown, where * represent a p-value of <0.05.*

Histology

Use of a dermatome was previously shown to remove the SC and epidermis of the skin (Chapter 5, Figure 5.12 and 5.13). This was also seen in WoundStat™ treated animals (Figure 6.21 and 6.22). All control (untreated) skin slides appeared normal.

There were only minimal changes observed between the unexposed and SM-exposed WoundStat™-treated damaged skins. There was minimal blood vessel dilation in the unexposed skin (WoundStat™-treated) but no blood vessel dilation was observed in SM-exposed skin receiving WoundStat™ treatment. The occurrence and severity of histopathological changes are summarised in Table 6.3. Both groups showed mild, perivascular PMN infiltrate in the dermis (Figure 6.21). Foci of fine, granular material was observed on the skin surface of half the samples from both groups. This was attributed to the presence of residual WoundStat™. Escharification and haemorrhage was slightly more severe in the WoundStat™ treated (with and without SM exposure) animals compared to animals which did not received WoundStat™ treatment (Figure 6.21). Hyper-eosinophilic, dermal collagen (which was interpreted as degenerate) at the surface of the exposed dermis was also present in animals receiving WoundStat™ treatment.

Overall, the microscopic changes seen in the two treatment sites (WoundStat™ with and without prior SM-exposure) were consistent with an acute, inflammatory response, secondary to the tissue damage caused by the dermatome. No significant changes were observed between the SM-exposed sites with and without decontamination with WoundStat™.

Lesion		Treatment Group			
		Control (n=6)	Damaged (n=6)	Damaged+ WS (n=6)	WS + SM (n=6)
Surface and follicular keratinocyte degeneration / necrosis	Occurrence	0	0	0	0
	Severity	Normal (6)	Normal (6)	Normal (6)	Normal (6)
Subepidemal separation/ vesiculation	Occurrence	0	0	0	0
	Severity	Normal (6)	Normal (6)	Normal (6)	Normal (6)
Blood vessel dilation-dermal	Occurrence	0	2	3	0
	Severity	Normal (6)	Normal (4) Minimal (2)	Normal (2) Minimal (1)	Normal (6)
Perivascular to diffuse, neutrophilic cell infiltrate-dermal	Occurrence	0	6	6	6
	Severity	Normal (6)	Mild (6)	Mild (6)	Mild (6)
Sero-cellular crusting-surface	Occurrence	0	6	6	6
	Severity	Normal (6)	Mild (1) Moderate (5)	Mild (1) Moderate (5)	Mild (2) Moderate (3) Marked (1)

Table 6-3: Occurrence and severity of histopathological findings for control (untreated) and damaged skin +/- WoundStat™ with and without SM exposure.

Lesions were histopathologically scored where; marked > moderate > mild > minimal > normal indicates the severity of the lesion. Number in brackets indicates number of animals in each severity group.

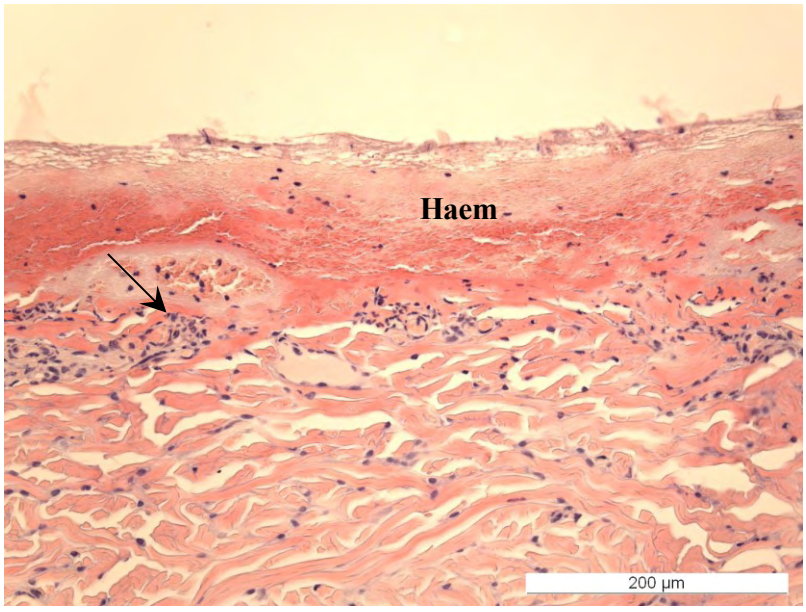

Figure 6.21: Histopathology of superficially damaged skin following treatment with WoundStat™ showing epidermal loss, marked surface haemorrhage (Haem) with fibrin and cellular debris.

Neutrophilic cell infiltrate is also shown (arrow). The haematoxylin and eosin stained section was viewed by light microscopy with bright field illumination at 20x zoom objective lens.

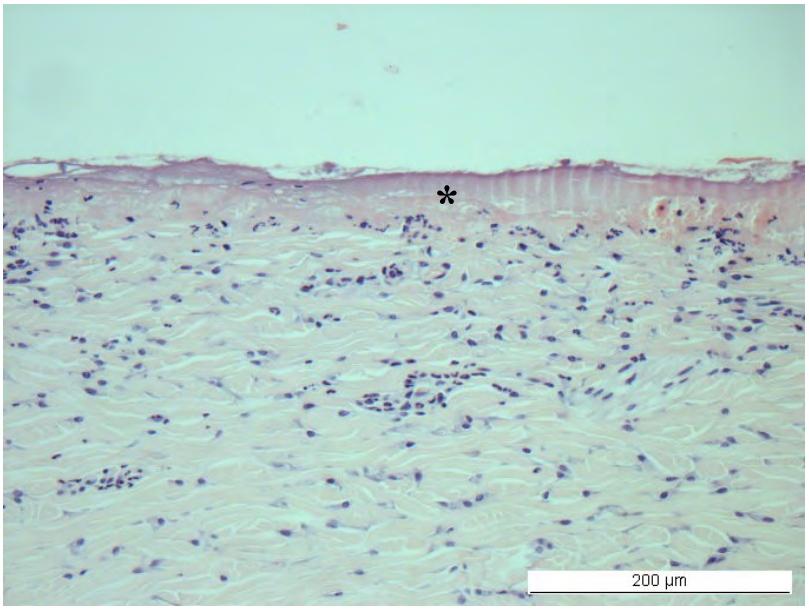

Figure 6.22: Histopathology of superficially damaged skin showing complete loss of epidermis and escharification and exposed dermal collagen (*).

The haematoxylin and eosin stained section was viewed by light microscopy with bright field illumination at 20x zoom objective lens.

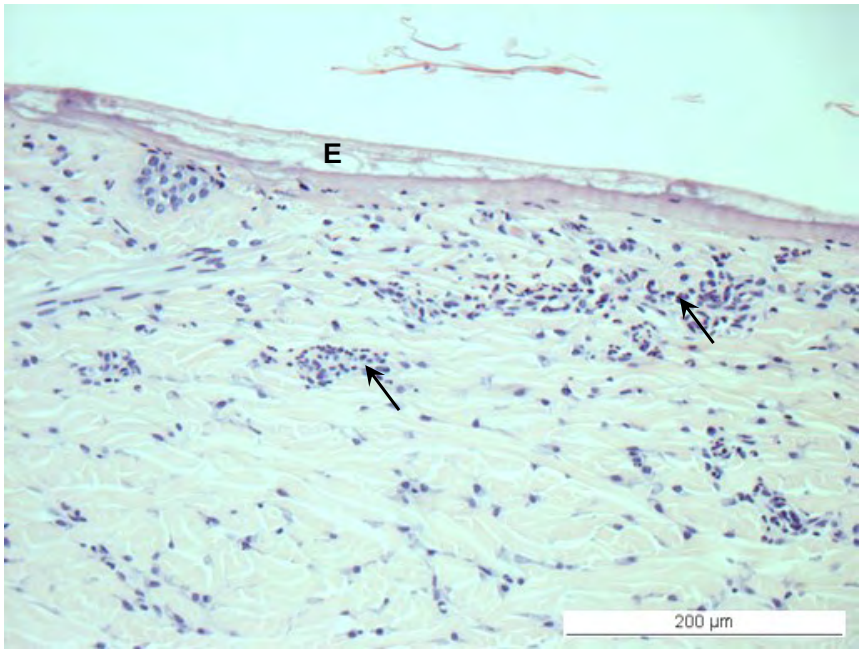

Figure 6.23: Histopathology of superficially damaged skin following treatment with WoundStat™ and SM showing loss of epidermis and escharification (E)

Neutrophilic cell infiltrate is also shown (arrow). The haematoxylin and eosin stained section was viewed by light microscopy with bright field illumination at 20x zoom objective lens.

Genomic Analysis

Relative mRNA levels for gene transcripts associated with skin from the different treatment sites were compared to identify up-regulated or down-regulated genes (as described in Chapter 2). Differential expression was defined as a Benjamini-Hochberg false discovery rate (FDR) corrected p value <0.05 and $\geq$ 2-fold change in relative mRNA levels. Approximately 0.6% of total transcripts (43663 probes) were found to have an altered expression pattern. Damaged (unexposed) skin treated with WoundStat™ had 107 transcripts whose relative mRNA levels statistically significantly differed to control (untreated) skin. Sulphur mustard-exposed, WoundStat™-treated damaged skin had 174 transcripts whose relative mRNA levels statistically significantly differed to control (untreated) skin. Of these differentially expressed transcripts, 74 were shared by both unexposed and SM exposed, WoundStat™-treated damaged skin.

As described in Chapter 5, sequences that did not have a characterised gene product (based on GenBank Accession number and Unigene identifier) were excluded from further *in silico* validation analysis. However, a full list of differently expressed gene transcripts; including those with uncharacterised or predicted gene products is provided in Appendix 1 (Tables 4 and 5).

The effects of WoundStat™ decontamination on relative gene transcript expression were determined by comparing SM-exposed skin with and without WoundStat™ treatment. In total 91 gene transcripts were found to be differentially expressed at the 6 h time point. Following further data mining as described above, 22 gene transcripts were found to up-regulated (Table 6.4) and 12 gene transcripts (Table 6.5) were found to be down-regulated as a result of combined skin damage, SM-exposure and WoundStat™ treatment.

Gene product	GenBank accession number	Fold change	Corrected p-value
Haemoglobin subunit alpha (Alpha-globin)	AK348963	7.1	0.0001
procollagen C-endopeptidase enhancer 2	AK235631	6.6	0.0001
interleukin 6 (interferon, β2)	NM_214399	6.6	0.02
claudin 11	AY609490	5.6	0.00008
superoxide dismutase 2, mitochondrial	NM_214127	4.3	0.00008
phosphoinositide-3-kinase, regulatory subunit 5	NM_213851	3.7	0.0001
amylase, alpha 2B (pancreatic)	NM_214195	3.7	0.008
amphiregulin	NM_214376	3.7	0.0005
carbonic anhydrase III, muscle specific	NM_001008688	3.3	0.0008
reticulon 4	NM_001129963	3.1	0.0002
signal sequence receptor, alpha	NM_001185167	2.7	0.0007
NADH dehydrogenase 1β subcomplex subunit 8, mitochondrial	AK236557	2.6	0.00008
actin, alpha 1, skeletal muscle	NM_001167795	2.4	0.02
glutaredoxin (thioltransferase)	AK230519	2.4	0.0002
glutamate dehydrogenase 1	AK235921	2.3	0.0006
putative deoxyribonuclease TATDN1-like	AK344100	2.3	0.0002
glutamate dehydrogenase 1	AK235921	2.2	0.0001
G-protein signalling modulator 3	NM_001123119	2.2	0.0001
insulin-like growth factor binding protein 6	AK240415	2.1	0.0001

matrix Gla protein	NM_214116	2.1	0.0005
proline-rich transmembrane protein 1	NM_001123170	2.1	0.0005
serine/arginine-rich splicing factor 2	AK235325	2.0	0.0001

Table 6-4: Differentially expressed upregulated gene transcripts in the skin following ^{14}C-SM percutaneous challenge and WoundStat™ treatment via superficially damaged skin.

Changes were determined by the mean expression ratio of WoundStat™ treated: WoundStat™ untreated SM-exposed damaged skin. Statistically significance differences in relative gene expression were identified by parametric t-test with a Benjamini and Hochberg False Discovery Rate (FDR) multiple-testing correction applied. Statistical significance was predefined as corrected p-value ≤0.05.

Gene product	GenBank accession number	Fold change	Corrected p-value
cytochrome P450 3A29	NM_214423	3.8	0.00009
tyrosyl-DNA phosphodiesterase 1	BI347194	3.2	0.02
claudin 20	NM_001159777	3.2	0.0001
feline leukaemia virus subgroup C cellular receptor 1	NM_001142846	3.0	0.001
nuclear receptor coactivator 1	EU346671	2.4	0.0005
DNA (cytosine-5-)-methyltransferase 3β	NM_001162404	2.3	0.0002
glycerol-3-phosphate acyltransferase	AK348444	2.3	0.0001
chromosome 6 open reading frame 15 ortholog	NM_001128447	2.1	0.0006
nuclear receptor coactivator 3	NM_001114276	2.0	0.0005
angiopoietin-like 7	NM_001142828	2.0	0.0008
RNA binding motif protein 4B	NM_001123188	2.0	0.00005
lysine (K)-specific demethylase 5C	NM_001097433	2.0	0.01

Table 6-5: Differentially expressed down regulated gene transcripts in the skin following ^{14}C-SM percutaneous challenge and WoundStat™ treatment via superficially damaged skin.

Changes were determined by the mean expression ratio of WoundStat™ treated: WoundStat™ untreated SM-exposed damaged skin. Statistically significance differences in relative gene expression were identified by parametric t-test with a Benjamini and Hochberg False Discovery Rate (FDR) multiple-testing correction applied. Statistical significance was predefined as corrected p-value ≤0.05.

DISCUSSION

As demonstrated in this study, the timely application of WoundStat™ can reduce the frequency of advanced signs of SM dermal toxicity, namely ulceration and significantly reduce the amount of ^{14}C radiolabel derived from ^{14}C-SM recovered from the blood and skin. The pig has been previously shown to be a suitable model for investigating the effects of SM and establishing the efficacy of therapeutic treatments *in vivo* (Price*, et al*. 2009, Chilcott*, et al*. 2007, Renshaw. 1946, Reid*, et al*. 2001). The overall limitations of this study were consistent with those described in Chapter 5. Primarily these were the lack of radio-isotope speciation, lack of historical data on short time course effects and different microarray slide versions used. Additionally, there were limitations surrounding the use of WoundStat™ as a decontaminant.

Application of WoundStat™

In "real-life" scenarios, haemostats are applied within a wound with sustained pressure to help arrest bleeding. Correspondingly, *in vivo* efficacy studies for WoundStat™ have incorporated continuous pressure at the site of application for up to four minutes (Ward*, et al*. 2007). Furthermore, the adsorptive nature of WoundStat™ may also create a tamponade effect within the wound. This may increase pressure in the wound and enhance absorption of SM in the wound. In this present *in vivo* study, no additional pressure was applied to the skin. Therefore, it would be desirable to develop a method of applying uniform, sustained pressure to a haemostat to assess whether this has an effect on dermal absorption of ^{14}C-SM.

Potential cytotoxic effects of WoundStat™

Aluminium phyllosilicates such as WoundStat™ have recently been shown to elicit cytotoxicity in endothelial cells *in vitro* (Bowman*, et al*. 2011) and *in vivo* (Kheirabadi*, et al*. 2010, Gerlach*, et al*. 2010). However, the relevance of this when WoundStat™ is applied to damaged skin is unclear. According to the manufacturer WoundStat™ was subject to cytotoxicity testing using fibroblast cell culture and WoundStat™ was not found to affect viability of transformed epithelial cells (HeLa) when used in concentrations of up to 100 μg ml^{-1} (Bowman*, et al*. 2011). This may indicate that WoundStat™ is non–toxic, epithelial cells are resistance to WoundStat™ toxicity or the cell line used (transformed, immortalised HeLa cells) are resistant to toxicity. Gene expression could be compared for unexposed damaged skin with and without the application of WoundStat™ to establish whether WoundStat™ results in expression of pro-apoptotic or necrotic genes.

Limitations to this model described in this chapter and Chapter 5 should be taken into consideration when drawing conclusions from the main findings of this study which are described below.

WoundStat™ has demonstrated equivalent efficacy as a decontaminant to fuller's earth *in vitro*, statistically significantly reducing both the amount of ^{14}C derived from ^{14}C-SM in the skin and penetrating through into the receptor fluid (Chapter 4). This efficacy was also evident *in vivo* as WoundStat™ treatment statistically reduced the amount of ^{14}C-SM in the blood circulation and within the skin at the exposure site. Similar to the *in vitro* experiments, the majority of the applied dose was recovered from WoundStat™, providing evidence of good *in vitro* and *in vivo* correlation. The primary suggested mechanism of haemostatic action for WoundStat™ is adsorption of plasma

from blood resulting in localised concentration of clotting factors (Carraway, *et al*. 2008, Ward, *et al*. 2007). Adsorption of toxic chemicals between the tetrahedral layers of fuller's earth is the primary mechanism of action for fuller's earth, an in-service military decontaminant (Wattana and Bey. 2009). Fuller's earth has also been shown to be efficacious in reducing the severity of SM lesions *in vivo* (Taysse, *et al*. 2007). Therefore, it is probable that the reductions seen in ^{14}C derived from ^{14}C-SM in the circulation and skin at the exposure site are due to adsorption of ^{14}C-SM by WoundStat™.

A statistically significant decrease in the amount of ^{14}C derived from ^{14}C-SM detected in the liver was also observed following decontamination with WoundStat™. The liver has been previously shown to be important in the conjugation and subsequent elimination for SM and its metabolites (Hambrook, *et al*. 1992, Maisonneuve, *et al*. 1993). WoundStat™ reduced dermal absorption of SM therefore it is probable that the amount of SM requiring metabolism and excretion is reduced. However, a statistically significant reduction in the amount of ^{14}C isotope in the kidneys following WoundStat™ treatment was not observed. Urinary excretion is reported to be the primary route of elimination of SM and its metabolites (Black, *et al*. 1992, Davison, *et al*. 1961, Graham, *et al*. 2000, Hambrook, *et al*. 1992, Maisonneuve, *et al*. 1993). However, SM conjugates and hydrolysis products have been detected in the urine from several days up to 3 months post exposure (potentially from red blood cell adducts) (Hambrook, *et al*. 1992, Maisonneuve, *et al*. 1993). Therefore, ^{14}C-labelled conjugates or hydrolysis products may be accumulating in the kidney.

Application of WoundStat™ to the exposure site appeared to reduce or delay the onset of advanced signs of SM dermal toxicity. Ulcerations or necrotic skin erosions

were not observed in any of the WoundStat™-treated animals during the 6 h study period (compared to all animals in the control group). The mode of cell death induced by SM is known to be dose-dependent in keratinocytes (Dabrowska*, et al*. 1996, Kehe*, et al*. 2000, Rosenthal*, et al*. 1998). Therefore, the significant reduction of ^{14}C-SM at the exposure site may have sufficiently reduced necrosis to prevent the development of skin erosions.

Frequency of ring-like blanching at the exposure site was also decreased, with only a third of animals displaying this symptom compared to animals not receiving WoundStat™ treatment. Furthermore, blood perfusion at the exposure site was also improved following the application of WoundStat™. Whilst SM caused a transient decrease in perfusion units compared to WoundStat™-treated unexposed skin the development of a low blood flow foci on the laser Doppler images did not occur (Figure 6.14). The effects of SM on dermal microvascular perfusion in undamaged skin are well documented (Brown*, et al*. 1998, Reid*, et al*. 2007, Graham*, et al*. 2002) and the effect of SM on damaged skin perfusion has been described in Chapter 5. However, the effect of decontaminating SM-exposed skin on cutaneous blood flow was not established prior to this study. Reduced dermal blood flow has been attributed to capillary necrosis and congestion (Reid*, et al*. 2007, Graham*, et al*. 2002). Therefore, it is probable that WoundStat™ treatment reduces inflammatory cell congestion of the subepidermal capillaries and so prevents a sustained decrease in perfusion at the exposure site.

Surprisingly, haemorrhage and clot formation at the exposure site were more apparent in WoundStat™-treated animals (both visual and histological observations) compared to control animals. The addition of WoundStat™ combined with SM caused reduced clot strength i*n vitro* in whole blood (Chapter 3). Although, the appearance of

haemorrhage was increased following WoundStat™ treatment (regardless of SM exposure) it is probable that WoundStat™ causes the coagulated blood to strongly adhere to the damaged skin surface which prevents removal by the cotton swabs.

Transepidermal water loss was statistically significantly increased at WoundStat™ and SM treatment sites compared to SM only from 120 min post SM challenge. This was surprising as scab formation would expected be to increase barrier function and therefore reduce TEWL. However, there was not a significant difference between WoundStat™ treated skin with and without prior SM exposure suggesting the effect is due to WoundStat™ alone and not as a result of SM decontamination. The phenomenon of increased TEWL and delayed in barrier repair following the application of semi-occlusive dressings has been previously reported (Schunck, *et al*. 2005). Therefore, WoundStat™ may act as a barrier to TEWL and so the increased TEWL signal that would normally stimulate re-epithelisation and associated barrier mechanism may be absent. Although in open wounds, rapid formation of a barrier layer is required to prevent ingress of harmful substances or bacteria (Schunck, *et al*. 2005).

Following WoundStat™ treatment, increased relative expression was observed for gene transcripts involved in inflammation, barrier function, regulation of cell differentiation/survival and oxidative stress. Interleukin-6 (IL-6) is a pleiotrophic cytokine, primarily produced by keratinocytes in the epidermis and fibroblasts in the dermis (Paquet and Piérard. 1996). Interleukin-6 modulates cell proliferation and differentiation and increased expression promotes wound healing (Sugawara, *et al*. 2001, Gallucci, *et al*. 2000, McFarland-Mancini, *et al*. 2010). Increased expression of IL-6 following SM exposure has been observed as early as 3 h post challenge (Sabourin, *et al*. 2000, Vallet, *et al*. 2012, Gerecke, *et al*. 2009, Rogers, *et al*. 2004).

However, IL-6 antibodies have been shown to mitigate the inflammatory effects of SM induced IL-6 release (Arroyo, *et al*. 2004b). From this study it is not possible to determine whether increased IL-6 expression is in response to the physical insult (removal of upper layers) or chemical insult (SM). Therefore, it is difficult to determine whether this is a positive effect (promotion of wound healing) or negative effect (terminal differentiation of keratinocytes) of WoundStat™ treatment.

Claudin 11 is a transmembrane protein which is thought to have involvement in the formation of tight junctions and maintenance of barrier function (Agarwal, *et al*. 2009). Claudin 11 is generally associated with myelination (Bronstein, *et al*. 2000). However, recently it has been suggested that claudin-11 may be associated with IL-4 activated macrophages (Van den Bossche, *et al*. 2012). Thus claudin-11 expression may be involved in the inflammatory response to SM.

Amphiregulin (AREG) is cytokine and epidermal growth factor (EGF) receptor ligand which is involved in autocrine keratinocyte proliferation (Stoll, *et al*. 2009). Increased expression of AREG has been attributed to keratinocyte terminal differentiation and induction of keratins 1/10 (Wakita and Takigawa. 1999). Interestingly, SM has been shown to increase expression of AREG and keratin 1 *in vivo* (Dillman III, *et al*. 2005) and promote keratin 1/10 induction *in vitro* (Rosenthal, *et al*. 1998). Furthermore, AREG has also been shown to be up-regulated in epidermolysis bullosa which is characterised by severe blistering at the epidermal-dermal junction similar to that caused by SM exposure (Niculescu, *et al*. 2011).

Phosphoinositide-3-kinase, regulatory subunit 5 also known as p101 is a non-catalytic subunit which forms a heterodimer with p110γ (catalytic subunit) to form a class 1 phosphoinositide-3-kinase γ (PI3Kγ) (Brock, *et al*. 2003). Class 1 PI3Kγs are

involved in cell signal transduction downstream of G-protein coupled receptors (Brazzatti, *et al*. 2011). PI3Kγ is able to activate the Akt signalling pathway which has numerous effector functions including cell survival, proliferation and differentiation (Cantrell. 2001). Activation of PI3Kγ has been shown to prevent anoikis or detachment induced apoptosis (Brazzatti, *et al*. 2011). Overexpression of the p101 subunit has been shown to enhance the activity of p110γ (Johnson, *et al*. 2007). Therefore increased expression of p101 may be a cellular defence mechanism to prevent anoikis which has previously been attributed to SM toxicity *in vitro* (Sourdeval, *et al*. 2006) and *in vivo* (Kan, *et al*. 2003).

Oxidative stress is reported as a major contributor to the cytotoxic effects of SM and SM has been shown to increase ROS (Pal, *et al*. 2009, Laskin, *et al*. 2010, Gould, *et al*. 2009). Reactive oxygen species are known to cause DNA damage (Cooke, *et al*. 2003), lipid perioxidation (Jafari. 2007) and protein oxidation (Pal, *et al*. 2009) and could therefore contribute to SM induced cytotoxicity. This study has identified a number of genes whose expression in the skin was increased by combined SM and WoundStat™ treatment; including SOD2 and CAIII. Superoxide dismutase (SOD2) has a role in the mitochondrial defence response to ROS (Figure 6.29) (Cadenas and Davies. 2000). Increased expression of SOD2 has been linked with protection against the apoptotic effects of ROS (Keller, *et al*. 1998). Increased expression of SOD2 in response to SM exposure has been previously observed (Gerecke, *et al*. 2009). Moreover, pre-treatment with SOD2 has been has been shown to reduce SM lesion severity (Eldad, *et al*. 1998). Thus increased SOD2 expression could reflect an adaptive cellular response against SM-induced oxidative stress. Carbonic anhydrase III (CAIII) is a metalloenzyme and is known to have an important role in oxidative stress response

(George, *et al*. 2011). It is thought that the enzyme catalyses the conversion of hydrogen peroxide to percarbonic acid as a means to protect cells from hydrogen peroxide induced apoptosis (Figure 6.29) (Kim, *et al*. 2004, Räisänen, *et al*. 1999)

Sulphur mustard has been shown to spontaneously form carbonium ions (Chapter 1, Figure 1.9) in solution (Kang and Spears. 1987). Enzymatic reduction of carbonium ions by thioredoxin reductase, NADPH or CYPs results in the production of carbon-centred free radicals (Chapter 1, Figure 1.9) which can result in DNA damage (Brimfield, *et al*. 2012, Brimfield, *et al*. 2009).

Reduced nicotinamide adenine dinucleotide (NADH) dehydrogenase 1β is an accessory subunit of NADH-ubiquinone oxidoreductase (Complex I) (Dutta, *et al*. 2006). It has been proposed that SM directly inhibits one or more of the enzymes in complex I (Martens and Smith. 2008). Impaired activity of NADH-ubiquinone oxidoreductase has been shown to enhance superoxide production (Hansford, *et al*. 1997, Papa, *et al*. 2008). Again, this could be an adaptive response to combat SM-induced oxidative stress and direct DNA damage by SM caused by increased free radical production. Sulphur mustard induced DNA strand breaks have been shown to increase poly (adenosine diphosphate-ribose) polymerase (PARP) activity which uses nicotinamide adenine dinucleotide (NAD^+) as a substrate (Rosenthal, *et al*. 2001, Bhat, *et al*. 2006). Depletion of cellular NAD^+ has been shown to induce necrotic cell death due to reduced cellular adenosine triphosphate (ATP) (Virag, *et al*. 2002, Platteborze. 2003). Complex I is responsible for catalysing the oxidation of NADH to NAD^+.

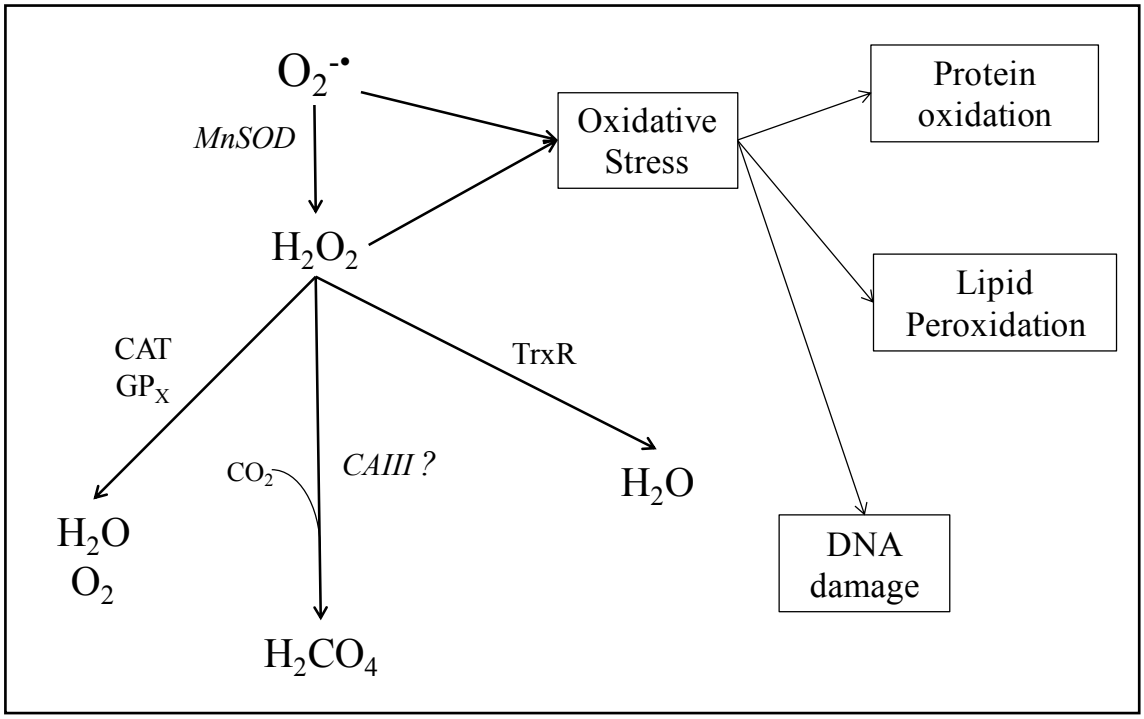

Figure 6.24: Summary of reactive oxygen species detoxification and cellular effects of oxidative stress.

Superoxide anion is metabolised in mitochondria by manganese superoxide dismutase (MnSOD or SOD2) to produce hydrogen peroxide. This is further metabolised by catalase (CAT), peroxidises i.e. glutathione peroxidase (GP_x) and thioredoxin reductases (TrxR) to produce water and oxygen. Carbonic anhydrase III (CAIII) involvement in hydrogen peroxide detoxification has also been implicated. However, if these detoxification systems become overwhelmed then accumulation of superoxide and hydrogen peroxide can occur, contributing to oxidative stress. Oxidative stress can result in protein oxidation, lipid peroxidation and DNA damage and may trigger cell death. Italics indicate that relative gene expression for this enzyme was found to be up-regulated by decontamination of SM-exposed skin using WoundStat™.

Up-regulation of NADH-ubiquinone oxidoreductase in response to SM has been previously observed *in vitro* (Platteborze. 2003). Therefore, the increase in expression of NADH dehydrogenase 1β may be a response to maintain intracellular levels of ATP.

Taken together this could suggest that a reduction in the dose of SM at the exposure site following WoundStat™ treatment allows increased expression of enzymes that are responsible for an adaptive cellular response against the formation of ROS as well as enzyme which respond to ROS-induced cell damage. However, a longer term study would be required to confirm whether the reduction of SM absorption at the exposure site was sufficient to prevent ROS-induced cellular death.

Overall treatment with WoundStat™ resulted in the relative down regulation of genes involved in transcription/translation including histone and epigenetic modifications and cell signalling. Cytochrome P450 3A29 (CYPs) is a pig orthologue of human cytochrome P450 3A4 which is involved in the oxidation and metabolism of many xenobiotics in the body (Anzenbacherová*, et al*. 2005). Upregulation of rodent CYPs have been observed in the lung in response to a SM aerosol challenge (Pons*, et al*. 2001). Sulphur mustard has been shown to inhibit CYPs activity *in vitro* by uncoupling electron transport at flavoenzyme reductase, resulting in electrons being diverted to xenobiotic reduction (Brimfield*, et al*. 2009) which can lead to free radical formation (Testa. 1995). The reduction in SM absorption following decontamination with WoundStat™ may explain the apparent reduction in cytochrome P450 expression in the skin compared to SM-exposed skin which was not decontaminated. If the amount of SM in the skin were reduced then a reduction in the expression of enzymes involved the xenobiotic metabolism of SM would be expected.

Sulphur mustard-induced alterations to epigenetic processes have been suggested as an underlying mechanism for the delayed toxic effects of SM (Korkmaz, *et al*. 2008). Molecular mechanisms involved in epigenetic gene regulation include: modifications to histones by histone acetyltransferases and DNA methylation by DNA methyltransferase (Yang and Seto. 2007, Bestor. 2000).

DNA methyltransferase 3β (DNMT3B) is involved in *de novo* methylation of DNA, in which a methyl group is covalently added to the 5-position of cytosine typically within gene promoter regions (Girault, *et al*. 2003, Yu, *et al*. 2012). Methylation of DNA is associated generally with the silencing of genes including potentially tumour suppressor genes which could lead to tumour promotion (Nandakumar, *et al*. 2011). Although the cellular damage attributed to the direct alkylation of DNA by SM is well established (Brookes and Lawley. 1960, Jowsey, *et al*. 2012, Simbulan-Rosenthal, *et al*. 1999) there is little known about the epigenetic effects of SM. Methylation of DNA has been proposed as a possible mechanism which results in the delayed toxic effects of SM (Korkmaz, *et al*. 2008) through the down regulation of affected genes. However, it is not known whether DNA methylation or direct alkylation may also contribute to acute SM toxicity. Both nuclear receptor coactivator 1 (NCOA1) and 3 (NCOA3) bind to oestrogen receptor-alpha and vitamin D receptor, respectively, to promote transcription of target genes (Bikle, *et al*. 2010). They are also able to induce transcription through disruption of nucleosome structure via histone acetyltransferase activity (Spencer, *et al*. 1997). Nuclear receptor coactivator 3 is thought to be in involved keratinocyte terminal differentiation (Bikle, *et al*. 2010). Although, there is also a proposed role for NCOA3 in keratinocyte proliferation and wound healing (Al-Otaiby, *et al*. 2012, Oda, *et al*. 2007).

Nuclear receptor coactivator 1 is also thought to have a role in increasing keratinocyte proliferation and subsequently the thickness of the epidermis (Kanda and Watanabe. 2003). Down-regulation of keratinocyte proliferation following WoundStat™ treatment was unexpected. However, down regulation of these genes may also reduce promotion of gene expression associated with histone acetyltransferase activity.

Angiopoietin-like 7 (ANGPTL7) is a member of the ANGPTL family and is a secreted glycoprotein and increased intracellular levels of ANGPTL7 have been shown to decrease fibronectin expression (Comes, *et al*. 2011). Fibronectin is an extracellular matrix protein (Faralli, *et al*. 2009) and is important in basement membrane stability (Zhang, *et al*. 1995a). Decreased expression of fibronectin in response to SM exposure and subsequent loss of cellular adhesion at the epidermal-dermal junction has been previously reported *in vitro* (Rosenthal, *et al*. 1998, Zhang, *et al*. 1995a). Therefore, reduced expression of ANGPTL7 may help to prevent blister formation.

Some genes whose relative expression was differentially regulated do not appear to have an obvious role in SM pathogenesis or at present have an unknown function.

RNA binding motif protein 4B is thought to be involved in suppression of translation during muscle cell differentiation (Lin and Tarn. 2009). Feline leukaemia virus subgroup C cellular receptor 1 (FLVCR) is involved in heme export from red blood cells to maintain iron haemostasis and is required for red blood cell differentiation (Yang, *et al*. 2010). As previously described in Chapter 5, the presence of blood vessels and other adnexal structure within the skin may result in genes being identified which do not have a direct role in cutaneous response to SM. As previously suggested further characterisation of protein and gene function of the pig genome would

be hugely advantageous for the use of this model to investigate the genomic effects of SM.

Conclusions

This study has found that WoundStat™ has shown promise as a decontaminant for superficially damaged skin against SM *in vivo*. Data from Chapter 5 have shown that removal of the SC and epidermis reduces the lag time between SM exposure and the appearance of advance signs of toxicity. Timely application of WoundStat™ has been shown to reduce the overt (gross) signs of SM-induced skin damage and significantly decrease the amount of ^{14}C-SM remaining within the skin at 6 h post-challenge. WoundStat™ also significantly reduced systemic absorption of ^{14}C-SM, with decreased ^{14}C-SM measured in the circulation and major routes of elimination and excretion (liver and small intestine). Furthermore, SM was previously shown to significantly reduce perfusion rates at the exposure site from 2 h post challenge onwards (Chapter 5) whilst only a transient decrease was observed in WoundStat™ treated animals. However, no significant microscopic changes were observed in between the two treatment groups (SM only and SM + WoundStat™ decontamination). Treatment with WoundStat™ was found to increase the relative mRNA levels of gene transcripts associated with cellular response to oxidative stress and inflammation, barrier function, and regulation of cell differentiation/survival compared to animals not receiving decontamination. Overall treatment with WoundStat™ resulted in the relative down regulation of genes involved in transcription/translation including histone and epigenetic modifications and cell signalling.

Recommendations for future work

This study has found that WoundStat™ has shown promise as a decontaminant for superficially damaged skin against SM *in vivo*.

- Chromatographic analysis should be used to for the speciation of sample containing ^{14}C-isotope to determine whether they contain the parent compound (SM) or a conjugate/hydrolysis product and thus to establish if the absorbed material is active/reactive.
- Relative changes in mRNA levels observed using cDNA microarray analysis should be quantified and validated using qRT-PCR.
- The efficacy of WoundStat™ as a haemostatic decontaminant should be evaluated in a SM-contaminated haemorrhaging wound model (Kheirabadi*, et al*. 2009). However, given recent safety concerns regarding embolised vessels in distal organs following WoundStat™ treatment (Kheirabadi*, et al*. 2010) reformulation of the product may be required. This could be achieved by containing product within non-woven surgical gauze similar to QuikClot ACS+® (Kheirabadi*, et al*. 2009). However, further experiments would be required to ensure encasing WoundStat™ did not have an adverse impact on efficacy as a decontaminant. WoundStat™ efficacy as a decontaminant *in vitro* (static diffusion cell system; Chapter 4) correlated with the *in vivo* data (Chapter 6). Therefore, the static diffusion cell system may be suitable for evaluating the decontaminant efficacy of a new formulation.

Chapter 7

General Discussion

GENERAL DISCUSSION

Contamination of wounds with highly toxic chemicals, such as SM, presents a hazard to civilian and military populations e.g. a "dirty bomb" scenario. Current decontamination regimes are contraindicated for intra-wound use and may adversely affect wound healing (Gibbs and Pooley. 1994, Sakula. 1961, Walters, *et al*. 2007). Therefore, there is a considerable need for the development of a skin decontaminant which is also safe for use on abraded skin and in open wounds. In addition to the capacity to decontaminate wounds, a product which could simultaneously clot haemorrhaging wounds would be of significant clinical benefit.

The work reported in this Thesis has successfully demonstrated the feasibility of developing a product (WoundStat™) to simultaneously arrest bleeding and reduce the ingress of a CW agent. Moreover, WoundStat™ is also an effective skin decontaminant, being equivocal in performance to existing military topical decontamination products such as fuller's earth, RSDL® and M291.

To be considered suitable for use as a haemostatic decontaminant a product must maintain the ability to rapidly coagulate blood even in the presence of potentially toxic chemicals. The acute effects of SM on blood coagulation are not well established. Although it was presumed based on published literature that SM may have a deleterious effect on clot formation and stability due to its ability to alkylate critical active site residues of thrombin and increase expression of enzymes associated with clot lysis. However, the use of whole blood TEG by this thesis has demonstrated that SM has no discernible effect on coagulation, either following direct addition to blood *in vitro* or following percutaneous exposure *in vivo*. Furthermore, TEG identified four haemostatic products (WoundStat™, ProQR®, VitaGel™ and FastAct®) which significantly

enhanced coagulation *in vitro*. The performance of three of these products (ProQR®, VitaGel™ and FastAct®) was completely unaffected by the presence of SM. Clot strength was significantly reduced in blood treated with WoundStat™ and SM compared to native, control or WoundStat™ only treated blood. As clot strength is a direct function of platelet and fibrin binding via $GPII_b/III_a$ receptor (Mousa*, et al*. 2000), it is possible that WoundStat™ in combination with SM affects the structure or function of $GPII_b/III_a$ integrins, platelets or fibrin. Although, these observations may be species specific as differences in $GPII_b/III_a$ integrins between human and porcine blood have been reported (Royo*, et al*. 1998). Sulphur mustard has been shown to increase u-PA expression which promotes clot lysis via activation of plasmin. Therefore, it is plausible that SM could prevent cross-linked fibrin clot formation through indirect activation of plasmin. However, the increased clot lysis observed with SM and WoundStat™ treated blood was limited to the *in vitro* findings as there was no significant difference in TEG parameters *in vivo* following SM percutaneous exposure and topical decontamination with WoundStat™. This suggests that the effects are either dose-dependent or require direct contact between SM, WoundStat™ and blood components.

The other three products tested (QuikClot ACS+®, HemCon® and Celox™) did not demonstrate efficacy *in vitro*. Whilst this is contrary to reported efficacy *in vivo*, it is in agreement with previous *in vitro* studies (Kheirabadi*, et al*. 2009). The successful products fell into two broad categories: absorptive granular products and liquid products containing activated clotting factors. The pro-coagulatory functions of the granular products are attributed to absorption of plasma in the interlayer or molecular spaces. Fuller's earth and M291 are able to absorb and sequester chemicals in the

interlayer spaces and effectively decontaminant the skin surface. Thus it was proposed that products which were effective in absorbing plasma may also be efficacious as topical decontaminants.

Measurement of percutaneous absorption of SM *in vitro* demonstrated good agreement with *in vivo* data and identified that superficial damage to the skin results in increased dermal and systemic absorption of SM. This further validates the use of *in vitro* diffusion cells for the initial screening of candidate decontaminants. Additionally, use of diffusion cells can minimise the number of animals required and so is in keeping with the "3 Rs" ethical framework. The pig was the chosen animal model in this Thesis as it is established for investigating SM toxicity in undamaged skin (Reid*, et al*. 2007, Chilcott*, et al*. 2007, Graham*, et al*. 2001, Graham*, et al*. 1999) and demonstrates good correlation with dermal absorption in man (Barbero and Frasch. 2009). There was no significant difference observed in either the rate or amount of SM percutaneous absorption through undamaged skin (control skin) between animals. However, there were significant differences in the amount of SM remaining within the skin. Interindividual differences in percutaneous absorption can be due, in part, to differences in the amount or ratio of filaggrin and intercellular lipids within the SC. Little is known about the role of filaggrin in the formation of reservoirs of active chemical within the SC (which could potentially contribute to systemic or dermal toxicity) which has been observed for SM (Hattersley*, et al*. 2008). Thus interindividual differences in filaggrin or intercellular lipids within the SC could present further challenges to topical decontamination in addition to contributing to differences in rate of percutaneous penetration through the skin.

Removal of the SC and epidermis using a dermatome resulted in the rapid onset of advanced signs of SM toxicity including ulceration, escharification and reduced dermal perfusion. Reduction in blood flow could be attributed to vasoconstriction as SM can act as a cholinergic agonist. However, SM can also down regulate expression of adrenergic receptors, responsible for vasoconstriction in the skin. Alternatively, reductions in blood flow could be attributed to capillary congestion identified by histological analysis. The increased rate of absorption *in vivo* correlated with earlier onset of advanced signs of toxicity than previously reported. This implies that the apparent latency in clinical signs associated with SM exposure may be due to the rate of absorption and not solely dependent of biochemical pathways as previously described. Additionally this thesis has demonstrated that some commonly used biophysical measurements may have limited value when investigating the effects of SM exposure via damaged skin as subtle changes in parameters could be masked by the initial injury. This thesis has built on previous work (Brown*, et al*. 1998, Chilcott. 2000, Braue*, et al*. 2007) in demonstrating the usefulness of laser Doppler imaging in measuring SM lesion progression, particularly early time point changes in perfusion and when the skin is damaged.

This Thesis is the first to examine the toxicokinetics and distribution of ^{14}C-SM when applied percutaneously to superficially damaged skin. Absorption of ^{14}C-SM into the circulation was rapid (dose peaked at 2 h post-challenge) and toxicokinetics of ^{14}C-SM in the blood followed a first-order one compartment model with a half life of 460 ± 62 min. The apparent long half-life in the blood could be attributed to the absorption of residual SM remaining at the dose site (after removal at 60 min). Whilst it has been demonstrated that SM forms a skin reservoir within the SC *in vitro* (Hattersley*, et al*.

2008) it is not clear if reservoir of active SM forms in the dermis if the SC is removed. Alternatively SM rapidly spreads across the surface of the skin *in vitro* (Chilcott*, et al*. 2000) and so could form a reservoir in the SC in the undamaged skin surrounding the area of damaged skin.

In vitro static diffusion cell studies identified WoundStat™ as being comparable, as a decontaminant, with in-service military decontaminants (M291 and fuller's earth). WoundStat™ is similar in structure to fuller's earth and thus it is reasonable to postulate that WoundStat™ is able to adsorb SM in the interlayer spaces of the smectite clay structure.

Overall, WoundStat™ showed *in vivo* efficacy as a decontaminant significantly reducing the amount of ^{14}C-SM at the exposure site (skin and skin surface swabs) and systemically absorbed (blood, liver and small intestines). Treatment with WoundStat™ also prevented the appearance of signs of severe toxicity e.g. ulceration and reduced the occurrence of other clinical observations (blanching and erythema). The reduction in blanching at the exposure site corresponded with a significant increase in maximal blood flow at WoundStat™ treated exposure sites when compared with the SM only exposure sites. This not only supports the hypothesis that haemostats could have a dual function as a haemostatic decontaminants but also further validates the use of *in vitro* diffusion cells in the identification of potential decontaminants.

The remaining haemostats tested were either ineffective or less efficacious than WoundStat™ (QuikClot ACS+® and Pro QR®) or significantly increased the dermal absorption of SM *in vitro* (VitaGel™, FastAct®, Celox™ and HemCon®). The significant increase in rate and amount of ^{14}C-SM absorption could be attributable to the formation of an occlusive layer preventing evaporative loss and/or

thermodynamically favourable partitioning of hydrophobic SM from an aqueous solution into the lipid-rich SC. The lack of efficacy for the other granular products is possibly due to preferentially adsorbing hydrophilic molecules.

This Thesis sought to develop a defined animal model to characterise the early time point effects of SM exposure via superficially damaged skin. Overall, this has been achieved. However, further work to characterise the biological function of porcine gene products and a better identification of gene sequences would be advantageous in allowing more extensive microarray studies to be conducted using the pig model. The mouse is currently widely used for investigating the genomic effects of SM *in vivo* due to its size, cost, availability of reagents and information regarding gene function. Absorption of chemicals in murine skin has been shown to be unrepresentative of absorption in human skin (Lu*, et al*. 1992, Wester and Maibach. 1993). Moreover, this Thesis has shown that SM-induced pathology and gene expression in the skin are affected by decreased barrier function (removal of the SC and epidermis). Therefore, the gene expression changes observed in the murine model which has more permeable skin (decreased barrier function) may not be representative of the genomic response to SM in man. Thus, use of an animal model like the pig which has shown good correlation with human skin (Barbero and Frasch. 2009, Simon and Maibach. 2000) may more accurately reflect the time course of effects.

Overall, treatment of damaged skin with SM was associated with down regulation of gene expression (summarised in Table 7.1) which is in contrast to the general upregulation of gene expression observed following SM exposure of undamaged skin (Vallet*, et al*. 2012, Gerecke*, et al*. 2009). The majority of the genes whose relative mRNA levels were down-regulated are involved in

inflammatory/immune response, oxidative stress response or cell differentiation/proliferation. Some of the genes identified as down-regulated in this Thesis (Chapter 5) have been shown to be up-regulated in previous studies (Gao*, et al*. 2008, Gerecke*, et al*. 2009, Wormser*, et al*. 2004, Steinritz*, et al*. 2009).

Although, this may be attributed to the combined damaged to the skin (wounding plus SM) particularly in the case of inducible nitric oxide synthase (iNOS). Sulphur mustard has been shown to increase iNOS function in undamaged skin (Gao*, et al*. 2008, Steinritz*, et al*. 2009) but decreased function was observed in a keratinocyte wound model (Ishida*, et al*. 2008). Therefore, targets for SM injury therapies identified using undamaged skin may not be effective (or have an adverse effect) when used on wounded skin.

Treatment site (Skin was superficially damaged for all treatment sites)	**Number of genes upregulated**	**Number of genes down regulated**
SM-exposed (vs. damaged unexposed)	1	18
WoundStat™-treated SM exposed (vs. WoundStat™-treated unexposed)	4	12
WoundStat™-treated SM exposed (vs. SM exposed)	18	8

Table 7-1: Summary of differential gene expression in the skin following application of WoundStat™ and/or SM

Differential gene expression was defined as a FDR corrected p-value of <0.05 and a fold change in relative mRNA levels of ≥ 2)

Thioredoxin interacting protein (TXNIP) was the only gene upregulated in damaged skin following exposure to SM (without decontamination). Thioredoxin interacting protein decreases detoxification of ROS through the inhibition of H_2O_2 metabolism by thioredoxin contributing to oxidative stress (Zhou*, et al*. 2010, Cadenas and Davies. 2000). A monofunctional SM analogue (CEES) reduces thioredoxin activity, although, the observed reduction in activity was attributed to decreased thioredoxin reductase activity and not increased TXNIP expression (Jan*, et al*. 2010). Thus inhibition of TXNIP may reduce cell death associated with SM-induced toxicity. Additionally TXNIP has been attributed to linking oxidative stress to increased inflammation via NLRP3 inflammasome binding which results in increased IL-1β production (Zhou*, et al*. 2010).

Surprisingly, decontamination of SM-exposed damaged skin using WoundStat™ increased the relative expression of gene transcripts (compared to SM-exposed damaged skin without decontamination) involved in inflammation, barrier function, regulation of cell differentiation/survival and oxidative stress. Some genes (IL-6, amphiregulin, p101) have a well characterised role in inflammation or cell regulation (proliferation, differentiation or survival) and have been previously been shown to up-regulated by SM and may contribute to SM pathogenesis (Gerecke*, et al*. 2009, Sabourin*, et al*. 2004, Rogers*, et al*. 2004). Interestingly, IL-6 has been observed to contribute to SM damage in the dermal layer and inhibition of the cytokine (by anti-IL-6 antibodies) may reduce associated inflammation (Arroyo*, et al*. 2004b).

Both AREG and p101 are associated with activation of downstream effector pathways involved in cell death and terminal differentiation (Wakita and Takigawa. 1999; Cantrell. 2001). Although they appear to have opposing effects in terms of

vesication as AREG is up-regulated in blistering diseases (epidermolysis bullosa) affecting the epidermal-dermal junction (Niculescu, *et al*. 2011) and activation of PI3Kγ (p101 is a subunit) prevents anoikis or detachment-induced apoptosis (Brazzatti, *et al*. 2011). Therefore, it is unclear whether WoundStat™ sufficiently reduces the dermal absorption of SM as to prevent vesication. Although, WoundStat™ may reduce SM to a level at which cellular death is shifted toward apoptosis rather than necrosis. Whilst it would be desirable for WoundStat™ to completely prevent cell death, apoptotic cell death would reduce the inflammatory response associated with necrotic cell death (Festjens, *et al*. 2006).

Oxidative stress is a major contributor to the cytotoxic effects of SM (Pal, *et al*. 2009, Laskin, *et al*. 2010, Gould, *et al*. 2009). Several genes (manganese superoxide dismutase; SOD2 and carbonic anhydrase III; CAIII) which were upregulated in WoundStat™ decontaminated, SM-exposed skin (compared to SM-exposed skin without decontamination) have a role in the ROS detoxification (Chapter 6; Figure 6.29). Increased expression of SOD2 and CAIII may be an adaptive cellular defence mechanism to prevent oxidative stress and associated cellular damage including DNA damage. Moreover, SM-induced skin lesion severity was reduced with pre-treatment using SOD2 (Eldad, *et al*. 1998). Furthermore, pre-treatment with antioxidants (e.g. glutathione) reduces SM cytotoxicity (Sawyer and Hamilton. 2000).

Overall, gene expression changes suggest that treatment of SM-exposed damaged skin with WoundStat™ sufficiently reduces the amount of SM at the exposure site to allow for compensatory mechanisms to counteract SM-induced severe cell damage which could result in necrosis. However, a number of genes whose expression was significantly altered by WoundStat™ treatment do not have defined function and

further characterisation of porcine gene products would be beneficial as previously described. This study has identified that WoundStat™ treatment can significantly reduce SM percutaneous absorption and promote compensatory mechanisms to counteract SM-induced cellular damage at a gene expression level. Although, the length of the study (6 h) may not have been long enough to ascertain whether WoundStat™ treatment will prevent the macroscopic and microscopic changes normally attributed to SM injury and a longer term (24 – 72 h) study may be necessary.

This Thesis formed part of a larger project investigating the suitability of commercial haemostats as decontaminants against three chemical warfare agents (SM, VX; *O*-ethyl-*S*-[2(di-isopropylamino)ethyl] methylphosphonothioate, and Soman; *O*-Pinacolyl methylphosphonofluoridate). Studies investigating the efficacy of haemostats against VX and Soman when applied percutaneously to superficially damaged skin *in vitro* and *in vivo* were conducted by Helen Lydon and Christopher Dalton, respectively. The studies were conducted using the same *in vitro* methodology (see Chapter 2). However, the nerve agent studies used a different *in vivo* model (agent applied percutaneously to the pig's ear) which has previously been described for nerve agent exposure studies (Chilcott*, et al*. 2005). Collectively, these studies have demonstrated that WoundStat™ is effective at reducing both SM and VX toxicity *in vivo* (Table 7.2). However, decontamination with WoundStat™ did not prevent death in Soman-exposed animals, although, there was an increase the survival time which could extend the window for therapeutic intervention (Table 7.2). Thus overall, the project represents a comprehensive evaluation of haemostatic products and all three component studies have converged in identifying WoundStat™ as the most effective product.

Agent		VX	Soman (GD)
Coagulation	*In vitro* findings	VX by itself was pro-coagulant. No adverse effect on haemostat efficacy *in vitro*.	GD by itself was pro-coagulant. No adverse effect on haemostat efficacy *in vitro.*
Percutaneous Absorption	*In vitro* findings	WoundStat™ was the most effective product at reducing amount of ^{14}C-VX percutaneously absorbed through undamaged or damaged skin	WoundStat™ was the most effective product at reducing amount of ^{14}C-GD percutaneously absorbed through undamaged or damaged skin
	In vivo findings	WoundStat™ significantly increased survival rate following a 5 x percutaneous LD_{50} challenge of ^{14}C-VX (6/6 animals survived 6 h study period). WoundStat™ also decreased frequency of severe signs of toxicity and the amount of ^{14}C-VX in the systemic circulation	WoundStat™ increased survival time following an estimated 5 x percutaneous LD_{50} challenge of ^{14}C-GD. However, 4 out of 6 animals still died and 2 surviving animals had severe signs of toxicity.

Table 7-2: Summary of in vitro and in vivo decontamination efficacy data from the nerve agent (VX and GD) studies.
(Summary data reproduced with kind permission from Helen Lydon and Christopher Dalton)

Future Work

All *in vitro* studies were conducted with either porcine blood (Chapter 3) or skin (Chapter 4) therefore it would be useful to conduct *in vitro* experiments with human blood and skin to ensure SM effects (or lack thereof) on blood coagulation and SM penetration through damaged skin was not species specific.

Microarray analysis conducted in Chapters 5 and 6 has identified some gene transcripts whose relative expression is changed in response to SM or decontamination of SM-exposed skin. Quantification and validation of these results by qRT-PCR would be required before definitive conclusions can be drawn as to the effects of SM exposure on gene expression in damaged skin and the efficacy of WoundStat™ decontamination.

WoundStat™ has been shown to display cytotoxic effects against endothelial cells but not transformed epithelial cells (HeLa). However the lack of cytotoxicity may be due to the transformed nature of these cells rather than a specific cell response to WoundStat™. This may have an impact on gene expression in the skin. Therefore, changes seen may be as a result of combined SM and WoundStat™ toxicity. To establish what effects WoundStat™ has on gene expression in the skin microarray analysis could be performed on damaged (unexposed) skin and damaged (unexposed) skin receiving WoundStat™ treatment. Unfortunately, this analysis was beyond the scope of this Thesis but it would be a useful comparison to clarify what effect WoundStat™ has on the skin.

This Thesis has included a study of the gene expression effects of SM on damaged skin. However, it would be interesting to conduct similar experiments using an undamaged pig model. This would allow direct comparison of the same species (most literature uses murine models) and thus allow the identification of gene

transcripts whose expression is altered in response to SM alone or whether superficial damage to the skin alters the gene-level response to SM. Moreover, the altered toxicodynamics (caused by removal of the SC) imply that the latent period associated with SM exposure is due to rate of absorption and not solely dependent on biochemical pathways. Future work should seek to further evaluate the role of the skin barrier in altering the toxicodynamics of SM in order to establish if the latent period associated with the pathology of SM lesions is due to kinetics of absorption and not metabolic mechanisms.

Speciation of the ^{14}C-isotopes would be useful to distinguish between SM parent molecule and radiolabelled degradation products. This would be of particular use in the *in vitro* screening studies to ascertain whether ^{14}C detected within the receptor fluid is SM, particularly for reactive decontaminants. However, rapid hydrolysis of SM within the aqueous ethanol may prevent this. Therefore, selection or development of a receptor fluid that allows identification of SM but does not limit percutaneous absorption would be required.

Chapter 8

References

REFERENCES

Agarwal, R., Mori, Y., Cheng, Y., Jin, Z., Olaru, A.V., Hamilton, J.P., David, S., Selaru, F.M., Yang, J., Abraham, J.M., Montgomery, E., Morin, P.J. and Meltzer, S.J., (2009) *Silencing of claudin-11 is associated with increased invasiveness of gastric cancer cells*. Public Library of Science ONE, 4:e8002.

Ahuja, N., Ostomel, T.A., Rhee, P., Stucky, G.D., Conran, R., Chen, Z., Al-Mubarak, G.A., Velmahos, G., Demoya, M. and Alam, H.B., (2006) *Testing of modified zeolite hemostatic dressings in a large animal model of lethal groin injury*. Journal of Trauma-Injury Infection & Critical Care, 61:1312-20.

Akiyama, M., (2011) *Updated molecular genetics and pathogenesis of ichthiyoses*. Nagoya Journal of Medical Science, 73:79-90.

Akomeah, F.K., Martin, G.P., Muddle, A.G. and Brown, M.B., (2008) *Effect of abrasion induced by a rotating brush on the skin permeation of solutes with varying physicochemical properties*. European Journal of Pharmaceutics and Biopharmaceutics, 68:724-734.

Alam, H.B., Chen, Z., Jaskille, A., Querol, R.I.L.C., Koustova, E., Inocencio, R., Conran, R., Seufert, A., Ariaban, N., Toruno, K. and Rhee, P., (2004) *Application of a zeolite hemostatic agent achieves 100% survival in a lethal model of complex groin injury in swine*. Journal of Trauma-Injury Infection & Critical Care, 56:974-83.

Alam, H.B., Uy, G.B., Miller, D., Koustova, E., Hancock, T., Inocencio, R., Anderson, D., Llorente, O. and Rhee, P., (2003) *Comparative analysis of hemostatic agents in a swine model of lethal groin injury*. Journal of Trauma-Injury Infection & Critical Care, 54:1077-1082.

Al-Otaiby, M., Tassi, E., Schmidt, M.O., Chien, C.D., Baker, T., Salas, A.G., Xu, J., Furlong, M., Schlegel, R., Riegel, A.T. and Wellstein, A., (2012) *Role of the nuclear receptor coactivator AIB1/SRC-3 in angiogenesis and wound healing*. The American Journal of Pathology, 180:1474-1484.

Ameziane-El-Hassani, R., Morand, S., Boucher, J., Frapart, Y., Apostolou, D., Agnandji, D., Gnidehou, S., Ohayon, R., Noël-Hudson, M., Francon, J., Lalaoui, K., Virion, A. and Dupuy, C., (2005) *Dual oxidase-2 has an intrinsic Ca2+-dependent H2O2-generating activity*. Journal of Biological Chemistry, 280:30046-30054.

Ankarcrona, M., Dypbukt, J.M., Orrenius, S. and Nicotera, P., (1996) *Calcineurin and mitochondrial function in glutamate-induced neuronal cell death*. FEBS Letters, 394:321-324.

Anzenbacherová, E., Baranová, J., Zuber, R., Pechová, A., Anzenbacher, P., Soucek, P. and Martínková, J., (2005) *Model systems based on experimental animals for studies on*

drug metabolism in man: (mini) pig cytochromes P450 3A29 and 2E1. Basic & Clinical Pharmacology & Toxicology, 96:244-245.

Arnaud, F., Tomori, T., Saito, R., McKeague, A., Prusaczyk, W.K. and McCarron, R., (2007) *Comparative efficacy of granular and bagged formulations of the hemostatic agent QuikClot*. Journal of Trauma-Injury Infection & Critical Care, 63:775-782.

Arroyo, C.M., Burman, D.L., Kahler, D.W., Nelson, M.R., Corun, C.M., Guzman, J.J., Smith, M.a., Purcell, E.D., Hackley, B.E., Soni, S. and Broomfield, C.a., (2004a) *TNF-alpha expression patterns as potential molecular biomarker for human skin cells exposed to vesicant chemical warfare agents: Sulfur mustard (HD) and lewisite (L)*. Cell Biology and Toxicology, 20:345-59.

Arroyo, C., Burman, D., Sweeney, R., Broomfield, C., Ross, M. and Hackley, B., (2004b) *Neutralization effects of interleukin-6 (IL-6) antibodies on sulfur mustard (HD)-induced IL-6 secretion on human epidermal keratinocytes*. Environmental Toxicology and Pharmacology, 17:87-94.

Arroyo, C.M., Broomfield, C.A., Hackley, B.E. and Jr, (2001a) *The role of interleukin-6 (IL-6) in human sulfur mustard (HD) toxicology.* International Journal of Toxicology, 20:281-296.

Arroyo, C.M., Schafer, R.J., Kurt, E.M., Broomfield, C.A. and Carmichael, A.J., (2001b) *Response of normal human keratinocytes to sulfur mustard: Cytokine release.* Journal of Applied Toxicology, 21:S63-S72.

Balali-Mood, M. and Hefazi, M., (2005) *The pharmacology, toxicology, and medical treatment of sulphur mustard poisoning*. Fundamental & Clinical Pharmacology, 19:297-315.

Balali-Mood, M., Hefazi, M., Mahmoudi, M., Jalali, E., Attaran, D., Maleki, M., Razavi, M.E., Zare, G., Tabatabaee, A. and Jaafari, M., (2005) *Long-term complications of sulphur mustard poisoning in severely intoxicated iranian veterans*. Fundamental & Clinical Pharmacology, 19:713-21.

Banin, S., Moyal, L., Shieh, S.-., Taya, Y., Anderson, C.W., Chessa, L., Smorodinsky, N.I., Prives, C., Reiss, Y., Shiloh, Y. and Ziv, Y., (1998) *Enhanced phosphorylation of p53 by ATM in response to DNA damage*. Science, 281:1674-1677.

Barbero, A.M. and Frasch, H.F., (2009) *Pig and guinea pig skin as surrogates for human in vitro penetration studies: A quantitative review*. Toxicology in Vitro, 23:1-13.

Baroni, A., Buommino, E., De Gregorio, V., Ruocco, E., Ruocco, V. and Wolf, R., (2012) *Structure and function of the epidermis related to barrier properties*. Clinics in Dermatology, 30:257-262.

Barry, B.W., (1991) *Modern methods of promoting drug absorption through the skin*. Molecular Aspects of Medicine, 12:195-241.

Barry, B.W., Harrison, S.M. and Dugard, P.H., (1985) *Vapour and liquid diffusion of model penetrants through human skin; correlation with thermodynamic activity*. Journal of Pharmacy and Pharmacology, 37:226-236.

Bartek, M.J., Labudde, J.A. and Maibach, H.I., (1972) *Skin permeability in vivo: Comparison in rat, rabbit, pig and man*. Journal of Investigative Dermatology, 58:114-123.

Bashir, S.J., Chew, A., Anigbogu, A., Dreher, F. and Maibach, H.I., (2001) *Physical and physiological effects of stratum corneum tape stripping*. Skin Research and Technology, 7:40-48.

Beisson, F., Aoubala, M., Marull, S., Moustacas-Gardies, A., Voultoury, R., Verger, R. and Arondel, V., (2001) *Use of the tape stripping technique for directly quantifying esterase activities in human stratum corneum*. Analytical Biochemistry, 290:179-185.

Bestor, T.H., (2000) *The DNA methyltransferases of mammals*. Human Molecular Genetics, 9:2395-2402.

Bharara, M., Cobb, J.E. and Claremont, D.J., (2006) *Thermography and thermometry in the assessment of diabetic neuropathic foot: A case for furthering the role of thermal techniques*. The International Journal of Lower Extremity Wounds, 5:250-260.

Bhat, K.R., Benton, B.J. and Ray, R., (2006) *Poly (ADP-ribose) polymerase (PARP) is essential for sulfur mustard-induced DNA damage repair, but has no role in DNA ligase activation.* Journal of Applied Toxicology, 26:452-457.

Bhat, K.R., Benton, B.J., Rosenthal, D.S., Smulson, M.E. and Ray, R., (2001) *Role of poly(ADP-ribose) polymerase (PARP) in DNA repair in sulfur mustard-exposed normal human epidermal keratinocytes (NHEK).* Journal of Applied Toxicology, 21:S13-S17.

Bikle, D.D., Teichert, A., Arnold, L.A., Uchida, Y., Elias, P.M. and Oda, Y., (2010) *Differential regulation of epidermal function by VDR coactivators*. The Journal of Steroid Biochemistry and Molecular Biology, 121:308-313.

Bjarnason, S., Mikler, J., Hill, I., Tenn, C., Garrett, M., Caddy, N. and Sawyer, T., (2008) *Comparison of selected skin decontaminant products and regimens against VX in domestic swine*. Human & Experimental Toxicology, 27:253-261.

Black, A.T., Hayden, P.J., Casillas, R.P., Heck, D.E., Gerecke, D.R., Sinko, P.J., Laskin, D.L. and Laskin, J.D., (2011) *Regulation of Hsp27 and Hsp70 expression in human and mouse skin construct models by caveolae following exposure to the model sulfur mustard vesicant, 2-chloroethyl ethyl sulfide*. Toxicology and Applied Pharmacology, 253:112-120.

Black, A.T., Hayden, P.J., Casillas, R.P., Heck, D.E., Gerecke, D.R., Sinko, P.J., Laskin, D.L. and Laskin, J.D., (2010) *Expression of proliferative and inflammatory markers in a full-thickness human skin equivalent following exposure to the model*

sulfur mustard vesicant, 2-chloroethyl ethyl sulfide. Toxicology and Applied Pharmacology.

Black, R.M., Brewster, K., Clarke, R.J., Hambrook, J.L., Harrison, J.M. and Howells, D.J., (1992) *Biological fate of sulphur mustard, 1,1'-thiobis((2-chloroethane): Isolation and identification of urinary metabolites following intraperitoneal administration to rat.* Xenobiotica, 22:405-418.

Black, R.M., Clarke, R.J., Cooper, D.B., Read, R.W. and Utley, D., (1993) *Application of headspace analysis, solvent extraction, thermal desorption and gas chromatography-mass spectrometry to the analysis of chemical warfare samples containing sulphur mustard and related compounds.* Journal of Chromatography, 637:71-80.

Black, R.M., Clarke, R.J., Harrison, J.M. and Read, R.W., (1997) *Biological fate of sulphur mustard: Identification of valine and histidine adducts in haemoglobin from casualties of sulphur mustard poisoning.* Xenobiotica, 27:499-512.

Black, R.M. and Read, R.W., (1995) *Biological fate of sulphur mustard, 1,1'-thiobis(2-chloroethane): Identification of beta-lyase metabolites and hydrolysis products in human urine*. Xenobiotica, 25:167-73.

Blank, I.H., (1965) *Cutaneous barriers*. The Journal of Investigative Dermatology, 45:249-256.

Bloch, W., Elischer, A., Schriek, M., Böhm, K., Moghbeli, F., Kehe, K., Szinicz, L. and Steinritz, D., (2007) *Comparison of sulfur mustard induced mechanism of cell damage in dependency of time course and cell type*. Toxicology, 233:223-223.

- -Sal - , M., (1997) *Influence of sodium lauryl sulphate on the in vitro percutaneous absorption of compounds with different lipophilicity*. European Journal of Pharmaceutical Sciences, 5:15-22.

Bos, J.D. and Meinardi, M.M., (2000) *The 500 dalton rule for the skin penetration of chemical compounds and drugs*. Experimental Dermatology, 9:165-169.

Bowbrick, V.A., Mikhailidis, D.P. and Stansby, G., (2000) *The use of citrated whole blood in thromboelastography*. Anesthesia & Analgesia, 90:1086-1088.

Bowman, P.D., Wang, X., Meledeo, M.A., Dubick, M.A. and Kheirabadi, B.S., (2011) *Toxicity of aluminum silicates used in hemostatic dressing toward human umbilical vein endothelial cells, HeLa cells, and RAW267.4 mouse macrophages.* Journal of Trauma - Injury, Infection and Critical Care, 71:727-732.

Brass, L.F., (2003) *Thrombin and platelet activation*. Chest, 124:18S-24S.

Braue, J., E.H, Graham, J.S., Doxzon, B.F., Hanssen, K.A., Lumpkin, H.L., Stevenson, R.S., Deckert, R.R., Dalal, S.J. and Mitcheltree, L.W., (2007) *Noninvasive methods for*

determining lesion depth from vesicant exposure. Journal of Burn Care and Research, 28:275-285.

Brazzatti, J.A., Klingler-Hoffmann, M., Haylock-Jacobs, S., Harata-Lee, Y., Niu, M., Higgins, M.D., Kochetkova, M., Hoffmann, P. and McColl, S.R., (2011) *Differential roles for the p101 and p84 regulatory subunits of PI3K[gamma] in tumor growth and metastasis*. Oncogene.

Brimfield, A.A., Mancebo, A.M., Mason, R.P., Jiang, J.J., Siraki, A.G. and Novak, M.J., (2009) *Free radical production from the interaction of 2-chloroethyl vesicants (mustard gas) with pyridine nucleotide-driven flavoprotein electron transport systems*. Toxicology and Applied Pharmacology, 234:128-134.

Brimfield, A.A., Soni, S.D., Trimmer, K.A., Zottola, M.A., Sweeney, R.E. and Graham, J.S., (2012) *Metabolic activation of sulfur mustard leads to oxygen free radical formation*. Free Radical Biology and Medicine, 52:811-817.

Brisson, P., (1974) *Percutaneous absorption*. Canadian Medical Association Journal, 110:1182-1185.

Brock, C., Schaefer, M., Reusch, H.P., Czupalla, C., Michalke, M., Spicher, K., Schultz, G. and Nürnberg, B., (2003) *Roles of G beta gamma in membrane recruitment and activation of p110 gamma/p101 phosphoinositide 3-kinase gamma.*. Journal of Cell Biology, 160:89-99.

Bronaugh, R.L., Stewart, R.F. and Congdon, E.R., (1982) *Methods for in vitro percutaneous absorption studies. II. animal models for humanskin*. Toxicology and Applied Pharmacology, 62:481-488.

Bronaugh, R.L., Collier, S.W., Macpherson, S.E. and Kraeling, M.E. , (1994) *Influence of metabolism in skin on dosimetry after topical exposure*. Environmental Health Perspectives, 102:71-74.

Bronaugh, R.L., (2004) *Methods for in vitro percutaneous absorption.* In. Dermatotoxicology, H. Zhai and H.I. Maibach eds., 6th ed. CRC Press, 519-529.

Bronaugh, R.L. and Franz, T.J., (1986) *Vehicle effects on percutaneous absorption: In vivo and in vitro comparisons with human skin*. British Journal of Dermatology, 115:1-11.

Bronaugh, R.L. and Stewart, R.F., (1985) *Methods for in vitro percutaneous absorption studies IV: The flow-through diffusion cell*. Journal of Pharmaceutical Sciences, 74:64-67.

Bronstein, J.M., Chen, K., Tiwari-Woodruff, S. and Kornblum, H.I., (2000) *Developmental expression of OSP/claudin-11*. Journal of Neuroscience Research, 60:284-290.

Brookes, P. and Lawley, P.D., (1961) *The reaction of mono- and di-functional alkylating agents with nucleic acids*. The Biochemical Journal, 80:496-503.

Brookes, P. and Lawley, P.D., (1960) *The reaction of mustard gas with nucleic acids in vitro and in vivo*. The Biochemical Journal, 77:478-84.

Brown, B.M., Ramirez, T., Rife, L. and Craft, C.M., (2010) *Visual arrestin 1 contributes to cone photoreceptor survival and light adaptation*. Investigative Ophthalmology & Visual Science, 51:2372-2380.

Brown, M.A., Daya, M.R. and Worley, J.A., (2007) *Experience with chitosan dressings in a civilian EMS system*. Journal of Emergency MedicineIn Press-7.

Brown, R.F., Rice, P. and Bennett, N.J., (1998) *The use of laser doppler imaging as an aid in clinical management decision making in the treatment of vesicant burns*. Burns : Journal of the International Society for Burn Injuries, 24:692-8.

Brown, R.F.R. and Rice, P., (1997) *Histopathological changes in yucatan minipig skin following challenge with sulphur mustard. A sequential study of the first 24 hours following challenge.* International Journal of Experimental Pathology, 78:9-20.

Cadenas, E. and Davies, K.J.A., (2000) *Mitochondrial free radical generation, oxidative stress, and aging*. Free Radical Biology and Medicine, 29:222-230.

Camenzind, V., Bombeli, T., Seifert, B., Jamnicki, M., Popovic, D., Pasch, T. and Spahn, D.R., (2000) *Citrate storage affects Thrombelastograph® analysis*. Anesthesiology, 92:1242-1249.

Cantrell, D.A., (2001) *Phosphoinositide 3-kinase signalling pathways*. Journal of Cell Science, 114:1439-1445.

Capacio, B.R., Smith, J.R., DeLion, M.T., Anderson, D.R., Graham, J.S., Platoff, G.E. and Korte, W.D., (2004) *Monitoring sulfur mustard exposure by gas chromatography-mass spectrometry analysis of thiodiglycol cleaved from blood proteins.* Journal of Analytical Toxicology, 28:306-310.

Carraway, J.W., Kent, D., Young, K., Cole, A., Friedman, R. and Ward, K.R., (2008) *Comparison of a new mineral based hemostatic agent to a commercially available granular zeolite agent for hemostasis in a swine model of lethal extremity arterial hemorrhage*. Resuscitation, 78:230-235.

Castellino, F.J., (1984) *Biochemistry of human plasminogen*. Seminars in Thrombosis and Hemostasis, 10:18,23-23.

Castellino, F.J., (1981) *Recent advances in the chemistry of the fibrinolytic system*. Chemical Reviews, 81:431-446.

Champion, H.C., Skaf, M.W. and Hare, J.M., (2003) *Role of nitric oxide in the pathophysiology of heart failure*. Heart Failure Reviews, 8:35-46.

Champliaud, M., Viel, A. and Baden, H.P., (2003) *The expression of vitamin D-upregulated protein 1 in skin and its interaction with sciellin in cultured keratinocytes*, 121:781-785.

Cheung, C., Davies, N.G., Hoog, J., Hotchkiss, S.A.M. and Smith Pease, C.K. , (2003) *Species variations in cutaneous alcohol dehydrogenases and aldehyde dehydrogenases may impact on toxicological assessments of alcohols and aldehydes*. Toxicology, 184:97-112.

Cheung, C., Smith, C.K., Hoog, J. and Hotchkiss, S.A.M. , (1999) *Expression and localization of human alcohol and aldehyde dehydrogenase enzymes in skin*. Biochemical and Biophysical Research Communications, 261:100-107.

R. P. Chilcott., (2000) *Vesicant Prophylaxis and Decontamination*.

Chilcott, R., (2000) *Non-invasive quantification of skin injury resulting from exposure to sulphur mustard and lewisite vapours*. Burns, 26:245-250.

Chilcott, R.P., Barai, N., Beezer, A.E., Brain, S.I., Brown, M.B., Bunge, A.L., Burgess, S.E., Cross, S., Dalton, C.H., Dias, M., Farinha, A., Finnin, B.C., Gallagher, S.J., Green, D.M., Gunt, H., Gwyther, R.L., Heard, C.M., Jarvis, C.A., Kamiyama, F., Kasting, G.B., Ley, E.E., Lim, S.T., McNaughton, G.S., Morris, A., Nazemi, M.H., Pellett, M.A., Du Plessis, J., Quan, Y.S., Raghavan, S.L., Roberts, M., Romonchuk, W., Roper, C.S., Schenk, D., Simonsen, L., Simpson, A., Traversa, B.D., Trottet, L., Watkinson, A., Wilkinson, S.C., Williams, F.M., Yamamoto, A. and Hadgraft, J., (2005) *Inter- and intralaboratory variation of in vitro diffusion cell measurements: An international multicenter study using quasi-standardized methods and materials*. Journal of Pharmaceutical Sciences, 94:632-638.

Chilcott, R.P., Jenner, J., Carrick, W., Hotchkiss, S.A. and Rice, P., (2000) *Human skin absorption of bis-2-(chloroethyl)sulphide (sulphur mustard) in vitro*. Journal of Applied Toxicology, 20:349-355.

Chilcott, R.P., Jenner, J., Hotchkiss, S.A.M. and Rice, P., (2001) *In vitro skin absorption and decontamination of sulphur mustard : Comparison of human and pig-ear skin*. Journal of Applied Toxicology, 21:279-283.

Chilcott, R.P., Dalton, C.H., Ashley, Z., Allen, C.E., Bradley, S.T., Maidment, M.P., Jenner, J., Brown, R.F.R., Gwyther, R.J. and Rice, P., (2007) *Evaluation of barrier creams against sulphur mustard: (II) in vivo and in vitro studies using the domestic white pig.* Cutaneous and Ocular Toxicology, 26:235-247.

Chilcott, R.P., Dalton, C.H., Emmanuel, A.J., Allen, C.E. and Bradley, S.T., (2002) *Transepidermal water loss does not correlate with skin barrier function in vitro.* Journal of Investigative Dermatology, 118:871-875.

Chilcott, R.P., Dalton, C.H., Hill, I., Davison, C.M., Blohm, K.l., Clarkson, E.D. and Hamilton, M.G., (2005) *In vivo skin absorption and distribution of the nerve agent VX (O-ethyl-S-[2(diisopropylamino)ethyl] methylphosphonothioate) in the domestic white pig*. Human & Experimental Toxicology, 24:347-352.

Chilcott, R.P., J. Jenner, C. Taylor and P. Rice. , (1996)*A rapid technique to identify structurally non-viable epidermal membranes during in vitro percutaneous penetration studies*British Toxicology Society Autumn Meeting. University of Oxford.

Clemedson, C.J., Kristoffersson, H., Sorbo, B. and Ullberg, S., (1963) *Whole body autoradiographic studies of the distribution of sulphur 35-labelled mustard gas in mice*. Acta Oncologica, 1:314.

Cochrane, C.G., Revak, S.D. and Wuepper, K.D., (1973) *Activation of hageman factor in solid and fluid phases: A critical role of kallikrein*. J. Exp. Med., 138:1564-1583.

Cole, R.P., Jones, S.G. and Shakespeare, P.G., (1990) *Thermographic assessment of hand burns.*. Burns, 16:60-63.

Collier, S.W., Sheikh, N.M., Sakr, A., Lichtin, J.L., Stewart, R.F. and Bronaugh, R.L., (1989) *Maintenance of skin viability during in vitro percutaneous absorption/metabolism studies*. Toxicology and Applied Pharmacology, 99:522-533.

Collombet, J., Mourcin, F., Grenier, N., Four, E., Masqueliez, C., Baubichon, D., Lallement, G. and Hérodin, F., (2005) *Effect of soman poisoning on populations of bone marrow and peripheral blood cells in mice*. Neurotoxicology, 26:89-98.

Comes, N., Buie, L.K. and Borrás, T., (2011) *Evidence for a role of angiopoietin-like 7 (ANGPTL7) in extracellular matrix formation of the human trabecular meshwork: Implications for glaucoma*. Genes to Cells, 16:243-259.

Cooke, M.S., Evans, M.D., Dizdaroglu, M. and Lunec, J., (2003) *Oxidative DNA damage: Mechanisms, mutation, and disease*. The Journal of the Federation of American Societies for Experimental Biology, 17:1195-1214.

Cooper, E.R. and Berner, B., (1985) *Skin permeability.* In. Methods In Skin Research, D. Skerrow and C.J. Skerrow eds., John Wiley, 407-432.

Cross, S.E., Magnusson, B.M., Winckle, G., Anissimov, Y. and Roberts, M.S., (2003) *Determination of the effect of lipophilicity on the in vitro permeability and tissue reservoir characteristics of topically applied solutes in human skin layers*. Journal of Investigative Dermatology, 120:759-764.

Cullumbine, H., (1947) *Medical aspects of mustard gas poisoning*. Nature, 159:151-153.

Dabrowska, M.I., Becks, L.L., Lelli, J.L., Levee, M.G. and Hinshaw, D.B., (1996) *Sulfur mustard induces apoptosis and necrosis in endothelial cells*. Toxicology and Applied Pharmacology, 141:568-83.

Dachir, S., Cohen, M., Fishbeine, E., Sahar, R., Brandies, R., Horwitz, V. and Kadar, T., (2010) *Characterization of acute and long-term sulfur mustard-induced skin injuries in hairless guinea-pigs using non-invasive methods*. Skin Research and Technology, 16:114-124.

Dacre, J.C. and Goldman, M., (1996) *Toxicology and pharmacology of the chemical warfare agent sulfur mustard.* Pharmacological Reviews, 48:289-326.

Dale, B.A., Resing, K.A. and Lonsdale-Eccles, J.D., (1985) *Filaggrin: A keratin filament associated protein*. Annals of the New York Academy of Sciences, 455:330-342.

Dale, B.A., Scofield, J.A.H., Hennings, H., Stanley, J.R. and Yuspa, S.H., (1983) *Identification of filaggrin in cultured mouse keratinocytes and its regulation by calcium*. J Investig Dermatol, 81:90s-95s.

Dalton, C.H., J. Jenner, R.P. Chilcott, H.I. Maibach and J.S. Graham. , (2006)*Preliminary evaluation of debriding agents*Proceedings of the U.S. Army Medical Defense Bioscience Review. Hunt Valley, MD, USA.

Dalton, C., Hattersley, I., Rutter, S. and Chilcott, R., (2006) *Absorption of the nerve agent VX (O-ethyl-S-[2(di-isopropylamino)ethyl] methyl phosphonothioate) through pig, human and guinea pig skin in vitro*. Toxicology in Vitro, 20:1532-1536.

Davies, D.J., Ward, R.J. and Heylings, J.R., (2004) *Multi-species assessment of electrical resistance as a skin integrity marker for in vitro percutaneous absorption studies*. Toxicology in Vitro, 18:351-358.

Davison, C., Rozman, R.S. and Smith, P.K., (1961) *Metabolism of bis-β-chloroethyl sulfide (sulfur mustard gas)*. Biochemical Pharmacology, 7:65-74.

Debiak, M., Kehe, K. and Burkle, A., (2009) *Role of poly(ADP-ribose) polymerase in sulfur mustard toxicity.* Toxicology, 263:20-25.

Detheux, M., Jijakli, H. and Lison, D., (1997) *Effect of sulphur mustard on the expression of urokinase in cultured 3T3 fibroblasts*. Archives of Toxicology, 71:243-249.

Dillman III, J.F., Hege, A.I., Phillips, C.S., Orzolek, L.D., Sylvester, A.J., Bossone, C., Henemyre-Harris, C., Kiser, R.C., Choi, Y.W., Schlager, J.J. and Sabourin, C.L., (2006) *Microarray analysis of mouse ear tissue exposed to bis-(2-chloroethyl) sulfide: Gene expression profiles correlate with treatment efficacy and an established clinical endpoint.* Journal of Pharmacology and Experimental Therapeutics, 317:76-87.

Dillman III, J.F., McGary, K.L. and Schlager, J.J., (2004) *An inhibitor of p38 MAP kinase downregulates cytokine release induced by sulfur mustard exposure in human epidermal keratinocytes.* Toxicology in Vitro, 18:593-599.

Dillman III, J.F., Phillips, C.S., Dorsch, L.M., Croxton, M.D., Hege, A.I., Sylvester, A.J., Moran, T.S. and Sciuto, A.M., (2005) *Genomic analysis of rodent pulmonary tissue following bis-(2-chloroethyl) sulfide exposure.* Chemical Research in Toxicology, 18:28-34.

Droog, E.J., Steenbergen, W. and Sjöberg, F., (2001) *Measurement of depth of burns by laser doppler perfusion imaging*. Burns, 27:561-568.

Duracher, L., Blasco, L., Hubaud, J., Vian, L. and Marti-Mestres, G., (2009) *The influence of alcohol, propylene glycol and 1, 2-pentanediol on the permeability of hydrophilic model drug through excised pig skin*. International Journal of Pharmaceutics, 374:39-45.

Dutta, R., McDonough, J., Yin, X., Peterson, J., Chang, A., Torres, T., Gudz, T., Macklin, W.B., Lewis, D.A., Fox, R.J., Rudick, R., Mirnics, K. and Trapp, B.D., (2006) *Mitochondrial dysfunction as a cause of axonal degeneration in multiple sclerosis patients*. Annals of Neurology, 59:478-489.

Eckert, R.L., Yaffe, M.B., Crish, J.F., Murthy, S., Rorke, E.A. and Welter, J.F., (1993) *Involucrin - structure and role in envelope assembly*. Journal of Investigative Dermatology, 100:613-617.

Eguchi, Y., Shimizu, S. and Tsujimoto, Y., (1997) *Intracellular ATP levels determine cell death fate by apoptosis or necrosis*. Cancer Research, 57:1835-1840.

Eldad, A., Meir, P.B., Breiterman, S., Chaouat, M., Shafran, A. and Ben-Bassat, H., (1998) *Superoxide dismutase (SOD) for mustard gas burns*. Burns, 24:114-119.

Elkeeb, R., Hui, X., Chan, H., Tian, L. and Maibach, H.I., (2010) *Correlation of transepidermal water loss with skin barrier properties in vitro: Comparison of three evaporimeters*. Skin Research and Technology, 16:9-15.

Elsayed, N.M. and Omaye, S.T., (2004) *Biochemical changes in mouse lung after subcutaneous injection of the sulfur mustard 2-chloroethyl 4-chlorobutyl sulfide.* Toxicology, 199:195-206.

Enders, G.H., (2008) *Expanded roles for Chk1 in genome maintenance*. Journal of Biological Chemistry, 283:17749-17752.

Essa, E.A., Bonner, M.C. and Barry, B.W., (2002) *Human skin sandwich for assessing shunt route penetration during passive and iontophoretic drug and liposome delivery*. Journal of Pharmacy and Pharmacology, 54:1481-1490.

Fairhall, S.J., Brown, R.F.R., Jugg, B.J.A., Smith, A.J., Mann, T.M., Jenner, J. and Sciuto, A.M., (2008) *Preliminary studies of sulphur mustard-induced lung injury in the terminally anesthetized pig: Exposure system and methodology*. Toxicology Mechanisms and Methods, 18:355-362.

Faralli, J.A., Schwinn, M.K., Gonzalez Jr., J.M., Filla, M.S. and Peters, D.M., (2009) *Functional properties of fibronectin in the trabecular meshwork*. Experimental Eye Research, 88:689-693.

Festjens, N., Vanden Berghe, T. and Vandenabeele, P., (2006) *Necrosis, a well-orchestrated form of cell demise: Signalling cascades, important mediators and concomitant immune response*. Biochimica Et Biophysica Acta, 1757:1371-1387.

Flynn, G.L., (1990) *Physicochemical determinants of skin absorption.* In. Principles of Route-to-Route Extrapolation for Risk Assessment, T.R. Gerrity and C.J. Henry eds., Elsevier Science Publishing Co, .

Forrester, K.R., Stewart, C., Tulip, J., Leonard, C. and Bray, R.C., (2002) *Comparison of laser speckle and laser doppler perfusion imaging: Measurement in human skin and rabbit articular tissue*. Medical and Biological Engineering and Computing, 40:687-697.

Forslind, B. and Lindberg, M., (2003) *Structure and function of the skin barrier: An introduction.* In. Skin, Hair and Nails: Structure and Function, B. Forslind and M. Lindberg eds., Marcel Dekker, 9-21.

Francis, C.W. and Marder, V.J., (1987) *Physiologic regulation and pathologic disorders of fibrinolysis*. Human Pathology, 18:263-274.

Franz, T.J., (1978) *The finite dose technique as a valid in vitro model for the study of percutaneous absorption in man.* Current Problems in Dermatology, 7:58-68.

Franz, T.J., (1975) *Percutaneous absorption. on the relevance of in vitro data.* Journal of Investigative Dermatology, 64:190-195.

Gallucci, R.M., Simeonova, P.P., Matheson, J.M., Kommineni, C., Guriel, J.L., Sugawara, T. and Luster, M.I., (2000) *Impaired cutaneous wound healing in interleukin-6– deficient and immunosuppressed mice*. The Journal of the Federation of American Societies for Experimental Biology, 14:2525-2531.

Gan, S.Q., McBride, O.W., Idler, W.W., Markova, N. and Steinert, P.M., (1990) *Organization, structure, and polymorphisms of the human profilaggrin gene*. Biochemistry, 29:9432-9440.

Gao, X., Ray, R., Xiao, Y., Barker, P.E. and Prabhati, R., (2007) *Inhibition of sulfur mustard-induced cytotoxicity and inflammation by the macrolide antibiotic roxithromycin in human respiratory epithelial cells*. BMC Cell Biology17-26.

Gao, X., Ray, R., Xiao, Y. and Ray, P., (2008) *Suppression of inducible nitric oxide synthase expression and nitric oxide production by macrolide antibiotics in sulfur mustard-exposed airway epithelial cells.* Basic and Clinical Pharmacology and Toxicology, 103:255-261.

Gattu, S. and Maibach, H.I., (2011) *Modest but increased penetration through damaged skin: An overview of the in vivo human model*. Skin Pharmacology and Physiology, 24:2-9.

George, J., Srivastava, A.K., Singh, R. and Shukla, Y., (2011) *Cypermethrin exposure leads to regulation of proteins expression involved in neoplastic transformation in mouse skin*. Proteomics, 11:4411-4421.

Gerecke, D.R., Chen, M., Isukapalli, S.S., Gordon, M.K., Chang, Y.-., Tong, W., Androulakis, I.P. and Georgopoulos, P.G., (2009) *Differential gene expression profiling of mouse skin after sulfur mustard exposure: Extended time response and inhibitor effect.* Toxicology and Applied Pharmacology, 234:156-165.

Gerlach, T., Grayson, J.K., Pichakron, K.O., Sena, M.J., DeMartini, S.D., Clark, B.Z., Estep, J.S. and Zierold, D., (2010) *Preliminary study of the effects of smectite granules (WoundStat) on vascular repair and wound healing in a swine survival model*. Journal of Trauma-Injury Infection & Critical Care, 69:1203-1209.

Gibbs, A.R. and Pooley, F.D., (1994) *Fuller's earth (montmorillonite) pneumoconiosis.* Occupational and Environmental Medicine, 51:644-646.

Girault, I., Tozlu, S., Lidereau, R. and Bièche, I., (2003) *Expression analysis of DNA methyltransferases 1, 3A, and 3B in sporadic breast carcinomas*. Clinical Cancer Research, 9:4415-4422.

Giuliani, I., Baeza-Squiban, A. and Marano, F., (1997) *Early cytotoxic effects of mechlorethamine, a nitrogen mustard, on mammalian airway epithelium*. Toxicology in Vitro, 11:695-702.

Gold, M.B., Bongiovanni, R., Scharf, B.A., Gresham, V.C. and Woodward, C.L., (1994) *Hypochlorite solution as a decontaminant in sulfur mustard contaminated skin defects in the euthymic hairless guinea pig.* Drug and Chemical Toxicology, 17:499-527.

Golden, G.M., Guzek, D.B., Kennedy, A.E., McKie, J.E. and Potts, R.O., (1987) *Stratum corneum lipid phase transitions and water barrier properties*. Biochemistry, 26:2382-2388.

Gordon, R.K., A.T. Gunduz, L.Y. Askins, S.J. Strating, B.P. Doctor, E.D. Clarkson, L.W. Mitchelree, B. Lukey, R. Railer, S. Schulz, M. Shutz, D.M. Maxwell, J.P. Skvorak and M. Ross. , (2002)*Decontamination And Detoxification Of Toxic Chemical Warfare Agents Using Polyurethane Sponges*Proceedings of the 2002 Joint Service

Scientific Conference on Chemical & Biological Defense Research. . Aberdeen Proving Ground, MD: Edgewood Chemical Biological Center.

Götz, C., Pfeiffer, R., Tigges, J., Ruwiedel, K., Hübenthal, U., Merk, H.F., Krutmann, J., Edwards, R.J., Abel, J., Pease, C., Goebel, C., Hewitt, N. and Fritsche, E. , (2012) *Xenobiotic metabolism capacities of human skin in comparison with a 3D-epidermis model and keratinocyte-based cell culture as in vitro alternatives for chemical testing: Phase II enzymes*. Experimental Dermatology, 21:364-369.

Gould, N.S., White, C.W. and Day, B.J., (2009) *A role for mitochondrial oxidative stress in sulfur mustard analog 2-chloroethyl ethyl sulfide-induced lung cell injury and antioxidant protection*. Journal of Pharmacology and Experimental Therapeutics, 328:732-739.

Graham, J.S., Martin, J.L., Zallnick, J.E., Nalls, C.R., Mitcheltree, L.W., Lee, R.B., Logan, T.P., Braue, J. and E.H, (1999) *Assessment of cutaneous sulfur mustard injury in the weanling pig.* Skin Research and Technology, 5:56-67.

Graham, J.S., Reid, F.M., Smith, J.R., Stotts, R.R., Tucker, F.S., Shumaker, S.M., Niemuth, N.A. and Janny, S.J., (2001) *A cutaneous full-thickness liquid sulfur mustard burn model in weanling swine: Clinical pathology and urinary excretion of thiodiglycol.* Journal of Applied Toxicology, 21:S161-S172.

Graham, J.S., Schomacker, K.T., Glatter, R.D., Briscoe, C.M., Braue, J., E.H and Squibb, K.S., (2002) *Bioengineering methods employed in the study of wound healing of sulphur mustard burns.* Skin Research and Technology, 8:57-69.

Graham, J.S., Chilcott, R.P., Rice, P., Milner, S.M., Hurst, C.G. and Maliner, B.I., (2005) *Wound healing of cutaneous sulfur mustard injuries: Strategies for the development of improved therapies*. Journal of Burns and Wounds, 4:e1-e45.

Graham, J.S., Reid, F.M., Smith, J.R., Stotts, R.R., Tucker, F.S., Shumaker, S.M., Niemuth, N.A. and Janny, S.J., (2000) *A cutaneous full-thickness liquid sulfur mustard burn model in weanling swine : Clinical pathology and urinary excretion of thiodiglycol* . Journal of Applied Toxicology, 172:161-172.

Gray, J.P., Mishin, V., Heck, D.E., Laskin, D.L. and Laskin, J.D., (2010) *Inhibition of NADPH cytochrome P450 reductase by the model sulfur mustard vesicant 2-chloroethyl ethyl sulfide is associated with increased production of reactive oxygen species*. Toxicology and Applied Pharmacology, 247:76-82.

Greenberg, S., Kamath, P., Petrali, J., Hamilton, T., Garfield, J. and Garlick, J.A., (2006) *Characterization of the initial response of engineered human skin to sulfur mustard*. Toxicological Sciences, 90:549-557.

Gross, C.L., Innace, J.K., Hovatter, R.C., Meier, H.L. and Smith, W.J., (1993) *Biochemical manipulation of intracellular glutathione levels influences cytotoxicity to*

isolated human lymphocytes by sulfur mustard. Cell Biology and Toxicology, 9:259-268.

Grummer, C. and Maibach, H.I., (1991) *Diffusion cell desgin.* In. *In vitro* Percutaneous Absorption: Principles, Fundamentals and Applications, R.L. Bronaugh and H.I. Maibach eds., CRC Press, 7-16.

Gunther, C., Kecskes, A., Staks, T. and Tauber, U., (1998) *Percutaneous absorption of methylprednisolone aceponate following topical application of Advantan® lotion on intact, inflamed and stripped skin of male volunteers*. Skin Pharmacology and Physiology, 11:35-42.

Guy, R.H., Hadgraft, J. and Maibach, H.I., (1985) *Percutaneous absorption in man: A kinetic approach*. Toxicology and Applied Pharmacology, 78:123-129.

Haake, A., Scott, G.A. and Holbrook, K.A., (2001) *Structure and function of the skin: Overview of the epidermis and dermis.* In. The Biology of the Skin, R.K. Freinkel and D.T. Woodley eds., 3rd ed. Informa Healthcare, 19-47.

Hadgraft, J., (2001) *Modulation of the barrier function of the skin*. Skin Pharmacology and Physiology, 14:72-81.

Hambrook, J.L., Harrison, J.M., Howells, D.J. and Schock, C., (1992) *Biological fate of sulphur mustard (1,1'-thiobis(2-chloroethane)): Urinary and faecal excretion of ^{35}S by rat after injection or cutaneous application of ^{35}S-labelled sulphur mustard.* Xenobiotica, 22:65-75.

Hamilton, M.G., Dorandeu, F.M., McCaffery, M., Lundy, P.M. and Sawyer, T.W., (1998) *Modification of cytosolic free calcium concentrations in human keratinocytes after sulfur mustard exposure.* Toxicology in Vitro, 12:365-372.

Hampton, J.R. and Mitchell, J.R.A., (1966) *Effect of glass contact on the electrophoretic mobility of human blood platelets*. Nature, 209:470-472.

Hansford, R.G., Hogue, B.A. and Mildaziene, V., (1997) *Dependence of H_2O_2 formation by rat heart mitochondria on substrate availability and donor age*. Journal of Bioenergetics and Biomembranes, 29:89-95.

Harrison, S.M., Barry, B.W. and Dugard, P.H., (1984) *Effects of freezing on human skin permeability*. Journal of Pharmacy and Pharmacology, 36:261-262.

Hartert, H., (1948) *Blutgerinnungsstudien mit der thrombelastographie, einem neuen untersuchungsverfahren*. Journal of Molecular Medicine, 26:577.

Hattersley, I.J., Jenner, J., Dalton, C., Chilcott, R.P. and Graham, J.S., (2008) *The skin reservoir of sulphur mustard*. Toxicology in Vitro, 22:1539-1546.

Hawkins, G.S. and Reifenrath, W.G., (1986) *Influence of skin source, penetration cell fluid, and, partition coefficient on in vitro skin penetration*. Journal of Pharmaceutical Sciences, 75:378-381.

Hayden, M.S. and Ghosh, S., (2008) *Shared principles in NF-κB signaling*. Cell, 132:344-362.

Heidrich, F.M., Zhang, K., Estrada, M., Huang, Y., Giordano, F.J. and Ehrlich, B.E., (2008) *Chromogranin B regulates calcium signaling, nuclear factor κB activity, and brain natriuretic peptide production in cardiomyocytes*. Circulation Research, 102:1230-1238.

Hewitt, P.G., Perkins, J. and Hotchkiss, S.A.M. , (2000) *Metabolism of fluroxypyr, fluroxypyr methyl ester, and the herbicide fluroxypyr methylheptyl ester. I: During percutaneous absorption through fresh rat and human skin in vitro*. Drug Metabolism and Disposition, 28:748-754.

Ho, J. and Hruza, G., (2007) *Hydrophilic polymers with potassium salt and microporous polysaccharides for use as hemostatic agents*. Dermatologic Surgery, 33:1430-1433.

Hoffman, M., (2003) *A cell-based model of coagulation and the role of factor VIIa*. Blood Reviews, 17:S1-S5.

Hua, A., Daniel, R., Jasseron, M.P. and Thiriot, C., (1993) *Early cytotoxic effects induced by bis-chloroethyl sulphide (sulphur mustard): [Ca^{2+}](i) rise and time-dependent inhibition of B77 fibroblast serum response.* Journal of Applied Toxicology, 13:161-168.

Hwa, C., Bauer, E.A. and Cohen, D.E., (2011) *Skin biology*. Dermatologic Therapy, 24:464-470.

Illel, B., Schaefer, H., Wepierre, J. and Doucet, O., (1991) *Follicles play an important role in percutaneous absorption*. Journal of Pharmaceutical Sciences, 80:424-427.

Ishida, H., Ray, R. and Ray, P., (2008) *Sulfur mustard downregulates iNOS expression to inhibit wound healing in a human keratinocyte model.* Journal of Dermatological Science, 49:207-216.

Ismail, I.H., Nyström, S., Nygren, J. and Hammarsten, O., (2005) *Activation of ataxia telangiectasia mutated by DNA strand break-inducing agents correlates closely with the number of DNA double strand breaks*. The Journal of Biological Chemistry, 280:4649-55.

Jacobi, U., Gautier, J., Sterry, W. and Lademann, J., (2005) *Gender-related differences in the physiology of the stratum corneum*. Dermatology, 211:312-317.

Jacobi, U., Tassopoulos, T., Surber, C. and Lademann, J., (2006) *Cutaneous distribution and localisation of dyes affected by vehicles all with different lipophilicity*. Archives of Dermatological Research, 297:303-310.

Jafari, M., (2007) *Dose- and time-dependent effects of sulfur mustard on antioxidant system in liver and brain of rat.* Toxicology, 231:30-39.

Jakasa, I., Verberk, M.M., Bunge, A.L., Kruse, J. and Kezic, S., (2006) *Increased permeability for polyethylene glycols through skin compromised by sodium lauryl sulphate*. Experimental Dermatology, 15:801-807.

Jan, Y., Heck, D.E., Gray, J.P., Zheng, H., Casillas, R.P., Laskin, D.L. and Laskin, J.D., (2010) *Selective targeting of selenocysteine in thioredoxin reductase by the half mustard 2-chloroethyl ethyl sulfide in lung epithelial cells*. Chemical Research in Toxicology, 23:1045-1053.

Jennemann, R., Sandhoff, R., Langbein, L., Kaden, S., Rothermel, U., Gallala, H., Sandhoff, K., Wiegandt, H. and Gröne, H., (2007) *Integrity and barrier function of the epidermis critically depend on glucosylceramide synthesis*. Journal of Biological Chemistry, 282:3083-3094.

Jewell, C., Ackermann, C., Payne, N.A., Fate, G., Voorman, R. and Williams, F.M. , (2007a) *Specificity of procaine and ester hydrolysis by human, minipig, and rat skin and liver*. Drug Metabolism and Disposition, 35:2015-2022.

Jewell, C., Prusakiewicz, J.J., Ackermann, C., Payne, N.A., Fate, G. and Williams, F.M. , (2007b) *The distribution of esterases in the skin of the minipig*. Toxicology Letters, 173:118-123.

Johansson, P., Stissing, T., Bochsen, L. and Ostrowski, S., (2009) *Thrombelastography and tromboelastometry in assessing coagulopathy in trauma*. Scandinavian Journal of Trauma, Resuscitation and Emergency Medicine, 17:45.

Johansson, P.I., Svendsen, M.S., Salado, J., Bochsen, L. and Kristensen, A.T., (2008) *Investigation of the thrombin-generating capacity, evaluated by thrombogram, and clot formation evaluated by thrombelastography of platelets stored in the blood bank for up to 7 days*. Vox Sanguinis, 94:113-118.

Johnson, C., Marriott, S.J. and Levy, L.S., (2007) *Overexpression of p101 activates PI3K-gamma signaling in T cells and contributes to cell survival*. Oncogene, 26:7049-7057.

Jowsey, P.A., Williams, F.M. and Blain, P.G., (2009) *DNA damage, signalling and repair after exposure of cells to the sulphur mustard analogue 2-chloroethyl ethyl sulphide.* Toxicology, 257:105-112.

Jowsey, P.A., Williams, F.M. and Blain, P.G., (2012) *DNA damage responses in cells exposed to sulphur mustard*. Toxicology Letters, 209:1-10.

Kalia, Y.N., Pirot, F. and Guy, R.H., (1996) *Homogeneous transport in a heterogeneous membrane: Water diffusion across human stratum corneum in vivo.* Biophysical Journal, 71:2692-2700.

Kan, R.K., Pleva, C.M., Hamilton, T.A., Anderson, D.R. and Petrali, J.P., (2003) *Sulfur mustard-induced apoptosis in hairless guinea pig skin.* Toxicologic Pathology, 31:185-190.

Kanda, N. and Watanabe, S., (2003) *17 beta-estradiol inhibits the production of RANTES in human keratinocytes*. Journal of Investigative Dermatology, 120:420-427.

Kang, S.I. and Spears, C.P., (1987) *Linear free energy relationships and cytotoxicities of para-substituted 2-haloethyl aryl selenides and bis(2-chloroethyl) selenides.*. Journal of Medicinal Chemistry, 30:597-602.

Kanikkannan, N., Locke, B.R. and Singh, M., (2002) *Effect of jet fuels on the skin morphology and irritation in hairless rats*. Toxicology, 175:35-47.

Kanitakis, J., (2002) *Anatomy, histology and immunohistochemistry of normal human skin*. European Journal of Dermatology, 12:390-401.

Kanwar, J.R., Kanwar, R.K., Burrow, H. and Baratchi, S., (2009) *Recent advances on the roles of NO in cancer and chronic inflammatory disorders.* Current Medicinal Chemistry, 16:2373-2394.

Karin, M. and Ben-Neriah, Y., (2000) *Phosphorylation meets ubiquitination: The control of NF-κB activity*. Annual Review of Immunology, 18:621-663.

Karin, M. and Greten, F.R., (2005) *NF-kappaB: Linking inflammation and immunity to cancer development and progression*. Nature Reviews.Immunology, 5:749-59.

Karoutsos, S., Nathan, N., Lahrimi, A., Grouille, D., Feiss, P. and Cox, D.J., (1999) *Thrombelastogram reveals hypercoagulability after administration of gelatin solution.* British Journal of Anaesthesia, 82:175-177.

Kasting, G.B., Francis, W.R., Bowman, L.A. and Kinnett, G.O., (1997) *Percutaneous absorption of vanilloids: In vivo and in vitro studies*. Journal of Pharmaceutical Sciences, 86:142-146.

Kaufmann, C.R., Dwyer, K.M., Crews, J.D., Dols, S.J.M.T. and Trask, A.L., (1997) *Usefulness of thrombelastography in assessment of trauma patient coagulation*. Journal of Trauma-Injury Infection & Critical Care, 42:716-722.

Kawasaki, H., Nagao, K., Kubo, A., Hata, T., Shimizu, A., Mizuno, H., Yamada, T. and Amagai, M., (2012) *Altered stratum corneum barrier and enhanced percutaneous immune responses in filaggrin-null mice*. Journal of Allergy and Clinical Immunology, In Press:.

Kawasaki, J., Katori, N., Kodaka, M., Miyao, H. and Tanaka, K.A., (2004) *Electron microscopic evaluations of clot morphology during thrombelastography®.* Anesthesia & Analgesia, 99:1440-1444.

Kehe, K., Balszuweit, F., Steinritz, D. and Thiermann, H., (2009) *Molecular toxicology of sulfur mustard-induced cutaneous inflammation and blistering.* Toxicology, 263:12-19.

Kehe, K., Raithel, K., Kreppel, H., Jochum, M., Worek, F. and Thiermann, H., (2008) *Inhibition of poly(ADP-ribose) polymerase (PARP) influences the mode of sulfur mustard (SM)-induced cell death in HaCaT cells*. Archives of Toxicology, 82:461-470.

Kehe, K., Reisinger, H. and Szinicz, L., (2000) *Sulfur mustard induces apoptosis and necrosis in SCL II cells in vitro*. Journal of Applied Toxicology, 20 Suppl 1:S81-6.

Kehe, K. and Szinicz, L., (2005) *Medical aspects of sulphur mustard poisoning*. Toxicology, 214:198-209.

Keller, J.N., Kindy, M.S., Holtsberg, F.W., St. Clair, D.K., Yen, H., Germeyer, A., Steiner, S.M., Bruce-Keller, A.J., Hutchins, J.B. and Mattson, M.P., (1998) *Mitochondrial manganese superoxide dismutase prevents neural apoptosis and reduces ischemic brain injury: Suppression of peroxynitrite production, lipid peroxidation, and mitochondrial dysfunction*. The Journal of Neuroscience, 18:687-697.

Kessler, U., Grau, T., Gronchi, F., Berger, S., Brandt, S., Bracht, H., Marcucci, C., Zachariou, Z. and Jakob, S.M., (2011) *Comparison of porcine and human coagulation by thrombelastometry*. Thrombosis Research, 128:477-482.

Kheirabadi, B.S., Acheson, E.M., Deguzman, R., Sondeen, J.L., Ryan, K.L., Delgado, A., J., D.E.,Jr and Holcomb, J.B., (2005) *Hemostatic efficacy of two advanced dressings in an aortic hemorrhage model in swine*. Journal of Trauma-Injury Infection & Critical Care, 59:25-35.

Kheirabadi, B.S., Edens, J.W., Terrazas, I.B., Estep, J.S.D.V.M., Klemcke, H.G., Dubick, M.A. and Holcomb, J.B., (2009) *Comparison of new hemostatic Granules/Powders with currently deployed hemostatic products in a lethal model of extremity arterial hemorrhage in swine*. Journal of Trauma-Injury Infection & Critical Care, 66:316-328.

Kheirabadi, B.S., Mace, J.E., Terrazas, I.B., Fedyk, C.G., Estep, J.S., Dubick, M.a. and Blackbourne, L.H., (2010) *Safety evaluation of new hemostatic agents, smectite granules, and kaolin-coated gauze in a vascular injury wound model in swine*. The Journal of Trauma: Injury, Infection, and Critical Care, 68:269-278.

Kheirabadi, B.S., Scherer, M.R., Estep, J.S.D.V.M., Dubick, M.A. and Holcomb, J.B., (2009) *Determination of efficacy of new hemostatic dressings in a model of extremity arterial hemorrhage in swine*. Journal of Trauma-Injury Infection & Critical Care, 67:450-460.

Khurana, R.N., Parikh, J.G., Saraswathy, S., Wu, G. and Rao, N.A., (2008) *Mitochondrial oxidative DNA damage in experimental autoimmune uveitis*. Investigative Ophthalmology & Visual Science, 49:3299-3304.

Khurana, S., Mattson, J.C., Westley, S., O'neill, W.W., Timmis, G.C. and Safian, R.D., (1997) *Monitoring platelet glycoprotein IIb/IIIa—fibrin interaction with tissue factor—activated thromboelastography*. Journal of Laboratory and Clinical Medicine, 130:401-411.

Kim, G.S., Jung, J.E., Narasimhan, P., Sakata, H. and Chan, P.H., (2012) *Induction of thioredoxin-interacting protein is mediated by oxidative stress, calcium, and glucose after brain injury in mice*. Neurobiology of Disease, 46:440-449.

Kim, G., Lee, T., Wetzel, P., Geers, C., Robinson, M.A., Myers, T.G., Owens, J.W., Wehr, N.B., Eckhaus, M.W., Gros, G., Wynshaw-Boris, A. and Levine, R.L., (2004) *Carbonic anhydrase III is not required in the mouse for normal growth, development, and life span*. Molecular and Cellular Biology, 24:9942-9947.

Kitson, N. and Thewalt, J., (2000) *Hypothesis: The epidermal permeability barrier is a porous medium*. Acta Derm Venereologica, 208:12-15.

Korkmaz, A., Yaren, H., Kunak, Z.I., Uysal, B., Kurt, B., Topal, T., Kenar, L., Ucar, E. and Oter, S., (2008) *Epigenetic perturbations in the pathogenesis of mustard toxicity; hypothesis and preliminary results*. Interdisciplinary Toxicology, 1:236-241.

Korkmaz, A. and Reiter, R.J., (2008) *Epigenetic regulation: A new research area for melatonin?*. Journal of Pineal Research, 44:41-44.

Korkmaz, A., Yaren, H., Topal, T. and Oter, S., (2006) *Molecular targets against mustard toxicity: Implication of cell surface receptors, peroxynitrite production, and PARP activation*. Archives of Toxicology, 80:662-70.

Kozen, B., Kircher, S., Henao, J., Godinez, F. and Johnson, A., (2007) *An alternative field hemostatic agent? comparison of a new chitosan granule dressing to existing chitosan wafer, zeolite and standard dressings, in a lethal hemorrhagic groin injury: 191*. Annals of Emergency Medicine, 50:S60-S61.

Kozen, B.G., Kircher, S.J., Henao, J., Godinez, F.S. and Johnson, A.S., (2008) *An alternative hemostatic dressing: Comparison of CELOX, HemCon, and QuikClot*. Acad Emerg Med, 15:74-81.

Krumbhaar, E.B. and Krumbhaar, H.D., (1919) *The blood and bone marrow in yellow cross gas (mustard gas) Poisoning*. The Journal of Medical Research, 40:497-508.

Kumar, O., Sugendran, K. and Vijayaraghavan, R., (2001) *Protective effect of various antioxidants on the toxicity of sulphur mustard administered to mice by inhalation or percutaneous routes*. Chemico-Biological Interactions, 134:1-12.

Kunamneni, A., Ravuri, B.D., Poluri, E., Prabhakhar, T. and Saisha, V., (2008) *Urokinase - A strong plasminogen activator*. Biotechnology and Molecular Biology Reviews, 3:58-70.

Lahiri, B.B., Bagavathiappan, S., Jayakumar, T. and Philip, J., (2012) *Medical applications of infrared thermography: A review*. Infrared Physics & Technology, In Press:.

Lahti, A., Kopola, H., Harila, A., Myllyla, R. and Hannuksela, M., (1993) *Assessment of skin erythema by eye, laser doppler flowmeter, spectroradiometer, two-channel erythema meter and minolta chroma meter*. Archives of Dermatological Research, 285:278-282.

Lampe, M.A., Burlingame, A.L., Whitney, J., Williams, M.L., Brown, B.E., Roitman, E. and Elias, P.M., (1983) *Human stratum corneum lipids: Characterization and regional variations*. Journal of Lipid Research, 24:120-130.

Laskin, J.D., Black, A.T., Jan, Y., Sinko, P.J., Heindel, N.D., Sunil, V., Heck, D.E. and Laskin, D.L., (2010) *Oxidants and antioxidants in sulfur mustard?induced injury*. Annals of the New York Academy of Sciences, 1203:92-100.

Lawley, P.D. and Brookes, P., (1968) *Cytotoxicity of alkylating agents towards sensitive and resistant strains of escherichia coli in relation to extent and mode of alkylation of cellular macromolecules and repair of alkylation lesions in deoxyribonucleic acids*. Biochemical Journal, 109:433-47.

Lawrence, J.N., (1997) *Electrical resistance and tritiated water permeability as indicators of barrier integrity of in vitro human skin*. Toxicology in Vitro, 11:241-249.

Lawrence, R.J., Smith, J.R., Boyd, B.L. and Capacio, B.R., (2008) *Improvements in the methodology of monitoring sulfur mustard exposure by gas chromatography-mass spectrometry analysis of cleaved and derivatized blood protein adducts.* Journal of Analytical Toxicology, 32:31-36.

Levin, J. and Maibach, H., (2005) *The correlation between transepidermal water loss and percutaneous absorption: An overview*. Journal of Controlled Release, 103:291-299.

Levine, S. and Saltzman, A., (1996) *Abdominal cocoon: An animal model for a complication of peritoneal dialysis*. Peritoneal Dialysis International, 16:613-616.

Levy, J.H., (2007) *Anti-inflammatory strategies and hemostatic agents: Old drugs, new ideas*. Hematology/Oncology Clinics of North America, 21:89-101.

Liederer, B.M. and Borchardt, R.T. , (2006) *Enzymes involved in the bioconversion of ester-based prodrugs*. Journal of Pharmaceutical Sciences, 95:1177-1195.

Lin, J. and Tarn, W., (2009) *RNA-binding motif protein 4 translocates to cytoplasmic granules and suppresses translation via Argonaute2 during muscle cell differentiation*. Journal of Biological Chemistry, 284:34658-34665.

Lippens, S., Denecker, G., Ovaere, P., Vandenabeele, P. and Declercq, W., (2005) *Death penalty for keratinocytes: Apoptosis versus cornification*. Cell Death and Differentiation, 12:1497-1508.

Liu, P. and Zhang, L., (2007) *Adsorption of dyes from aqueous solutions or suspensions with clay nano-adsorbents*. Separation and Purification Technology, 58:32-39.

Liu, Y., Chen, J., Shang, H., Liu, C., Wang, Y., Niu, R., Wu, J. and Wei, H., (2010) *Light microscopic, electron microscopic, and immunohistochemical comparison of bama minipig (sus scrofa domestica) and human skin*. Comparative Medicine, 60:142-148.

Lockley, D.J., Howes, D. and Williams, F.M. , (2004) *Percutaneous penetration and metabolism of 2-butoxyethanol*. Archives of Toxicology, 78:617-628.

Lockley, D.J., Howes, D. and Williams, F.M. , (2002) *Percutaneous penetration and metabolism of 2-ethoxyethanol*. Toxicology and Applied Pharmacology, 180:74-82.

Lotte, C., Rougier, A., Wilson, D. and Maibach, H.I., (1987) *In vivo relationship between transepidermal water loss and percutaneous penetration of some organic compounds in man: Effect of anatomic site.* Archives of Dermatological Research, 279:351-356.

Lu, M.F., Lee, D. and Rao, G.S., (1992) *Percutaneous absorption enhancement of leuprolide*. Pharmaceutical Research, 9:1575-1579.

Ludlum, D.B., Kent, S. and Mehta, J.R., (1986) *Formation of O^6-ethylthioethylguanine in DNA by reaction with the sulfur mustard, chloroethyl sulfide, and its apparent lack of repair by O^6-alkylguanine DNA alkyltransferase.* Carcinogenesis, 7:1203-1206.

Ludlum, D.B., Tong, W.P. and Mehta, J.R., (1984) *Formation of O^6-ethylthioethyldeoxyguanosine from the reaction of chloroethyl ethyl sulfide with deoxyguanosine.* Cancer Research, 44:5698-5701.

Luo, J. and Chen, A.F., (2005) *Nitric oxide: A newly discovered function on wound healing*. Acta Pharmacologica Sinica, 26:259-264.

Ma, X., Fang, L., Guo, J., Zhao, N. and He, Z., (2010) *Effect of counter-ions and penetration enhancers on the skin permeation of flurbiprofen*. Journal of Pharmaceutical Sciences, 99:1826-1837.

Mahdy, A.M. and Webster, N.R., (2004) *Perioperative systemic haemostatic agents*. British Journal of Anaesthesia, 93:842-58.

Mahmoudi, M., Hefazi, M., Rastin, M. and Balali-Mood, M., (2005) *Long-term hematological and immunological complications of sulfur mustard poisoning in iranian veterans.* International Immunopharmacology, 5:1479-1485.

Maibach, H.I., Feldmann, R.J., Hilby, T.H. and Serat, W.F., (1971) *Regional variation in percutaneous absorption in man.* Archives of Environmental Health, 23:208-211.

Maisonneuve, A., Callebat, I., Debordes, L. and Coppet, L., (1993) *Biological fate of sulphur mustard in rat: Toxicokinetics and disposition.* Xenobiotica, 23:771-780.

Mallett, S.V. and Cox, D.J.A., (1992) *Thrombelastography*. British Journal of Anaesthesia, 69:307-313.

Markova, N.G., Marekov, L.N., Chipev, C.C., Gan, S.Q., Idler, W.W. and Steinert, P.M., (1993) *Profilaggrin is a major epidermal calcium-binding protein*. Molecular and Cellular Biology, 13:613-625.

Marshall, E.K., (1919) *Mustard gas*. Journal of the American Medical Association, 73:684-686.

Martens, M.E. and Smith, W.J., (2008) *The role of NAD^+ depletion in the mechanism of sulfur mustard-induced metabolic injury.* Cutaneous and Ocular Toxicology, 27:41-53.

Maynard, R.L., (2007) *Mustard gas.* In. Chemical Warfare Agents: Toxicology and Treatments, T.C. Marrs, R.L. Maynard and F.R. Sidell eds., 2nd ed. Wiley-Blackwell, 375-408.

Mcadams, A.J., (1956) *A study of mustard vesication*. The Journal of Investigative Dermatology, 26:317-26.

McCarver, D.G. and Hines, R.N. , (2002) *The ontogeny of human drug-metabolizing enzymes: Phase II conjugation enzymes and regulatory mechanisms*. Journal of Pharmacology and Experimental Therapeutics, 300:361-366.

McFarland-Mancini, M.M., Funk, H.M., Paluch, A.M., Zhou, M., Giridhar, P.V., Mercer, C.A., Kozma, S.C. and Drew, A.F., (2010) *Differences in wound healing in mice with deficiency of IL-6 versus IL-6 receptor*. The Journal of Immunology, 184:7219-7228.

McGrath, J.A., Eady, R.A. and Pope, F.M., (2010) *Anatomy and organization of human skin.* In. Rook's Textbook of Dermatology, T. Burns, S. Breathnach, N. Cox and C. Griffiths eds., 8th ed. Wiley-Blackwell, .

McGrath, J.A. and Uitto, J., (2008) *The filaggrin story: Novel insights into skin-barrier function and disease*. Trends in Molecular Medicine, 14:20-27.

Meyer, W. and Neurand, K. , (1976) *The distribution of enzymes in the skin of the domestic pig*. Laboratory Animals, 10:237-247.

Michaels, A.S., Chandrasekaran, S.K. and Shaw, J.E., (1975) *Drug permeation through human skin: Theory and in vitro experimental measurement*. Journal of the American Institute of Chemical Engineers, 21:985-996.

Miller, M.A. and Kasting, G.B., (2010) *Toward a better understanding of pesticide dermal absorption: Diffusion model analysis of parathion absorption in vitro and in vivo.*. Journal of Toxicology and Environmental Health, Part A, 73:284-300.

Minsavage, G.D. and Dillman III, J.F., (2007) *Bifunctional alkylating agent-induced p53 and nonclassical nuclear factor kappaB responses and cell death are altered by caffeic acid phenethyl ester: A potential role for antioxidant/electrophilic response-element signaling.* Journal of Pharmacology and Experimental Therapeutics, 321:202-212.

Mitcheltree, L.W., Mershon, M.M., Wall, H.G., Pulliam, J.D. and Manthei, J.H., (1989) *Microblister formation in vesicant-exposed pig skin.* Journal of Toxicology - Cutaneous and Ocular Toxicology, 8:309-319.

Mol, M.A.E. and De Vries-Van de Ruit, A.-.B.C., (1992) *Concentration- and time-related effects of sulphur mustard on human epidermal keratinocyte function.* Toxicology in Vitro, 6:245-251.

Mol, M.A.E. and Smith, W.J., (1996) *Ca^{2+} homeostasis and Ca^{2+} signalling in sulphur mustard-exposed normal human epidermal keratinocytes.* Chemico-Biological Interactions, 100:85-93.

Monash, S.B.,H., (1958) *Location and reformation of the epithelial barrier to water vapor*. Archives of Dermatology, 78:710-714.

Monroe, D.M. and Hoffman, M., (2006) *What does it take to make the perfect clot?*. Arteriosclerosis, Thrombosis, and Vascular Biology, 26:41-48.

Monroe, D.M., Hoffman, M. and Roberts, H.R., (2002) *Platelets and thrombin generation*. Arteriosclerosis, Thrombosis, and Vascular Biology, 22:1381-1389.

Monteiro-Riviere, N.A., (2004) *Anatomical factors affecting barrier function.* In. Dermatotoxicology, H. Zhai and H.I. Maibach eds., 6th ed. CRC Press, 43-70.

Monteiro-Riviere, N.A., Bristol, D.G., Manning, T.O., Rogers, R.A. and Riviere, J.E., (1990) *Interspecies and interregional analysis of the comparative histologic thickness and laser doppler blood flow measurements at five cutaneous sites in nine species.* Journal of Investigative Dermatology, 95:582-586.

Monteiro-Riviere, N.A., (2005) *Structure and function of skin.* In. Dermal Absorption Models in Toxicology and Pharmacology, J.E. Riviere ed., Informa Healthcare, 1-20.

Monteiro-Riviere, N.A. and Inman, A.O., (2000) *Characterization of sulfur mustard-induced toxicity by enzyme histochemistry in porcine skin.* Toxicology Methods, 10:127-142.

Monteiro-Riviere, N.A., Inman, A.O., Babin, M.C. and Casillas, R.P., (1999) *Immunohistochemical characterization of the basement membrane epitopes in bis(2-chloroethyl) sulfide-induced toxicity in mouse ear skin.* Journal of Applied Toxicology, 19:313-328.

Moore, P.a., (1981) *Preparation of whole blood for liquid scintillation counting*. Clinical Chemistry, 27:609-11.

Mousa, S.A., Khurana, S. and Forsythe, M.S., (2000) *Comparative in vitro efficacy of different platelet glycoprotein IIb/IIIa antagonists on platelet-mediated clot strength induced by tissue factor with use of thromboelastography : Differentiation among glycoprotein IIb/IIIa antagonists*. Arteriosclerosis, Thrombosis, and Vascular Biology, 20:1162-1167.

Munro, N.B., Talmage, S.S., Griffin, G.D., Waters, L.C., Watson, A.P., King, J.F. and Hauschild, V., (1999) *The sources, fate, and toxicity of chemical warfare agent degradation products*. Environ Health Perspect, 107:.

Nagy, S.M., Golumbic, C., Stein, W.H., Fruton, J.S. and Bergmann, M., (1946) *The penetration of vesicant vapors into human skin*. The Journal of General Physiology, 29:441-469.

Najjar, S.F., Healey, N.A., Healey, C.M., McGarry, T., Khan, B., Thatte, H.S. and Khuri, S.F., (2004) *Evaluation of poly-N-acetyl glucosamine as a hemostatic agent in patients undergoing cardiac catheterization: A double-blind, randomized study*. Journal of Trauma-Injury Infection & Critical Care, 57:S38-41.

Nakai, J.S., Stathopulos, P.B., Campbell, G.L., Chu, I., Li-Muller, A. and Aucoin, R., (1999) *Penetration of chloroforn, trichloroethylene, and tetrachloroethylene through human skin*. Journal of Toxicology and Environmental Health, Part A, 58:157-170.

Nakanishi, G., Fujimoto, W. and Arata, J., (1997) *IRF-1 expression in normal human epidermal keratinocytes*. Archives of Dermatological Research, 289:415-420.

Nandakumar, V., Vaid, M. and Katiyar, S.K., (2011) *(−)-Epigallocatechin-3-gallate reactivates silenced tumor suppressor genes, Cip1/p21 and p16INK4a, by reducing DNA methylation and increasing histones acetylation in human skin cancer cells*. Carcinogenesis, 32:537-544.

Ng, S., Rouse, J., Sanderson, F., Meidan, V. and Eccleston, G., (2010) *Validation of a static franz diffusion cell system for in vitro permeation studies*. AAPS PharmSciTech, 11:1432-1441.

Niculescu, C., Ganguli-Indra, G., Pfister, V., Dupé, V., Messaddeq, N., De Arcangelis, A. and Georges-Labouesse, E., (2011) *Conditional ablation of integrin alpha-6 in mouse epidermis leads to skin fragility and inflammation*. European Journal of Cell Biology, 90:270-277.

Nielsen, V.G., Gurley, W.Q. and Burch, T.M., (2004) *The impact of factor XIII on coagulation kinetics and clot strength determined by thrombelastography*. Anesthesia & Analgesia, 99:120-123.

Nilsson, G.E., (1977) *Measurement of water exchange through skin*. Medical and Biological Engineering and Computing, 15:209-218.

Noort, D., Fidder, A., Hulst, A.G., de Jong, L.P.A. and Benschop, H.P., (2000) *Diagnosis and dosimetry of exposure to sulfur mustard: Development of a standard operating procedure for mass spectrometric analysis of haemoglobin adducts: Exploratory research on albumin and keratin adducts.* Journal of Applied Toxicology, 20:S187-S192.

Noort, D., Fidder, A., Hulst, A.G., Woolfitt, A.R., Ash, D. and Barr, J.R., (2004) *Retrospective detection of exposure to sulfur mustard: Improvements on an assay for liquid chromatography-tandem mass spectrometry analysis of albumin/sulfur mustard adducts*. Journal of Analytical Toxicology, 28:333-338.

Noort, D., Verheij, E.R., Hulst, A.G., De Jong, L.P.A. and Benschop, H.P., (1996) *Characterization of sulfur mustard induced structural modifications in human hemoglobin by liquid chromatography-tandem mass spectrometry.* Chemical Research in Toxicology, 9:781-787.

Norlen, L., Nicander, I., Lundh Rozell, B., Ollmar, S. and Forslind, B., (1999) *Inter- and intra-individual differences in human stratum corneum lipid content related to physical parameters of skin barrier function in vivo.* The Journal of Investigative Dermatology, 112:72-77.

Oda, Y., Ishikawa, M.H., Hawker, N.P., Yun, Q. and Bikle, D.D., (2007) *Differential role of two VDR coactivators, DRIP205 and SRC-3, in keratinocyte proliferation and differentiation*. The Journal of Steroid Biochemistry and Molecular Biology, 103:776-780.

Odanagi, M., Kikuchi, Y., Yamazaki, T., Kaneko, T., Nakano, H., Tamai, K., Vitto, J. and Hanada, K., (2004) *Transcriptional regulation of the 230-kDa bullous pemphigoid antigen gene expression by interferon regulatory factor 1 and interferon regulatory factor 2 in normal human epidermal keratinocytes*. Experimental Dermatology, 13:773-779.

OECD., (2004) *Test no. 428: Skin absorption in vitro methods.* In. Organisation for Economic Co-operation and Development guidelines for the testing of chemicals Section 4: Health Effects, OECD Publishing, 1-8.

Oestmann, E., Lavrijsen, A.P.M., Hermans, J. and Ponec, M., (1993) *Skin barrier function in healthy volunteers as assessed by transepidermal water loss and vascular response to hexyl nicotinate: Intra- and inter-individual variability*. British Journal of Dermatology, 128:130-136.

Olsen, A.K., Kornerup Hansen, A., Jespersen, J., Marckmann, P. and Bladbjerg, E.M., (1999) *The pig as a model in blood coagulation and fibrinolysis research*. Scandinavian Journal of Laboratory Animal Science, 26:214-224.

Ostomel, T.A., Stoimenov, P.K., Holden, P.A., Alam, H.B. and Stucky, G.D., (2006) *Host-guest composites for induced hemostasis and therapeutic healing in traumatic injuries*. Journal of Thrombosis & Thrombolysis, 22:55-67.

Pal, A., Tewari-Singh, N., Gu, M., Agarwal, C., Huang, J., Day, B.J., White, C.W. and Agarwal, R., (2009) *Sulfur mustard analog induces oxidative stress and activates signaling cascades in the skin of SKH-1 hairless mice.* Free Radical Biology and Medicine, 47:1640-1651.

Papa, S., De Rasmo, D., Scacco, S., Signorile, A., Technikova-Dobrova, Z., Palmisano, G., Sardanelli, A.M., Papa, F., Panelli, D., Scaringi, R. and Santeramo, A., (2008) *Mammalian complex I: A regulable and vulnerable pacemaker in mitochondrial respiratory function*. Biochimica Et Biophysica Acta - Bioenergetics, 1777:719-728.

Papirmeister, B., Feister, A.J., Robinson, S.I. and Ford, R.D., 1991. *Medical Defense Against Mustard Gas: Toxic Mechanisms and Pharmacological Implications.* CRC Press.

Papirmeister, B., Gross, C.L., Meier, H.L., Petrali, J.P. and Johnson, J.B., (1985) *Molecular basis for mustard-induced vesication*. Fundamental and Applied Toxicology : Official Journal of the Society of Toxicology, 5:S134-49.

Papirmeister, B., Gross, C.L., Petrali, J.P. and Hixson, C.J., (1984) *Pathology produced by sulfur mustard in human skin grafts on athymic nude mice. I. gross and light microscopic changes.* Journal of Toxicology - Cutaneous and Ocular Toxicology, 3:371-391.

Paquet, P. and Piérard, G.E., (1996) *Interleukin-6 and the skin*. International Archives of Allergy and Immunology, 109:308-317.

Paromov, V., Qui, M., Yang, H., Smith, M. and Stone, W.L., (2008) *The influence of N-acetyl-L-cysteine on oxidative stress and nitric oxide synthesis in stimulated macrophages treated with a mustard gas analogue*. BMC Cell Biology, 9:33-47.

Patwari, P., Chutkow, W.A., Cummings, K., Verstraeten, V.L.R.M., Lammerding, J., Schreiter, E.R. and Lee, R.T., (2009) *Thioredoxin-independent regulation of metabolism by the α-arrestin proteins*. Journal of Biological Chemistry, 284:24996-25003.

Pershing, L.K., Lambert, L.D., Shah, V.P. and Lam, S.Y., (1992) *Variability and correlation of chromameter and tape-stripping methods with the visual skin blanching assay in the quantitative assessment of topical 0.05% betamethasone dipropionate bioavailability in humans*. International Journal of Pharmaceutics, 86:201-210.

Petrali, J.P., Oglesby, S.B. and Hamilton, T.A., (1994) *Morphologic accounts of a human skin equivalent exposed to mustard gas.* In Vitro Toxicology: Journal of Molecular and Cellular Toxicology, 7:95-98.

Petrali, J.P., Oglesby, S.B. and Justus, T.A., (1991) *Morphologic effects of sulfur mustard on a human skin equivalent.* Journal of Toxicology - Cutaneous and Ocular Toxicology, 10:315-324.

Pham, M., Magdalou, J., Siest, G., Lenoir, M., Bernard, B.A., Jamoulle, J. and Shroot, B., (1990) *Reconstituted epidermis: A novel model for the study of drug metabolism in human epidermis*. Journal of Investigative Dermatology, 94:749-752.

Platteborze, P.L., (2003) *Effects of sulfur mustard on transcription in human epidermal keratinocytes: Analysis by mRNA differential display*. Journal of Applied Toxicology, 23:249-54.

Poet, T.S. and McDougal, J.N., (2002) *Skin absorption and human risk assessment*. Chemico-Biological Interactions, 140:19-34.

Pons, F., Calvet, J., Haag, M., Raeppel, V., Keravis, T. and Frossard, N., (2001) *Altered expression of lung cytochrome P450 3A1 in rat after exposure to sulfur mustard*. Pharmacology & Toxicology, 88:40-44.

Popp, T., Egea, V., Kehe, K., Steinritz, D., Schmidt, A., Jochum, M. and Ries, C., (2011) *Sulfur mustard induces differentiation in human primary keratinocytes: Opposite roles of p38 and ERK1/2 MAPK*. Toxicology Letters, 204:43-51.

Price, J.A., Rogers, J.V., McDougal, J.N., Shaw, M.Q., Reid, F.M. and Graham, J.S., (2009) *Transcriptional changes in porcine skin at 7 days following sulfur mustard and thermal burn injury.* Cutaneous and Ocular Toxicology, 28:129-140.

Prior, J.J., Powers, N. and DeLustro, F., (2000) *Efficacy of a novel hemostatic agent in animal models of impaired hemostasis*. Journal of Biomedical Materials Research, 53:252-7.

Pryzdial, E.L.G., Lavigne, N., Dupuis, N. and Kessler, G.E., (1999) *Plasmin converts factor X from coagulation zymogen to fibrinolysis cofactor*. Journal of Biological Chemistry, 274:8500-8505.

Pugh, W.J. and Chilcott, R.P., (2008) *Principles of diffusion and thermodynamics.* In. Principles and Practice of Skin Toxicology, R.P. Chilcott and S. Price eds., Wiley, 83-108.

Pusateri, A.E., McCarthy, S.J., Gregory, K.W., Harris, R.A., Cardenas, L., McManus, A.T. and W., G.C.,Jr, (2003a) *Effect of a chitosan-based hemostatic dressing on blood loss and survival in a model of severe venous hemorrhage and hepatic injury in swine*. Journal of Trauma-Injury Infection & Critical Care, 54:177-182.

Pusateri, A.E., Modrow, H.E., Harris, R.A., Holcomb, J.B., Hess, J.R., Mosebar, R.H., Reid, T.J., Nelson, J.H., W., G.C.,Jr, Fitzpatrick, G.M., McManus, A.T., Zolock, D.T., Sondeen, J.L., Cornum, R.L. and Martinez, R.S., (2003b) *Advanced hemostatic dressing development program: Animal model selection criteria and results of a study of nine hemostatic dressings in a model of severe large venous hemorrhage and hepatic injury in swine*. Journal of Trauma-Injury Infection & Critical Care, 55:518-526.

Qvist, M.H., Hoeck, U., Kreilgaard, B., Madsen, F. and Frokjaer, S., (2000) *Evaluation of göttingen minipig skin for transdermal in vitro permeation studies*. European Journal of Pharmaceutical Sciences, 11:59-68.

Räisänen, S.R., Lehenkari, P., Tasanen, M., Rahkila, P., Härkönen, P.L. and Väänänen, H.K., (1999) *Carbonic anhydrase III protects cells from hydrogen peroxide-induced apoptosis*. The Journal of the Federation of American Societies for Experimental Biology, 13:513-522.

Ramsey, J.D., Woollen, B.H., Auton, T.R. and Scott, R.C., (1994) *The predictive accuracy of in vitro measurements for the dermal absorption of a lipophilic penetrant (fluazifop-butyl) through rat and human skin*. Toxicological Sciences, 23:230-236.

Rappeneau, S., Baeza-Squiban, A., Marano, F. and Calvet, J.-., (2000) *Efficient protection of human bronchial epithelial cells against sulfur and nitrogen mustard cytotoxicity using drug combinations*. Toxicological Sciences, 58:153-160.

Rawlings, A.V. and Harding, C.R., (2004) *Moisturization and skin barrier function*. Dermatologic Therapy, 17:43-48.

Ray, R., Hauck, S., Kramer, R. and Benton, B., (2005) *A convenient fluorometric method to study sulfur mustard-induced apoptosis in human epidermal keratinocytes monolayer microplate culture.* Drug and Chemical Toxicology, 28:105-116.

Rebholz, B., Kehe, K., Ruzicka, T. and Rupec, R.A., (2008) *Role of NF-kappaB/RelA and MAPK pathways in keratinocytes in response to sulfur mustard.* Journal of Investigative Dermatology, 128:1626-1632.

Reddy, G., Major, M.A. and Leach, G.J., (2005) *Toxicity assessment of thiodiglycol.* International Journal of Toxicology, 24:435-442.

Reid, F.M., Graham, J., Niemuth, N.A., Singer, A.W., Janny, S.J. and Johnson, J.B., (2000) *Sulfur mustard-induced skin burns in weanling swine evaluated clinically and histopathologically*. Journal of Applied Toxicology, 160:153-160.

Reid, F.M., Graham, J., Niemuth, N.A., Singer, A.W., Janny, S.J. and Johnson, J.B., (2001) *Sulfur mustard-induced skin burns in weanling swine evaluated clinically and histopathologically.* Journal of Applied Toxicology, 21:S153-S160.

Reid, F.M., Niemuth, N.A., Shumaker, S.M., Waugh, J.D. and Graham, J.S., (2007) *Biomechanical monitoring of cutaneous sulfur mustard-induced lesions in the weanling pig model for depth of injury.* Skin Research and Technology, 13:217-225.

Reifenrath, W.G., Chellquist, E.M., Shipwash, E.A. and Jederberg, W.W., (1984) *Evaluation of animal models for predicting skin penetration in man*. Fundamental and Applied Toxicology, 4:S224-S230.

Reifenrath, W.G., Hawkins, G.S. and Kurtz, M.S., (1991) *Percutaneous penetration and skin retention of topically applied compounds: An in vitro-in vivo study*. Journal of Pharmaceutical Sciences, 80:526-532.

Renshaw, B., (1947) *Observation on the role of water in the susceptibility of human skin to injury by vesicant vapors.* Journal of Investigative Dermatology, 9:75-85.

Renshaw, B., (1946) *Mechanism in production of cutaneous injuries by sulfur and nitrogen mustards.* N. D. C. US Office of Scientific Research and Development, Chemical Warfare Agents and Related Chemical Problems478-520.

Rettie, A.E., Williams, F.M., Rawlins, M.D., Mayer, R.T. and Danny Burke, M. , (1986) *Major differences between lung, skin and liver in the microsomal metabolism of homologous series of resorufin and coumarin ethers*. Biochemical Pharmacology, 35:3495-3500.

Ricketts, K.M., Santai, C.T., France, J.A., Granziosi, A.M., Doyel, D., Gazaway, M.Y. and Casillas, R.P., (2001) *Inflammatory cytokine response in sulfur mustard-exposed mouse skin.* Journal of Applied Toxicology, 21:S73-S76.

Ring, E.F.J., (1990) *Quantitative thermal imaging*. Clinical Physics and Physiological Medicine, 11:87-95.

Rivard, G.E., Brummel, K., Mann, K.G., Fan, L., Hofer, A. and Cohen, E., (2005) *Evaluation of the profile of thrombin generation during the process of whole blood clotting as assessed by thromboelastography*. Journal of Thrombosis and Haemostasis, 3:2039.

Riviere, J.E., Brooks, J.D., Williams, P.L. and Monteiroriviere, N.A., (1995) *Toxicokinetics of topical sulfur mustard penetration, disposition, and vascular toxicity in isolated perfused porcine skin*. Toxicology and Applied Pharmacology, 135:25-34.

Roberts, H.R., Monroe, D.M. and Escobar, M.A., (2004) *Current concepts of hemostasis: Implications for therapy.* Anesthesiology, 100:722-30.

Roberts, J.J. and Warwick, G.P., (1963) *Studies of the mode of action of alkylating agents—VI the metabolism of bis-2-chloroethylsulphide (mustard gas) and related compounds*. Biochemical Pharmacology, 12:1329-1334.

Rogan, E.G., Devanesan, P.D., RamaKrishna, N.V.S., Higginbotham, S., Padmavathi, N.S., Chapman, K., Cavalieri, E.L., Jeong, H., Jankowiak, R. and Small, G.J. , (1993) *Identification and quantitation of benzo[a]pyrene-DNA adducts formed in mouse skin*. Chemical Research in Toxicology, 6:356-363.

Rogers, J.V., Choi, Y.W., Kiser, R.C., Babin, M.C., Casillas, R.P., Schlager, J.J. and Sabourin, C.L.K., (2004) *Microarray analysis of gene expression in murine skin exposed to sulfur mustard*. Journal of Biochemical and Molecular Toxicology, 18:289-99.

Roper, C.S., Howes, D., Blain, P.G. and Williams, F.M. , (1997) *Percutaneous penetration of 2-phenoxyethanol through rat and human skin*. Food and Chemical Toxicology, 35:1009-1016.

Rosenblatt, D.H., Small, M.J., Kimmell, T.A. and Anderson, A.W., (1996) *Background chemistry for chemial warfare agents and decontamination processes in support of delisting water streams at the U.S. army dugway proving ground, utah*.

Rosenthal, D.S., Simbulan-Rosenthal, C., Liu, W.F., Velena, a., Anderson, D., Benton, B., Wang, Z.Q., Smith, W., Ray, R. and Smulson, M.E., (2001) *PARP determines the mode of cell death in skin fibroblasts, but not keratinocytes, exposed to sulfur mustard*. The Journal of Investigative Dermatology, 117:1566-73.

Rosenthal, D.S., Simbulan-Rosenthal, C.M.G., Iyer, S., Spoonde, A., Smith, W., Ray, R. and Smulson, M.E., (1998) *Sulfur mustard induces markers of terminal differentiation and apoptosis in keratinocytes via a Ca^{2+}-calmodulin and caspase-dependent pathway.* Journal of Investigative Dermatology, 111:64-71.

Rosenthal, D.S., Velena, A., Chou, F.-., Schlegel, R., Ray, R., Bentont, B., Anderson, D., Smith, W.J. and Simbulan-Rosenthal, C.M., (2003) *Expression of dominant-negative fas-associated death domain blocks human keratinocyte apoptosis and vesication induced by sulfur mustard.* Journal of Biological Chemistry, 278:8531-8540.

Roskos, K.V., Maibach, H.I. and Guy, R.H., (1989) *The effect of aging on percutaneous absorption in man.* Journal of Pharmacokinetics and Biopharmaceutics, 17:617-630.

Rounds, S., Likar, L.L., Harrington, E.O., Kim, K.C., Smeglin, A., Heins, K. and Parks, N., (1999) *Nucleotide-induced PMN adhesion to cultured epithelial cells: Possible role of MUC1 mucin*. American Journal of Physiology - Lung Cellular and Molecular Physiology, 277:L874-L880.

Royo, T., Vidal, M. and Badimon, L., (1998) *Porcine platelet von willebrand antigen II (vW AgII): Inhibitory effect on collagen-induced aggregation and comparative distribution with human platelets.* Thrombosis and Haemostasis, 80:677-685.

Rubio, L., Alonso, C., López, O., Rodríguez, G., Coderch, L., Notario, J., de la Maza, A. and Parra, J.L., (2011) *Barrier function of intact and impaired skin: Percutaneous penetration of caffeine and salicylic acid*. International Journal of Dermatology, 50:881-889.

Ruff, A.L. and Dillman III, J.F., (2007) *Signaling molecules in sulfur mustard-induced cutaneous injury*. Eplasty, 8:e2.

Ruminski, J., Kaczmarek, M., Renkielska, A. and Nowakowski, A., (2007) *Thermal parametric imaging in the evaluation of skin burn depth*. Biomedical Engineering, IEEE Transactions on, 54:303-312.

Ryatt, K.S., Mobayen, M., Stevenson, J.M., Maibach, H.I. and Guy, R.H., (1988) *Methodology to measure the transient effect of occlusion on skin penetration and stratum corneum hydration in vivo*. British Journal of Dermatology, 119:307-312.

Sabourin, C.L.K., Rogers, J.V., Choi, Y.W., Kiser, R.C., Casillas, R.P., Babin, M.C. and Schlager, J.J., (2004) *Time- and dose-dependent analysis of gene expression using microarrays in sulfur mustard-exposed mice.* Journal of Biochemical and Molecular Toxicology, 18:300-312.

Sabourin, C.L.K., Danne, M.M., Buxton, K.L., Casillas, R.P. and Schlager, J.J., (2002) *Cytokine, chemokine, and matrix metalloproteinase response after sulfur mustard injury to weanling pig skin*. Journal of Biochemical and Molecular Toxicology, 16:263-272.

Sabourin, C.L.K., Petrali, J.P. and Casillas, R.P., (2000) *Alterations in inflammatory cytokine gene expression in sulfur mustard-exposed mouse skin*. Journal of Biochemical and Molecular Toxicology, 14:291-302.

Sakula, A., (1961) *Pneumoconiosis due to fuller's earth*. Thorax, 16:176-179.

Sambasivan, C.N., Cho, S.D., Zink, K.A., Differding, J.A. and Schreiber, M.A., (2009) *A highly porous silica and chitosan-based hemostatic dressing is superior in controlling hemorrhage in a severe groin injury model in swine*. The American Journal of Surgery, 197:576-580.

Sawyer, T.W. and Hamilton, M.G., (2000) *Effect of intracellular calcium modulation on sulfur mustard cytotoxicity in cultured human neonatal keratinocytes*. Toxicology in Vitro, 14:5-9.

Sawyer, T.W., Lundy, P.M. and Weiss, M.T., (1996) *Protective effect of an inhibitor of nitric oxide synthase on sulphur mustard toxicity in vitro.* Toxicology and Applied Pharmacology, 141:138-144.

Sayer, N.M., Whiting, R., Green, a.C., Anderson, K., Jenner, J. and Lindsay, C.D., (2010) *Direct binding of sulfur mustard and chloroethyl ethyl sulphide to human cell membrane-associated proteins; implications for sulfur mustard pathology*. Journal of

Chromatography.B, Analytical Technologies in the Biomedical and Life Sciences, 878:1426-32.

Schaefer, H. and Redelmeier, T.E., (1996) In. Skin Barrier: Principles of Percutaneous Absorption, Karger, .

Schaefer, H., Redelmeier, T.E. and Lademann, J., (2011) *Skin penetration.* In. Contact Dermatitis, J.D. Johansen, P.J. Frosch and J. Lepoittevin eds., Springer Berlin Heidelberg, 215-227.

Scheuplein, R.J. and Blank, I.H., (1971) *Permeability of the skin*. Physiological Reviews, 51:702-747.

Scheuplein, R., (1967) *Mechanism of percutaneous absorption. II. transient diffusion and the relative importance of various routes of skin penetration*. The Journal of Investigative Dermatology, 48:79-88.

Schiffer, R., Neis, M., Holler, D., Rodriguez, F., Geier, A., Gartung, C., Lammert, F., Dreuw, A., Zwadlo-Klarwasser, G., Merk, H., Jugert, F. and M Baron, ‚Jens, (2003) *Active influx transport is mediated by members of the organic anion transporting polypeptide family in human epidermal keratinocytes*. J Investig Dermatol, 120:285-291.

Schmook, F.P., Meingassner, J.G. and Billich, A., (2001) *Comparison of human skin or epidermis models with human and animal skin in in-vitro percutaneous absorption*. International Journal of Pharmaceutics, 215:51-56.

Schunck, M., Neumann, C. and Proksch, E., (2005) *Artificial barrier repair in wounds by semi-occlusive foils reduced wound contraction and enhanced cell migration and reepithelization in mouse skin*. J Investig Dermatol, 125:1063-1071.

Schwentker, A., Vodovotz, Y., Weller, R. and Billiar, T.R., (2002) *Nitric oxide and wound repair: Role of cytokines?*. Nitric Oxide, 7:1-10.

Scott, R.C. and Ramsey, J.D., (1987) *Comparison of the in vivo and in vitro percutaneous absorption of a lipophilic molecule (cypermethrin, a pyrethroid insecticide)*. Nature, 89:142-146.

Shakarjian, M.P., Bhatt, P., Gordon, M.K., Chang, Y.-., Casbohm, S.L., Rudge, T.L., Kiser, R.C., Sabourin, C.L., Casillas, R.P., Ohman-Strickland, P., Riley, D.J. and Gerecke, D.R., (2006) *Preferential expression of matrix metalloproteinase-9 in mouse skin after sulfur mustard exposure.* Journal of Applied Toxicology, 26:239-246.

Shakarjian, M.P., Heck, D.E., Gray, J.P., Sinko, P.J., Gordon, M.K., Casillas, R.P., Heindel, N.D., Gerecke, D.R., Laskin, D.L. and Laskin, J.D., (2010) *Mechanisms mediating the vesicant actions of sulfur mustard after cutaneous exposure*. Toxicological Sciences, 114:5-19.

Shen, D.D., (2008) *Toxicokinetics.* In. Casarett & Doull's Toxicology: The Basic Science of Poisons, C.D. Klaassen ed., 7th ed. McGraw-Hill Medical, 305-327.

Sidell, F.R., Urbanetti, J.S. and Smith, W.J., (1997) *Vesicants.* In. Medical Aspects of Chemical and Biological Warfare, F.R. Sidell, E.T. Takafuji and D.R. Franz eds., Office of The Surgeon General at TMM Publications, 197-228.

Sierra, D.H., (1993) *Fibrin sealant adhesive systems: A review of their chemistry, material properties and clinical applications*. Journal of Biomaterials Applications, 7:309-52.

Sies, H., (1997) *Oxidative stress: Oxidants and antioxidants*. Experimental Physiology, 82:291-295.

Sies, H., (1993) *Strategies of antioxidant defense*. European Journal of Biochemistry, 215:213-219.

Siller-Matula, J.M., Plasenzotti, R., Spiel, A., Quehenberger, P. and Jilma, B., (2008) *Interspecies differences in coagulation profile*. Thrombosis and Haemostasis, 100:397-404.

Simbulan-Rosenthal, C., Rosenthal, D.S., Iyer, S., Boulares, H. and Smulson, M.E., (1999) *Involvement of PARP and poly(ADP-ribosyl)ation in the early stages of apoptosis and DNA replication*. Molecular and Cellular Biochemistry, 193:137-48.

Simbulan-Rosenthal, C., Ray, R., Benton, B., Soeda, E., Daher, A., Anderson, D., Smith, W.J. and Rosenthal, D.S., (2006) *Calmodulin mediates sulfur mustard toxicity in human keratinocytes*. Toxicology, 227:21-35.

Simon, G.A. and Maibach, H.I., (2000) *The pig as an experimental animal model of percutaneous permeation in man: Qualitative and quantitative observations – an overview.* Skin Pharmacology and Applied Skin Physiology, 13:229-234.

Singh, P.K. and Hollingsworth, M.A., (2006) *Cell surface-associated mucins in signal transduction*. Trends in Cell Biology, 16:467-476.

Smith, G., Wolf, C.R., Deeni, Y.Y., Dawe, R.S., Evans, A.T., Comrie, M.M., Ferguson, J. and Ibbotson, S.H. , (2003) *Cutaneous expression of cytochrome P450 CYP2S1: Individuality in regulation by therapeutic agents for psoriasis and other skin diseases*. The Lancet, 361:1336-1343.

Smith, K.J., Smith, W.J., Hamilton, T., Skelton, H.G., Graham, J.S., Okerberg, C., Moeller, R. and Hackley, B.E., (1998) *Histopathologic and immunohistochemical features in human skin after exposure to nitrogen and sulfur mustard*. American Journal of Dermatopathology, 20:22-28.

Smith, K.J., (1999) *The prevention and treatment of cutaneous injury secondary to chemical warfare agents: Application of these finding to other dermatologic conditions and wound healing.* Dermatologic Clinics, 17:41-60.

Smith, K.J., Casillas, R., Graham, J., Skelton, H.G., Stemler, F., Jr., H. and B.E, (1997) *Histopathologic features seen with different animal models following cutaneous sulfur mustard exposure*. Journal of Dermatological Science, 14:126-135.

Sourdeval, M., Lemaire, C., Deniaud, A., Taysse, L., Daulon, S., Breton, P., Brenner, C., Boisvieux-Ulrich, E. and Marano, F., (2006) *Inhibition of caspase-dependent mitochondrial permeability transition protects airway epithelial cells against mustard-induced apoptosis*. Apoptosis : An International Journal on Programmed Cell Death, 11:1545-59.

Southwell, D., Barry, B.W. and Woodford, R., (1984) *Variations in permeability of human skin within and between specimens*. International Journal of Pharmaceutics, 18:299-309.

Spencer, T.E., Jenster, G., Burcin, M.M., Allis, C.D., Zhou, J., Mizzen, C.A., McKenna, N.J., Onate, S.A., Tsai, S.Y., Tsai, M. and O'Malley, B.W., (1997) *Steroid receptor coactivator-1 is a histone acetyltransferase*. Nature, 389:194-198.

Spoo, J.W., Monteiro-Riviere, N.A. and Riviere, J.E., (1995) *Detection of sulfur mustard bis (2-chloroethyl) sulfide and metabolites after topical application in the isolated perfused porcine skin flap.* Life Sciences, 56:1385-1394.

Spratt, D.E., Taiakina, V., Palmer, M. and Guillemette, J.G., (2007) *Differential binding of calmodulin domains to constitutive and inducible nitric oxide synthase enzymesâ€ .* Biochemistry, 46:8288-8300.

Squadrito, G.L. and Pryor, W.A., (1998) *Oxidative chemistry of nitric oxide: The roles of superoxide, peroxynitrite, and carbon dioxide.* Free Radical Biology and Medicine, 25:392-403.

Steinritz, D., Elischer, A., Balszuweit, F., Gonder, S., Heinrich, A., Bloch, W., Thiermann, H. and Kehe, K., (2009) *Sulphur mustard induces time- and concentration-dependent regulation of NO-synthesizing enzymes.* Toxicology Letters, 188:263-269.

Steinritz, D., Emmler, J., Hintz, M., Worek, F., Kreppel, H., Szinicz, L. and Kehe, K., (2007) *Apoptosis in sulfur mustard treated A549 cell cultures.* Life Sciences, 80:2199-2201.

Steinsträsser, I. and Merkle, H.P. , (1995) *Dermal metabolism of topically applied drugs: Pathways and models reconsidered*. Pharmaceutica Acta Helvetiae, 70:3-24.

Stoll, S.W., Johnson, J.L., Bhasin, A., Johnston, A., Gudjonsson, J.E., Rittie, L. and Elder, J.T., (2009) *Metalloproteinase-mediated, context-dependent function of amphiregulin and HB-EGF in human keratinocytes and skin*. The Journal of Investigative Dermatology, 130:295-304.

Sugawara, T., Gallucci, R.M., Simeonova, P.P. and Luster, M.I., (2001) *Regulation and role of interleukin 6 in wounded human epithelial keratinocytes.* Cytokine, 15:328-336.

Sun, J., Wang, Y.X. and Sun, M.J., (1999) *Apoptosis and necrosis induced by sulfur mustard in HeLa cells.* Acta Pharmacologica Sinica, 20:445-448.

Szinicz, L., Worek, F., Thiermann, H., Kehe, K., Eckert, S. and Eyer, P., (2007) *Development of antidotes: Problems and strategies.* Toxicology, 233:23-30.

Tamura, T., Ishihara, M., Lamphier, M.S., Tanaka, N., Oishi, I., Aizawa, S., Matsuyama, T., Mak, T.W., Taki, S. and Taniguchi, T., (1995) *An IRF-1-dependent pathway of DNA damage-induced apoptosis in mitogen-activated T lymphocytes*. Nature, 376:596-599.

Taysse, L., Daulon, S., Delamanche, S., Bellier, B. and Breton, P., (2007) *Skin decontamination of mustards and organophosphates: Comparative efficiency of RSDL and fuller's earth in domestic swine.* Human and Experimental Toxicology, 26:135-141.

Taysse, L., Dorandeu, F., Daulon, S., Foquin, A., Perrier, N., Lallement, G. and Breton, P., (2011) *Cutaneous challenge with chemical warfare agents in the SKH-1 hairless mouse (II): Effects of some currently used skin decontaminants (RSDL and Fuller's earth) against liquid sulphur mustard and VX exposure*. Human & Experimental Toxicology, 30:491-498.

Testa, B., (1995) *Reductions catalyzed by cytochrome P450 and other oxidoreductases.* In. The Metabolism of Drugs and Other Xenobiotics, Biochemistry of Redox Reactions, B. Testa and J. Caldwell eds., Academic Press, 434-437.

Thorps, D., (1963) *Fuller's earth as a decontamination powder*. Porton Technical Paper 866, Ministry of Supply.

Tripathi, D., Sugendran, K., Malhotra, R., Bhattacharya, A. and Das Gupta, S., (1995) *Studies on urine and tissues of rats, guineapigs and mice exposed to sulphur mustard using mass spectrometry*. Journal of Biosciences, 20:29-33.

Tuthill, D.D., Bayer, V., Gallagher, A.M., Drohan, W.N. and MacPhee, M.J., (2001) *Assessment of topical hemostats in a renal hemorrhage model in heparinized rats*. Journal of Surgical Research, 95:126-132.

Twizell, E.H. and Kubota, K., (1994) *Lag time in the dual sorption model for percutaneous absorption with finite skin-receptor boundary clearance*. Mathematical Biosciences, 123:1-23.

Vallet, V., Cruz, C., Josse, D., Bazire, A., Lallement, G. and Boudry, I., (2007) *In vitro percutaneous penetration of organophosphorus compounds using full-thickness and split-thickness pig and human skin*. Toxicology in Vitro, 21:1182-1190.

Vallet, V., Poyot, T., Cléry-Barraud, C., Coulon, D., Sentenac, C., Peinnequin, A. and Boudry, I., (2012) *Acute and long-term transcriptional responses in sulfur mustard-exposed SKH-1 hairless mouse skin*. Cutaneous and Ocular Toxicology, 31:38-47.

Van de Sandt, J.J.M., van Burgsteden, J.A., Cage, S., Carmichael, P.L., Dick, I., Kenyon, S., Korinth, G., Larese, F., Limasset, J.C., Maas, W.J.M., Montomoli, L., Nielsen, J.B., Payan, J.-., Robinson, E., Sartorelli, P., Schaller, K.H., Wilkinson, S.C. and Williams, F.M., (2004) *In vitro predictions of skin absorption of caffeine, testosterone, and benzoic acid: A multi-centre comparison study*. Regulatory Toxicology and Pharmacology, 39:271-281.

Van de Sandt, J.J.M., Meuling, W.J.A., Elliott, G.R., Cnubben, N.H.P. and Hakkert, B.C., (2000) *Comparative in Vitro–in vivo percutaneous absorption of the pesticide propoxur*. Toxicological Sciences, 58:15-22.

Van den Bossche, J., Laoui, D., Morias, Y., Movahedi, K., Raes, G., De Baetselier, P. and Van Ginderachter, J.A., (2012) *Claudin-1, claudin-2 and claudin-11 genes differentially associate with distinct types of anti-inflammatory macrophages in vitro and with parasite- and tumor-elicited macrophages in vivo*. Scandinavian Journal of Immunology, In Press:.

Varley, C.L., Bacon, E.J., Holder, J.C. and Southgate, J., (2008) *FOXA1 and IRF-1 intermediary transcriptional regulators of PPAR gamma-induced urothelial cytodifferentiation*. Cell Death and Differentiation, 16:103-114.

Vasquez, Y., Williams, C.H. and Hardaway, R.M., (1998) *Effect of urokinase on disseminated intravascular coagulation*. Journal of Applied Physiology, 85:1421-1428.

Velik-Salchner, C., Schnürer, C., Fries, D., Müssigang, P.R., Moser, P.L., Streif, W., Kolbitsch, C. and Lorenz, I.H., (2006) *Normal values for thrombelastography (ROTEM®) and selected coagulation parameters in porcine blood*. Thrombosis Research, 117:597-602.

Virag, L., Szabo, E., Bakondi, E., Bai, P., Gergely, P., Hunyadi, J. and Szabo, C., (2002) *Nitric oxide-peroxynitrite-poly(ADP-ribose) polymerase pathway in the skin*. Experimental Dermatology, 11:189-202.

Wakita, H. and Takigawa, M., (1999) *Activation of epidermal growth factor receptor promotes late terminal differentiation of cell-matrix interaction-disrupted keratinocytes*. Journal of Biological Chemistry, 274:37285-37291.

Walters, T.J., Kauvar, D.S., Reeder, J. and Baer, D.G., (2007) *Effect of reactive skin decontamination lotion on skin wound healing in laboratory rats.* Military Medicine, 172:318-321.

Wang, Y., Barbacioru, C., Hyland, F., Xiao, W., Hunkapiller, K.L., Blake, J., Chan, F., Gonzalez, C., Zhang, L. and Samaha, R.R., (2006) *Large scale real-time PCR validation on gene expression measurements from two commercial long-oligonucleotide microarrays*. BMC Genomics, 7:59-75.

Ward, K.R., Tiba, M.H., Holbert, W.H., Blocher, C.R., Draucker, G.T., Proffitt, E.K., Bowlin, G.L., Ivatury, R.R. and Diegelmann, R.F., (2007) *Comparison of a new hemostatic agent to current combat hemostatic agents in a swine model of lethal extremity arterial hemorrhage*. Journal of Trauma-Injury Infection & Critical Care, 63:276-284.

Waring, M.J., Monger, L., Hollingsbee, D.A., Martin, G.P. and Marriott, C., (1993) *Assessment of corticosteroid-induced skin blanching: Evaluation of the minolta chromameter CR200*. International Journal of Pharmaceutics, 94:211-222.

Warner, R.R., Stone, K.J. and Boissy, Y.L., (2003) *Hydration disrupts human stratum corneum ultrastructure*. J Investig Dermatol, 120:275-284.

Wattana, M. and Bey, T., (2009) *Mustard gas or sulfur mustard: An old chemical agent as a new terrorist threat*. Prehospital and Disaster Medicine, 24:19-31.

Watts, M.E., Arnold, S. and Chaplin, D.J., (1996) *Changes in coagulation and permeability properties of human endothelial cells in vitro induced by TNF-alpha or 5,6 MeXAA*. Br J Cancer, 27:S164-S167.

Weatherall, I.L. and Coombs, B.D., (1992) *Skin color measurements in terms of CIELAB color space values*. Journal of Investigative Dermatology, 99:468-473.

Wertz, P.W., (2004) *Percutaneous absorption: Role of lipids.* In. Dermatotoxicology, H. Zhai and H.I. Maibach eds., 6th ed. CRC Press, 71-82.

Wester, R.C. and Maibach, H.I., (2001) *In vivo methods for percutaneous absorption measurements.* Journal of Toxicology: Cutaneous and Ocular Toxicology, 20:411-422.

Wester, R.C. and Maibach, H.I., (1993) *Animal models for percutaneous absorption.* In. Topical Drug Bioavailability, Bioequivalence and Penetration, V.P. Shah and H.I. Maibach eds., 1st ed. Springer, 333-349.

Wester, R.C., Christoffel, J., Hartway, T., Poblete, N., Maibach, H.I. and Forsell, J., (1998) *Human cadaver skin viability for in vitro percutaneous absorption: Storage and detrimental effects of heat-separation and freezing*. Pharmaceutical Research, 15:82-84.

Wester, R.C. and Maibach, H.I., (1992) *Percutaneous absorption of drugs*. Clinical Pharmacokinetics, 23:253-266.

Wheeler, G., (1962) *Studies related to the mechanisms of action of cytotoxic alkylating agents : A review*. Cancer Research, 22:651-688.

Whitfield, J.F., Bird, R.P., Chakravarthy, B.R., Isaacs, R.J. and Morley, P., (1995) *Calcium-cell cycle regulator, differentiator, killer, chemopreventor, and maybe, tumor promoter.* J Cell Biochem Suppl, 22:74-91.

Wilkinson, S., Maas, W., Nielsen, J., Greaves, L., van de Sandt, J. and Williams, F., (2006) *Interactions of skin thickness and physicochemical properties of test compounds in percutaneous penetration studies*. International Archives of Occupational and Environmental Health, 79:405-413.

Williams, A.C. and Barry, B.W., (2004) *Penetration enhancers*. Advanced Drug Delivery Reviews, 56:603-618.

Williams, F.M., (2006) *In vitro studies – how good are they at replacing in vivo studies for measurement of skin absorption.* Environmental Toxicology and Pharmacology, 21:199-203.

Williams, G.D., Bratton, S.L., Riley, E.C. and Ramamoorthy, C., (1999) *Coagulation tests during cardiopulmonary bypass correlate with blood loss in children undergoing cardiac surgery*. Journal of Cardiothoracic and Vascular Anesthesia, 13:398-404.

Williams, P.L., Carver, M.P. and Riviere, J.E. , (1990) *A physiologically relevant pharmacokinetic model of xenobiotic percutaneous absorption utilizing the isolated perfused porcine skin flap*. Journal of Pharmaceutical Sciences, 79:305-311.

Wormser, U., Brodsky, B. and Sintov, A., (2002) *Skin toxicokinetics of mustard gas in the guinea pig: Effect of hypochlorite and safety aspects.* Archives of Toxicology, 76:517-522.

Wormser, U., Langenbach, R., Peddada, S., Sintov, A., Brodsky, B. and Nyska, A., (2004) *Reduced sulfur mustard-induced skin toxicity in cyclooxygenase-2 knockout and celecoxib-treated mice.* Toxicology and Applied Pharmacology, 200:40-47.

Yang, X. and Seto, E., (2007) *HATs and HDACs: From structure, function and regulation to novel strategies for therapy and prevention*. Oncogene, 26:5310-5318.

Yang, Z., Philips, J.D., Doty, R.T., Giraudi, P., Ostrow, J.D., Tiribelli, C., Smith, A. and Abkowitz, J.L., (2010) *Kinetics and specificity of feline leukemia virus subgroup C receptor (FLVCR) export function and its dependence on hemopexin*. Journal of Biological Chemistry, 285:28874-28882.

Yaraee, R., Ghazanfari, T., Ebtekar, M., Ardestani, S.K., Rezaei, A., Kariminia, A., Faghihzadeh, S., Mostafaie, A., Vaez-Mahdavi, M.R., Mahmoudi, M., Naghizadeh, M.M., Soroush, M.R. and Hassan, Z.M., (2009) *Alterations in serum levels of inflammatory cytokines (TNF, IL-1alpha, IL-1beta and IL-1Ra) 20 years after sulfur mustard exposure: Sardasht-iran cohort study.* International Immunopharmacology, 9:1466-1470.

Ye, J., Esmon, N.L., Esmon, C.T. and Johnson, A.E., (1991) *The active site of thrombin is altered upon binding to thrombomodulin. two distinct structural changes are detected by fluorescence, but only one correlates with protein C activation.* Journal of Biological Chemistry, 266:23016-23021.

Yourick, J.J. and Bronaugh, R.L. , (2000) *Percutaneous penetration and metabolism of 2-nitro-p-phenylenediamine in human and fuzzy rat skin*. Toxicology and Applied Pharmacology, 166:13-23.

Yu, Q., Zhou, B., Zhang, Y., Nguyen, E.T., Du, J., Glosson, N.L. and Kaplan, M.H., (2012) *DNA methyltransferase 3a limits the expression of interleukin-13 in T helper 2 cells and allergic airway inflammation*. Proceedings of the National Academy of Sciences, 109:541-546.

Zhai, H. and Maibach, H.I., (2002) *Occlusion vs. skin barrier function*. Skin Research and Technology, 8:1-6.

Zhang, B.Z. and Wu, Y., (1987) *Toxicokinetics of sulfur mustard*. Chinese Journal of Pharmacology and Toxicology, 1:188-194.

Zhang, Z., Peters, B.P. and Monteiro-Riviere, N., (1995a) *Assessment of sulfur mustard interaction with basement membrane components*. Cell Biology and Toxicology, 11:89-101.

Zhang, Z., Riviere, J.E. and Monteiro-Riviere, N.A., (1995b) *Topical sulfur mustard induces changes in prostaglandins and interleukin-1alpha in isolated perfused porcine skin.* In Vitro Toxicology: Journal of Molecular and Cellular Toxicology, 8:149-158.

Zhou, R., Tardivel, A., Thorens, B., Choi, I. and Tschopp, J., (2010) *Thioredoxin-interacting protein links oxidative stress to inflammasome activation*. Nature Immunology, 11:136-140.

Zhu, Z., Hotchkiss, S.A., Boobis, A.R. and Edwards, R.J. , (2002) *Expression of P450 enzymes in rat whole skin and cultured epidermal keratinocytes*. Biochemical and Biophysical Research Communications, 297:65-70.

Chapter 9

Appendix 1

Sample ID	Nanodrop		Bioanalyser
	RNA concentration (ng μl^{-1})	A_{260}/A_{280} ratio	RIN value
3 control	396.3	2.06	7.8
4 control	278.46	2.03	8.9
5 control	469.05	2.01	7.4
6 control	576.14	2.08	8.1
7 control	327.82	2.01	7.5
8 control	163.66	2.07	7.0
9 control	277.32	2.04	8.1
10 control	218.16	2.04	7.7
11 control	431.44	2.05	7.5
12 control	535.25	2.11	7.7
13 control	342.67	2.07	7.2
14 control	295.84	2.04	7.7
3 damaged	392.53	2.03	8.4
4 damaged	199.96	2.05	9.1
5 damaged	343.01	2.06	9.1
6 damaged	614.73	2.11	8.2
7 damaged	124.44	2.00	7.3
8 damaged	231.1	2.08	7.9
9 WS	272.84	2.07	8.2
10 WS	181.26	2.03	8.1
11 WS	518.7	2.07	7.6
12 WS	204.91	2.08	8.0
13 WS	240.32	2.09	8.1
14 WS	228.48	2.05	8.1
3 SM	371.82	2.07	8.7
4 SM	299.09	2.04	7.6
5 SM	427.92	2.03	6.6
6 SM	458.57	2.01	7.3
7 SM	224.37	2.02	7.4
8 SM	144.2	2.07	6.2
9 SM + WS	221.14	1.89	8.2
10 SM + WS	164.58	2.03	7.1
11 SM + WS	164.62	2.08	9.1
12 SM + WS	266.71	2.08	8.3
13 SM + WS	328.66	2.05	7.5
14 SM + WS	179.36	2.08	7.2

Table 1: Final RNA concentration, purity and integrity measurements for skin samples. *Skin samples included: untreated (control) skin, unexposed damaged skin without (damaged) and with WoundStat™ (WS) treatment, and exposed damaged skin without (SM) and with WoundStat™ (SM + WS) treatment.*

Probe ID	p-value	F/C	Gene name	GenBank accession number
A_72_P399653	0.006	7.6	(PADT) Sus scrofa cDNA 3', mRNA sequence	EB416880
A_72_P472742	0.01	6.6	S-antigen; retina and pineal gland (arrestin)	NM_214079
A_72_P489515	0.01	6.6	methionine adenosyltransferase I, alpha	NM_001243187
A_72_P790675	0.0004	6.6	Sus scrofa kinesin-like protein KIF13A-like	XM_003128197
A_72_P575039	0.003	6.4	CLASP1 protein	XM_001924533
A_72_P706062	0.004	6.3	myeloid-associated differentiation marker-like	XM_003482234
A_72_P490425	0.0007	5.7	heat shock 70kDa protein 12A	XM_001925611
A_72_P472030	0.0005	5.3	Uncharacterized protein	XM_003133566
A_72_P474549	0.04	4.8	Uncharacterized protein	XM_003125683
A_72_P444501	0.01	4.5	dual oxidase 2	NM_213999
A_72_P535979	0.04	4.5	armadillo repeat gene deleted in velocardiofacial syndrome	XM_001929642
A_72_P472260	0.04	4.4	Uncharacterized protein	AK351203
A_72_P441773	0.002	4.4	uroplakin 2	NM_214012
A_72_P634826	0.0003	4.4	RNA binding motif protein 19	XM_001928156
A_72_P178456	0.0007	4.2	Fc fragment of IgA, receptor for	NM_001123112
A_72_P466051	0.003	4.2	Uncharacterized protein	XM_003135157
A_72_P777866	0.003	4.1	Sus scrofa mRNA, clone: PTG010087E10, expressed in pituitary gland.	AK349501
A_72_P597688	0.006	4.0	E1A binding protein p300	XM_001929213
A_72_P441997	0.008	3.9	adrenergic, alpha-1D-, receptor	NM_001123073
A_72_P658293	0.04	3.9	chromogranin B (secretogranin 1)	NM_214081
A_72_P477007	0.04	3.6	RAB44, member RAS oncogene family	XM_001927576
A_72_P491077	0.004	3.6	uncharacterized protein C6orf211 homolog	NM_001243637

A_72_P156111	0.002	3.5	PDZ domain containing 3	XM_003129933
A_72_P373153	0.01	3.5	nitric oxide synthase 2, inducible	NM_001143690
A_72_P444592	0.03	3.5	Uncharacterized protein	XM_003122137
A_72_P444993	0.006	3.5	mucin 13, cell surface associated	NM_001105293
A_72_P450318	0.03	3.5	transcription factor GATA-5-like	XM_001924182
A_72_P562834	0.03	3.4	progesterone receptor membrane component 2	NM_001097521
A_72_P534494	0.004	3.4	immunoglobulin superfamily, member 1	AK349537
A_72_P366808	0.004	3.4	potassium voltage-gated channel subfamily C member 4-like	XM_003125860
A_72_P705052	0.03	3.3	sorting nexin 1	XM_001928499
A_72_P564459	0.02	3.2	outer dense fibre protein 2-like	EW159310
A_72_P443218	0.002	3.2	prostaglandin-endoperoxide synthase 2 (prostaglandin G/H synthase and cyclooxygenase)	NM_214321
A_72_P505875	0.008	3.1	fragile X mental retardation syndrome-related protein 1-like	XM_003132553
A_72_P477641	0.04	3.1	myeloid-associated differentiation marker-like	XM_001925007
A_72_P242552	0.0003	3.1	NADH dehydrogenase (ubiquinone) 1 beta subcomplex, 8, 19kDa	AK236557
A_72_P455180	0.009	3.1	Uncharacterized protein	DB791121
A_72_P350373	0.04	3.0	vav 2 guanine nucleotide exchange factor	XM_001927141
A_72_P434779	0.004	2.9	RIMS binding protein 3	XM_001926953
A_72_P479603	0.03	2.9	Uncharacterized protein	XM_003128783
A_72_P569539	0.009	2.9	albumin	NM_001005208
A_72_P105036	0.004	2.9	PR domain containing 10	AK239583
A_72_P443879	0.01	2.7	progestin and adipoQ receptor family member VIII	NM_213740
A_72_P649894	0.0003	2.7	adenosine monophosphate deaminase 1	NM_001123076
A_72_P704643	0.01	2.7	Sus scrofa tenascin-like	XM_001926573

A_72_P444567	0.0004	2.7	pregnancy-associated plasma protein-A	XM_001926753
A_72_P493687	0.0004	2.6	Uncharacterized protein	XM_003121740
A_72_P105546	0.01	2.6	Src-like-adaptor 2	AK236978
A_72_P440716	0.0005	2.6	retrotransposon-like 1	NM_001134358
A_72_P444674	0.01	2.6	gastrin	NM_001004036
A_72_P679769	0.004	2.5	pancreatic lipase-related protein 1	NM_001142897
A_72_P547186	0.01	2.5	Uncharacterized protein	AK232259
A_72_P162486	0.02	2.5	steroid sulfatase (microsomal), isozyme S	DN129273
A_72_P413548	<0.0001	2.5	sarcalumenin-like	AF128841
A_72_P150631	0.003	2.5	CHD3-like protein	EU780792
A_72_P499554	0.0003	2.4	heterogeneous nuclear ribonucleoprotein F	XM_003133036
A_72_P476531	0.04	2.3	Uncharacterized protein	XM_001929101
A_72_P034771	0.02	2.3	MARC 2PIG Sus scrofa cDNA 5', mRNA sequence	BF190050
A_72_P653771	0.002	2.3	multicatalytic proteinase subunit K	AY610111
A_72_P440506	0.0002	2.3	hepatocyte nuclear factor 4, alpha	NM_001044571
A_72_P107346	0.007	2.2	WD repeat domain 46	AK348376
A_72_P490065	0.008	2.2	cytochrome P450 2C33	NM_214414
A_72_P250907	0.0009	2.2	Sus scrofa obscurin, cytoskeletal calmodulin and titin-interacting RhoGEF	XM_003123629
A_72_P475097	<0.0001	2.2	tumour necrosis factor, alpha-induced protein 8-like 2	NM_001204370
A_72_P233892	<0.0001	2.2	annexin A9	NM_001243348
A_72_P472516	0.002	2.2	Uncharacterized protein	XM_001926448
A_72_P515198	0.004	2.1	carnitine palmitoyltransferase 1B (muscle)	NM_001007191
A_72_P166401	0.03	2.0	MARC 2PIG Sus scrofa cDNA 5', mRNA sequence	BI360438

A_72_P620564	0.02	2.0	creatine kinase, muscle	NM_001129949
A_72_P097066	0.03	2.0	kinesin family member C1	AK233842
A_72_P477233	0.03	2.0	Uncharacterized protein	XM_001929304
A_72_P225252	0.02	1.9	MARC 4PIG Sus scrofa cDNA 3', mRNA sequence	CN166189
A_72_P748722	<0.0001	1.9	vitronectin	NM_214104
A_72_P715808	0.01	1.9	Sus scrofa mRNA, clone: UTR010026F01, expressed in uterus.	AK352210
A_72_P455827	0.002	1.9	histidine ammonia-lyase-like	XM_001925061
A_72_P413613	0.04	1.9	solute carrier family 9 (sodium/hydrogen exchanger), member 3	AF123280
A_72_P587986	0.02	1.8	receptor-binding cancer antigen expressed on SiSo cells-like	XM_001925514
A_72_P440536	0.001	1.8	parkinson protein 2, E3 ubiquitin protein ligase (parkin)	NM_001044603
A_72_P440046	0.04	1.8	ADAM metallopeptidase domain 2	NM_213957
A_72_P537720	0.008	1.8	killer cell immunoglobulin-like receptor, two domains, long cytoplasmic tail, 1	NM_001113218
A_72_P502529	0.01	1.8	transcription elongation factor A (SII)-like 4	XM_001924869
A_72_P413533	0.04	1.8	potassium voltage-gated channel, subfamily H (eag-related), member 2	AB030030
A_72_P555885	0.003	1.8	adenylate cyclase 4	XM_001927556
A_72_P773846	0.01	1.8	forkhead box protein Q1-like	XM_001928048
A_72_P567814	0.02	1.8	ubiquitin carboxyl-terminal esterase L3 (ubiquitin thiolesterase)	NM_001077227
A_72_P303589	0.0003	1.8	Uncharacterized protein	XR_131178
A_72_P306044	0.02	1.8	protocadherin 17	XM_001927267
A_72_P494665	0.002	1.7	transmembrane protein 8B-like	XM_003122009
A_72_P219367	0.02	1.6	popeye domain containing 2	NM_001144114

A_72_P473103	0.003	1.6	Uncharacterized protein	XM_003125434
A_72_P070251	0.05	1.6	c-X-C chemokine receptor type 2-like	AK237564
A_72_P490729	0.03	1.6	forkhead box protein I2-like	XM_001928234
A_72_P365643	0.003	1.6	Uncharacterized protein	XM_003134357
A_72_P168736	0.03	1.5	MARC 4PIG Sus scrofa cDNA 5', mRNA sequence	DN112477
A_72_P028406	0.03	1.5	integrin, alpha 5 (fibronectin receptor, alpha polypeptide)	XM_001925252
A_72_P724928	0.006	1.5	transmembrane protein 70	AK231606
A_72_P495810	0.02	1.5	sarcosine dehydrogenase	XM_001929498
A_72_P477263	0.003	1.5	tight junction associated protein 1 (peripheral)	XM_003128424

Table 2: Differentially expressed gene transcripts which are down regulated in damaged skin following SM exposure compared to damaged, unexposed skin. *Differentially expressed genes are based on a 1.5-fold change (F/C) cut-off with a FDR < 0.05.*

Probe ID	p-value	F/C	Gene name	GenBank accession number
A_72_P673176	0.0002	2.2	thioredoxin interacting protein	NM_001044614
A_72_P252863	0.01	2.1	uncharacterized protein C6orf62 homolog	XM_001928389
A_72_P709750	0.001	2.0	pantothenate kinase 1	XM_001926022
A_72_P585156	<0.0001	1.9	thioredoxin interacting protein	NM_001044614
A_72_P649754	0.006	1.9	snurportin 1	AK350475
A_72_P709040	0.01	1.9	chromosome 6 open reading frame 106 ortholog	NM_001243026
A_72_P592864	0.0001	1.9	thioredoxin interacting protein	NM_001044614
A_72_P612897	0.0000	1.9	thioredoxin interacting protein	AK349227
A_72_P721303	0.0004	1.8	Histone H3.3	AK239851
A_72_P512479	0.0007	1.8	actin-related protein 8	XM_001929049
A_72_P725763	0.002	1.8	serine/arginine-rich splicing factor 9	AK347688
A_72_P391653	0.02	1.7	eukaryotic translation initiation factor 4E-binding protein 2-like	XM_003133058
A_72_P562489	<0.0001	1.7	thioredoxin interacting protein	NM_001044614
A_72_P574349	0.0003	1.7	thioredoxin interacting protein	AK349227
A_72_P630319	0.03	1.7	scavenger receptor class B, member 2	NM_001244155
A_72_P548796	0.003	1.6	unactive progesterone receptor, 23 kD	AY610476
A_72_P733718	0.0009	1.6	B-cell translocation gene 1, anti-proliferative	NM_001099936
A_72_P587931	0.01	1.6	tyrosine 3-monooxygenase/ tryptophan 5-monooxygenase activation protein, beta polypeptide	AK231708
A_72_P549696	0.001	1.6	thioredoxin interacting protein	NM_001044614
A_72_P557625	0.001	1.6	CD9 molecule	NM_214006
A_72_P298634	0.005	1.6	Uncharacterized protein	XM_003133519

A_72_P546521	0.01	1.6	epithelial splicing regulatory protein 1-like	XM_003125564
A_72_P760377	0.001	1.5	lipoprotein lipase	NM_214286
A_72_P665410	0.02	1.5	nexin-1	NM_214287

Table 3: Differentially expressed gene transcripts which are up regulated in damaged skin following SM exposure compared to damaged, unexposed skin. *Differentially expressed genes are based on a 1.5-fold change (F/C) cut-off with a FDR < 0.05.*

Probe ID	p-value	F/C	Gene name	GenBank accession number
A_72_P454116	0.007	7.5	homeobox protein Hox-C4-like	XM_001925128
A_72_P755349	0.0001	3.8	cytochrome P450 3A29	NM_214423
A_72_P062611	0.008	3.6	MARC 3PIG Sus scrofa cDNA 5', mRNA sequence	DY427469
A_72_P530870	0.02	3.2	tyrosyl-DNA phosphodiesterase 1	BI347194
A_72_P440981	0.0001	3.2	claudin 20	NM_001159777
A_72_P497066	0.007	3.1	nonhomologous end-joining factor 1	XM_001925512
A_72_P441189	0.001	3.0	feline leukaemia virus subgroup C cellular receptor 1	NM_001142846
A_72_P344208	0.004	2.8	sphingosine-1-phosphate lyase 1	XM_001928140
A_72_P490438	0.03	2.5	shootin-1-like	XM_001925635
A_72_P474419	0.005	2.5	poliovirus receptor-related protein 4-like	XM_001927467
A_72_P489836	0.02	2.4	solute carrier family 16, member 12 (monocarboxylic acid transporter 12)	XM_001928811
A_72_P020616	0.0004	2.4	nuclear receptor coactivator 1	EU346671
A_72_P449170	0.0001	2.4	isthmin 1 homolog (zebrafish)	XM_001925000
A_72_P541658	0.0001	2.4	ACP6 protein	XM_001928346
A_72_P441184	0.0002	2.3	DNA (cytosine-5-)-methyltransferase 3 beta	NM_001162404
A_72_P501805	0.0001	2.3	inhibitor of kappa light polypeptide gene enhancer in B-cells, kinase complex-associated protein	XM_001924394
A_72_P632621	0.0001	2.3	glycerol-3-phosphate acyltransferase	AK348444
A_72_P532333	0.0001	2.3	Sus scrofa similar to Inositol polyphosphate multikinase	XM_001926840
A_72_P490263	0.005	2.2	inositol 1,4,5-triphosphate receptor-interacting protein-like	XM_001927312
A_72_P399768	0.001	2.2	porcine adipose tissue cDNA library (PADT) Sus scrofa cDNA 3', mRNA sequence	EB415041
A_72_P666205	0.005	2.2	carbonic anhydrase II	XM_001927805

A_72_P473691	0.001	2.1	epithelial splicing regulatory protein 1	XM_001925874
A_72_P489597	0.0004	2.1	multimerin 2	XM_001927177
A_72_P445143	0.0006	2.1	chromosome 6 open reading frame 15 ortholog	NM_001128447
A_72_P440331	0.0005	2.0	nuclear receptor coactivator 3	NM_001114276
A_72_P475537	0.0001	2.0	uncharacterized protein C1orf88-like	XM_001926563
A_72_P675956	0.009	2.0	SH2 domain-containing adapter protein F-like	XM_001925071
A_72_P440611	0.0008	2.0	angiopoietin-like 7	NM_001142828
A_72_P441972	0.0001	2.0	RNA binding motif protein 4B	NM_001123188
A_72_P410688	0.0003	2.0	MARC 3PIG Sus scrofa cDNA 3', mRNA sequence	DY412467
A_72_P443134	0.01	2.0	lysine (K)-specific demethylase 5C	NM_001097433
A_72_P738358	0.0001	2.0	Sus scrofa mRNA, clone: AMP010001F07, expressed in alveolar macrophage	AK230481
A_72_P506470	0.003	1.9	hypothetical protein LOC100155045	XM_001925366
A_72_P443329	0.0001	1.9	homeobox D13	XM_001926027
A_72_P489530	0.0002	1.9	tetraspanin-14-like	XM_001926602
A_72_P427239	0.006	1.9	cadherin-24-like	AK348514
A_72_P644426	0.002	1.9	programmed cell death 4 (neoplastic transformation inhibitor)	XM_001927049
A_72_P553731	0.001	1.9	RALBP1 associated Eps domain containing 1	XM_001925993
A_72_P559179	0.0004	1.8	MAX interactor 1	XM_001925277
A_72_P795364	0.0002	1.8	ubiquitin protein ligase E3B	EW061474
A_72_P562464	0.001	1.8	prolyl endopeptidase	NM_001004050
A_72_P491390	0.0003	1.8	trace amine-associated receptor 8a-like	XM_001926037
A_72_P221067	0.01	1.8	v-crk sarcoma virus CT10 oncogene homolog (avian)	NM_001137636
A_72_P708895	0.0001	1.7	sortilin 1	AK236900

A_72_P557625	0.003	1.7	CD9 molecule	NM_214006
A_72_P472491	0.0004	1.7	nexin-1	NM_214287
A_72_P299229	0.0009	1.7	Y55F3AM.9	XM_001929665
A_72_P665999	0.0003	1.7	Kruppel-like factor 10	NM_001134344
A_72_P307758	0.004	1.6	protein interacting with PRKCA 1	XM_001925023
A_72_P270094	0.0003	1.6	protein tyrosine phosphatase, receptor type, G	XM_001926989
A_72_P442584	0.001	1.6	Uncharacterized protein C5orf4	AK233246
A_72_P493602	0.0004	1.6	alpha-kinase 2	XM_001925970
A_72_P685060	0.0008	1.6	bactericidal/ permeability-increasing protein	NM_001159307
A_72_P746188	0.005	1.6	amyloid beta (A4) precursor protein	NM_214372
A_72_P163251	0.003	1.6	CST complex subunit STN1-like	XM_001929419
A_72_P723273	0.008	1.6	MGC159817 protein	XM_001928319
A_72_P265767	0.0003	1.6	Sus scrofa mRNA, clone: THY010202C04, expressed in thymus	AK239751
A_72_P000076	0.0001	1.6	SH2B adaptor protein 3	XM_001929523
A_72_P555186	0.0001	1.5	sarcolipin	NM_001044566
A_72_P318468	0.0005	1.5	zinc finger protein 174	XM_003124674
A_72_P441119	0.0006	1.5	claudin 6	NM_001161645
A_72_P797349	0.0003	1.5	Sus scrofa similar to hCG2040023	XM_001925825

Table 4: Differentially expressed gene transcripts which are down regulated in damaged skin following SM exposure and decontamination with WoundStat™ compared to SM-exposed skin without decontamination. *Differentially expressed genes are based on a 1.5-fold change (F/C) cut-off with a FDR < 0.05.*

Probe ID	p-value	F/C	Gene name	GenBank accession number
A_72_P159746	0.0001	7.1	Haemoglobin subunit alpha (Alpha-globin)	AK348963
A_72_P365563	0.0001	6.6	procollagen C-endopeptidase enhancer 2	AK235631
A_72_P680394	0.02	6.6	interleukin 6 (interferon, beta 2)	NM_214399
A_72_P008421	0.0004	6.3	C27H2.2a	XM_001928606
A_72_P273359	0.0002	5.8	MARC 3PIG Sus scrofa cDNA 5', mRNA sequence	DY410803
A_72_P558764	0.0001	5.6	claudin 11	AY609490
A_72_P502819	<0.0001	4.6	collagen, type VIII, alpha 1	XM_001926443
A_72_P669424	0.0001	4.3	superoxide dismutase 2, mitochondrial	XM_001926440
A_72_P269404	0.0001	4.1	potassium large conductance calcium-activated channel, subfamily M, beta member 4	XM_001928917
A_72_P723223	0.0001	3.7	phosphoinositide-3-kinase, regulatory subunit 5	NM_213851
A_72_P730788	0.008	3.7	amylase, alpha 2B (pancreatic)	NM_214195
A_72_P440121	0.0005	3.7	amphiregulin	NM_214376
A_72_P001121	0.0002	3.5	Sus scrofa mRNA, clone: PBL010105F02, expressed in peripheral blood mononuclear cell	AK237103
A_72_P715808	0.003	3.5	translation initiation factor IF-3, mitochondrial-like	XM_001926477
A_72_P262637	0.0006	3.3	Leucine rich repeat containing 23	XM_003126523
A_72_P615820	0.0008	3.3	carbonic anhydrase III, muscle specific	NM_001008688
A_72_P206097	0.0003	3.2	Porcine Brain Library Sus scrofa cDNA clone PBL 5', mRNA sequence	CD572107
A_72_P532834	<0.0001	3.2	transmembrane 6 superfamily member 1	XM_001929144
A_72_P502516	0.001	3.2	SIX homeobox 1	XM_001928937
A_72_P676302	0.0001	3.2	electron-transfer-flavoprotein, alpha polypeptide	XM_001928732
A_72_P602553	0.0002	3.1	reticulon 4	NM_001129963

A_72_P069731	0.0001	2.8	asparagine-linked glycosylation 5, dolichyl-phosphate beta-glucosyltransferase homolog (S. cerevisiae)	AK238941
A_72_P374788	0.0001	2.7	crystallin, alpha B	XM_003129866
A_72_P532628	0.0007	2.7	signal sequence receptor, alpha	NM_001185167
A_72_P731188	0.0001	2.7	cytochrome c oxidase subunit 5A, mitochondrial-like	XM_001927220
A_72_P242552	0.0001	2.6	Sus scrofa mRNA, clone: OVRM10202E03, expressed in ovary	AK236557
A_72_P704827	0.0003	2.5	Sus scrofa mRNA, clone: OVRM10218H12, expressed in ovary	AK348632
A_72_P763429	0.02	2.4	actin, alpha 1, skeletal muscle	NM_001167795
A_72_P514974	0.0002	2.4	glutaredoxin (thioltransferase)	AK230519
A_72_P677500	0.0003	2.3	ribosomal protein S6 modification-like protein B-like	XR_115935
A_72_P624481	0.0006	2.3	glutamate dehydrogenase 1	AK235921
A_72_P351818	0.0008	2.3	Sus scrofa mRNA, clone:PTG010104H11, expressed in pituitary gland	AK349562
A_72_P473343	0.0002	2.3	putative deoxyribonuclease TATDN1-like	AK344100
A_72_P552836	0.0001	2.2	glutamate dehydrogenase 1	AK235921
A_72_P404238	0.0009	2.2	Sus scrofa mRNA, clone:OVRM10114A05, expressed in ovary	AK348273
A_72_P442002	0.0001	2.2	G-protein signalling modulator 3	NM_001123119
A_72_P633842	0.0004	2.1	SMAD family member 6	XM_001926127
A_72_P710138	0.0001	2.1	insulin-like growth factor binding protein 6	AK240415
A_72_P729913	0.0005	2.1	matrix Gla protein	NM_214116
A_72_P441908	0.0005	2.1	proline-rich transmembrane protein 1	NM_001123170
A_72_P400753	0.0000	2.0	MARC 4PIG Sus scrofa cDNA 5', mRNA sequence	CK453658

A_72_P230782	0.0001	2.0	Sus scrofa mRNA, clone: THY010088C01, expressed in thymus	AK239275
A_72_P276754	0.0000	2.0	Sus scrofa mRNA, clone: PTG010078F03, expressed in pituitary gland	AK349467
A_72_P640265	0.0001	2.0	serine/arginine-rich splicing factor 2	AK235325
A_72_P514959	0.02	2.0	glycoprotein m6b	XM_001927816
A_72_P501854	0.0001	1.9	Sus scrofa similar to GDNF-inducible zinc finger protein 1	XM_001926993
A_72_P654023	0.002	1.8	cytochrome c, somatic	NM_001129970
A_72_P727423	0.0002	1.8	H3 histone, family 3A	AK235071
A_72_P609774	0.002	1.8	tubulin, alpha 1b	NM_001044544
A_72_P541728	0.005	1.8	MTERF domain containing 1	AK347886
A_72_P532882	0.0002	1.8	aldo-keto reductase family 1 member C1-like	NM_001044569
A_72_P158071	0.009	1.8	UDP-N-acteylglucosamine pyrophosphorylase 1	XM_001928643
A_72_P015106	0.004	1.8	dystonin	XM_001927053
A_72_P735133	0.0005	1.7	PRP39 pre-mRNA processing factor 39 homolog (S. cerevisiae)	XM_001927120
A_72_P516849	0.0001	1.7	translocase of outer mitochondrial membrane 20 homolog (yeast)	XM_001926935
A_72_P629589	0.0002	1.7	UDP-N-acteylglucosamine pyrophosphorylase 1	XM_001928643
A_72_P490497	0.0007	1.7	antioxidant protein	AK235228
A_72_P588691	0.002	1.7	UDP-N-acteylglucosamine pyrophosphorylase 1	XM_001928643
A_72_P502441	0.0040	1.6	cyclin-dependent kinase 2 associated protein 1	NM_001190166
A_72_P544737	0.0002	1.6	pumilio domain-containing protein KIAA0020-like	XM_001927669
A_72_P755406	0.0003	1.6	H3 histone, family 3A	BP171840
A_72_P603353	0.0002	1.5	matrilin 2	AK234298
A_72_P583711	0.007	1.5	meningioma expressed antigen 5 (hyaluronidase)	XM_001928026

A_72_P442806	0.03	1.5	membrane-bound transcription factor peptidase, site 1	XM_003126835
A_72_P292894	0.0005	1.5	MARC 2PIG Sus scrofa cDNA 5', mRNA sequence	BI343668
A_72_P047996	0.01	1.5	MARC 1PIG Sus scrofa cDNA 5', mRNA sequence	AW360248
A_72_P499726	0.0002	1.5	Friend of PRMT1 protein-like	XM_001929572
A_72_P581292	0.0005	1.5	syndecan 2	XM_001926939
A_72_P531692	0.0001	1.5	Sus scrofa mRNA, clone: LVR010071B05, expressed in liver	AK232553
A_72_P677030	0.0004	1.5	UDP-N-acteylglucosamine pyrophosphorylase 1	XM_001928643
A_72_P136196	0.004	1.5	Sus scrofa mRNA, clone: LNG010001F06, expressed in lung	AK231609

Table 5: Differentially expressed gene transcripts which are upregulated in damaged skin following SM exposure and decontamination with WoundStat™ compared to SM-exposed skin without decontamination. *Differentially expressed genes are based on a 1.5-fold change (F/C) cut-off with a FDR < 0.05.*

PUBLICATIONS AND PRESENTATIONS

Hall, C.A., Lydon, H.L., Dalton, C.H., Chipman, J.K., Chilcott, R.P. and Graham, J.S., **(2009)** *The in vitro efficacy of haemostatic products in the presence of chemical warfare agents—Sulphur mustard (HD) and VX*. Toxicology, 262:9-10. Abstract

Hall, C.A., Lydon, H.L., Dalton, C.H., Chipman, J.K., Chilcott, R.P. and Graham, J.S., **(2010)** *Novel decontaminant Role for COTS Haemostats for the CW Agent Sulphur Mustard*. DTRA CBD S&T, Orlando, Florida, Abstract and Poster

Hall, C.A., Lydon, H.L., Dalton, C.H., Chipman, J.K., Chilcott, R.P. and Graham, J.S., **(2011)** *Developing a Haemostatic Decontaminant for Sulphur Mustard; An in vivo feasibility study.* Society of Toxicology Washington DC, USA, Abstract and Poster,

PUBLICATIONS ARISING

Hall, C.A., Lydon, H.L., Dalton, C.H., Chipman, J.K., Chilcott, R.P. and Graham, J.S., *The in vitro efficacy of haemostatic products in the presence of chemical contaminants.*

Lydon, H.L., Hall, C.A., Dalton, C.H., Chipman, J.K., Chilcott, R.P. and Graham, J.S., *Development of haemostatic decontaminants for treatment of wounds contaminated with chemical warfare agents: Evaluation of topical decontamination efficacy using undamaged skin.*

Dalton, C.H., Hall, C.A., Lydon, H.L., Chipman, J.K., Chilcott, R.P. and Graham, J.S., *Development of haemostatic decontaminants for treatment of wounds contaminated with chemical warfare agents: Evaluation of de contamination efficacy from damaged skin.*